The Synthesis and Study of Multimetallic Platinum Group Metal Complexes as *in vitro* Pharmacological Agents

Prinessa Chellan

University of Cape Town

April 2013

The Synthesis and Study of Multimetallic Platinum Group Metal Complexes as *in vitro* Pharmacological Agents

A thesis submitted to the

University of Cape Town

in fulfillment of the requirements for the degree of

Doctor of Philosophy

by

Prinessa Chellan

Supervisor: Dr Gregory S. Smith

Co-supervisor: Prof Kelly Chibale

Department of Chemistry
University of Cape Town
Rondebosch
7701
Cape Town

April 2013

Declaration

I know the meaning of Plagiarism and declare that all of the work in the document, **"*The Synthesis and Study of Multimetallic PGM complexes as in vitro Pharmacological Agents*"**, is my own work and to the best of my knowledge has never been submitted for examination for any degree at any university. All sources of information are cited and fully referenced.

_____ Date:_____

Miss Prinessa Chellan

Acknowledgements

I would like to thank my supervisor, Dr Gregory Smith for his guidance, invaluable advice and faultless attention to detail during the write-up of this thesis. My co-supervisor, Prof Kelly Chibale for his helpful discussions and advice on synthetic methods, as well as biological mechanisms and studies.

I would also like to acknowledge the following people for their assistance, Mr P. Roberts and Mr N. Hendricks for recording some of the NMR spectra. Mr G. Benincasa for microanalytical analyses and Electron Impact Mass Spectral analyses, Dr M. Stander (University of Stellenbosch) for Electro-Spray Ionisation Mass spectral analyses and Dr H. Su for X-ray diffraction analyses. Prof P. J. Dyson, Dr T. Riedel and Dr. F. Edafe (École Polytechnique Fédérale de Lausanne) for conducting anticancer experiments. Prof P. J. Smith, Dr C. de Kock and Dr D. Taylor (UCT Department of Clinical Pharmacology) for antimalarial screenings. Prof K. M. Land and his research group (University of the Pacific) for the *T. vaginalis* studies. Dr J. Mao and his research group at the Key Laboratory of Organic Synthesis of Jiangsu Province, Soochow University, for the catalytic studies.

Special thanks go to my friends, Dr Emma Hager and Miss Tameryn Stringer. I would also like to thank the rest of the Organometallic Research group for the amicable atmosphere that made working in the lab a pleasure. Mr David Kuter and Miss Katheryn Wicht of the Bioinorganic Research Group at UCT for discussions on physico-chemical properties.

For funding, I thank the UCT Chemistry Equity Development Programme, K. W. Johnstone bursary programme, the Stella and Paul Loewenstein Medical Research Fund and the National Research Foundation.

Finally, I would like to thank my family in particular my Dad, Mr Munsami Chellan. Dad, you keep us all sane and I couldn't have finished my studies without your support. This thesis is as much for you as it is for me.

Abstract

The success of cisplatin and its analogues for the treatment of different cancers has had a profound effect on establishing the application of metal complexes in medicine. Lately, increasing drug resistance and the emergence of unwanted side effects to currently available therapies have bred a need for novel pharmacological agents. Thus, the design and study of organometallic complexes as potential chemotherapeutics may potentially identify new drug candidates. Apart from platinum based compounds, platinum-like metals such as ruthenium(II), rhodium(III) and iridium(III), have been identified as biologically relevant metals. The purpose of this study is to synthesize three classes of polynuclear complexes containing metals from the Platinum Group Metal (PGM) series and evaluate each class for pharmacological activity *in vitro*. Each complex class is based on a different ligand type.

New mono- and polynuclear organometallic Platinum Group Metal (PGM) complexes based on three ligand classes have been synthesised and characterised using several analytical and spectroscopic techniques including ^{1}H, ^{13}C and ^{31}P NMR, infrared and UV-vis spectroscopy. The first complex series is based on the thiourea containing ligand, 3,4-dichloroacetophenonethiosemicarbazone, which has demonstrated *in vitro* pharmacological activity. This ligand was reacted with $K_2[PtCl_4]$ to afford a tetranuclear cycloplatinated thiosemicarbazone complex (**2.2**). Reaction of **2.2** with different mono- and diphosphanes yielded two mono- and three dinuclear Pt(II) thiosemicarbazone ligands (**2.3**-**2.7**). In all of the complexes (**2.2**-**2.7**), the thiosemicarbazone ligands act as a dinegative tridentate [C,N,S] donor to each metal centre. Single crystal X-ray analyses of three of the complexes in this series, including the tetraplatinum derivative, confirmed the structural integrity of these complexes. Reactivity studies of the mononuclear platinum(II) complexes revealed that one complex is able to undergo oxidative addition reactions with different aryl iodide substrates. *In vitro* pharmacological studies of a selection of these complexes as antiparasitic agents have been carried out against the *P. falciparum* strains, D10 (cisplatin sensitive) and Dd2 (cisplatin resistant)) and *Trichomonas vaginalis* T1. Their cytotoxic effects on the A2780 (cisplatin sensitive) and A2780*cis*R (cisplatin resistant) human ovarian carcinoma cell line has also been determined. All of the complexes demonstrated moderate cytotoxic effects as

antiparasitics and antitumor agents. No correlation between the number of platinum-thiosemicarbazone moieties and pharmacological activity could be discerned. Instead, the type of ancillary ligand used to prepare each complex may influence the lipophilic nature of each complex thus explaining the trend observed.

The second and third complex series are based on di- and tri-pyridyl aromatic ethers and esters respectively. The di- and tri-pyridyl aromatic ether ligands (**4.1** and **4.2**) were prepared using the Williamson ether synthetic method. The di- and tri-pyridyl ester ligands (**5.1** and **5.2**) were isolated upon alkylation of the appropriate carboxylic acid derivative. Functionalization of these ligands (**4.1**, **4.2**, **5.1** and **5.2)** with either dichloro(*p*-cymene)-ruthenium(II), dichloro(pentamethylcyclopentadienyl)rhodium(III) or dichloro(pentamethyl-cyclopenta-dienyl)iridium(III) moieties yielded the corresponding di- or trinuclear organometallic complexes (**4.3**-**4.8** and **5.3**-**5.8**). All of the ligands act as monodentate donors to each metal centre and this coordination mode of the polyaromatic ether and ester ligands were confirmed upon elucidation of the molecular structures for three of the dinuclear complexes (**4.5**, **5.4** and **5.5**).

The di- and trinuclear platinum group metal complexes synthesized were evaluated for inhibitory effects on the *P. falciparum* strain NF54 (chloroquine sensitive), the *T. vaginalis* strain T1 and the tumor cell lines cisplatin-sensitive A2780 and cisplatin-resistant A2780cisR human ovarian cancer. All of the complexes were found to have moderate to high antiplasmodial activities and the compounds with the best activities were evaluated for their ability to inhibit formation of synthetic hemozoin in a cell free medium. The *in vitro* antitumor evaluations of these complexes revealed that the pyridyl ether complex series (**4.2**-**4.8**) have no significant cytotoxic effect. In contrast, the pyridyl ester containing PGM complexes demonstrated moderate activities against these two tumor cell lines and was also found to be less toxic to healthy cells.

Four Pd(II) analogues (**7.1**-**7.4**) of the cycloplatinated complexes (**2.2**-**2.8**) were prepared in order to assess the potential of palladium thiosemicarbazone complexes as catalyst precursors for the Suzuki-Miyaura cross couplings of a variety of aryl halides and aryl boronic acids. One mononuclear (**7.2**), two dinuclear (**7.3** and **7.4**) and one tetranuclear complex were tested. The dinuclear cyclopalladated thiosemicarbazone complex **7.4**, which contains the bis(diphenylphosphino)ferrocene spacer, was found to be a robust catalyst. It was able to

efficiently catalyze the coupling of various aryl halides and aryl boronic acids, irrespective of the type of electron-withdrawing or electron-donating substituent on the aromatic ring.

Publications

Journal Article:

1. Hong Yan, Prinessa Chellan, Tingyi Li, Jincheng Mao, Kelly Chibale and Gregory S. Smith, Cyclometallated Pd(II) thiosemicarbazone complexes: new catalyst precursors for Suzuki-coupling reactions, Tetrahedron Letters, **2013**, 54, 154-157.
2. Prinessa Chellan, Kirkwood M. Land, Ajit Shokar, Aaron Au, Seung Hwan An, Catherine M. Clavel, Paul J. Dyson, Carmen de Kock, Peter J. Smith, Kelly Chibale and Gregory S. Smith, *Exploring the Versatility of Cycloplatinated Thiosemicarbazones as Antitumor and Antiparasitic Agents*, Organometallics, **2012**, 31, 5791−5799.

Conference Contributions

1. **Poster Presentation:** Prinessa Chellan, Kelly Chibale and Gregory S. Smith, *Tridentate [O,N,S] and [C,N,S] Pd(II) Thiosemicarbazone Complexes: A New Class of Catalyst Precursors for Coupling Reactions*, presented at CATSA 2012, Langebaan, Western Cape, South Africa, 2012.
2. **Poster with Oral Flash Presentation**: Prinessa Chellan, Kelly Chibale, Gregory S. Smith, Exploring the Versatility of Cyclometalated Pd(II) and Pt(II) Thiosemicarbazones in Biology and Catalysis, presented at International Conference on Organometallic Chemistry 2012, Lisbon, Portugal, 2012
3. **Poster Presentation**: Prinessa Chellan, Kelly Chibale, Gregory S. Smith, *Tridentate Pd(II) Thiosemicarbazone Complexes Prepared by C-H Activation: New Catalyst Precursors for Coupling Reactions*, presented at CATSA 2011, Gauteng, South Africa, 2011.
4. **Poster Presentation**: Prinessa Chellan, Kelly Chibale, Gregory S. Smith, *Synthesis and Characterisation of Mono- and Multinuclear Cycloplatinated Thiosemicarbazone Complexes,* presented at SACI 2011, Johannesburg, 2011.
5. **Poster Presentation**: Prinessa Chellan, Kelly Chibale, Gregory S. Smith, *Organometallic Palladium(II) Complexes Containing Tridentate [C,N,S] Thiosemicarbazone Ligands: Synthesis, Structure and Antimalarial activity*, presented at the 5th International Symposium on Bioorganometallic Chemistry, Bochum, Germany, 2010.

List of Abbreviations and Symbols

%	percent
°C	degrees celcius
Å	Ångstrom
A2780	cisplatin-sensitive Human Ovarian Carcinoma cell line
A2780cisR	cisplatin-resistant Human Ovarian Carcinoma cell line
ACT	artemisinin-based combined therapy
ADME	Absorption Distribution Metabolism and Excretion
Ala	alanine
Arg	arginine
ATR	Attenuated Total Reflection (infrared spectroscopy)
ClogP	calculated logP
cm^{-1}	reciprocal centimeters
COSY	Correlation Spectroscopy
Cp*	1,2,3,4,5-pentamethylcyclopentadienyl
CQ	chloroquine
CQR	chloroquine-resistant
CQS	chloroquine-sensitive
d	doublet
D10	CQS *P. falciparum* strain
DCC	N,N'-dicyclohexylcarbodiimide
DCM	dichloromethane
Dd2	CQR *P. falciparum* strain
Decomp.	decomposition
DHFR	dihydrofolate reductase
DMAP	4-dimethylaminopyridine
DMF	dimethylformamide
DMSO	dimethylsulfoxide
dppe	*trans*-bis(diphenylphosphino)ethylene
dppf	bis(diphenylphopshino)ferrocene

dppp	bis(diphenylphosphino)propane
EA	elemental analysis
EI	Electron Impact
ESI	Electro-Spray Ionisation
FDA	Food and Drug Administration
FT-IR	Fourier Transform-Infrared
Gly	glycine
Hb	hemoglobin
HEK	human embryonic kidney cells
HEPES	(4-(2-hydroxyethyl)-1-piperazineethanesulfonic acid)
His	histidine
HSQC	Heteronuclear Spin-Quantum Coupling Spectroscopy
Hz	Hertz
IC_{50}	minimum concentration of test compound to induce 50% cell growth inhibition
IR	Infrared
J	Coupling constant
lit.	literature
LMCT	ligand to metal charge transfer
Lys	lysine
m	mulitplet (NMR), medium intensity (IR)
m.p.	melting point
m/z	mass-charge ratio (MS)
Me	methyl
Met	methionine
MHz	megahertz
MLCT	metal to ligand charge transfer
mM	millimolar
MS	mass spectrometry
MTT	3-(4,5-Dimethylthiazol-2-yl)-2,5-diphenyltetrazolium bromide
NADPH	nicotinamide adenine dinucleotide phosphate
NF54	CQS *P. falciparum* strain

NMR	nuclear magentic spectroscopy
NOESY	Nuclear Overhauser Effect Spectroscopy
NP-40	Nonidet P40
PBS	phosphate buffered saline
PGM	platinum group metal
PPh_3	triphenylphosphane
ppm	parts per million
PTA	1,3,5-triaza-7-phosphaadamantane
q	quartet (NMR)
RI	resistance index
RT	room temperature
s	singlet (NMR)
t	triplet (NMR)
T1	T. vaginalis strain
THF	tetrahydrofuran
TMS	trimethylsilane
Trp	trytophan
TSC	thiosemicarbazone
TYM	medium of trypticase, yeast extract, maltose and serum
UV	ultraviolet
vis	visible
w	weak intensity (IR)
XRD	X-ray Diffraction
µg	microgram
µM	micromolar

Table of Contents

CHAPTER 1

Multinuclear Platinum Group Metal Complexes as Pharmacological Agents: A Review

1.1. Introduction

There are several focus areas in the design and application of medicinal compounds, with the greatest emphasis being placed on control of side effects, targeting of the drug to the specific organs, cells or tissues where it is needed, optimizing bioavailability of the drug, enhancing permeability and retention of the drug and overcoming intrinsic or acquired resistance to existing therapies.[1,2] In this regard, the use of metal complexes as therapeutic and diagnostic agents is an area of important research.

Certain metals play crucial roles in biological processes so it is only logical that the study of metal complexes, particularly transition metal complexes, would be an area of great potential in the treatment of diseases and other illnesses. Metal containing compounds offer several properties which may be beneficial to the design and synthesis of better therapeutic agents compared to purely organic compounds.[3] Depending on the metal, these complexes can possess a wide range of coordination numbers, geometries, thermodynamic and kinetic properties as well as accessible redox states; all of which can be exploited in the pursuit for better drug therapies.[3]

The use of synthetic organometallic complexes as therapeutic agents dates back to the early twentieth century.[4] Paul Ehrlich, now known as the founding father of bioorganometallic chemistry, realized the potential of organoarsenic compounds as antiparasitics.[4] The first patented organometallic drug, which also happens to be multinuclear, was Salvarsan® (Structure **1.1**, Figure 1.1) and was used for the treatment of syphilis along with it second generation analogue, Neosalvarsan® (**1.2**).[4] Not long after the discovery of these organoarsenicals, came the implementation of organomercury compounds in syphilis treatment. In time, the use of these organometallic complexes in drug therapies began to decrease as their highly toxic side effects became evident.[4]

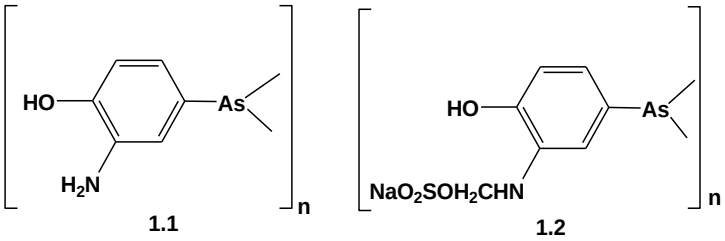

Figure 1.1. The proposed structures of bioorganometallic compounds Salvarsan (**1.1**) and Neosalvarsan (**1.2**).[4]

Years later, the discovery of cisplatin and its analogues as antitumoral agents had a profound influence on establishing the field of metal complexes in medicine [5] and the amount of research already accomplished within this area is substantial.[3,6-8] However, despite the considerable quantity of work completed there are still many avenues of research waiting to be explored particularly in the application of multinuclear organometallic complexes as chemotherapeutic agents.

Cancer and parasitic diseases such as malaria are a serious threat, with the number of diagnosed cases increasing exponentially every year. For these illnesses, resistance to currently available drug therapies has led to a pressing need for new drug designs. The study of multinuclear Platinum Group Metal (PGM) complexes as potential chemotherapeutics against cancer and parasitic diseases has emerged as an area of great potential. By combining the biological properties of certain functional groups present in purely organic ligands to the various biological, thermodynamic, kinetic and redox properties of each metal in the platinum group series has yielded several possibilities for the treatment of these diseases. This review highlights the application of multinuclear PGM complexes against cancer and parasitic diseases. Against cancer, they have found application as both cytotoxic agents and pro-drugs for targeted photoactivated therapies.

1.2. Multinuclear Platinum Group Metal Complexes: Cancer Chemotherapeutics.

1.2.1. Cytotoxic Agents.

Cancer is a class of disease that is known to affect millions of South Africans and is a leading cause of death worldwide. In 2008, it accounted for 7.8 million deaths worldwide.[9] According to the National Cancer Institute, cancer is a broad term used to define a set of

diseases wherein abnormal cells rapidly divide and invade other tissues.[10] There are several types of cancers and they can be divided into subcategories[10]:

- Sarcoma: Cancers that originate in connective or supportive tissues such as bone, cartilage and muscle.
- Carcinoma: Cancers that originate in the skin and tissues that cover internal organs.
- Lymphoma and myeloma: Cancers that originate in the cells of the immune system.
- Leukemia: Cancers that originate in bone marrow and other blood forming tissues.
- Central nervous system cancers: Cancers that originate in the brain and spinal cord tissue.

The most common form of cancer treatment is chemotherapy which employs different drugs as cytotoxic agents all of which target DNA and/or cellular replication and expression.[11] Figure 1.2 depicts the biological targets of some currently used clinical cytotoxic agents. These compounds act as anti-metabolites, intercalating agents or mitotic spindle inhibitors.[11]

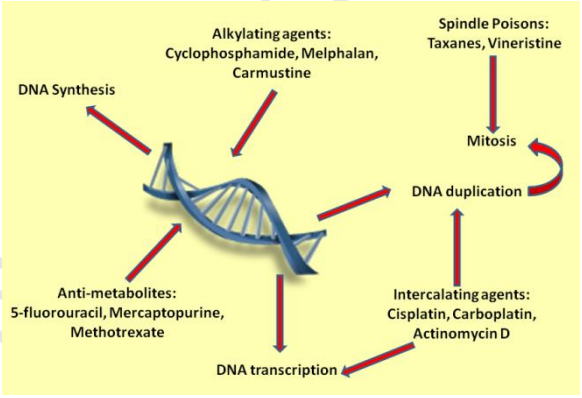

Figure 1.2. Targets of some currently used clinical drugs for cancer chemotherapy.[11]

While most of the drugs clinically used today have some success, drug resistance is fast becoming a major obstacle particularly in recurring cases. There are two proposed causes of this resistance; genetic characteristics may render tumor cells inherently resistant or they may acquire resistance following exposure.[11] In addition to intrinsic and acquired drug resistance, the processes targeted by these compounds also occur in healthy cells and thus they are also vulnerable to attack by these drugs leading to unwanted side effects. In particular, bone marrow cells and intestinal lining cells are susceptible.[11] Consequently, in the design of

improved chemotherapies against cancer, the preferential targeting of cancer cells over healthy normal cells is essential.

The investigation of metal complexes as chemotherapeutic agents has long been of interest and the most well-known complexes clinically used today are cisplatin and its analogues (Figure 1.3) which are known to interact with DNA leading to death of the cancer cell.

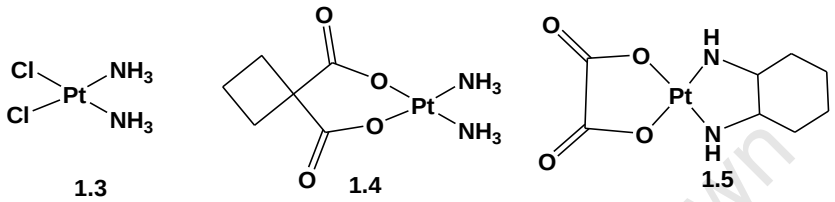

Figure 1.3. Structures of cisplatin (**1.3**), carboplatin (**1.4**) and oxaliplatin (**1.5**).[12,13]

The well-established cytotoxic activity of cisplatin against cancer is believed to be through exchange of the labile chlorido ligands with water or hydroxido ligands yielding partially hydrolyzed species which can then bind to biological macromolecules.[13,14] In some cases, these hydrolysed/aqua species are able to bind to two adjacent guanine bases in the DNA chain causing distortions in the DNA structure which cannot be easily repaired by the cell's existing enzymatic mechanisms thus triggering apoptotic cell death (Figure 1.4).[15,16]

However, in order for cisplatin to exert its antiproliferative activity it needs to diffuse into the cell nucleus unchanged where it can then undergo hydrolysis or aquation.[13,15,16] It has been found that up to 98 % of the intravenously administered dose of cisplatin is deactivated before it can reach its target.[2] There are several proposed deactivation mechanisms (Figure 1.4); the complex undergoes aquation in the extracellular membranes leading to formation of adducts with proteins such as serum albumin[2] and further deactivation can transpire through binding of cisplatin to intracellular sulfur donors such as glutathione in the cytoplasm.[15,17] Apart from the deactivation of cisplatin prior to reaching its target, the complex is known to have high systemic toxicity and there is a tendency of patients developing tumor resistance to the drug.[18,19] These problems can be partially overcome when cisplatin is used in combination therapy[20] but a more preferable alternative would be the use of platinum complexes with lower general toxicity.[13]

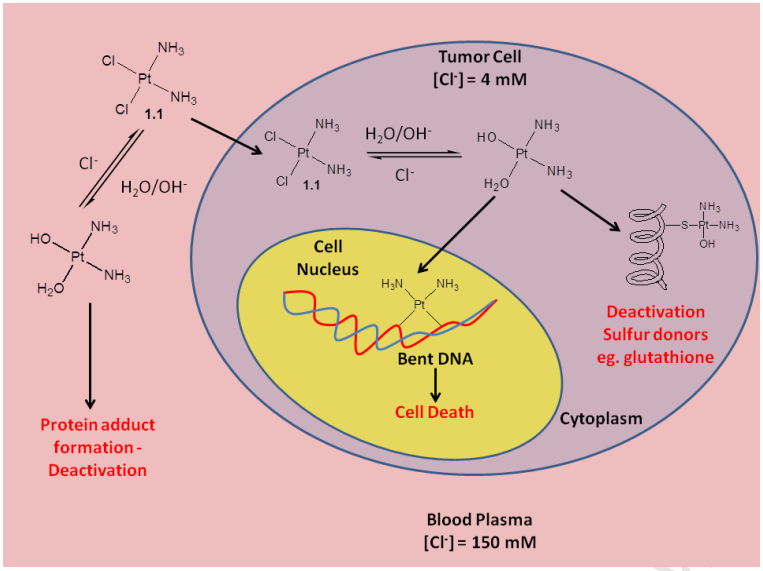

Figure 1.4. A basic schematic representation of the mechanism of action of cisplatin and its proposed deactivation pathways.[13,15]

For these reasons research moved toward the design of platinum complexes with structural similarities to cisplatin. This first wave of research yielded only two complexes that reached broad clinical use, carboplatin and oxaliplatin.[21,22] The replacement of the chlorido ligands with a carboxylato ligand and use of the inert chelating nitrogen donor ligand led to an increase in water solubility and favourably altered ligand exchange reaction rates.[23,24] These findings have prompted studies into the use of other types of ligand systems that can achieve a similar stabilization of platinum. For example, the use of polydentate ligands or the coordination of one or more platinum metal ions to polyaromatic or heteraromatic ligands which are less likely to undergo dissociation before reaching the cell nucleus. These premises have thus led to an ever increasing amount of research into the anticancer activities of multinuclear platinum complexes.

1.2.1.1. Multinuclear Platinum Complexes as Cytotoxic Agents

One of the earliest reports on the development of polynuclear platinum complexes capable of DNA interactions was published by Farrel and co-workers in the late 1980's.[25] Consequent intensive studies of the *cis* or *trans* geometries of the metal, the flexibility of the polyamine linker, the nature of the ancillary ligands and the overall molecular charge yielded a potential

antitumor candidate.[26-31] The polyamine-bridged triplatinum complex BBR3464 (**1.6**, Figure 1.5) demonstrated high tumor cytotoxicity compared to cisplatin.[32] It was able to form long range intra- or interstrand DNA crosslinks to a much higher degree than cisplatin.[31] The antitumor efficacy of BBR3464 was 2-3 orders of magnitude higher than cisplatin against cisplatin-resistant cell lines *in vitro*.[27,32] It successfully completed phase I clinical trials against non-small cell lung, pancreatic, melanoma and ovarian cancers.[33] However, it failed phase II trials due to a lack of major response in small cell lung cancer and in patients with gastric and gastro-esophageal adenocarcinoma.[34-36] Nevertheless, the marginal success of BBR3464 demonstrated the validity of the concept of polynuclearity in the development of potential metallo-chemotherapeutics and ever-increasing reports are appearing in the literature of polynuclear complexes containing not only platinum but also other PGM metals.

Two dinuclear platinum complexes (**1.7** and **1.8**, Figure 1.5) containing an aromatic diamine spacer have shown appreciable activity against the COC1 human ovarian cancer cell line.[37] Complexes **1.7** and **1.8** exhibited IC_{50} values of 1.08 and 4.97 µM respectively, lower than that of cisplatin (IC_{50} = 7.02 µM) in this cell line. Studies into the mode of cell death using flow cytometric assays found that these complexes induced apoptotic cell death. Cell cycle perturbation studies of **1.7**and **1.8** showed that they arrest the cell cycle in the G2 (resting phase) and M (mitosis) phases. Cisplatin exhibits S phase (DNA synthesis) arrest on cell cycle progression suggesting that these diplatinum complexes have a different interaction with the cancer cells compared to cisplatin.[37]

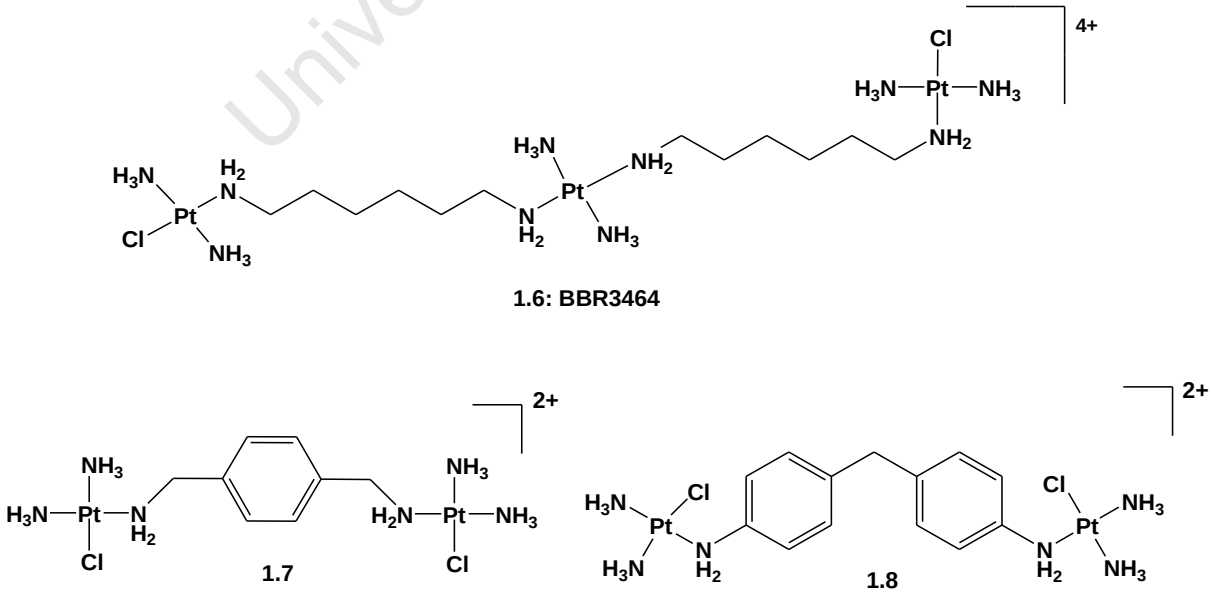

Figure 1.5. Structure of BBR3464[32] and the dinuclear complexes **1.6** and **1.7** that exhibit activities better than cisplatin against the COC1 cell line.[37]

A trinuclear platinum complex (**1.9**) containing a central phenyl core was screened for *in vitro* cytotoxic activity against human non-small cell lung cancer (A-549) and the murine leukemia (P-388) cell lines.[38] At a concentration of 10^{-7} M, complex **1.9** displayed percent cell inhibitions against P-388 and A-549 cell lines of 27.2 and 33.9 % respectively. These values compare favourably with cisplatin which showed inhibition rates of 3.4 % (P-388) and 0.6 % (A-549) at the same concentration. DNA binding studies of complex **1.9** using UV, fluorescence and circular dichroism (CD) spectroscopy and an agarose gel mobility shift assay found that it binds strongly to DNA and that it unwinds supercoiled DNA.

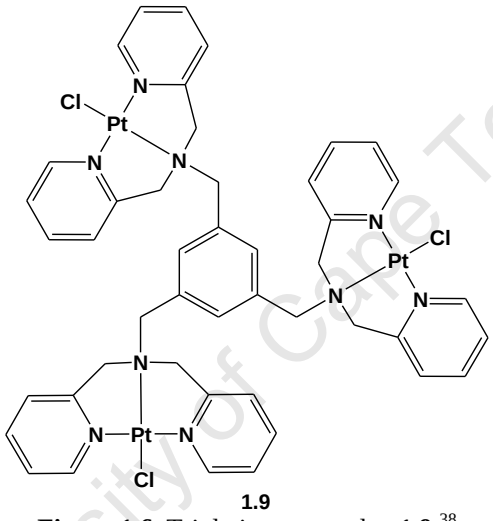

1.9

Figure 1.6. Triplatinum complex **1.9**.[38]

The effect of the triplatinate complexes **1.10** – **1.12** (Figure 1.7) on cancer cell viability as well as cytotoxic effect in four cancer cell lines was investigated in comparison to cisplatin.[39] All of the complexes reduced cell viability in a dose-dependent manner with the maximum reduction in cell viability being reached at 50 µM. Table 1.1. lists the IC_{50} values for the complexes **1.10** – **1.12** as well cisplatin against the human HT29 colon-rectal carcinoma, HepG2 hepatoma, MDA-MB-231 breast cancer and MG63 osteosarcoma cell lines.

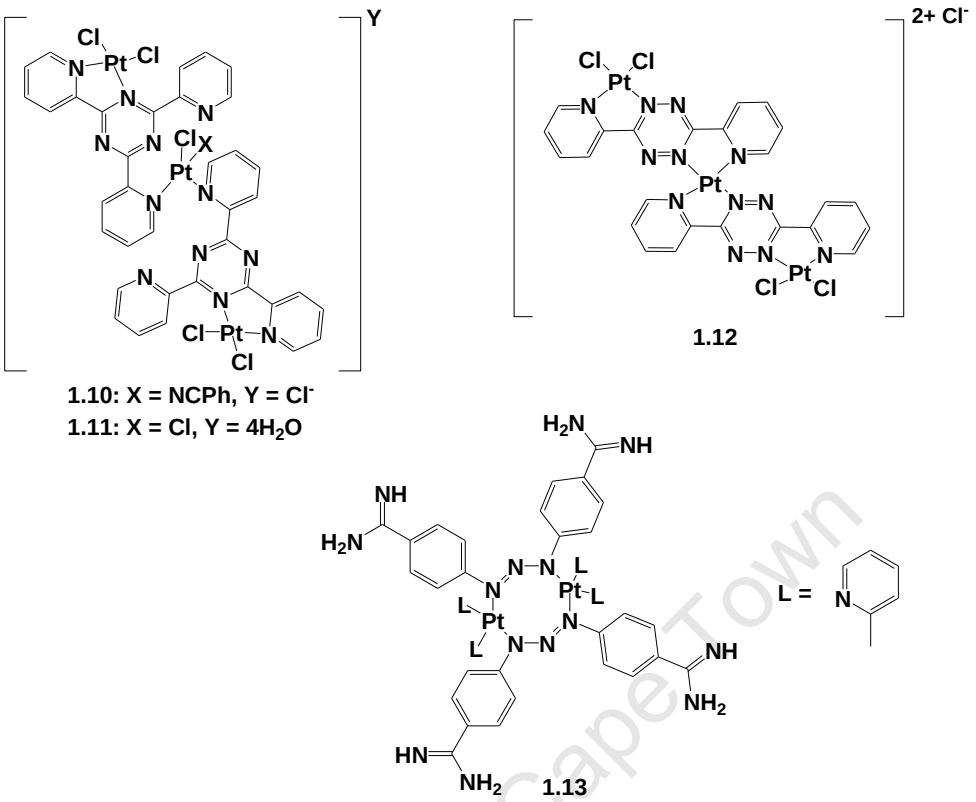

Figure 1.7. Structures of triplatinated complexes **1.10** – **1.12** and diplatinum complex **1.13**.[39,40]

Table 1.1. Cytotoxic Values of Complexes **1.10** – **1.12** and cisplatin Against Four Cancer Cell Lines[39]

Complex	IC_{50} (μM)			
	HT29	**HepG2**	**MG63**	**MDA-MB-231**
cisplatin	58	65	60	66
1.10	9	26	10	28
1.11	21	28	8	23
1.12	29	53	54	36

All of the complexes showed better cytotoxicity than cisplatin against all four cell lines. Complex **1.10** was a better cytotoxic agent than **1.11** and **1.12** against the cell lines HT29 and HepG2 displaying IC_{50} values of 9 and 26 μM respectively. An IC_{50} value of 8 μM was displayed by complex **1.11** in the MG63 cell line. Complexes **1.10** and **1.12** exhibited similar activities in the MDA-MB-231 cell line. The polypyridyl ligands used to prepare these complexes were tested for activity and found to exhibit no inhibitory effects. Overall, it was found that these trinuclear platinum complexes prepared from heterocyclic ligands showed better anticancer activity than cisplatin *in vitro*.

The diplatinum containing metallacycle **1.13** was able to decrease the cell viability of both estrogen receptor-positive (MCF-7) and estrogen receptor-negative (MDA-MB-231) breast cancer cell lines in a dose-dependent manner *in vitro*.[40] Complex **1.13** showed a significantly higher potency against both cell lines compared to cisplatin and when the antiproliferative effects of **1.13** on DNA synthesis was ascertained it was found that it was more than five times more active than cisplatin (16 μM for **1.13** vs 86 μM for cisplatin) in the MDA-MB-231 line and 4.5 times more active than cisplatin (21 μM for **1.13** vs 98 μM for cisplatin) in the MCF-7 line.

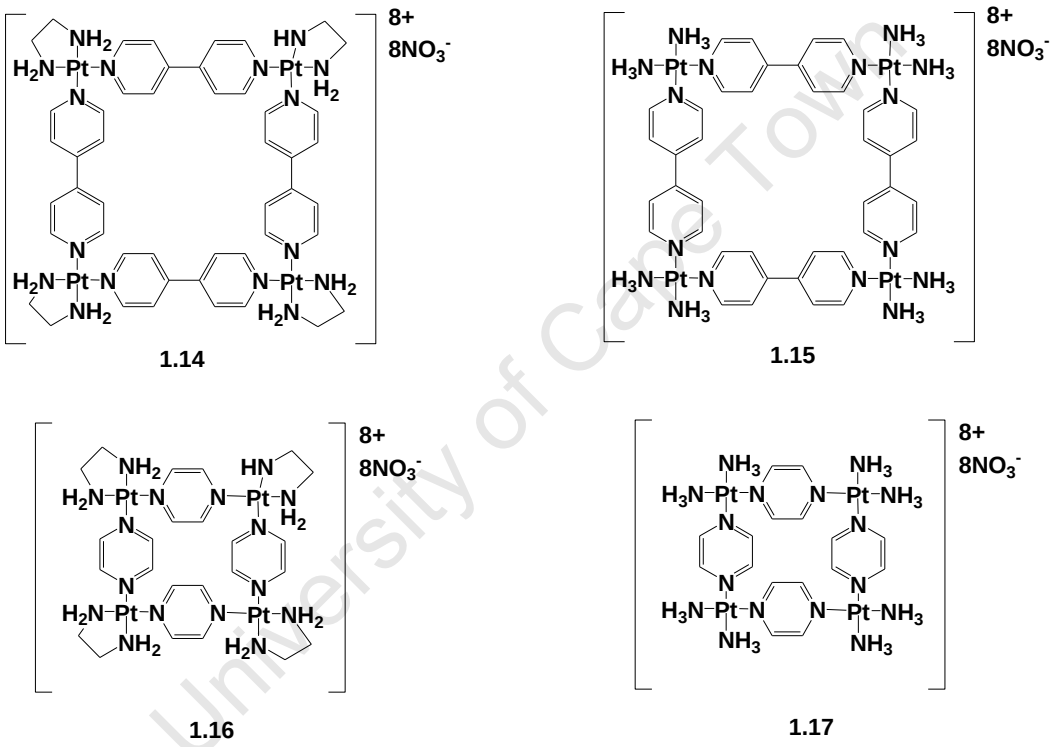

Figure 1.8. Metallasquares showing promising telomerase inhibition *in vitro*.[41]

Four tetranuclear Pt(II) metallasquares (**1.14 -1.17**, Figure 1.8) were found to selectively bind to *htelo* G-quadruplexes over promoter G-quadruplexes (*bcl2*) and duplex DNA in cell free assays.[41] *In vitro* assessments of the cyctotoxic effect of **1.14-1.17** on HeLa (human cervical cancer), HepG2 (Human hepatocellular liver carcinoma), MCF-7 (human breast adenocarcinoma), A549 (cisplatin-sensitive human lung adenocarcinoma) and A549/cis-R (cisplatin-resistant human lung adenocarcinoma) epithelial cell lines revealed these compounds to decrease cell viability in a dose-dependent manner.[41] The cytotoxic activities of all complexes were found be either higher or comparable to cisplatin. Complex **1.15**

displayed activities against all cell lines that were significantly higher than cisplatin. Against the cisplatin-sensitive A549 and cisplatin-resistant A549/*cis*R cell lines, complexes **1.14**-**1.17** displayed similar activity profiles suggesting that these tetranuclear complexes may be able to overcome cisplatin resistance and possibly have a mechanism of action that is distinct from cisplatin.[41]

1.2.1.2. Polynuclear Complexes containing other Platinum Group Metals as Cytotoxic Agents

The relevance of ruthenium complexes in biology was first realized by Francis Dwyer and co-workers in the 1950's.[42] They investigated simple ruthenium coordination complexes containing 2,2-bipyridine and 1,10-phenanthroline ligands and discovered that these complexes exhibited tumor growth inhibition in a mouse xeno graph model as well as showing bacteriostatic and bacteriocidal activities.[43-45] Their research was largely forgotten until Rosenberg and co-workers discovered the promising activity of cisplatin.[12,13]

As mentioned earlier, the systemic toxicity, intrinsic and acquired drug resistance found in patients as well as the rapid deactivation of cisplatin before reaching its target has bred a need for alternative drug therapies. Apart from designing platinum complexes with different ligand systems, ruthenium and the other platinum group metals soon gained attention as potential chemotherapeutics. Ruthenium is capable of accessing a range of oxidation states (Ru(II), Ru(III) and Ru(IV)) under physiological conditions and its compounds have also been shown to be less toxic than those of platinum.[24,46-49] This reduced toxicity is believed to be a consequence of ruthenium being able to mimic iron in the binding to biological molecules like albumin and transferrin.[24] Cancer cells rapidly divide and so exhibit a greater demand for iron causing transferrin receptors to be over-expressed thus leading to ruthenium based drugs to be more effectively delivered to cancer cells.[48,49]

Rh(III) and Ir(III) are also gaining attention as potential anti-tumor metals. An account of the anti-tumor properties of $RhCl_3 \cdot 3H_2O$ actually predates the discovery of cisplatin[50] but the cytotoxic abilities of Rh(III) and Ir(III) were not seriously considered until recently.[51,52] This lack of interest has been attributed to the kinetic inertness of these metal ions.[51-54] However, it has been proposed that this lack of reactivity can be overcome using one of two rational approaches, (i) the use of one or more ligands that provide a strong *trans* effect to improve the rate of substitution and (ii) complexation of these metals to ligands that display independent cytotoxic activities and can thus interact with specific biological targets.[52]

One of the earliest reports of a potential ruthenium complex with anticancer activity was proposed by Clarke and co-workers (**1.18**, Figure 1.9) and thought to achieve its cytotoxic function by binding to DNA.[55,56] The trinuclear complex ruthenium red (**1.19**) is also one of the earlier examples studied and believed to selectively bind to Ca(II)-transporting proteins thus arresting Ca(II) transport into cells.[55] One of the biggest hurdles to the biological studies of these complexes was their poor water solubility. This led to the next set of ruthenium complexes under investigation to be the highly water soluble Ru(II) chlorido-DMSO complexes such as **1.20**, first discovered by Sava et al.[57-59] This early work eventually led to the discovery of complex **1.21**, also known as NAMI-A, which acts as an anti-metastatic agent by either inhibiting metastasis formation[60] or reducing metastases size.[61] It has recently completed phase I clinical trials[62-65] and is currently undergoing phase II clinical evaluations.

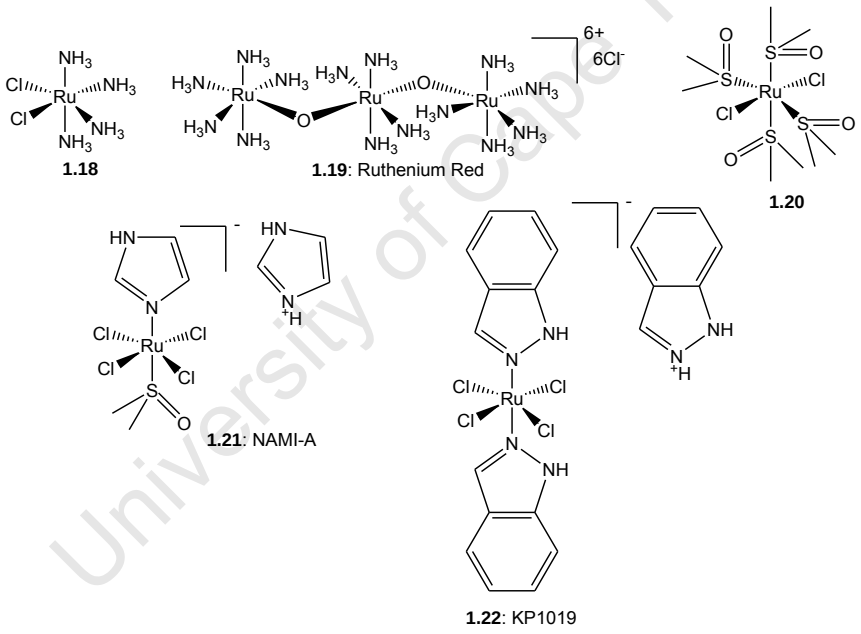

Figure 1.9. Structures of Complexes **1.18** – **1.22**.[55-59,62-64,66,67]

In parallel with the discovery of NAMI-A, Keppler and co-workers found the promising activity of KP-1019 (**1.22**). In contrast to NAMI-A, KP1019 is an antineoplastic agent that induces apoptosis via the intrinsic mitochondrial pathway. It exhibits high selectivity and low toxicity through accumulation in transferrin-receptor over-expressing tumor cells and reduction to a Ru(II) species in the tumor environment.[66] KP1019 has also completed phase I clinical trials[65-67] and it shows better cellular uptake compared to NAMI-A as well as significant activity in primary cisplatin-resistant colorectal tumors.[68-72]

The discovery of these two inorganic ruthenium complexes (**1.21** and **1.22**) has given rise to the investigation of organoruthenium complexes for cancer activities and most of the examples found in literature are largely made up of Ru(II) arene complexes which were first developed by two distinct research groups, Dyson and co-workers[24,73,74] and Sadler and co-workers.[17,71] The basis for the design and study of these arene-ruthenium(II) complexes was the suggestion that the previously studied Ru(III) complexes such as **1.21** and **1.22** were precursors from which the active Ru(II) species was generated *in vivo*. Thus, it makes sense for research to move toward the preparation of Ru(II) complexes.[17,71] The ruthenium-arene PTA complex **1.23** (Figure 1.10) and the extended arene-Ru(II) complex **1.24** were among the first complexes of these type to be studied. They both showed great potential as cancer chemotherapeutics but were eventually found to have low selectivity for cancer cells and were only active against certain cancer cell lines.[75-78]

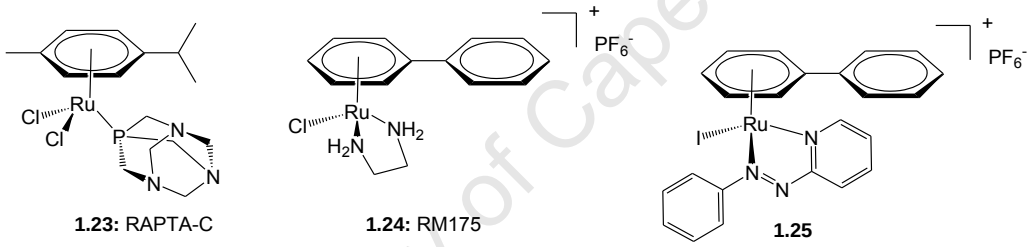

Figure 1.10. Ruthenium-arene complexes **1.23** – **1.25**.[17,24,79]

Nevertheless, subsequent studies of analogous complexes have shed light on the structure-activity relationships of these compounds. It has been found that by changing the nature of the metal, the arene ligand or by introducing a chelating ligand, the activity of piano-stool complexes could be fine-tuned.[80-85] For example, complex **1.25** which contains an iodo leaving group, the phenyl-pyridin-2-yl-diazene chelating group and an extended biphenyl arene system has been found to be highly water soluble. It has been proposed that this complex is able to enter the cytoplasm intact, where it proceeds to act as a catalyst of glutathione oxidation leading to increased oxidative stress and eventual apoptotic cell death.[79]

Further to these studies, the application of complexes containing multiple metal-arene moieties either as cluster compounds or supported on different mono- or polydentate ligands is now emerging as an area of great potential. Therrien and co-workers reported on the *in vitro* activity of tri- and tetranuclear ruthenium arene cluster compounds (**1.26** – **1.30**, Figure 1.11) against the cisplatin sensitive (A2780) and cisplatin resistant (A2780*cis*R) human

ovarian carcinoma cell lines.[86] While the tetranuclear complexes (**1.28 - 1.30**) did not exhibit any activity at the highest concentration tested (100 μM), the trinuclear complexes exhibited activities in the low micromolar range (Table 1.2.).[86] It was suggested that the marked difference in activities between the tri- and tetraruthenium complexes was a consequence of complexes **1.26** and **1.27** containing a hydrophobic pocket and a μ-oxo ligand and could thus form supramolecular interactions with hydrophobic arene units and hydroxyl groups present inside proteins.[86] The inhibitory activities of **1.26** and **1.27**were not as low as that of cisplatin in either cell line but it was noted that the compounds were much more active than the anti-metastatic mononuclear ruthenium complex, RAPTA-C (**1.23**).[86]

The influence of several structural features in the di- or trimetallic ruthenium and osmium complexes **1.31** – **1.38** (Figure 1.12) on *in vitro* antitumor activity was investigated by Mendoza-Ferri *et al*.[87] They wished to compare the effect of the type of metal centre, the leaving halide ligand, nature of arene group and the number of metal centers on activity. The complexes were screened for activity against two cancer cell lines and their water solubility was also evaluated (Table 1.3.).

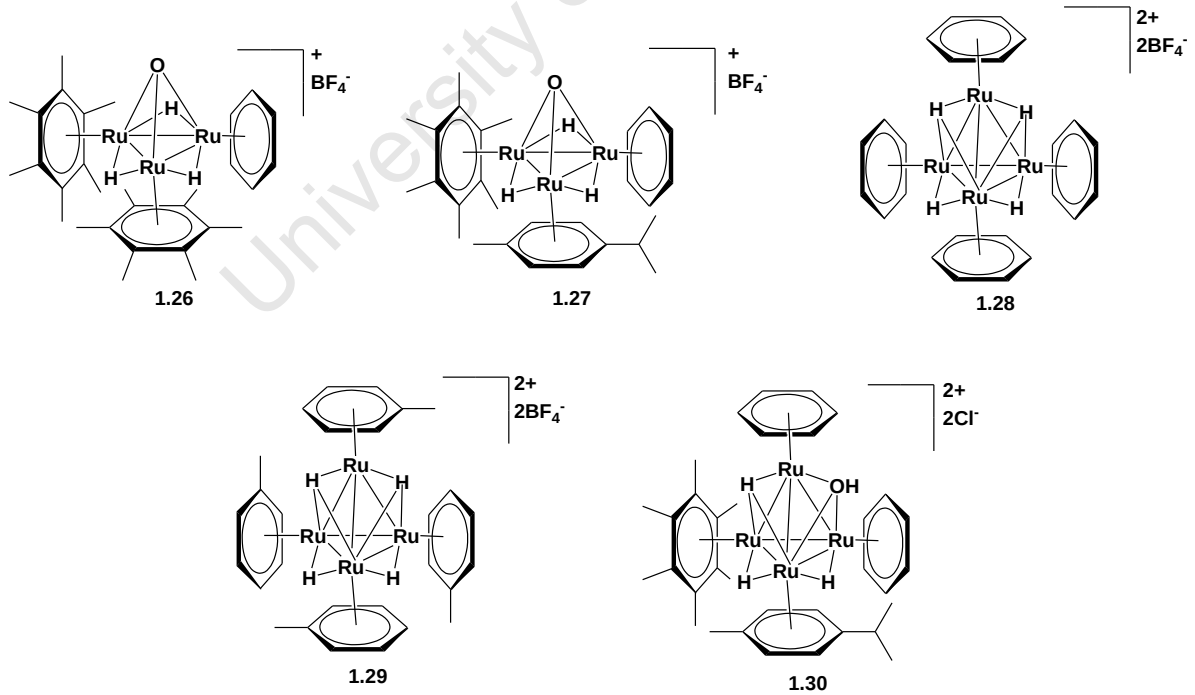

Figure 1.11. Structure of tri- and tetraruthenium arene clusters (**1.26** – **1.30**) screened against A2780 and A2780*cis*R ovarian carcinoma cell lines.[86]

Table 1.2. Inhibition of cell viability (IC_{50}) of complexes **1.26** – **1.30** on A2780 and A2780*cisR* ovarian carcinoma cell lines

Complex	IC_{50} (µM)	
	A2780	**A2780*cis*R**
1.26	9.8 ± 0.2	14.6 ± 0.7
1.27	9.1 ± 0.9	28.9 ± 2.8
1.28	>100	>100
1.29	>100	>100
1.30	>100	>100
RAPTA-C (1.23)	>100	>100
cisplatin	1.5 ± 0.3	8.7 ± 1.6

The water solubility was used as a measure for lipophilicity and it was found that for the dimetallic complexes **1.31** – **1.35** increasing the length of the spacer increases the lipophilic nature of the complex and a corresponding increase in activity is observed. Changing the metal centre also influenced activity, the osmium complexes **1.31** and **1.33** were 3 – 6 times less active than their ruthenium analogues **1.32** and **1.34** against the SW480 tumor cell line.

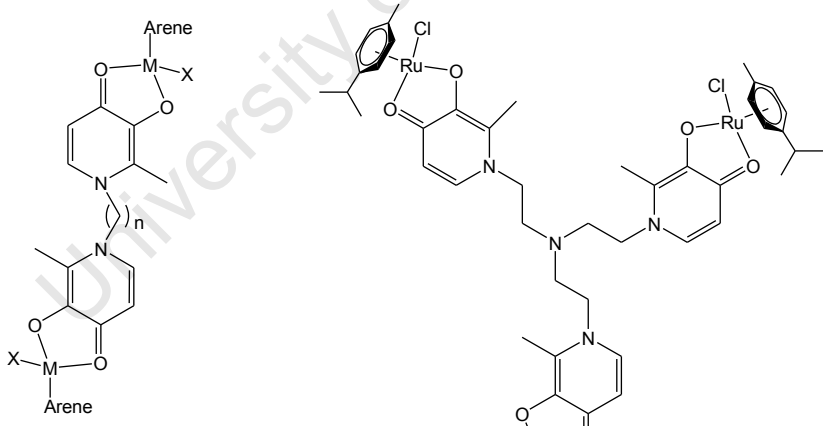

1.31: M = Os, n = 6, arene = p-cymene, X = Cl
1.32: M= Ru, n = 6, arene = p-cymene, X = Cl
1.33: M = Os, n = 8, arene = p-cymene, X = Cl
1.34: M = Ru, n = 8, arene = p-cymene, X = Cl
1.35: M = Ru, n = 6, arene = p-cymene, X = Br
1.36: M = Ru, n = 6, arene = p-cymene, X = I
1.37: M = Ru, n = 6, arene = biphenyl, X = Cl

Figure 1.12. Structure of di- and tri-organometallic complexes **1.31** – **1.38**.[87]

Table 1.3. Solubility and Cytotoxic Values for Complexes **1.31** – **1.38** against SW480 and A2780

		IC_{50} (μM)	
Compound	**Solubility (mM)**	**SW480**	**A2780**
1.31	1.6	88 ± 4	n/d[a]
1.32	3.9	26 ±8	30 + 6
1.33	0.2	15 ± 5	29 + 13
1.34	2.2	2.5 ± 0.2	5.7 + 0.5
1.35	0.6	54 ± 4	52 + 15
1.36	0.1	33 ± 4	36 + 2
1.37	0.6	25.7 ± 0.3	43 + 1
1.38	7.4	59 ± 18	80 + 7

[a]Not determined

The trinuclear complex **1.38** was more water soluble than the dinuclear complexes **1.31** – **1.36** but its activity against the A2780 tumor cell line was much lower than the other complexes. It also exhibited an IC_{50} value (59 μM) higher than most of the dimetallic complexes in the SW480 cell line. Only minor effects on the activity occur when the arene group is changed from *p*-cymene to biphenyl or when the leaving halide group is changed from chlorido to bromido or iodo.

Water soluble triosmium carbonyl clusters (**1.39** - **1.42**, Figure 1.13) containing a cyclometallated benzoheterocycle have been investigated as telomerase inhibitors. Telomerase is crucial in cancer progression as it is a ribonucleoprotein that sustains the length of DNA by adding hexameric units to the end of the 3' single strand terminus.[88,89] The complexes containing sulfonated phosphine ligands were found to be the best inhibitors of telomerase function when tested on enzymes in a cell free medium. However, they were found to have decreased activity when tested for telomerase inhibition in the MCF-7 breast cancer cell line.

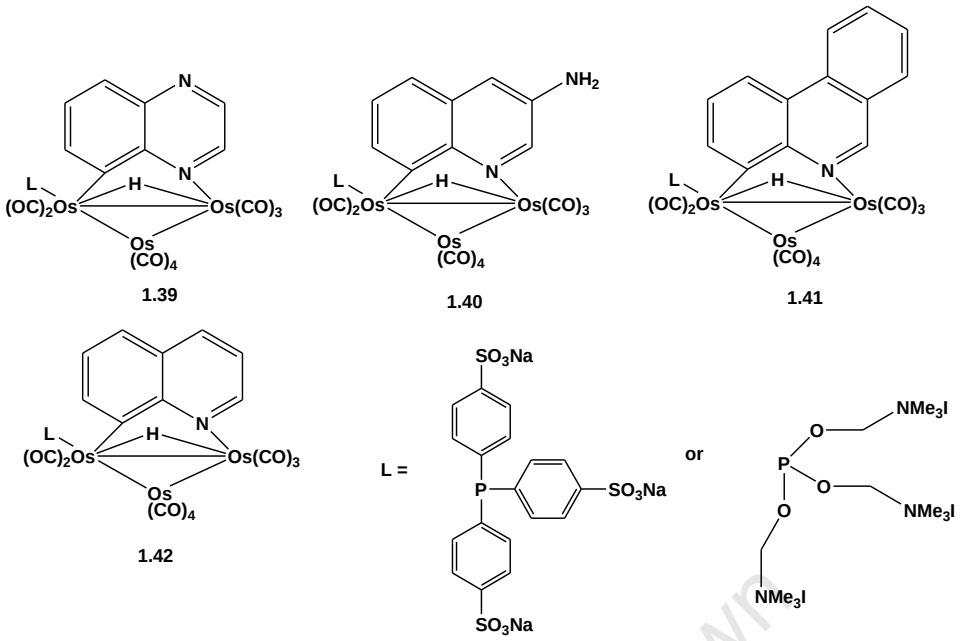

Figure 1.13. Organometallic triosmium complexes studied for telomerase inhibiton.[88]

Tetraruthenium molecular rectangles (**1.43**-**1.55**) have been investigated for their anti-proliferative activities.[90-92] Complexes **1.43** and **1.44** (Figure 1.14) were found to be robust coordination assemblies that did not undergo ligand exchange reactions with N-donor or S-donor biorelevant ligands.[92] Studies of the DNA binding abilities revealed these compounds to have non-covalent interactions with DNA which did induce significant conformational changes in DNA. *In vitro*, both complexes displayed IC_{50} values in the low micromolar range against the human ovarian carcinoma cell lines, cisplatin-sensitive A2780 [IC_{50} = 19 μM (**1.43**) and 15 μM (**1.44**)] and the cisplatin-resistant A2780*cis*R [IC_{50} = 4.6 μM (**1.43**) and 8.3 μM (**1.44**)].[92]

The metalla-rectangles **1.45**-**1.47** (Figure 1.15) were screened for activity against SK-hep-1 (liver cancer), HeLa (ovarian cancer), HCT-15 (colon cancer), A-549 (lung cancer) and MDA-MB-231 (breast cancer) cell lines.[91] Complexes **1.45** and **1.46** did not display any significant inhibitory effects while **1.47** showed activities that were higher than cisplatin against the SK-hep-1 and HCT-15 cell lines and were similar to cisplatin against the HeLa, A-549 and MDA-MB-231 cell lines.[91]

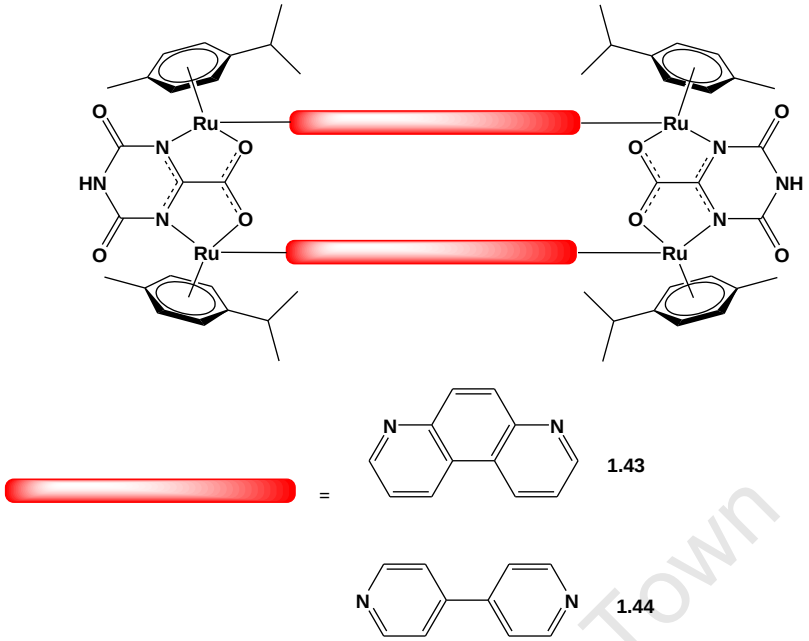

Figure 1.14. Structure of molecular rectangles **1.43** and **1.44**.[92]

Complexes **1.48**-**1.55** demonstrated large differences in activities compared to each other when screened for inhibitory effects in vitro against SK-hep-l and HCT-15. Complexes **1.50** and **1.53** displayed the highest cytotoxic activities against both cell lines; in the low micromolar range (6 -10 μM) while, **1.48** and **1.49** were not active. Complexes **1.51** and **1.55** were moderately active with IC_{50} values between 16-39 μM. Complexes **1.52** and **1.53** showed poor activity with IC_{50} values greater than 50 μM.[91]

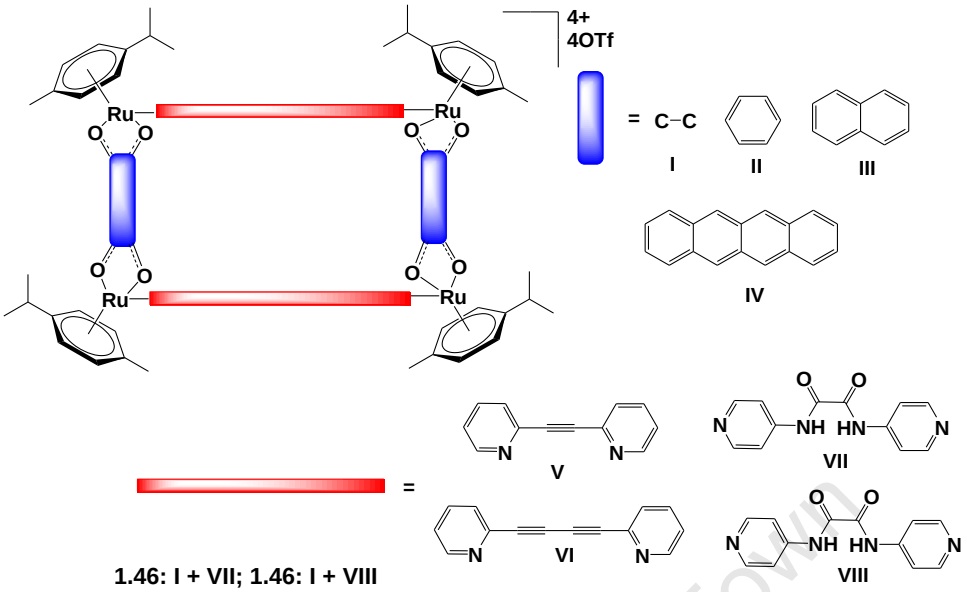

1.46: I + VII; 1.46: I + VIII
1.47: III + VII; 1.48: I + V
1.49: II + V; 1.50: III + V
1.51: IV + V; 1.52: I + VI
1.53: II + VI; 1.54: III + VI
1.55: IV + VI

Figure 1.15. Ruthenium containing metalla-rectangles **1.46**-**1.55**.[90,91]

1.2.2. Multinuclear PGM Complexes as Phototoxic Agents.

Apart from the use of metal complexes simply as cytotoxic agents, they are being studied for their potential as photochemotherapeutics for Photodynamic Therapy (PDT) and Photoactivated Therapy (PACT). The redox active nature of metals such as rhodium, iridium and ruthenium make them attractive for targeted therapies like PDT and PACT. In both types of therapies, the potentially photoactive drug should ideally show preferential uptake by tumor cells but this is often not the case thus, alternatively, they should show little or no effect on either healthy or tumor cells in the absence of light.[93]

Two mixed metal trinuclear complexes, containing Rh(III) and either Ru(II) or Os(II) metal ions (**1.56** and **1.57**, Figure 1.16) have been studied for their effect to inihibt cell growth in mammalian cells upon photoexcitation.[94] Previous studies of complexes **1.56** and **1.57** showed that they were able to cleave plasmid DNA upon exposure to light of > 460 nm for 20 min.[95] Thus, these complexes were tested on African green monkey (*Chlorocebus sabaceus*) kidney epithelial (Vero) cells.

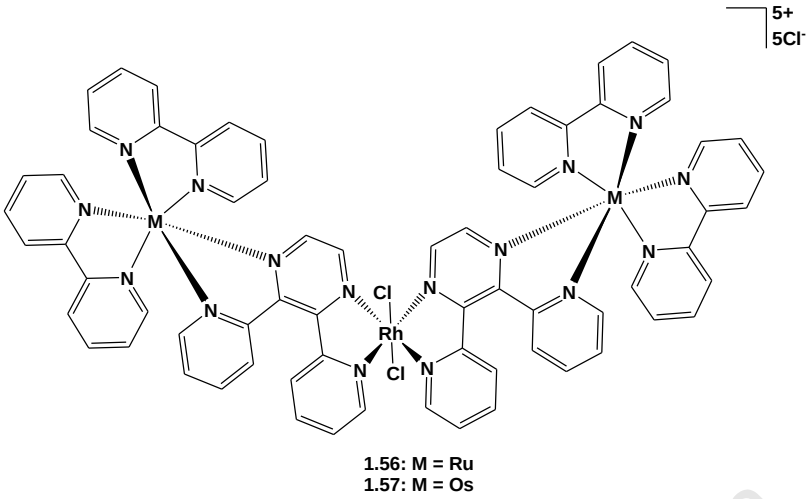

Figure 1.16. Structure of trimetallic complexes **1.56** and **1.57**.[95]

The cells were dosed with increasing concentrations of each complex starting at 3 μM. The treated cells were exposed to focused light of > 460 nm for 4 min before being incubated again for 48 hours. It was found that upon light exposure, complexes **1.56** and **1.57** were able to inhibit cell replication with the greatest cell death being observed for concentrations greater than 12 μM. Cells that were dosed with either **1.56** or **1.57** and not exposed to light showed normal growth confirming that these complexes only act upon photoexcitation. In the case of complex **1.56**, its believed that its phototoxic effect arises from the MLCT excitation of ruthenium(II) resulting in charge transfer from Ru(II) to Rh(III) via the bridging π-ligands. The Rh(II) metal center acts as an electron acceptor which consequently cleaves DNA.[96]

The phototoxic effect of three tetranuclear ruthenium functionalised porphyrin conjugates was studied in the MDA-MB-231 breast cancer cell line (**1.58** – **1.60**).[93] The cell cultures were exposed for 24 hours to concentrations of each conjugate ranging from 0.1 – 10 μM before being irradiated at 590-700 nm with a fluence rate of 25 mW/cm^2 and light doses from 1 to 10 J/cm^2.[93] A set of control cell cultures were also used, one containing only the cancer cells and culture medium was also irradiated and showed cell proliferation inhibition. The other control cell culture consisted of the cells dosed with the complexes and kept in the dark (dark cytotoxicity). Table 1.4 summarises the IC_{50} determinations for complexes **1.58** – **1.60**.

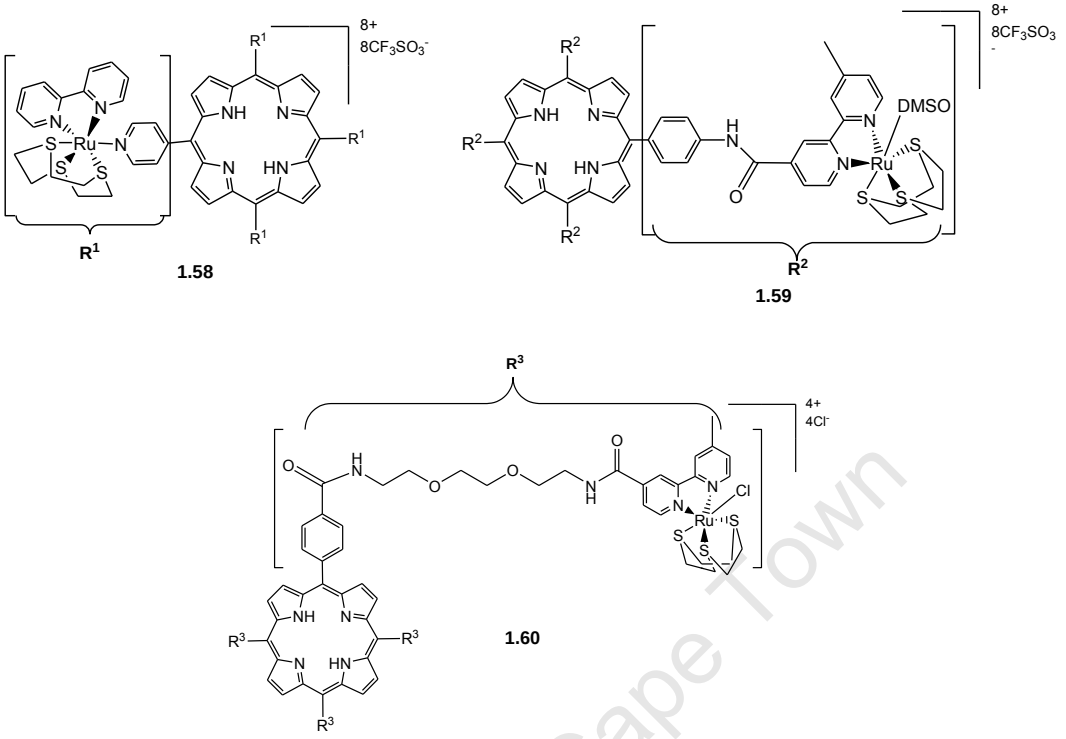

1.58 **1.59** **1.60**

Figure 1.17. Metalloporphyrin conjugates **1.58** – **1.60**.[93]

In the dark, all three complexes exhibit cytotoxic effect with **1.60** showing the best IC_{50} value of 2.09 µM. Upon irradiation, all three complexes exhibited an increase in its cell proliferation activity and the effect shows a positive increase with increasing light doses. At moderate light doses (5 J/cm^2), complex **1.58** is rendered 12 times (IC_{50} = 0.29 µM) more active compared to its dark cytotoxicity (IC_{50} = 3.34 µM). All three complexes were deemed good potential photosensitizers for PDT with complex **1.59** being the most potent inhibitor.

Table 1.4. IC_{50} values of Complexes **1.58 – 1.60** in MDA-MB-231 cell line

Complex	IC_{50} (µM)			
	Dark	**1 J/cm^2**	**5 J/cm^2**	**10 J/cm^2**
1.58	3.34 ± 1.87	1.73 ± 1.10	0.29 ± 0.02	0.13 ± 0.04
1.59	24.62 ± 6.38	10.64 ± 1.61	3.93 ± 1.24	1.71 ± 0.64
1.60	2.09 ± 0.78	0.56 ± 0.12	0.24 ± 0.10	0.10 ± 0.04

Schmitt and co-workers have screened a series of tetranuclear iridium, rhodium and ruthenium porphyrin complexes (Figure 1.18) for activity as dual photosensitizers and chemotherapeutics in human melanoma Me300 cells.[97,98]

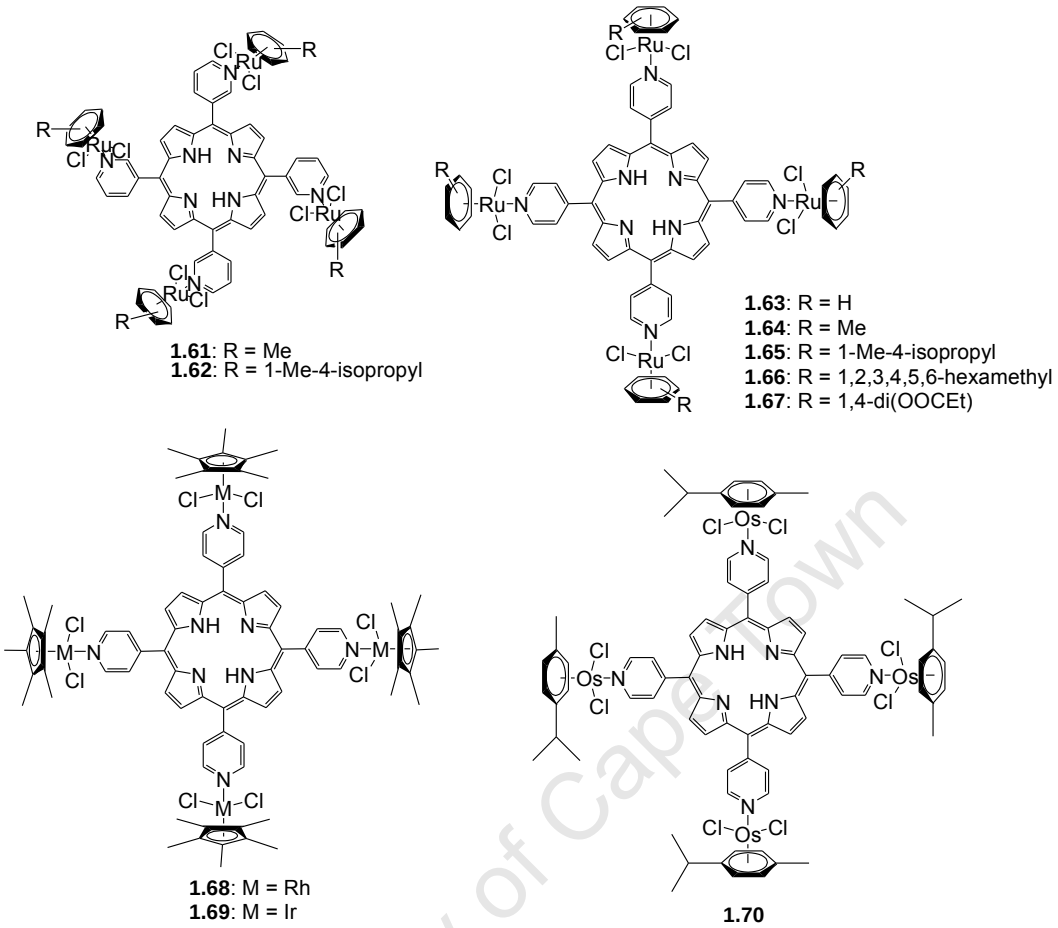

Figure 1.18. Tetranuclear porphyrin complexes (**1.61**-**1.70**) screened for activity as dual photosensitizers and chemotherapeutics.[97]

The dark cytotoxicities, absence of laser exposure, were determined for all complexes. After exposure for 24 hours, complexes **1.65**, **1.66** and **1.70** exhibited moderate cytoxicity (≈ 50 μM) against the melanoma cells while **1.63**, **1.64** and **1.67** exhibited cytotoxicities greater than 100 μM. The rhodium complex (**1.68**) showed no activity.[97] The complexes **1.64** and **1.65** were rescreened against the cell line along with complexes **1.61** and **1.62**, this time the melanoma cells were exposed to the compounds for 72 hours. The cytotoxic values were much lower than observed for the previous screening; **1.64**, **1.65** and **1.62** exhibited values of approximately 20 μM and complex **1.61** showed activity of *ca.* 10 μM.[98]

Fluorescence studies of these complexes in the melanoma cells showed that complex **1.68** was not taken up by the cells and would explain why the complex did not exhibit activity. The ruthenium complexes were found to accumulate in the cytoplasm and organelles. The photoxicity studies using red laser light irradiating at 652 nm revealed that, at a complex

concentration of 10 µM, the ruthenium complexes **1.64** – **1.67** leads to 60-80 % phototoxicity for just 5 J/cm^2 light exposition. The same level of phototoxicity was only reached for complex **1.70** with 30 J/cm^2 exposition. As expected, complex **1.68** did not exhibit phototoxicity.

The phototoxicity of two octanuclear porphyrin-ruthenium metalla-cubes (Figure 1.19, **1.71** and **1.72**) in the cervix (HeLa) and pulmonary (A549) cancer cell lines.[99] In the dark, these complexes exhibited cytotoxicities greater than 70 µM. When cell cultures treated with 1 µM of each complex were exposed to irradiation at 652 nm with a fluence of 20 mW/cm^2 and light doses from 2-20 J/cm^2, they were found to exhibit good phototoxicity. The complexes show LD_{50} (light dose that induces death of 50 % of cells) values between 2 and 7 J/cm^2.[99]

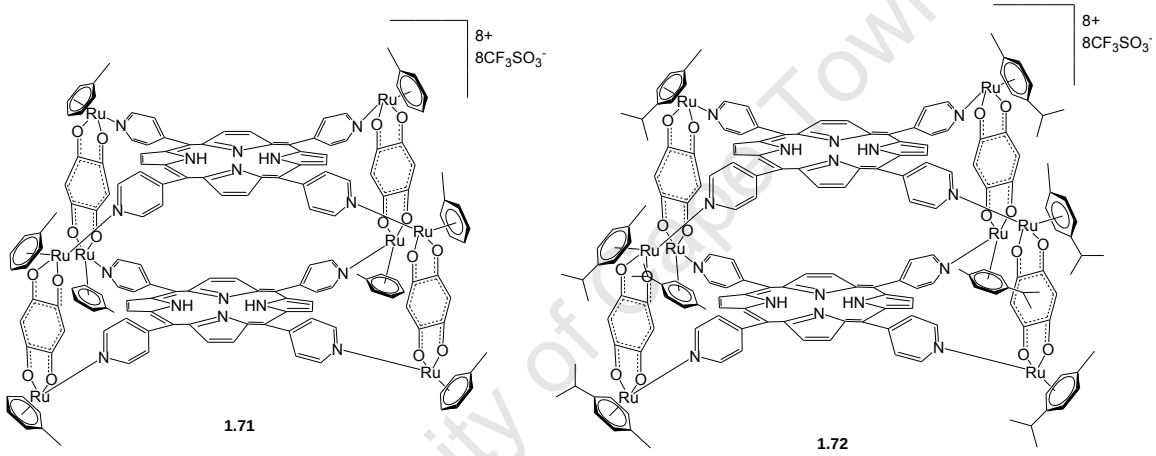

Figure 1.19. Octanuclear metalla-cubes **1.71** and **1.72**.[99]

1.3. Application of Platinum Group Metal Complexes Against Malaria

Parasitic diseases have proven to be a major health problem particularly in developing countries. Presently, there are only a few effective drugs available for their treatment. The frequent manifestation of resistance to these current therapies have posed a serious impediment to their use making the discovery of new drugs leads an urgent and challenging task.[100] In the past, big pharmaceutical companies were reluctant to invest in the research and development of parasitic disease chemotherapies as these illnesses mostly plague poorer, less developed countries where only low financial returns could be realized.[100,101] However, in the last ten years, intervention by several international non-profit organizations has breathed new life into this much needed area of research.[100]

The application of metal containing compounds for the treatment of parasitic diseases is a crucial area of research as they can show distinct selectivity toward parasite biomolecules over host biomolecules. Several strategies govern the study of metallo-antiparasitics; incorporation of a metal into established antiparasitics could enhance its pharmacological action or favourably alter its pharmacokinetic parameters.[100] Additionally, new metallo-antiparasitic agents could be developed which are able to deliver potent metal containing fragments capable of selectively interacting with parasite targets.[100]

Malaria is amongst the deadliest and most widespread parasitic diseases found today. A recent World Health Organisation (WHO) report estimated that 216 million cases of malaria infection were reported in 2010 with 655 000 resulting deaths mainly among African children.[102] In fact, most of these malarial infections and deaths occurred in sub-Saharan Africa.

There are four parasite species which cause malaria in humans:

- *Plasmodium falciparum*
- *Plasmodium vivax*
- *Plasmodium malariae*
- *Plasmodium ovale*

All four species are transmitted to humans through the bite of an infected female *Anopheles* mosquito and *P. falciparum* is responsible for the greatest number of malarial deaths.[102] The life cycle of the malaria parasite consists of two categories, the sexual stages in the insect vector and the asexual stages in the human host (Figure 1.20).[101,103]

The bite of the female Anopheles mosquito injects parasite sporozoites into the human's bloodstream. They rapidly invade liver cells (hepatocytes) where they evolve into the asexual form of the parasite known as schizonts containing a vast number of small round merosoites.[101] These schizonts undergo asexual replication known as exoerythrocytic schizogony into erythrocytes and this ultimately results in the liver cells swelling and bursting thereby releasing merozoites into the bloodstream where they infect red blood cells in the host. Within the infected red blood cells they begin the trophozoite stage wherein they experience a period of active metabolism for the synthesis of proteins. This metabolism includes the proteolysis of hemoglobin into amino acids and the ingestion of cytoplasm.[101]

Within the red blood cells, some of the merozoites develop into micro-gametocytes, the sexual form of the parasite, and circulate in the blood stream until a female Anopheles mosquito bites the person and ingests the infected blood. The micro-gametocytes quickly grow into macro-gametocytes producing oocysts which eventually rupture and release infectious sporozoites that migrate to the mosquito's salivary glands where they can then infect the next human host.[101]

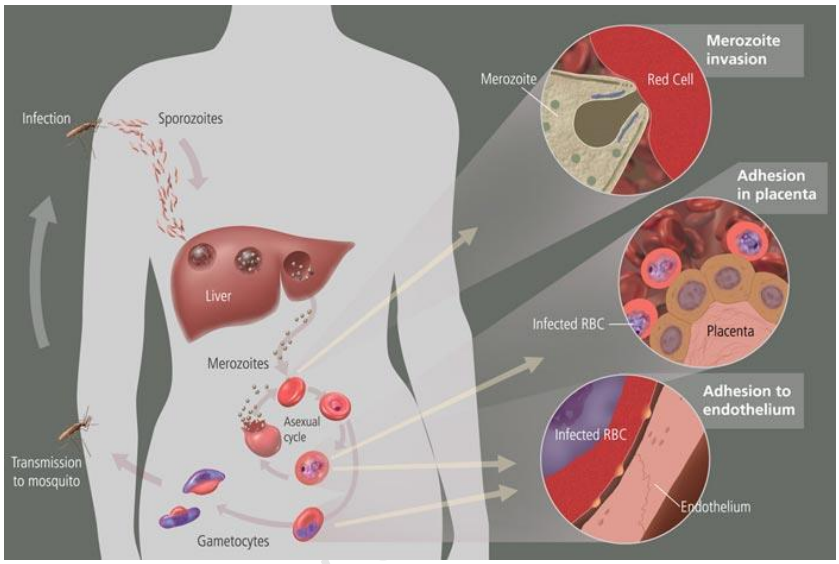

Figure 1.20. Schematic representation of the life cycle malaria parasite.[104,105]

P. falciparum infections were largely treated with chemotherapies using chloroquine (**1.73**, Figure 1.21) but employment of chloroquine for malaria treatment has been greatly reduced due to the emergence of resistance in most parts of the world. These days, it is only effective to treat *P. falciparum* in Egypt and a few countries in the Middle East and Central America.[106] Currently, the standard first line therapy for uncomplicated *P. falciparum* malaria infections is artemisinin-based combined therapy (ACT).[106,107] Artemisinin has demonstrated great effectiveness for the treatment of *P. falciparum* infections. It is fast acting and able to eliminate malaria parasites at a rapid rate.[108] ACT is a combination of artemisinin or an artemisinin derivative and a second drug with a separate parasite target in order to enhance efficiency and decrease the risk of resistance development. The five ACT treatments recommended by the WHO are Artemether/lumefantrine, artesunate/amodiaquine,

artesunate/mefloquine, artesunate/sulfadoxine pyrimethamine and dihydroartemisinin/piperaquine (Figure 1.21).[108]

Chloroquine and other related aminoquinolines have been shown to selectively build up within the parasite and are believed to target the formation of hemozoin. The digestion of the infected host's hemoglobin to provide essential amino acids for its growth and nutrition for the parasite is a vital step.[109] A side product of this hemoglobin digestion is free heme which is toxic to the parasite. The parasite removes this threat by conversion of the free heme into a crystalline solid known as hemazoin which is nontoxic to the parasite. Aminoquionlines can efficiently obstruct the formation of hemazoin through π-π stacking of the hydrophobic quinoline residues with heme thus causing a build-up of toxic heme and eventual death of the parasite.[110,111]

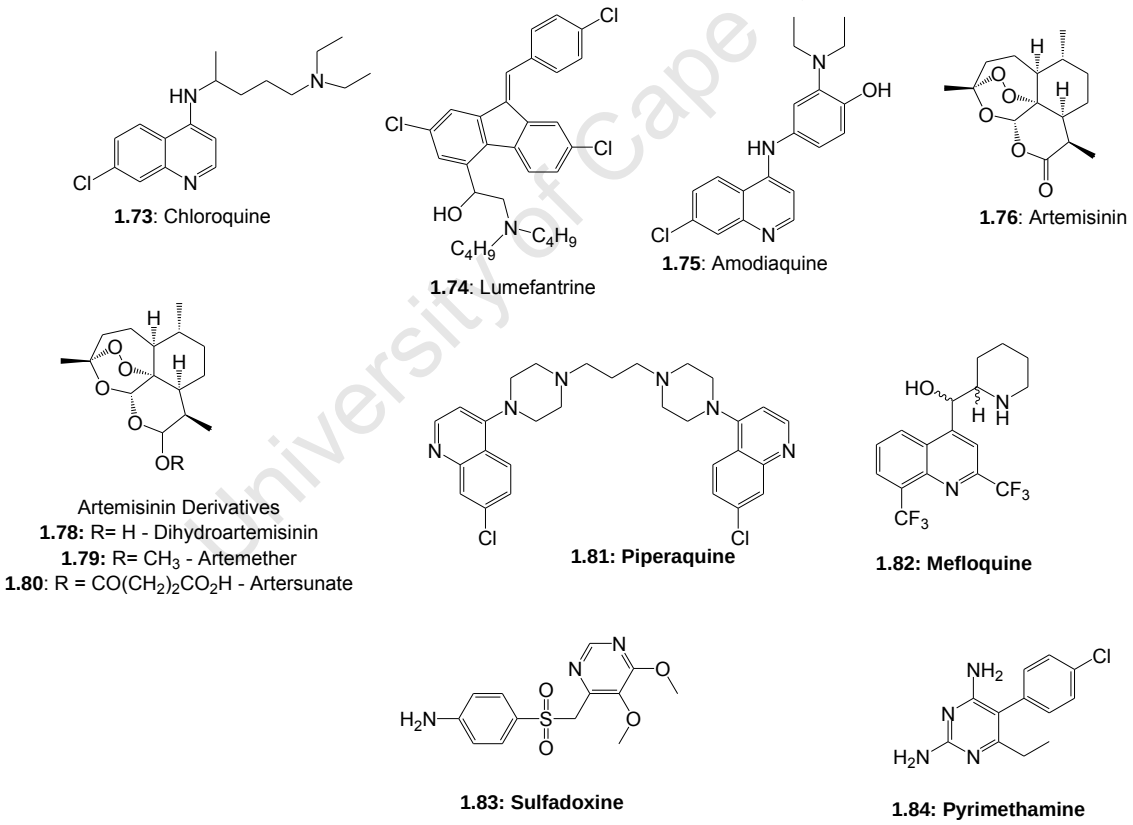

Figure 1.21. Structure of chloroquine (**1.73**) and the drugs currently recommended for ACT treatment (**1.74**-**1.84**).[106]

In the case of artemisinin and its derivatives, the actual mode of inhibition has yet to be clearly defined but it is accepted that these drugs selectively target parasites because of their enhanced uptake by parasitized erythrocytes.[112] Despite the effectiveness of ACT treatments, the emergence of resistance to these drugs is a very real possibility and is under intense monitoring.[107] Resistance of *P. falciparum* to artemisinins was observed at the Cambodia-Thailand border.[113] Suspected resistance has also been reported in Cambodia, Vietnam, Myanmar and Thailand.[114] The artesunate/mefloquine and dihydroartemisinin/piperaquine combination therapies have both presented resistance.[115-117] Measures are being taken to limit the spread of artemisinin-resistant strains,[114] however it is still of great import to find alternative drug candidates as most of the currently developed drugs are mainly artemisinin derivatives and may eventually become susceptible to parasite resistance as well.

One of the earliest attempts to produce metal complexes with antimalarial activity was published in 1987.[118] An extensive series of complexes were prepared using amodiaquine (**1.75**) and primaquine and a variety of metals including Cr(III), Fe(III), Pd(II) and Rh(III). However the results were disappointing, most of the complexes showed no enhancement in activity compared to the uncomplexed drugs. Study of metal conjugates of chloroquine has shown much more promise.

Sánchez-Delgado et al reported that a [Ru(II)-chloroquine]$_2$ dimer and mononuclear Rh(I) complex (Figure 1.22) proved active against *P. falciparum* strains *in vitro*.[119] The dinuclear ruthenium complex (**1.85**) is 4.5 times more active than chloroquine diphosphate against two chloroquine resistant *P. falciparum* strains, FcB1 and FcB2. The rhodium complex (**1.86**) exhibited activities similar to chloroquine diphosphate. *In vivo* studies of the complexes in the rodent malaria parasite *P. berghei* showed that at the same concentration of chloroquine diphosphate required to kill 50 % of parasitemia, **1.85** reduced parasitemia by 94 % and **1.86** by 74 %.

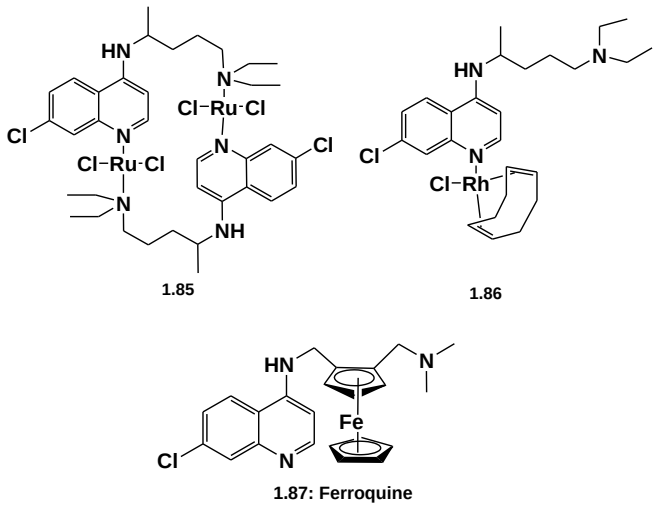

Figure 1.22. Structure of ruthenium (**1.85**) and rhodium (**1.86**) chloroquine metalloconjugates and ferroquine (**1.87**).[101,119,120]

Consequent to the initial chloroquine metal conjugate work pioneered by Sánchez-Delgado *et al*, came the discovery of the chloroquine analogue, Ferroquine (**1.87**).[121] The metallocene containing complex has shown impressive antiplasmodial activity and is even active in chloroquine resistant strains.[120-123] It has completed Phase I clinical trials and is expected to complete Phase II clinical trials against uncomplicated malaria soon. Ruthenium-arene chloroquine conjugates (**1.88**-**1.91**) have been extensively studied for their antiplasmodial activities.[124]

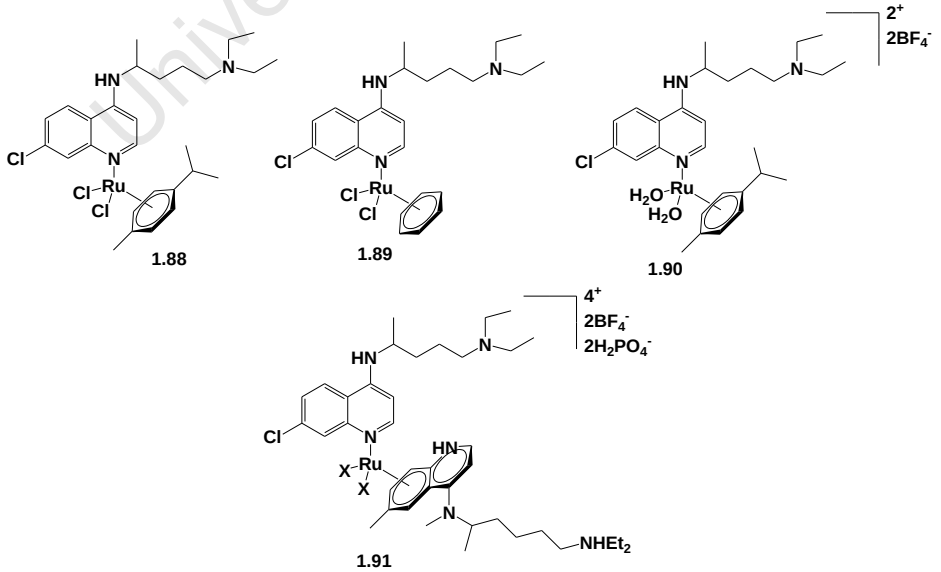

Figure 1.23. Ruthenium arene chloroquine conjugates **1.88** – **1.91**.[124]

They were evaluated for *in vitro* activity against three chloroquine resistant (W2, Dd2 and K1) and four chloroquine sensitive (FcB1, 3D7, PFB and F32) *P. falciparum* strains. Complexes **1.88** – **1.91** were found to be moderate inhibitors of the chloroquine sensitive *P. falciparum* strains with activities lower than chloroquine diphosphate. Against the chloroquine-resistant strains these complexes displayed consistently better activities compared to chloroquine diphosphate. The most potent inhibitor was found to be complex **1.90** which was 5 times more potent than CQDP against the Dd2 and K1 strains. The results obtained in this study clearly illustrate the concept of enhanced activity of metal-chloroquine conjugates against resistant malarial strains.

Iridium-chloroquine analogues (**1.92** – **1.94**) have also been studied for *in vitro* antiplasmodial activity on cultures of *P. Berghei* (Figure 1.24).[125] These complexes were able to inhibit parasite growth at nanomolar concentrations. They displayed IC_{50} values of 72 nM (**1.92**), 59 nM (**1.93**) and 126 nM (**1.94**). The dinuclear derivative (**1.93**) was more active than the two mononuclear complexes and the cationic complex was the least active.

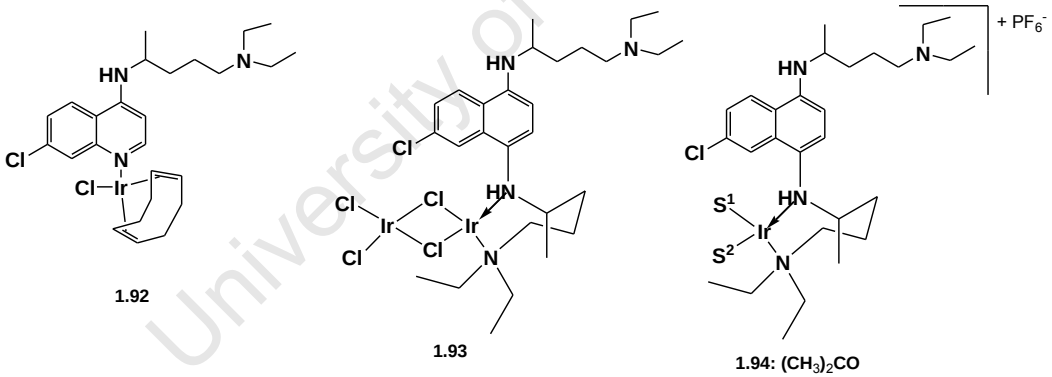

Figure 1.24. Iridium-CQ conjugates displaying nanomolar activity against *P. berghei*.[125]

Arene ruthenium complexes containing bis-chelating chloroquine analogues (**1.95**-**1.97**, Figure 1.25) have also shown promising activities against a chloroquine sensitive (D10) and a chloroquine resistant (Dd2) *P. falciparum* strain.[126] Against the D10 parasitic strain, all three complexes displayed activities in the low micromolar range. Complex **1.97** exhibited the best IC_{50} value (0.07 μM) which was only slightly higher than chloroquine (IC_{50} = 0.025 μM). The complexes were much less active compared to chloroquine against the Dd2 strain.

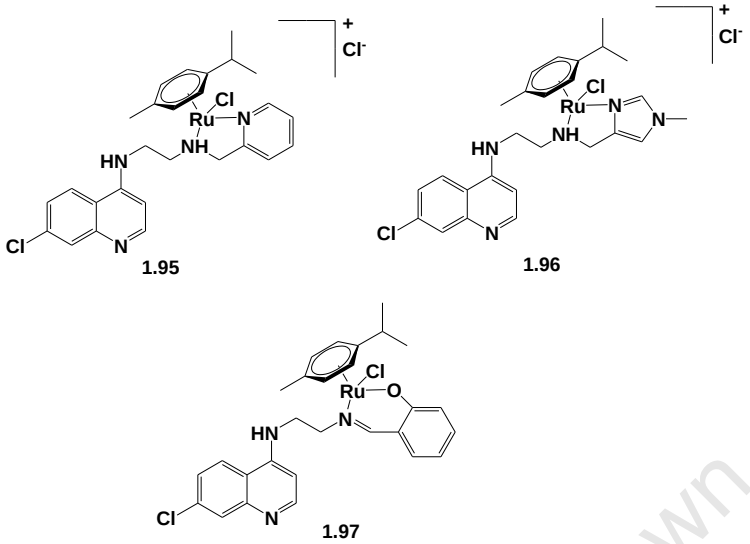

Figure 1.25. Structures of ruthenium arene complexes containing bis-chelating chloroquine analogues (**1.92** – **1.94**).[126]

There are fewer examples of antiplasmodial PGM metal complexes that are non-quinolone based. A series of cationic platinum complexes containing substituted bipyridyl and phenanthroline ligands were tested for antiplasmodial activity against the D10 (chloroquine sensitive) and K1 (chloroquine resistant) strains.[127] They inhibited parasite growth at concentrations in the nanomolar range. Several examples of mononuclear ruthenium and palladium thiosemicarbazone complexes (Figure 1.26) were reported to show antiplasmodial activity in the micromolar range against NF54 (chloroquine sensitive),[128] Dd2 (chloroquine resistant),[128] W2 (chloroquine resistant)[129] and D10 (chloroquine sensitive)[129] *P. falciparum* strains.

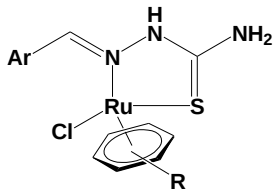

1.98: Ar = phenyl, 5-chlorophenyl, naphthyl or ferrocenyl
R = H or 1-ipropyl-3-methyl

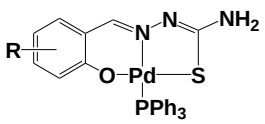

1.99: R = H, 3-OMe, 3-^{t}Bu or 5-Cl

Figure 1.26. Ruthenium and Palladium thiosemicarbazone complexes that have been studied for antiplasmodial activity.[128-131]

While there are several reports on the use of mononuclear PGM complexes as antiparasitics agents, there are few examples of multinuclear derivatives. The encouraging data published for mononuclear derivatives emphasize the potential of multinuclear analogues as antiparasitics agents.

Mono and multinuclear cyclopalladated complexes containing tridentate thiosemicarbazone ligands (**1.00** – **1.109**, Figure 1.26) showed promising activities against two P. falciparum strains, the 3D7 (chloroquine sensitive) and K1 (chloroquine resistant) strains.[130] Two tetranuclear (**1.100** and **1.101**), two mononuclear (**1.102** and **1.103**) and six dinuclear (**1.102-1.109**) complexes were screened in this study. Complexes **1.106** – **1.107** did not show any appreciable inhibitory effect on either strain; this was attributed to their poor solubility in DMSO and water. The rest of the complexes displayed activities in the mid to low micromolar range with best activities observed against the 3D7 strain. Complexes **1.102** – **1.104** showed the best antiplasmodial activities (IC_{50} = 2.43, 3.03 and 2.94 µM respectively). While they were not as potent as chloroquine in either strain, complexes **1.101** – **1.109** were more vastly more active than their free ligands emphasizing that chelation to a metal can beneficially alter the bioactivities of certain organic molecules.

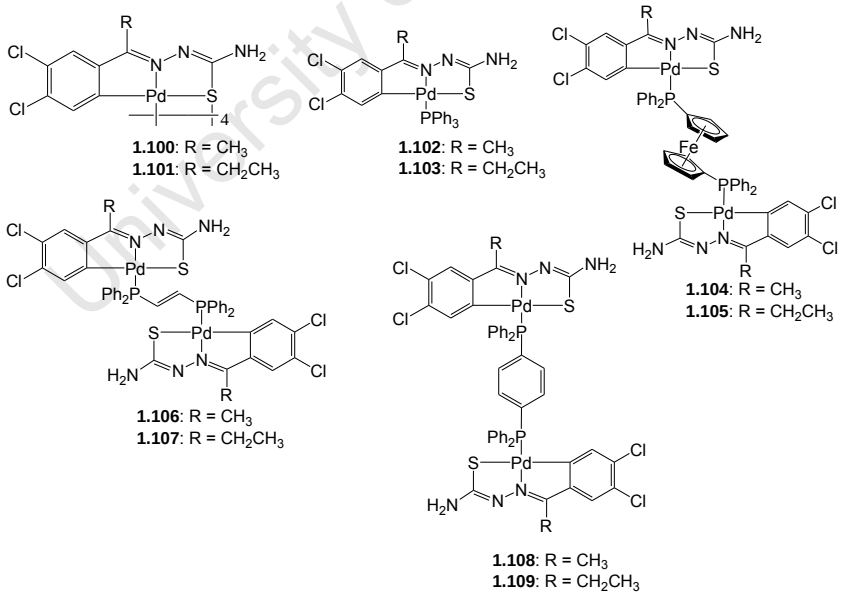

Figure 1.27. Cyclopalladated thiosemicarbazone complexes **1.96** – **1.105**.[130]

1.4. Conclusions

Cancer and parasitic diseases such as malaria pose a serious threat, with the number of diagnosed cases increasing exponentially every year. Intrinsic and acquired drug resistance and systemic toxicity to currently used chemotherapies has led to an urgent need for new drug leads. Multinuclear PGM complexes have emerged as valid candidates to circumvent the problems currently faced by purely organic molecules. In cancer, not only can these types of complexes be employed as cytotoxic agents, they can also be used as photoactivated chemotherapeutics for localized tumor inhibition.

Whilst there are scant reports on the use multinuclear PGM complexes as antiparasitals, the promising results obtained for mononuclear complexes serves as motivation for the investigation of their multimeric derivatives.

1.5. Aims and Objectives

1.5.1. Aim

The overall aim of this research project was to synthesize new platinum group mono- or multinuclear organometallic complexes and evaluate their activity as (i) biological agents against malaria and cancer or (ii) as catalyst precursors for cross coupling reactions.

1.5.2. Specific Objectives

1.5.2.1. Synthesis

The synthetic objectives of this project were to prepare new mono- and polynuclear complexes containing platinum, palladium, ruthenium, rhodium or iridium and fully characterize these compounds using several analytical and spectrometric techniques. The type of complex prepared is divided into three sub-categories. These sub-categories are based on the synthesis of three different types of ligand systems, each of which was used to prepare new complexes with different platinum group metals.

i. The preparation of **mono- and polynuclear cycloplatinated thiosemicarbazone complexes** where the ligand acts a tridentate donor to the metal (**I**) using 3,4-dichloroacetophenone thiosemicarbazone.

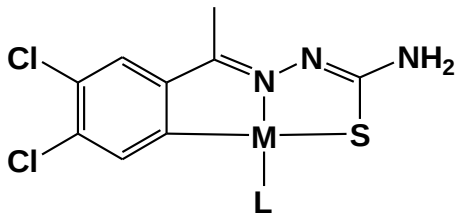

I

Figure 1.28. General structure of cycloplatinated thiosemicarbazone complexes prepared.

ii. The synthesis of di- and trinuclear **ruthenium(II), rhodium(III) and iridium(III) pyridyl ether complexes** with the general structure **II** and **III** containing benzyl alcohol or a central heteroaromatic core.

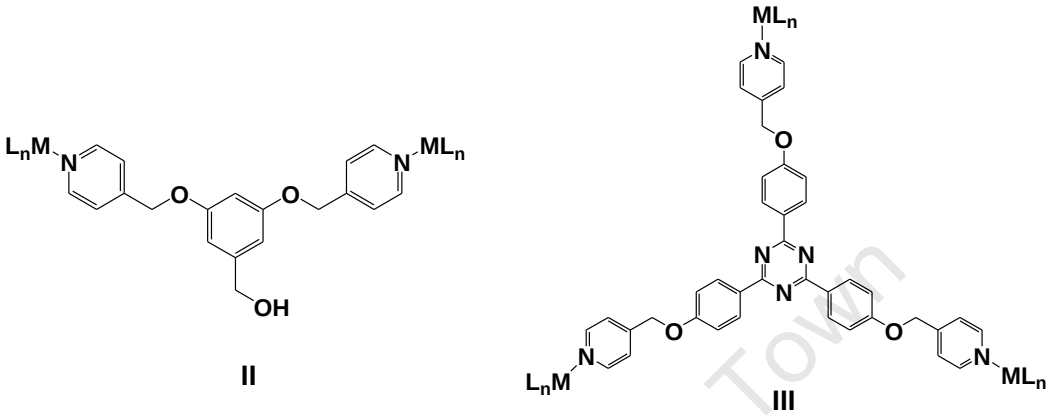

Figure 1.29. General structures of di- and trinuclear complexes containing pyridyl ether scaffolds

iii. The preparation of di- and trinuclear **ruthenium(II), rhodium(III) and iridium(III) pyridyl ester complexes** with general structures **IV** and **V** from ligands containing the central spacers, 1,4-benzene-dimethanol or 1,3,5-tricarboxylic acid.

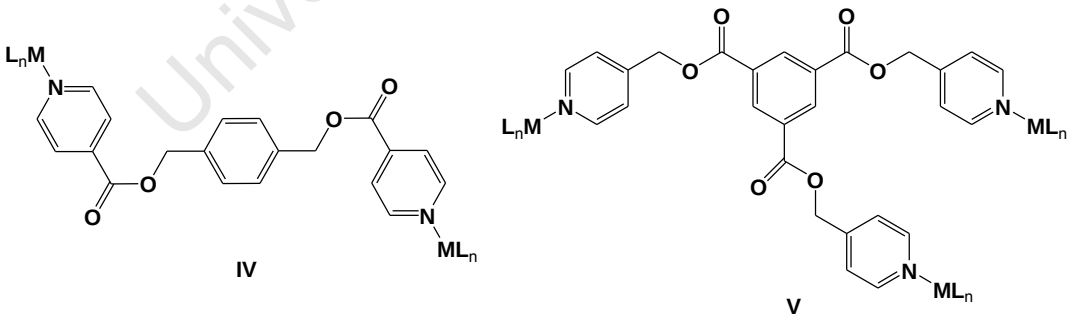

Figure 1.30. General structures of di- and trinuclear complexes containing pyridyl ester scaffolds

1.5.2.2. Pharmacological Studies

A selection of the PGM complexes synthesized were evaluated *in vitro* for activity as antiparasitic and antiproliferative agents. Previous studies have revealed that the mono- and

polynuclear cyclopalladated complexes of the thiosemicarbazone, 3,4-dichloroacetophenone thiosemicarbazone were able to moderately inhibit *P. falciparum* parasite growth *in vitro*.[130] The purpose for preparation of cycloplatinated derivatives is to assess whether replacing palladium with the biologically active metal, platinum, will lead to an increase in antiparasitic activity.

The biological activity of mono- and polynuclear 4-pyridyl ruthenium arene complexes has been established.[132] The rationale behind synthesizing pyridyl ether and ester ligands is to potentially increase the lipophilic nature of the scaffolds to which the metal-moieties will be conjugated thus increasing pharmacological activity and to determine if the number of metal moieties (2 vs 3 moieties) has an effect on pharmacological activity. Further to this, the effect of changing the metal moieties from [dichloro(*p*-cymene)ruthenium] to [dichloro(pentamethylcyclopentadienyl)rhodium] or [dichloro(pentamethylcyclopenta-dienyl)iridium] moieties on antiparasitic and anticancer activities will be evaluated.

1.5.2.3. Preliminary Screening of Cyclopalladated Thiosemicarbazone Complexes as Catalyst Precursors

Four **cyclopalladated thiosemicarbazone complexes** that are analogous to the cycloplatinated complexes have been prepared (**I**, Figure 1.28). These complexes were evaluated for their ability to catalyze the Suzuki-Miyaura cross coupling reaction of a variety of aryl halides and aryl boronic acids. This is a preliminary investigation to determine if there is potential in these types of tridentate Pd(II) complexes as catalyst precursors for cross coupling reactions.

1.6. References

(1) L. Ronconi and P. J. Sadler, *Coord. Chem. Rev.* **2007**, *251*, 1633.

(2) J. Reedijk, *Macromol. Symp.* **2008**, *270*, 193.

(3) P. C. A. Bruijnincx and P. J. Sadler, *Curr. Opin. Chem. Biol.* **2008**, *12*, 197.

(4) G. Jaouen, W. Beck and M.J. McGlinchey, A Novel Field of Research: Bioorganometallic Chemistry, Origins, and Founding Principles In *Bioogranometallics: Biomolecules, Labeling, Medicine*; Jaouen, G., Ed.; Wiley-VCH Verlag GmbH & Co.: KGaA, Weinheim,2006 Vol., Chapter 1.

(5) *Cisplatin. Chemistry and Biochemistry of a Leading Anticancer Drug*; VCHA & Wiley-VCH: Zurich, 1999.

(6) Z. Guo and P. J. Sadler, *Angew. Chem. Int. Ed.* **1999**, *38*, 1512.

(7) A. Garoufis, S.K. Hadjikakou and N. Hadjiliadis, *Coord. Chem. Rev.* **2009**, *253*, 1384.

(8) A. Garoufis, S.K. Hadjikakou and N. Hadjiliadis; *Metallotherapeutic Drugs and Metal-based Diagnostic Agents: The Use of Metals in Medicine*; John Wiley & Sons Ltd, 2005.

(9) www.who.int/mediacentre/factsheets/fs297/en/, Date accessed: 30/04/2012

(10) http://www.cancer.gov/cancertopics/cancerlibrary/what-is-cancer, Date accessed: 30/04/2012

(11) M. R. Chorawala, P. M. Oza and G. B. Shah, *Int. J. Pharm. Sci. Drug Discov.* **2012**, *4* (4), 1.

(12) B. Rosenberg, L. Van Camp and T. Krigas, *Nature* **1965**, *205*, 698.

(13) A. Levina, A. Mitra and P.A. Lay, *Metallomics* **2009**, *1*, 458.

(14) J. Reedijk, *Platinum Met. Rev.* **2008**, *52*, 2.

(15) R. A. Alderden, M .D. Hall and T. W. Hambley, *J. Chem. Educ.* **2006**, *83*, 728.

(16) J. Reedijk, *Eur. J. Inorg. Chem.* **2009**, 1303.

(17) A. F. A. Peacock and P. J. Sadler, *Chem.-Asian J.* **2008**, *3*, 1890.

(18) K. Barabas, R. Milner, D. Lurie and C. Adin, *Vet. Comp. Oncol.* **2008**, *6*, 1.

(19) P. Borst, S. Rottenberg and J. Jonkers, *Cell Cycle* **2008**, *7*, 1353.

(20) S. P. Fricker, *Dalton Trans.* **2007**, 4903.

(21) M. J. Cleare, P. C. Hydes, B. W. Malerbi and D. M. Watkins, *Biochimie* **1978**, *60*, 835.

(22) I. E. Smith and B. D. Evans, *Cancer Treat. Rev.* **1985**, *12*, 73.

(23) M. A. Jakupec, M. Galanski, V. B. Arion, C.G. Hartinger and B.K. Keppler, *Dalton Trans.* **2008**, 183.

(24) W. H. Ang and P. J. Dyson, *Eur. J. Inorg. Chem.* **2006**, 4003

(25) N. P. Farrell, S. G. De Almeida and K. A. Skov, *J. Am. Chem. Soc* **1988**, *110*, 5018.

(26) N. Farrell, *Metal Ions in Biological Systems* **2004**, *42*, 251.

(27) J. D. Roberts, J. Peroutka and N. Farrell, *J. Inorg. Biochem.* **1999** *77*, 51.

(28) Y. Qu, S. Gama de Almeida and N. Farrell *Inorg. Chim. Acta* **1992**, *201*, 123.

(29) A. L. Harris, X. Yang, A. Hegmans, L. Povirk, J. J. Ryan, L. Kelland and N. P. Farrell, *Inorg. Chem.* **2005**, *44*, 9598.

(30) G. Zhao, L. Guanghua Z. Huakuan, S. Shourong, H. Hongwei and Y. Yunti *Anti-Cancer Drug Des.* **1998**, *13*, 769.

(31) J. Kašpárková, O. Nováková, O. Vrána, N. Farrell and V. Brabec, *Biochemistry* **1999**, *38*, 10997.

(32) C. Manzotti, G. Pratesi, E. Menta, R. Di Domenico, E. Cavalletti, H. H. Fiebig, L. R. Kelland, N. Farrell, D. Polizzi, R. Supino, G. Pezzoni, and F. Zunino, *Clin. Cancer. Ress.* **2000**, *6*, 2626.

(33) C. G. Hartinger, A. D. Phillips and A. A. Nazarov, *Curr. Top. Med. Chem.* **2011**, *11* (11), 2688.

(34) D. I. Jodrella, T. R. J. Evans, W. Steward, D. Cameron, J. Prendiville, C. Aschele, C. Noberasco, M. Lind, J. Carmichael, N. Dobbs, G. Camboni, B. Gatti, F. De Braud, *Eur. J. Cancer* **2004**, *40*, 1872.

(35) I. Kostova, *Recent Patents on Anti-Cancer Drug Discov.* **2006**, *1*, 1.

(36) T. A. Hensing, N. H. Hanna, H. H. Gillenwater, M. G. Camboni, C. Allievi and M. A. Socinski, *Anti-Cancer Drugs* **2006**, *17*, 697.

(37) M. Lin, X. Wang, J. Zhu, D. Fan, Y. Zhang, J. Zhang and Z. Guo, *Apoptosis* **2011**, *16*, 288.

(38) Y. Zhao, W. He, P. Shi, J. Zhu, L. Qiu, L. Lin and Z. Guo, *Dalton Trans.* **2006**, 2617.

(39) S. Rubino, P. Portanova, A. Girasolo, G. Calvaruso, S. Orecchio and G.C. Stocco, *Eur. J. Med. Chem.* **2009**, *44*, 1041.

(40) A. Bielawska, B. Popławska, A. Surażyński, R. Czarnomysy and K. Bielawski, *Eur. J. Pharm.* **2010**, *643*, 34.

(41) X. -H. Zheng, Y. -F. Zhong, C. -P. Tan, L. -N. Ji and Z. -W. Mao, *Dalton Trans.* **2012**, *41*, 11807.

(42) E. Meggers, *Curr. Opin. Chem. Biol.* **2007**, *11*, 287.

(43) F. P. Dwyer, E. C. Gyarfas, W. P. Rogers and J. H. Koch, *Nature* **1952**, *170*, 190.

(44) F. P. Dwyer, E. Mayhew, E. M. F. Roe and A. Shulman, *Br. J. Cancer* **1965**, *19*, 195.

(45) F. P. Dwyer, I .K. Reid, A. Shulman, G. M. Laycock and S. Dixson, *Aust J Exp Biol Med Sci* **1969**, *47*, 203.

(46) C. S. Allardyce and P. J. Dyson, *Platinum Met. Rev.* **2001**, *45*, 62.

(47) I. Kostova, *Curr. Med. Chem.* **2006**, *13*, 1085.

(48) C. S. Allardyce, A. Dorcier, C. Scolaro and P. J. Dyson, *Appl. Organomet. Chem.* **2005**, *19*, 1.

(49) M. Galanski, V. B. Arion, M. A. Jakupec and B. K. Keppler, *Curr. Pharm. Des.* **2003**, *9*, 2078.

(50) A. Taylor and N. Carmichael, *Cancer Studies* **1953**, *2*, 36.

(51) N. Katsaros and A. Anagnostopoulou, *Crit. Rev. Oncol.* **2002**, *42*, 297.

(52) Y. Geldmacher, M. Oleszak and W. S. Sheldrick, *Inorg. Chim. Acta* **2012**, *393*, 84.

(53) L. Messori, G. Marcon, P. Orioli, M. Fontani, P. Zanello, A. Bergamo, G. Sava and P. Mura, *J. Inorg. Biochem.* **2003**, *95*, 37.

(54) G. Mestroni, E. Alessio, A. Sessanti o Santi, S. Geremia, A. Bergamo, G. Sava, A. Boccarelli, A. Schettino and M. Coluccia, *Inorg. Chim. Acta* **1998**, *273* 62.

(55) M. J. Clarke, *Coord. Chem. Rev.* **2003**, *236*, 209.

(56) M. J. Clarke, *Coord. Chem. Rev.* **2002**, *232*, 69.

(57) E. Alessio, G. Mestroni, G. Nardin, W. M. Attia, M. Calligaris, G. Sava and S. Zorzet, *Inorg. Chem.* **1988**, *27*, 4099.

(58) G. Mestroni, E. Alessio, G. Sava, S. Pacor, M. Coluccia and A. Boccarelli, *Met-Based. Drugs* **1994**, *1*, 41.

(59) I. Bratsos, A. Bergamo, G. Sava, T. Gianferrara, E. Zangrando and E. Alessio, *J. Inorg. Biochem.* **2008**, *102*, 606.

(60) M. Cocchietto, S. Zorzet, A. Sorc and G. Sava, *Invest. New Drugs* **2003**, *21*, 55.

(61) G. Sava, S. Zorzet, C. Turrin, F. Vita, M. Soranzo, G. Zabucchi, M. Cocchietto, A. Bergamo, S. DiGiovine, G. Pezzoni, L. Sartor and S. Garbisa, *Clin. Cancer Res.* **2003**, *9*, 1898.

(62) I. Bratsos, S. Jedner, T. Gianferrara and E. Alessio, *Chimia* **2007**, *61*, 692.

(63) A. Bergamo and G. Sava, *Dalton Trans.* **2007**, 1267.

(64) G. Sava, I. Capozzi, K. Clerici, G. Gagliardi, E. Alessio and G. Mestroni, *Clin. Exp. Metastasis* **1998**, *16*, 371.

(65) A. Bergamo, C. Gaiddon, J. H. M. Schellens, J. H. Beijnen and G. Sava,, *J. Inorg. Biochem.* **2012**, *106*, 90.

(66) C. G. Hartinger, M. A. Jakupec, S. Zorbas-Seifried, M. Groessl, A. Egger, W. Berger, H. Zorbas, P. J. Dyson and B. K. Keppler, *Chem. Biodiversity* **2008**, *5*, 2140.

(67) F. Lentz, A. Drescher, A. Lindauer, M. Henke, R. A. Hilger, C. G. Hartinger, M. E. Scheulen, C. Dittrich, B. K. Keppler and U. Jaehde, *Anti-Cancer Drugs* **2009**, *20*, 97.

(68) M. Groessl, E. Reisner, C. G. Hartinger, R. Eichinger, O. Semenova, A. R. Timerbaev, M. A. Jakupec, V. B. Arion and B. K. Keppler, *J. Med. Chem.* **2007**, *50*, 2185.

(69) S. Kapitza, M. Pongratz, M. A. Jakupec, P. Heffeter, W. Berger, L. Lackinger, B. K. Keppler and B. Marian, *J. Cancer Res. Clin. Oncol.* **2005**, *131*, 101.

(70) A. V. Vargiu, A. Robertazzi, A. Magistrato, P. Ruggerone and P. Carloni, *J. Phys. Chem. B* **2008**, *112*, 4401.

(71) E. Reisner, V. B. Arion, B. K. Keppler and A. J. L. Pombeiro, *Inorg. Chim. Acta* **2008**, *361*, 1569.

(72) B. K. Keppler, WO Application 2002059135, *Chem. Abstr.* **2002**, *vol. 137*, ref. 119658.

(73) P. J. Dyson, *Chimia* **2007**, *61*, 698.

(74) W. H. Ang, *Chimia* **2007**, *61*, 140.

(75) S. M. Guichard, R. Else, E. Reid, B. Zeitlin, R. Aird, M. Muir, M. Dodds, H. Fiebig and P. J. Sadler, *Biochem. Pharmacol.* **2006**, *71*, 408.

(76) C. Scolaro, A. Bergamo, L. Brescacin, R. Delfino, M. Cocchietto, G. Laurenczy,T. J. Geldbach,G. Sava and P. J.Dyson, *J. Med. Chem.* **2005**, *48* (4161-4171),

(77) A. K. Renfrew, A. D. Phillips, E. Tapavicza, R. Scopelliti, U. Rothlisberger and P. J. Dyson, *Organometallics* **2009**, *28*, 5061.

(78) G. S. Smith and B. Therrien, *Dalton Trans.* **2011**, *40*, 10793.

(79) S. J. Dougan, A. Habtemariam, S. E. McHale, S. Parsons and P. J. Sadler, *Proc. Natl. Acad. Sci. U. S. A.* **2008**, *105*, 11628.

(80) M. Mathew, G. J. Palenik and G. R. Clark, *Inorganic Chemistry* **1973**, *12*, 446.

(81) F. Wang, A. Habtemariam, E. P. L. van der Geer, R. Fernandez, M. Melchart, R. J. Deeth, R. Aird, S. Guichard, F. P. A. Fabbiani, P. Lozano-Casal, I. D. H. Oswald, D.

I. Jodrell, S. Parsons and P. J. Sadler, *Proc. Natl. Acad. Sci. U. S. A.* **2005**, *102*, 18269.

(82) C. Scolaro, A. Bergamo, L. Brescacin, R. Delfino, M. Cocchietto, G. Laurenczy, T. J. Geldbach, G. Sava and P. J. Dyson, *J. Med.Chem.* **2005**, *48*, 4161.

(83) A. Habtemariam, M. Melchart, R. Fernandez, S. Parsons, I. D. H. Oswald, A. Parkin, F. P. A. Fabbiani, J. E. Davidson, A. Dawson, R. E. Aird, D. I. Jodrell and P. J. Sadler, *J. Med. Chem.* **2006**, *49*, 6858.

(84) C. Scolaro, A. B. Chaplin, C. G. Hartinger, A. Bergamo, M. Cocchietto, B. K. Keppler, G. Sava and P. J. Dyson, *Dalton Trans.* **2007**, 5065.

(85) A. Casini, C. G. Hartinger, A. A. Nazarov and P. J. Dyson, *Top. Organomet. Chem.* **2010**, *32*, 57.

(86) B. Therrien, W.H. Ang, F. Cherioux, L. Vieille-Petit, L. Juillerat-Jeanneret, G. Suess-Fink and P. J. Dyson, *J. Cluster Sci.* **2007**, *18*, 741.

(87) M. G. Mendoza-Ferri, C. G. Hartinger, A. A. Nazarov, R. E. Eichinger, M. A. Jakupec, K. Severin and B. K. Keppler, *Organometallics* **2009**, *28*, 6260.

(88) G. Gasser, I. Ott and N. Metzler-Nolte, *J. Med. Chem.* **2011**, *54*, 3.

(89) D. Colangelo, A.L. Ghiglia, A.R. Ghezzi, M. Ravera, E. Rosenberg, E.; F. Spada, D. Osella, *J. Inorg. Biochem.* **2005**, *99*, 505.

(90) V. Vajpayee, Y. H. Song, Y. J. Jung, S. C. Kang, H. Kim, I. S. Kim, M. Wang, T. R. Cook, P. J. Stang and K. -W. Chi, *Dalton Trans.* **2012**, *41*, 3046.

(91) V. Vajpayee, Y. H. Song, Y. J. Jung, S. C. Kang, H. Kim, I. S. Kim, M. Wang, P. J. Stang and K. -W. Chi,, *Organometallics* **2011**, *30*, 3242.

(92) F. Linares, M. A. Galindo, S. Galli, M. A. Romero, J. A. R. Navarro and E. Barea, *Inorg. Chem.* **2009**, *48*, 7413.

(93) T. Gianferrara, A. Bergamo, I. Bratsos, B. Milani, C. Spagnul, G. Sava and E. Alessio, *J. Med. Chem.* **2010**, *53* (12), 4678.

(94) A. A. Holder, D. F. Zigler, M. T. Tarrago-Trani, B. Storrie and K. J. Brewer, *Inorg. Chem.* **2007**, *46* (12), 4760.

(95) A. A. Holder, S. Swavey and K. J. Brewer, *Inorg. Chem.* **2004**, *43* (1), 303.

(96) N. J. Farrer, L. Salassa and P. J. Sadler, *Dalton Trans.* **2009**, 10690.

(97) F. Schmitt, P. Govindaswamy, G. Süss-Fink, W. H. Ang, P. J. Dyson, L. Juillerat-Jeanneret and Bruno Therrien, *J. Med. Chem.* **2008**, *51*, 1811.

(98) F. Schmitt, P. Govindaswamy, O. Zava, G. Suss-Fink, L. Juillerat-Jeanneret and B. Therrien, *J. Biol. Inorg. Chem.* **2009**, *14*, 101.

(99) F. Schmitt, N. P. E. Barry, L. Juillerat-Jeanneret and B. Therrien, *Bioorg. Med. Chem. Lett.* **2012**, *22*, 178.

(100) M. Navarro, C. Gabbiani, L Messor and D. Gambino, *Drug Discov. Today* **2010**, *15* (23-24), 1070.

(101) R. A. Sánchez-Delgado, A. Anzellotti and L. Suarez, Metal Complexes as Chemotherapeutic Agents Against Tropical Diseases In *Metal Ions in Biological Systems*; A. Sigel and H. Sigel, Ed.; CRC Press,2004 Vol., Chapter 12.

(102) http://www.who.int/mediacentre/factsheets/fs094/en/index.html, Date accessed: 29/04/2012

(103) http://www.cdc.gov/malaria/about/biology/index.html, Date Acessed: 01/05/2012

(104) http://history.nih.gov/exhibits/bowman/SSmalaria.html, Date accessed: 20/03/2013

(105) http://en.wikipedia.org/wiki/File:MalariacycleBig.jpg, Date accessed: 20/02/2013

(106) P. F. Salas, C. Herrmann and C. Orvig, *Chem. Rev.* **2013**, *113*, 3450.

(107) World Health Organization: Guidelines for the Treatment of Malaria, 2nd ed.; WHO Press: Geneva.

(108) World Health Organization. Global Report on Antimalarial Drug Efficacy and Drug Resistance: 2000−2010, WHO Press: Geneva.

(109) D. E. Goldberg, A. F. Slater, A. Cerami and G. B. Henderson, *Proc. Natl. Acad. Sci. U. S. A.* **1990**, *87*, 2931.

(110) R. A. Sanchez-Delgado, A. Anzellotti and L. Suarez, Metal Complexes as Chemotherapeutic Agents Against Tropical Diseases In *Metal Ions in Biological Systems*; A. Sigel and H. Sigel, Ed.; CRC Press,2004 Vol., Chapter 12.

(111) T. J. Egan and H. M. Marques, *Coord. Chem. Rev.* **1999**, *190-192*, 493.

(112) R. Ridley, *Nature* **2002**, *415*, 686.

(113) M. Enserink, *Science* **2010**, *328*, 844.

(114) (GPARC), World Health Organization. Global plan for artemisinin resistance containment, WHO Press: Geneva.

(115) H. Noedl, Y. Se, K. Schaecher, B. L. Smith, D. Socheat and M. M. N. Fukuda, *Engl. J. Med.* **2008**, *359*, 2619.

(116) A. M. Dondorp, F. Nosten, P. Yi, D. Das, A. P. Phyo, J. Tarning, K. M. Lwin, F. Ariey, W. Hanpithakpong, S. J. Lee, P. Ringwald, K. Silamut, M. Imwong, K. Chotivanich, P. Lim, T. Herdman, S. An, S. Yeung, P. Singhasivanon, N. P. J. Day, N. Lindegardh, D. Socheat and N. J. N. White, *Engl. J. Med.* **2009**, *361*, 455.

(117) N. Gargano, F. Cenci and Q. Bassat, *Trop. Med. Int. Health* **2011**, *16*, 1466.

(118) N. Wash, H.B. Singh, A. Gajanana, and A.N. Raichowdhary, *Inorg. Chim. Acta.* **1987**, *135*, 133.

(119) R. A. Sánchez-Delgado, M. Navarro, H. Perez, and J. A. Urbina, *J. Med. Chem.* **1996**, *39*, 1095.

(120) M. Navarro, W. Castro and C. Biot, *Organometallics* **2012**, *31*, 5715.

(121) C. Biot, G. Glorian, L. A. Maciejewski, J. S. Brocard, O. Domarle, G. Blampain, P. Millet, A. J. Georges, H. Abessolo, D. Dive, and J. Lebibi,, *J. Med. Chem.* **1997**, *40*, 3715.

(122) M. Henry, S. Briolant, A. Fontaine, J. Mosnier, E. Baret, R. Amalvict, T. Fusai, L. Fraisse, C. Rogier, and B. Pradines, *Antimicrob. Agents. Chem.* **2008**, *52*, 2755.

(123) C. Biot, F. Nosten, L. Fraisse, D. Ter-minassian, J. Khalife and D. Dive, *Parasite* **2011**, *18*, 207.

(124) C. S. K. Rajapakse, A. Martınez, B. Naoulou, A. A. Jarzecki, L. Suarez, C. Deregnaucourt, V. Sinou, J. Schrevel, E. Musi, G. Ambrosini, G. K. Schwartz and R. A. Sanchez-Delgado, *Inorg. Chem.* **2009**, *48* (1122-1131),

(125) M. Navarro, S. Pekerar and H. A. Perez, *Polyhedron* **2007**, *26*, 2420.

(126) L. Glans, A. Ehnbom, C. de Kock, A. Martínez, J. Estrada, P. J. Smith, M. Haukka, R. A. Sánchez-Delgado and E. Nordlander, *Dalton Trans.* **2012**, *41*, 2764.

(127) T. J. Egan, K. R. Koch, P. L. Swan, D. A. Van Schalkwyk and P. J. Smith, *J. Med. Chem.* **2004**, *47*, 2926.

(128) M. Adams, Y. Li, H. Khot, C. De Kock, P. J. Smith, K. Land, K. Chibale and G. S. Smith, *Dalton Trans* **2013**, *42*, 4677.

(129) P. Chellan, N. Shunmoogam-Gounden, D. T. Hendricks, J. Gut, P. J. Rosenthal, C. Lategan, P. J. Smith, K. Chibale and G. S. Smith, *J. Eur. Med. Chem.* **2010**, 3520.

(130) P. Chellan, S. Nasser, L. Vivas, K. Chibale and G. S. Smith, *J. Organomet. Chem.* **2010**, *695*, 2225.

(131) P. Chellan, S. Nasser, L. Vivas, K. Chibale, and G. S. Smith,, *J. Organomet. Chem.* **2010**, *695*, 2225.

(132) P. Govender, N. C. Antonels, J. Mattsson, A. K. Renfrew, P. J. Dyson, J. R. Moss, B. Therrien and G. S. Smith, *J. Organomet. Chem.* **2009**, *694*, 3470.

CHAPTER 2

Synthesis and Characterisation of Mono-, Di- and Tetranuclear Cycloplatinated Thiosemicarbazone Complexes

2.1. Introduction

Thiosemicarbazones are a class of Schiff base compounds that contain a thiourea moiety. They are well known for their biological activity as antiparasitic,[1-6] antibacterial[7-9] and antitumoral agents.[10-14] As chemotherapeutics their mode of action is believed to be through the inhibition of ribonucleotide reductase thus arresting DNA synthesis.[15] As antiplasmodial agents, thiosemicarbazones may affect processes, some associated with hemoglobin (Hb) digestion in the food vacuole of the parasite, through several possible inhibitory mechanisms of action.[5,16-21] The ability of thiosemicarbazones to form stable complexes with a variety of metals is also believed to be of great importance to their biological activities. The lipophilic nature of the complex might be enhanced compared to the free ligand and certain side effects may decrease or be altogether avoided since the ligand could dissociate and the metal ion can then interact with its intended target.[22-24]

Research into the synthesis and application of thiosemicarbazone metal complexes as biological agents is thus an area of great promise. The discovery of cisplatin and its analogues as antitumoral agents had a profound influence on establishing the field of metal complexes in medicine[25] and the amount of research already accomplished within this area is substantial.[26-31] Despite the considerable quantity of work completed, there are still many little-researched avenues such as the preparation of mono- and polynuclear complexes from biologically active hybrid ligands. Hybrid ligands are defined as bis- or polydentate molecules which contain at least two different functionalities containing donor atoms capable of binding to a metal.[32] Thiosemicarbazones are prime hybrid candidates as they fulfill this basic criterion.

Several bonding modes have been observed for thiosemicarbazones.[33-39] For arylthiosemicarbazones the most common type of bonding modes observed are the tridentate [D,N,S] (**I**, **Figure 2.1**; where D = *ortho* carbon or heteroatom on the *ortho* carbon) or bidentate [N,S] (**II**). Depending on the metal, sulfur can coordinate either as a neutral (thione) or anionic (thiol) donor.[40]

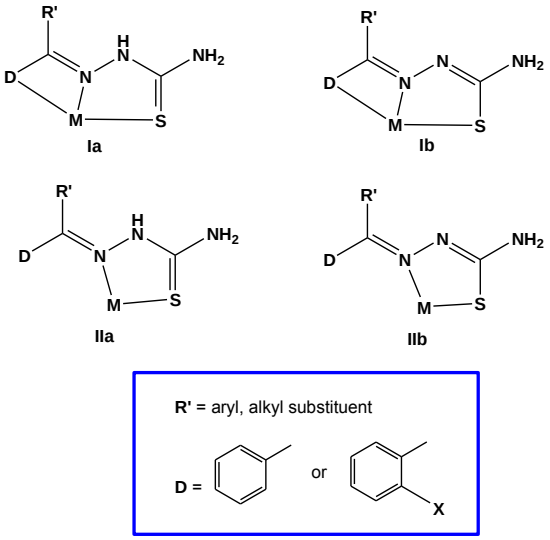

Figure 2.1. Different bonding modes of arylthiosemicarbazones.[40]

The coordination chemistry of thiosemicarbazones is a well established area with reviews on the subject being published as far back as 1974.[41] There have been extensive reports on the synthesis of thiosemicarbazone complexes with metals including vanadium,[42,43] zinc,[44] cobalt,[45] gold,[46] nickel,[47,48] silver,[49] copper,[50-52] and iron.[53] Thiosemicarbazone complexes containing metals from the Platinum Group Metal (PGM) series have also been reported.[40,54,55] PGM thiosemicarbazone complexes are gaining attention not just because of the structurally diverse complexes that can be prepared but due to the potential applications of these compounds in biology as well as catalysis.[54-69] Coupling the known bioactivities of thiosemicarbazones to the potentially beneficial biological properties of PGM metals such as palladium and platinum may result in a cooperative effect whereby the thiosemicarbazone ligand helps the metal reach its intended target (DNA) and the ligand can then dissociate and inhibit its cellular target.

Mononuclear thiosemicarbazone Pt(II) complexes have been widely studied for their *in vitro* pharmacological activity.[70-76] From these studies, certain trends in bioactivities have been discerned. Many thiosemicarbazones have demonstrated broad spectrum bioactivities[3,77-79] and consequent complexation with platinum brings about an enhancement in these bioactivities.[70] In the case of aryl-thiosemicarbazones, it has been observed that ortho-platination of the ring leads to high antitumor activity.[80,81] Variation of the substituents on the ligand also greatly influences activity; in particular the presence of at least one N-H group in

platinum thiosemicarbazone complexes is believed to be integral to its interaction with cellular components.[82]

In contrast, the extension of these evaluations of Pt(II) thiosemicarbazones as pharmacological agents to polynuclear derivatives remains relatively unexplored. Di- (**III**) and tetranuclear (**IV**) platinum thiosemicarbazone complexes (**Figure 2.2**) have shown antileukemic activity *in vitro* that is comparable to cisplatin.[80,83,84] In the tetranuclear complex, the thiosemicarbazone ligand chelates platinum in a tridentate fashion and this cyclometalated derivative showed better activity than the dinuclear derivative. Dinuclear Pt(II) complexes containing bis(thiosemicarbazones) (**V**) derived from 3,5-diacetyl-1,2,4-triazol demonstrated *in vitro* activities in the low micromolar range against the cisplatin sensitive (A2780) and cisplatin resistant (A2780*cis*R) human ovarian carcinoma cell lines.[85] These examples attest to the viability of polynuclear Pt(II) thiosemicarbazone complexes as pharmacological agents.

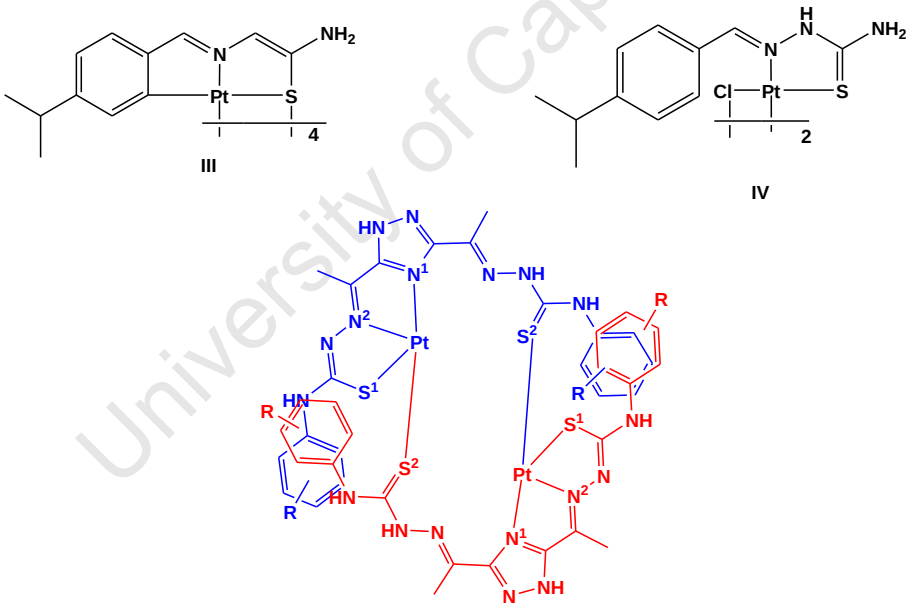

Figure 2.2. Examples of di- and tetranuclear platinum complexes studied for *in vitro* antitumor activity.

In this chapter, the synthesis, characterisation and reactivity of a series of cycloplatinated thiosemicarbazone complexes is discussed. The thiosemicarbazone ligand employed is 3,4-dichloroacetophenonethiosemicarbazone (**2.1**) which has been extensively studied for activity as an antiparasitic agent.[1,86,87] The DNA damaging effects of platinum is well known[88,89] and incorporation of this metal into the thiosemicarbazone moiety may enhance the bioactivities of **2.1**. Structure-activity studies of mononuclear Pt(II) thiosemicarbazone complexes have shown that tridentate [C,N,S] cycloplatinated thiosemicarbazones demonstrate better activities compared to bidentate [N,S] Pt(II) derivatives[70] and on this premise cycloplatinated complexes of **2.1** were synthesized. Further to this, di- and tetranuclear Pt(II) thiosemicarbazone complexes have been reported to have the ability to form DNA interhelical cross-links unlike cisplatin, indicating that these complexes have a different biochemical mechanism of action to cisplatin.[70] This may result in these polynuclear cycloplatinated complexes not being susceptible to the same deactivation and resistance mechanisms as cisplatin. The antiproliferative and antiparasitic studies of these complexes will be presented in Chapter 3.

2.2. Results and Discussion

*2.2.1. Synthesis of 3,4-dichloroacetophenonethiosemicarbazone (**2.1**)*

The ligand **2.1** was synthesized by Schiff base reaction of thiosemicarbazide with 3,4-dichloroacetophenone in the presence of acetic acid (**Scheme 2.1.**). This ligand has been reported and characterization of **2.1** with proton and carbon NMR and infrared spectroscopy agrees with the literature.[1] A broad singlet observed at 10.23 ppm in the ^{1}H NMR spectrum is assigned to the hydrazinic proton of the thiourea moiety and the terminal amine protons are observed as two singlets at 8.29 and 8.13 ppm due to restricted rotation of the C-NH_2 bond as a consequence of delocalization of the nitrogen's lone pair of electrons.[40,90-92] The aromatic protons H_a and H_b are observed as doublets at 7.86 and 7.59 ppm respectively due to mutual coupling to each other. A strong intensity absorption band at 1594 cm^{-1} in the infrared spectrum is characteristic of the C=N bond vibraton and confirms formation of the Schiff base product.

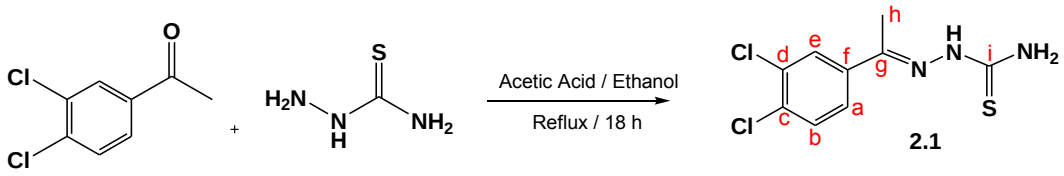

Scheme 2.1.

2.2.2. Synthesis and Characterization of Cycloplatinated Complexes

The tetranuclear complex **2.2** was prepared by stirring a suspension of the ligand **2.1** and $K_2[PtCl_4]$ in an ethanol-water mixture at 50 °C for five days (**Scheme 2.2.**) yielding a tetranuclear complex that is formed by a Pt_4S_4 core. The mono- and di-platinum complexes (**2.3 - 2.7**) were synthesized by cleavage of the bridging Pt-S bonds of **2.2** with either a mono- or diphosphane in acetone at room temperature. All of the complexes were isolated as orange amorphous solids in moderate to high yields.

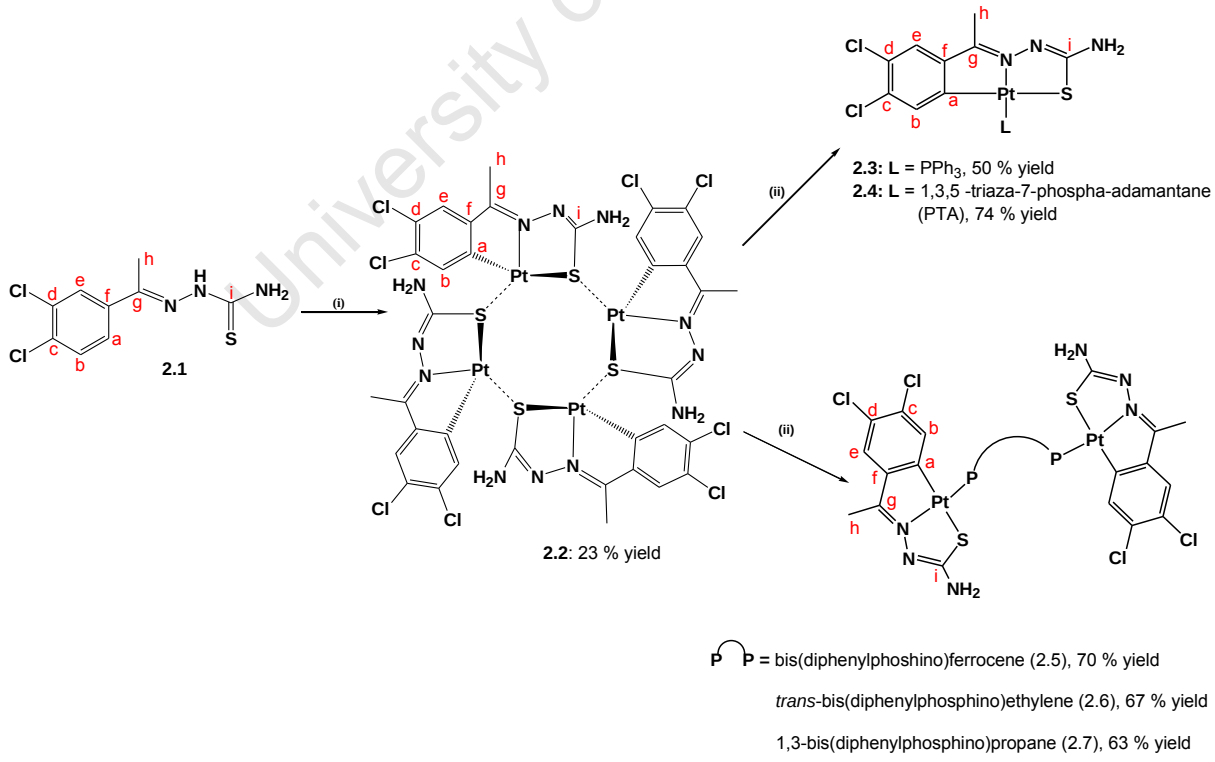

Scheme 2.2. Reaction Conditions: (i) $K_2[PtCl_4]$ / EtOH-H_2O / 50 °C / 5 days; (ii) L or P^P / acetone / RT / 3h.

On examination of the ^{1}H NMR spectral data for complex **2.2** (**Figure 2.3**), the absence of the proton resonances for the thioamide and *ortho*-protons (observed at 10.23 and 7.85 ppm respectively for **2.1**) presents evidence of the coordination of the *ortho*-carbon to platinum and the formation of a second imine bond thus suggesting that sulfur bonds to the metal in the thiolato form. In the free ligand **2.1**, the amine protons resonate as two distinct singlets at 8.29 and 8.13 ppm. Coordination to platinum effectively 'locks' the ligand into one conformation, most likely the *trans* conformation as this gives rise to a highly conjugated stable system, and the NH_2 protons are observed as a broad singlet upfield at 7.32 ppm. The remaining aromatic protons also experience this shielding effect and shift upfield. This shift in the proton resonances upon coordination is in agreement with similar cycloplatinated tetranuclear thiosemicarbazones complexes.[84,93]

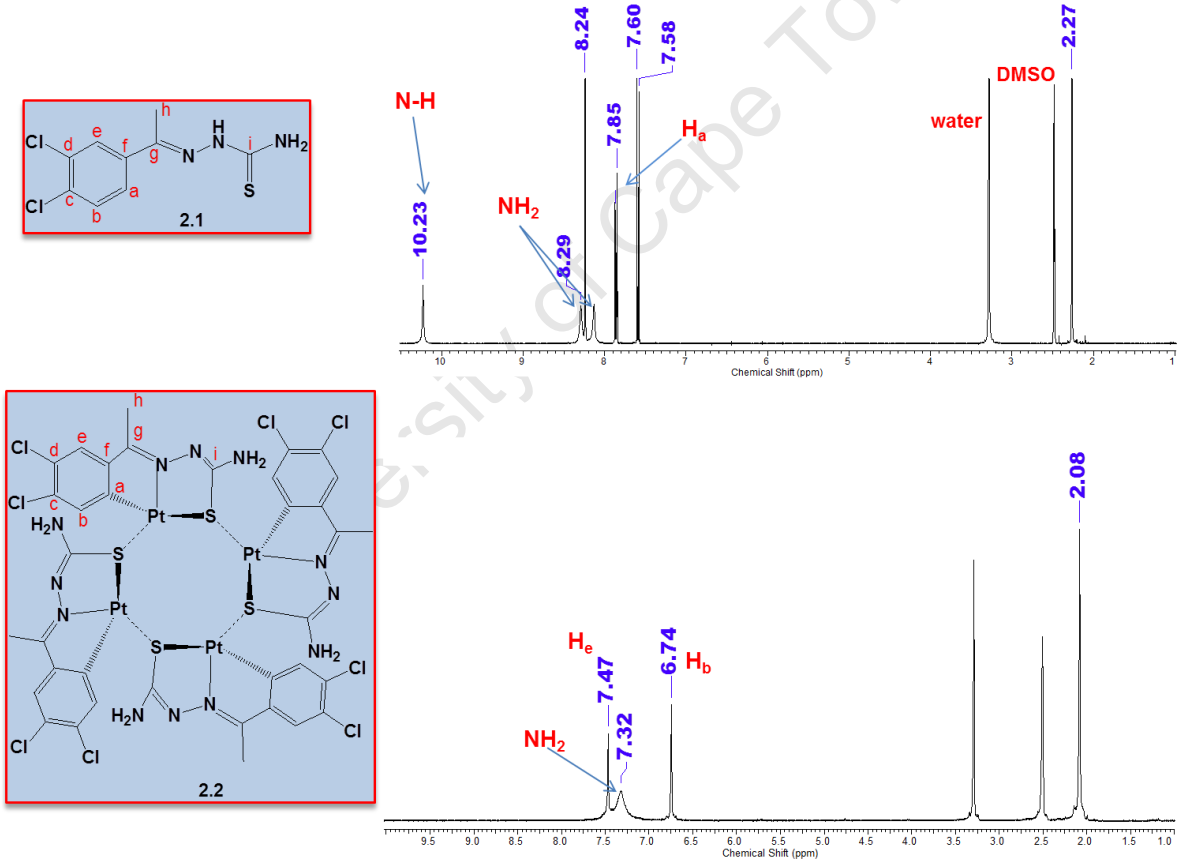

Figure 2.3. Proton NMR spectra for the free ligand **2.1** and complex **2.2**.

The ^{13}C NMR spectrum reveals the resonance of the carbon bonded to sulfur shifts from 179.1 ppm for the free ligand (**2.1**) to 166.6 ppm for **2.2** agreeing with coordination of sulfur in the thiolato formation. The *ortho*-carbon shifts downfield from 128.0 ppm to 153.8 ppm,

further evidence of coordination to platinum. The imine carbon (C_g) also shifts downfield, from 145.2 ppm in **2.1** to 165.0 in **2.2**, as a result of coordination of the imine nitrogen to the metal. The infrared spectrum for **2.2** shows only two strong absorption bands in the N-H region at 3321 and 3149 cm^{-1} agreeing with only two N-H bonds now present in the complex. Absorption bands at 1598 and 1561 cm^{-1} correspond to two C=N bonds, the high frequency band is assigned to the newly formed imine and the lower energy band to the metal coordinated (via nitrogen) imine.

Compared to the tetranuclear complex **2.2**, a slight upfield shift is observed for protons H_b and H_e for complexes **2.3** and **2.5 - 2.7**. This shielding of the aromatic protons is not observed for complex **2.4**, where the resonances for the aromatic and amine protons overlap to form a multiplet between 7.19 and 7.21 ppm. For complexes **2.3** and **2.5 - 2.7**, satellites are observed for the proton resonance of H_b. **Figure 2.4.** shows the proton NMR spectra for complex **2.3** where these satellites are clearly visible. A coupling constant of 20-25 Hz is observed and this corresponds to a ^3J coupling of ^{195}Pt to H_b. This type of coupling has been reported for other Pt(II) complexes.[94,95]

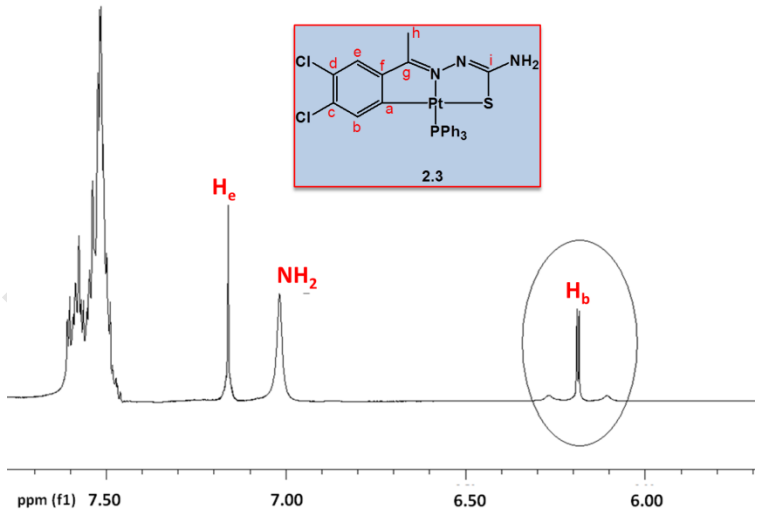

Figure 2.4. Expansion of the ^{1}H NMR aromatic region of complex **2.3**; the proton resonance with Pt satellites is circled.

A downfield shift of the azomethyl protons by approximately 0.25 ppm is observed for **2.3-2.7** compared to **2.2**. This is consistent with deshielding of these protons upon coordination of the imine nitrogen to the metal. For complex **2.4**, two sets of resonances are observed for the PTA ancillary ligand. A singlet at 4.20 ppm is assigned to the CH_2 protons adjacent to

phosphorus. The CH_2 protons of the N-CH_2-N moiety usually exhibit two doublets due to geminal coupling between $H_{equatorial}$ and H_{axial}.[96,97] In complex **2.4**, these protons are observed as a quartet possibly due to the influence of platinum.

In the ^{31}P NMR spectra for complexes **2.3**-**2.7**, only one phosphorus resonance is observed with platinum satellites confirming coordination of the phosphane to platinum. A ^{1}J coupling constant of between 1680 and 1888 Hz is consistent with similar cycloplatinated complexes.[93] In complex **2.6**, where the bridging ligand is *trans*-bis(diphenylphosphino)ethylene, a triplet with platinum satellites is observed (**Figure 2.5.**). This is attributed to phosphorus-phosphorus as well as phosphorus-platinum coupling.

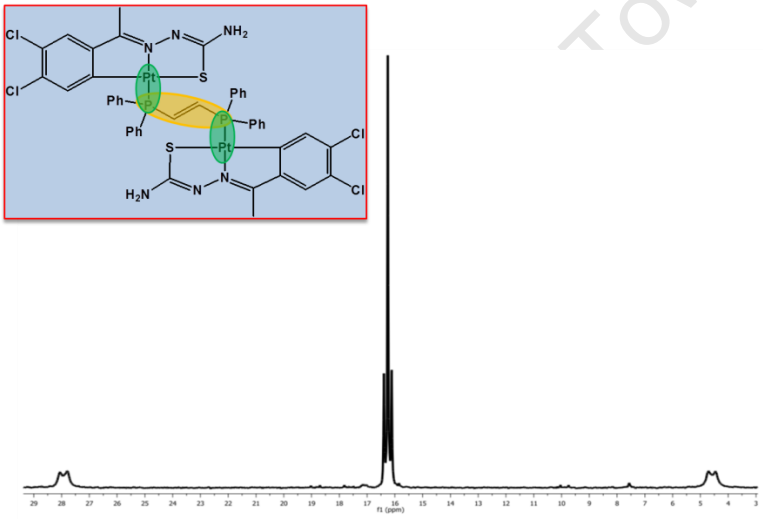

Figure 2.5. ^{31}P NMR spectrum for complex **2.6**

In the ^{13}C NMR spectra for complexes **2.3** – **2.7**, the C-S carbon resonates at approximately 177.0 ppm, similar to that of the tetranuclear complex (**2.2**). The *ortho*-carbon is observed at between 154.0 and 155.0 ppm. The chloro-substituted carbons of the coordinated thiosemicarbazone ligand appear to be equivalent and are observed at *ca.* 131.0 ppm. For complex **2.4**, two distinct resonances are seen at 135.3 and 133.15. The methyl carbon for all of the complexes resonates at approximately 13.0 ppm.

The IR spectra shows the expected two absorption bands in the imine region between 1627 and 1563 cm^{-1} for complexes **3**-**6** agreeing with the presence of two C=N bonds. Also, two

strong absorption bands in the N-H region, between 3300 and 3500 cm^{-1}, is consistent with only two N-H bonds present in the complexes.

Complexes **2.2** - **2.7** were all analysed using electro spray ionisation mass spectrometry (ESI-MS) run in the positive mode. Each complex exhibited a *m/z* peak corresponding to the [M + H] adduct.

2.2.3. X-ray Structure Analysis

Single crystals of complexes **2.2 – 2.4** suitable for single-crystal X-ray diffraction were obtained by exposing dimethyl sulfoxide solutions of each complex to air. **Table 2.1.** summarizes the data collection and processing parameters for each complex and **Table 2.2.** lists selected bond angles and lengths. Complex **2.2** (**Figure 2.6.**) crystallizes with 3 solvent molecules of DMSO with a monoclinic system. Each platinum center is bridged by the sulfur of the adjacent Pt-thiosemicarbazone unit to form an 8-membered Pt_4S_4 core around which the four thiosemicarbazone ligands reside. Each metal center is coordinated to the iminic nitrogen, *ortho*-carbon and sulfur of one thiosemicarbazone ligand and the fourth coordination site is occupied by the sulfur of the adjacent thiosemicarbazone ligand. A slightly distorted square-planar geometry is observed around each metal center.

a) b)

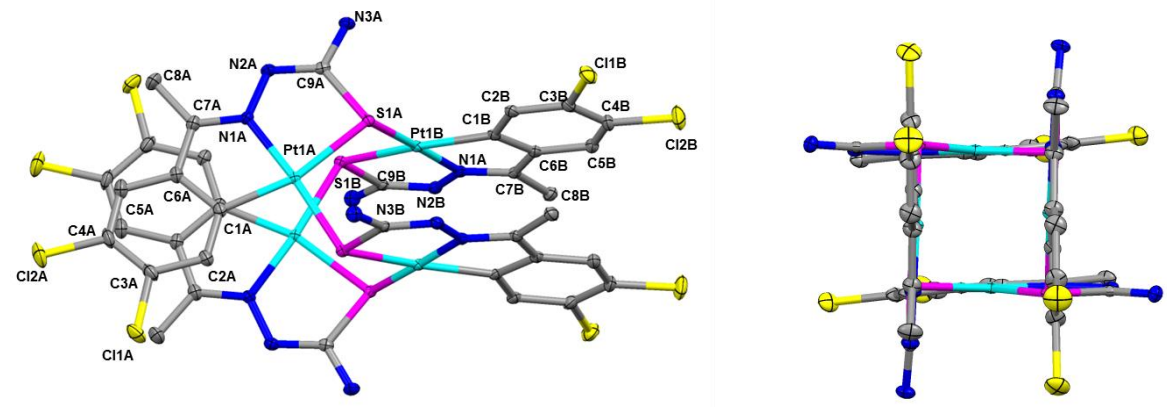

Figure 2.6. a) Molecular structure of **2.2** with ellipsoidal model of 25% probability level and another half molecule was generated via symmetry code of 1-x, y, 0.5-z. Solvent molecules and hydrogen atoms have been omitted for clarity. **b)** View of complex **2.2** down the 010 plane showing ring formed by the Pt_4S_4 core. Atom labeling, solvent molecules and hydrogen atoms omitted for clarity.

The bond lengths observed between platinum and each coordinated atom agree with those reported for similar tetranuclear platinum thiosemicarbazone complexes.[98] A lengthening of the C-S bond for S(1A)-C(9A) and the S(1B)-C(9B) is observed with values for the bond distances in close agreement with the bond length expected for a C-S single bond (1.82 Å) rather than a normal C=S double bond (1.56 Å),[99] corroborating that sulfur coordinates to palladium in the thiolato form.[100] The bond angles, N(1A)-Pt(1A)-S(1B)#2, N(1B)-Pt(1B)-S(1A) , C(1A)-Pt(1A)-S(1A) and C(1B)-Pt(1B)-S(1B) are all less than 180° confirming the slight deviation from the expected square-planar geometry around platinum.

Table 2.1. Data Collection and Processing Parameters for **2.2·3DMSO** , **2.3·2DMSO** and **2.4**

	2.2·3DMSO	**2.3·2DMSO**	**2.4**
Formula	$C_{42}H_{46}Cl_8N_{12}O_3Pt_4S_7$	$C_{31}H_{34}Cl_2N_3O_2PPtS_3$	$C_{15}H_{19}Cl_2N_6PPtS$
Formula weight	2055.29	873.75	612.38
Crystal system, Space group	Monoclinic,C2/c	Orthorhombic, *P*ca21	Monoclinic, *P*21/c
a (Å)	14.7265(6)	15.9511(4)	19.176(4)
b (Å)	30.6788(14)	9.2259(2)	6.0493(12)
c (Å)	14.2547(6)	23.0990(6)	17.977(4)
β (deg)	111.9020(10)	90	114.13(3)
V/Å^3	5975.3(4)	3399.32(14)	1903.2(7)
Z	4	4	4
Dc (g cm^{-3})	2.285	1.707	2.137
μ (mm^{-1})	9.987	4.550	7.860
θ range for data collection (deg.)	1.63 to 28.33	3.49 to 28.28	3.36 to 28.28
Limiting indices	$-19 \le h \le 18$ $-40 \le k \le 40$ $-19 \le l \le 19$	$-21 \le h \le 21$ $-12 \le k \le 12$ $-30 \le l \le 30$	$-25 \le h \le 23$ $-8 \le k \le 0$ $0 \le l \le 23$
no. of reflns measd	67775	136324	4703
no. of reflns used (R_{int})	7432 (0.0358)	8405 (0.0498)	4703 (0.0000)
no. of params	342	414	237
final R [I > 2σ(I)]			
R1	0.0204	0.0214	0.0182
wR2	0.0454	0.0382	0.0389
R (all data)			
R1	0.0269	0.0280	0.0216
wR2	0.0485	0.0403	0.0402
goodness of fit on F^2	1.068	1.145	1.126

The mononuclear complexes **2.3** and **2.4** (**Figures 2.7a and 2.7b**) crystallize with orthorhombic and monoclinic systems respectively. The molecular structure of each complex confirms that the platinum-sulfur bridging bonds in complex **2.2** are cleaved and the tridentate coordination of the thiosemicarbazone remains intact. As with **2.2**, there is a

distorted square-planar coordination sphere around the metal and this is confirmed by the slight deviation of the bond angles observed around platinum for complexes **2.3** and **2.4**.

Table 2.2. Selected bond lengths (Å) and angles (deg.) for **2.2**-**2.4**

	2.2·3DMSO		**2.3·2DMSO**	**2.4**
	A	**B**		
Pt1-C1	2.004(3)	1.999(4)	2.039(3)	2.027(3)
Pt1-N1	1.996(3)	1.995(3)	2.038(2)	2.035(2)
Pt1-S1	2.3169(8)	2.3513(8	2.2359(7)	2.3322(11)
Pt1-P1	-	-	2.2359(7)	2.2101(7)
N1-C7	1.307(4)	1.302(5)	1.298(3)	1.301(3)
N2-C9	1.293(5)	1.300(5)	1.316(4)	1.313(3)
C1-Pt1-S1	164.12(11)	100.70(3)	163.57(8)	163.74(7)
C1-Pt1-P1	-	-	97.00(8)	98.56(8)
N1-Pt1-C1	80.61(13)	81.42(15)	80.78(10)	80.73(9)
N1-Pt1-S1	83.97(9)	84.08(9)	82.80(7)	83.07(6)
N1-Pt1-P1	-	-	177.17(7)	168.56(6)
P1-Pt1-S1	-	-	99.43(3)	97.59(3)

a) b)

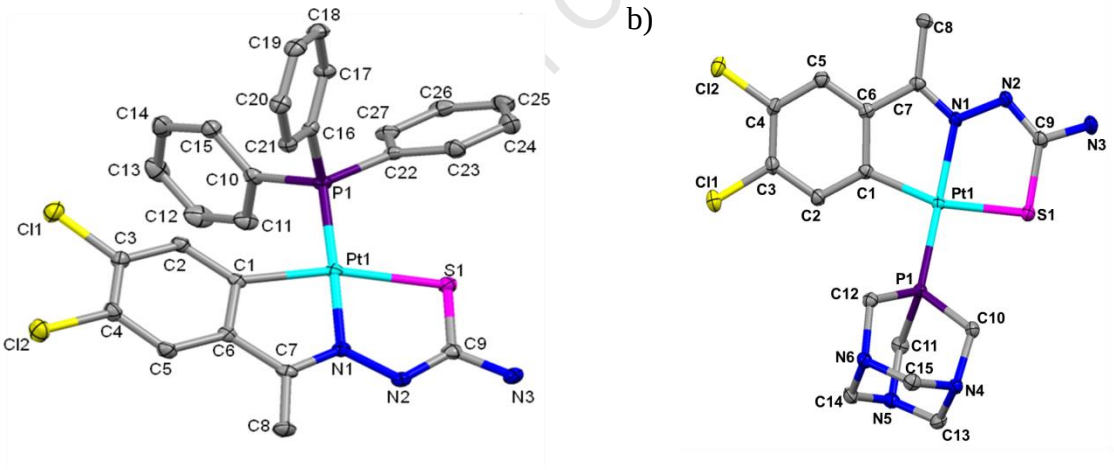

Figure 2.7. a) Structure of complex **2.3·2DMSO** with ellipsoidal model of 30% probability level; b) Structure of complex **2.4** with ellipsoidal model of 40% probability level.

The bond distances observed between the metal and the coordinated carbon, nitrogen and sulfur atoms in **2.3** and **2.4** are similar to the tetranuclear complex **2.2** indicating that the electron density distribution between platinum and the thiosemicarbazone ligand does not change after cleavage. These bond distances are also in close agreement with similar mononuclear platinum thiosemicarbazone complexes.[101,102]

2.2.4. Reactivity Studies of Mononuclear Cycloplatinated Thiosemicarbazone Complexes

The ability of the mononuclear Pt(II) complexes **2.3** and **2.4** to undergo oxidative addition reactions was evaluated using different mono-, di- and tri-halomethylbenzenes. These reactions were first carried out using complex **2.3** (**Scheme 2.3.**). The reaction was allowed to stir at room temperature for 18 hours. No change in the proton and phosphorus NMR was observed for the isolated solid.

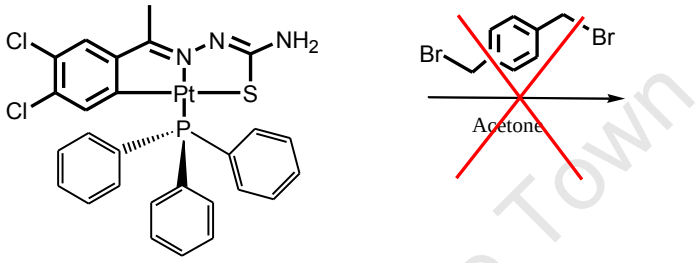

2.3

Scheme 2.3.

Platinum is able to easily access its +4 oxidation state and there is literature evidence of Pt(II) complexes undergoing oxidative addition reactions.[103,104] Thus, there are two possible reasons why complex **2.3** was not reactive; the metal center is not easily accessible due to the steric bulk of the triphenylphosphine ligand or the carbon-bromide bond was too strong to add across these types of tridentate cycloplatinated complexes.

Further reactivity studies were carried out using **2.4** which has less steric bulk around the metal compared to **2.3**, as evidenced by their molecular structures (section 2.2.2), and iodomethylbenzenes (**Scheme 2.4.**). Complex **2.4** was suspended in DCM and the appropriate mono-, bis- or tris-(iodomethyl)benzene was added and the reaction allowed to proceed at room temperature for 18 hours. Pale orange solids were isolated and the products of these reactivity studies were analyzed using ^{1}H and $^{31}P\{1H\}$ NMR and IR spectroscopies and mass spectrometry. For the reaction of **2.4** with iodomethylbenzene to give **2.8**, COSY, HSQC and NOESY 2D NMR studies were also used to ascertain the structural properties of the complex.

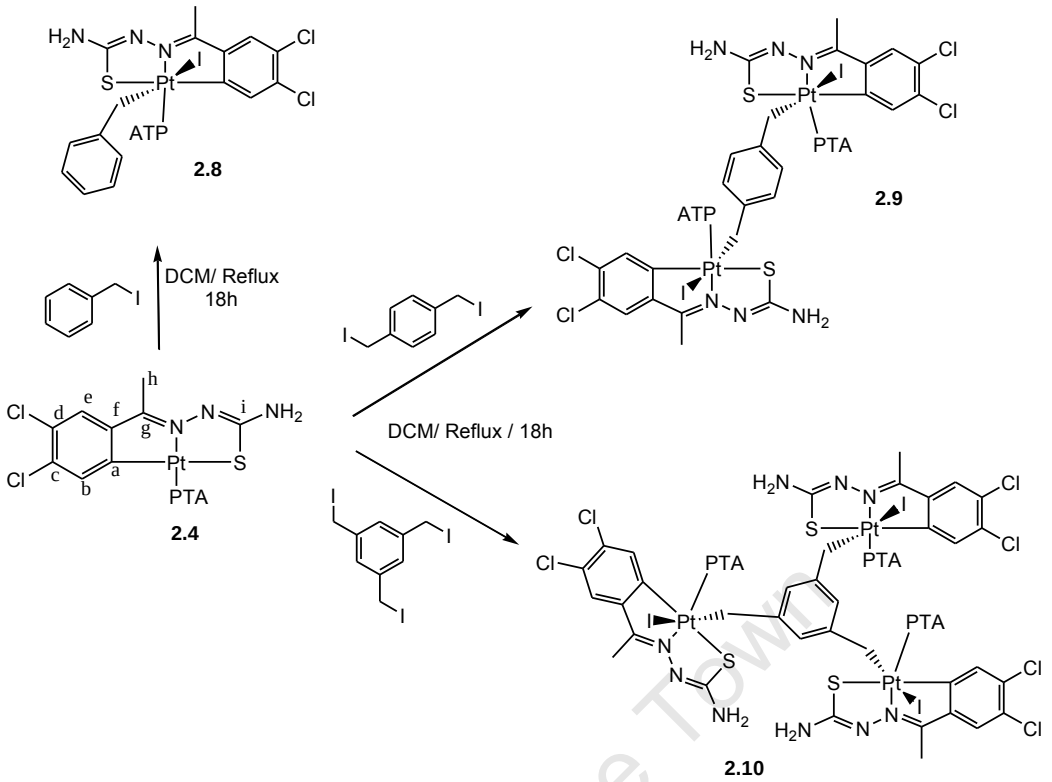

Scheme 2.4.

Comparison of the proton NMR spectrum of **2.8** to that of **2.4** reveals that the NH_2 protons of the thiosemicarbazone ligand shift downfield from 7.09 to 7.20 ppm (**Figure 2.7.**). The proton H_b shifts upfield from 7.19 ppm in the precursor complex (**2.4**) to 7.11 ppm in **2.8** and this slight shielding of this proton could be due to greater electron density around the metal center. The aromatic protons of the methyl benzene group occur as a multiplet at 7.55 ppm.

The alkyl region of the spectrum was harder to assign. Several signals are observed in this region, a doublet of doublets between 5.40 and 5.10 ppm, a doublet with platinum satellites and a multiplet between 4.21 and 4.72 ppm. Integration of this region suggests that the PTA protons as well as the methyl protons of the benzyl group occur in this region. Definite assignment of a PTA proton to a specific resonance is not possible as there may be through space coupling of the methylbenzene group and PTA. Thus, 2D NMR experiments were carried out. Correlation Spectroscopy (COSY) is a two-dimensional homonuclear (^{1}H-^{1}H) technique which can be used to ascertain which protons undergo through-bond spin-spin coupling to other protons in the molecule. The COSY 2D NMR for **2.8** reveals that the doublet of doublets observed between 5.00 and 5.50 ppm couple to each other as well as one of the resonances in the multiplet observed at 4.67 ppm (**Figure 2.8**).

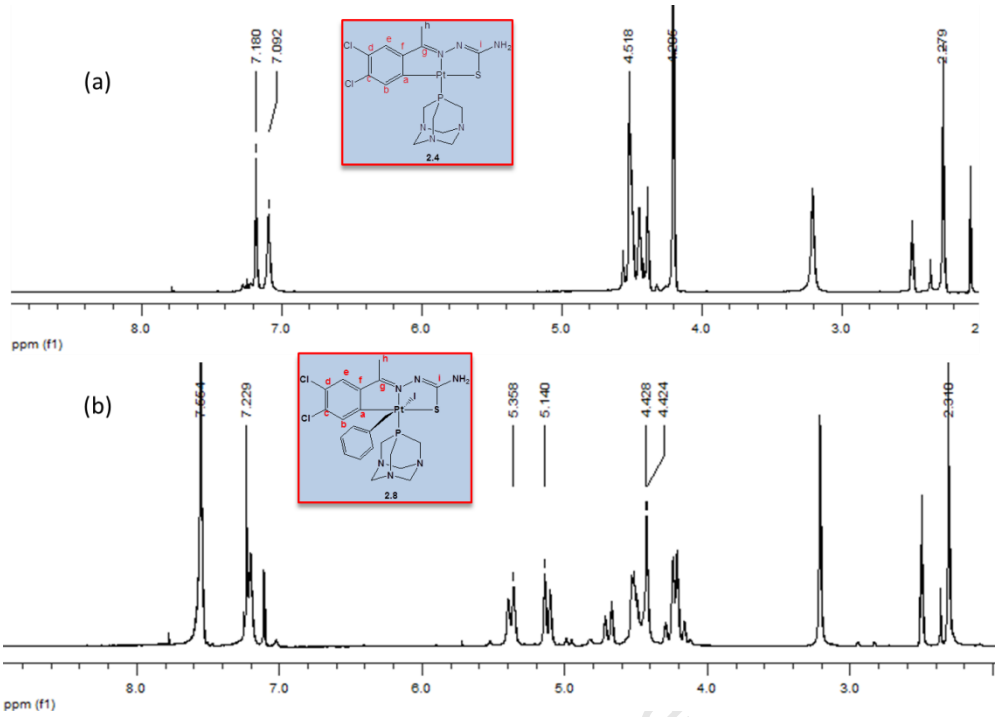

Figure 2.7. ^{1}H NMR spectra for **2.4** (a) and **2.8** (b).

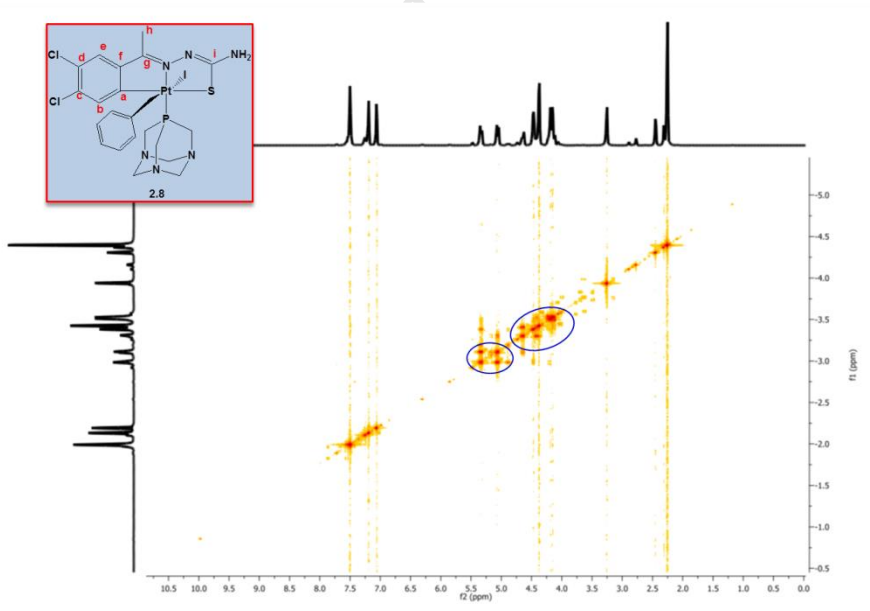

Figure 2.8. {^{1}H-^{1}H}COSY 2D NMR spectrum for complex **2.8**

Nuclear Overhauser Effect spectroscopy (NOESY) is a homonuclear (^{1}H-^{1}H) 2D technique that can be used to determine which protons experience through-space coupling to other protons in the molecule. Heteronuclear Spin-Quantum Coupling Spectroscopy (HSQC)

assists in showing which protons couple to other nuclei such as ^{13}C and thus allowing us to correlate which protons are on the same carbon. HSQC and NOESY NMR experiments for complex **2.8** were thus used to determine which proton resonances are on the same carbon and if there is through space coupling (**Figures 2.9.** and **2.10.**).

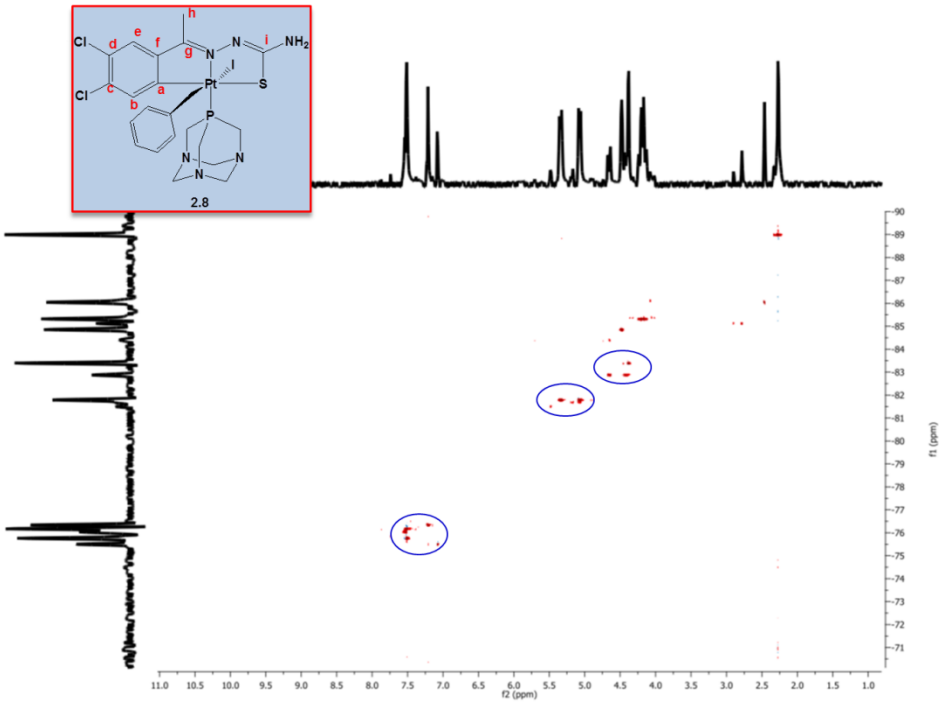

Figure 2.9. {^{1}H-^{13}C} HSQC 2D NMR spectrum for complex **2.8**

The HSQC 2D NMR spectrum shows that the doublet of doublets observed are for protons attached to the same carbon and is most likely the protons H_β and the doublet with platinum satellites seen upfield also occur on the same carbon and can be assigned to H_α protons; a coupling of ca. 24 Hz is in agreement with a ^{3}J(Pt-H) coupling.[94,105] The other multiplet observed in the alkyl region is also due to protons on the same carbon and is thus the alkyl protons of the benzyl ligand. The splitting of these proton signals is most likely due to through space coupling to the PTA proton resonances. This is confirmed by the NOESY NMR spectrum. The PTA resonances show through space coupling to the aromatic protons of the benzyl ligand.

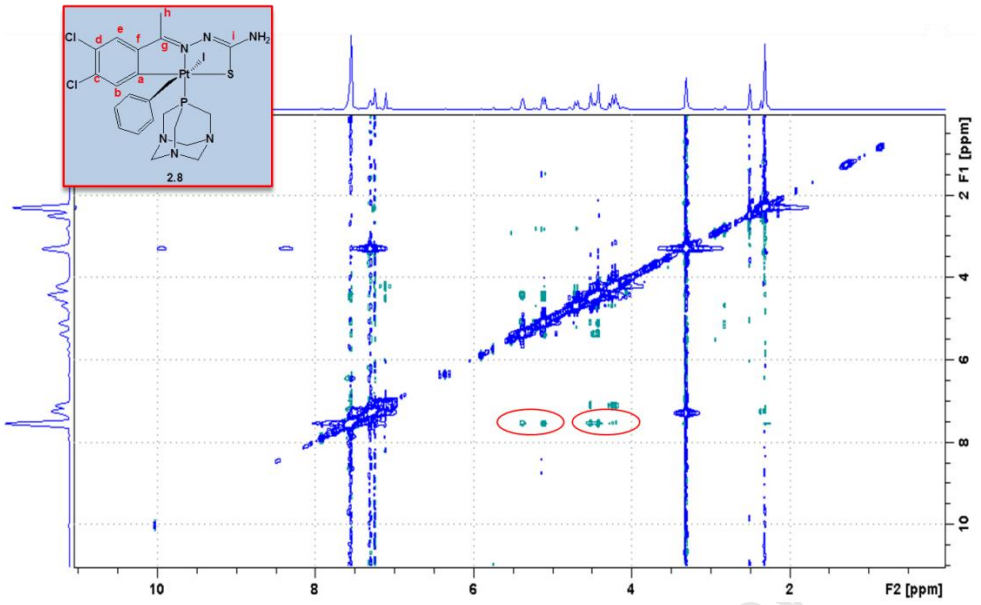

Figure 2.10. {^{1}H-^{1}H} NOESY NMR spectrum for complex **2.8**

The phosphorus NMR shows a shift of the PTA phosphorus resonance from -61.25 ppm in complex **2.4** to -39.79 ppm for complex **2.8**. Greater shielding of the phosphorus nucleus in **2.8** compared to **2.4** would be expected if there was greater electron density around the metal due to oxidative addition of benzyl iodide. The IR spectrum for **2.8** shows a shift of the C=N vibration of the uncoordinated imine from 1625.8 (for complex **2.4**) to 1601.9 cm^{-1}, agreeing with greater electron density around the metal leading to shortening of the Pt-S bond and thus elongation of the N=C bond.

The proton NMR for complexes **2.9** and **2.10** were found to be similar to that **2.8**. The same splitting pattern of the PTA and methyl protons is observed. As determined through 2D Proton NMR experiments for complex **2.8**, these broad signals are due to through-space interactions of the PTA and central benzene ring protons because of steric effects. Additionally, there may be interactions between the TSC-Pt-PTA moieties for complex **2.10**. The phosphorus NMR for **2.9** shows a singlet at -39.90 ppm suggesting that the complex formed is similar to that of **2.8**. For complex **2.10**, three phosphorus resonances are observed; singlets at -42.61 and -47.15 ppm and a doublet at -44.04 ppm, all with platinum satellites. This pattern could be due to two possibilities; the orientation of the TSC-Pt-PTA moieties may be different at each position relative to each other and there may also be through-space phosphorus-phosphorus interactions between the moieties.

Complex **2.8** was also analysed using low resolution Electrospray Ionisation Mass Spectrometry (ESI-MS). A base peak corresponding to the complex with loss of the iodo ligand was observed (**Figure 2.11**). This data confirms that oxidative addition of the iodobenzyl bond does occur across the platinum center.

(a) Complex **2.8**: $[M\text{-}I]^+ = 704$

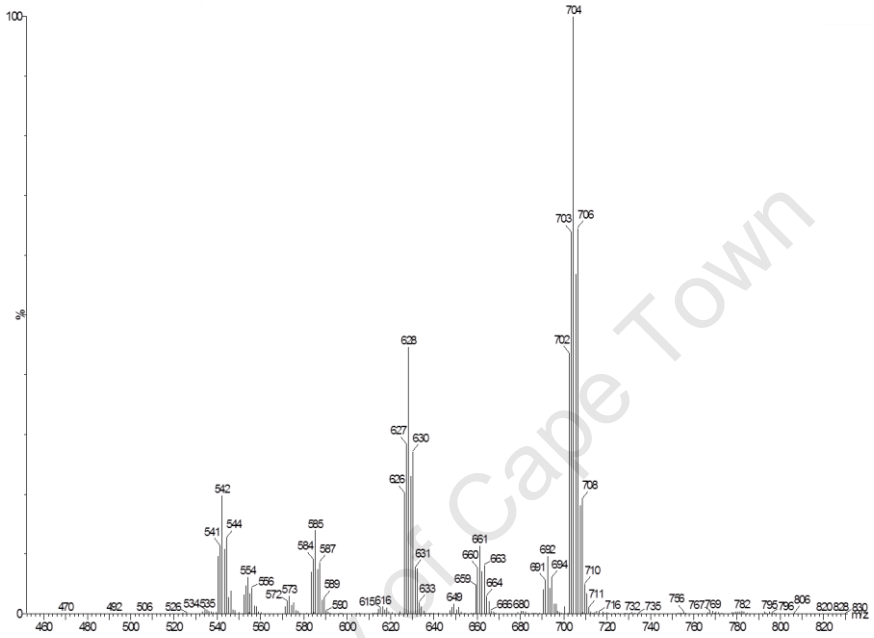

Figure 2.11. ESI-MS Traces for **2.8**

2.3. Summary

Six new cycloplatinated thiosemicarbazone complexes (**2.2**-**2.7**) have been prepared using the ligand 3,4-dichloroacetophenonethiosemicarbazone (**2.1**) in moderate to good yields. The complexes have been characterized using NMR and IR spectroscopies and mass spectrometry. The molecular structures of **2.2**-**2.4** were determined using single crystal X-ray diffraction and show that the ligand coordinates to platinum in the expected tridentate manner via the *ortho*-carbon, imine nitrogen and thiolato sulfur. Reactivity studies of the mononuclear complex 2.4 with mono-, bis- and tris-(iodomethyl)benzene revealed that this complex was able to undergo oxidative addition reactions.

A selection of these complexes have been evaluated for antiparasitic and antiproliferative activities and the results are discussed in detail in Chapter 3.

2.4. Experimental

2.4.1. General Methods

Thiosemicarbazide, 3,4-dichloro-acetophenone, triphenylphosphane, 1,3,5-triaza-7-phospha-adamantane, bis(diphenylphosphinoferrocene) and *trans*-bis(diphenylphosphino)-ethylene were purchased from Sigma-Aldrich and used without further purification. Potassium tetrachloroplatinate was kindly donated by AngloAmerican Platinum Limited. Ligand **2.1**, 3,4-dichloroacetophenonethiosemicarbazone, was prepared using a previously reported literature method.[1] All solvents used were analytical grade and dried over molecular sieves. Nuclear Magnetic Resonance (NMR) Spectra were recorded on a Varian Unity XR400 MHz (^{1}H at 399.95 MHz, ^{13}C at 100.58 MHz, ^{31}P at 161.90 MHz), Varian Mercury XR300 (^{1}H at 300.08 MHz, ^{13}C at 75.46 MHz, ^{31}P at 121.47 MHz) or Bruker Biospin GmbH (^{1}H at 400.22 MHz, ^{13}C at 100.65 MHz, ^{31}P at 162.00 MHz) spectrometer at ambient temperature. Chemical shifts for ^{1}H and ^{13}C{^{1}H} NMR shifts are reported using tetramethylsilane (TMS) as the internal standard and ^{31}P{^{1}H} NMR spectra were measured relative to H_3PO_4 as the external standard. NMR spectra were recorded in deuterated dimethylsulfoxide (DMSO-D_6) unless otherwise stated. Infrared (IR) absorptions were measured on Perkin-Elmer Spectrum 100 FT-IR Spectrometer as KBr pellets. Microanalyses for C, H, and N were carried out using a Thermo Flash 1112 Series CHNS-O Analyser and melting points were determined using a Büchi Melting Point Apparatus B-540. Mass Spectrometry determinations were carried out on all new compounds using either electron impact (EI) on a JEOL GC Matell instrument or electrospray ionisation (ESI) on a Waters API Quattro Micro instrument in either the positive or negative mode.

*2.4.2. Synthesis of 3,4-Dichloroacetophenone thiosemicarbazone (**2.1**)*[1]

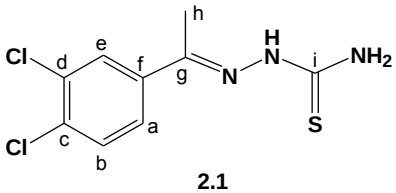

2.1

A solution of the 3,4-dichloroacetophenone (1.00 g, 5.30 mmol) in ethanol (10 cm^3) was added dropwise to a stirred suspension of thiosemicarbazide (0.55 g, 5.99 mmol) in ethanol (20 cm^3). Acetic acid (1cm^3) was then added and the reaction mixture was stirred at reflux for 18 hours. Upon cooling to room temperature, the product (**2.1**) precipitated out of solution and was collected by filtration, washed with ethanol and diethyl ether and dried under vacuum. The product (**2.1**) was isolated as a fluffy white solid (0.485 g, 35%). M.p.: 191-192 ºC (lit. mp.: 196 – 198 ºC). ^{1}H NMR (300.08 MHz, DMSO-d_6): δ (ppm) = 10.23 (br s, 1H, NH), 8.29 (s, 1H, NH_2), 8.26 (s, 1H, H_e), 8.13 (s, 1H, NH_2), 7.86 (d, $^3J(H_aH_b)$ = 8.52 Hz, 1H, H_a), 7.59 (d, $^3J(H_bH_a)$ = 8.52 Hz, 1H, H_b), 2.27 (s, 3H, H_h). ^{13}C NMR (75.46 MHz, DMSO-d_6): δ (ppm) = 179.1 (C_i), 145.2 (C_g), 138.2 (C_f), 131.5 (C_c), 131.2 (C_e), 130.0 (C_d), 128.0 (C_a), 126.5 (C_b), 13.6 (C_h). IR (KBr, cm^{-1}) υ = 3421 (s, N-H), 3181 (m, N-H), 3141 (m, N-H), 1594 (s, C=N), 1091 (s, C=S).

*2.4.3. Synthesis of [Pt(3,4-Dichloro-acetophenone thiosemicarbazone)]$_4$ (**2.2**)*

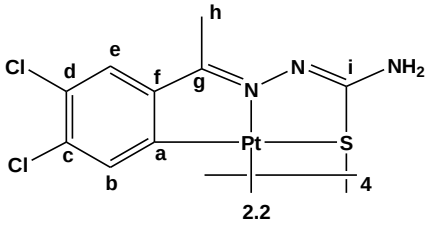

2.2

$K_2[PtCl_4]$ (0.862 g, 2.08 mmol) was dissolved in deionized water (10 cm^3) and ethanol (150 cm^3) added. The ligand **2.1** (0.520 g, 2.08 mmol) was then added to the resulting milky orange suspension. The reaction mixture was heated to 50 °C for 5 days before being cooled to room temperature. The orange-yellow product (**2.2**) was isolated by vacuum filtration, washed with ethanol (3 x 10 cm^3) and dried. Yield: 0.880 g, 23 %. Mp: 226-228 °C, decomposition without melting). ^{1}H NMR (300 MHz, DMSO-d_6): δ (ppm) = 7.47 (s, 4H, H_e), 7.25 (br s, 8H, NH_2), 6.74 (s, 4H, H_b), 2.08 (s, 12H, H_h). ^{13}C NMR (300 MHz, DMSO-d_6): δ (ppm) = 166.6 (C_i), 165.0 (C_g), 153.8 (C_a), 149.2 (C_f), 130.88 (C_c, C_d), 126.4 (C_e), 124.5 (C_b), 13.2 (C_h). IR (KBr, cm^{-1}) υ = 3321(w, N-H), 3149 (w, N-H), 1598 (s, C=N), 1561(m, C=N), 1561 (s, C=$C_{aromatics}$). Elemental Analysis for $C_{36}H_{28}Cl_8N_{12}Pt_4S_4$: found C 25.42; H, 2.36; N, 8.34 %; calculated for $C_{36}H_{28}Cl_8N_{12}Pt_4S_4 \cdot C_4H_{18}O$: C, 25.35; H, 2.44; N, 8.87. ESI-MS: *m/z* 1821.8 ($[C_{36}H_{28}Cl_8N_{12}Pt_4S_4 + H]^+$, 20%)

2.4.4. General Method for Synthesis of Mono- and Bis-phosphane Pt(II) Thiosemicarbazone Complexes

The tetrameric complex, **2.2**, (1 mol. equiv.) was suspended in acetone (15 cm^3). For complexes **2.3** and **2.4**, the monophosphane (4 mol. equiv.) was added and for complexes **2.5**-**2.7**, the bis(diphenylphoshane) (2 mol equiv.) was added and the reaction was stirred at room temperature for 3 hours. The product was collected as an orange solid by filtration, washed with acetone (2 x 5 cm^3) and dried under vacuum.

*2.4.4.1. [Pt(3,4-Dichloro-acetophenone thiosemicarbazone)(PPh_3)] (**2.3**)*

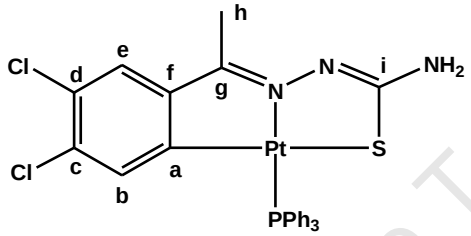

2.3

Triphenylphosphane (0.145 g, 0.552 mmol) was reacted with complex **2.2** (0.255 g, 0.140 mmol). The product (**2.3**) was isolated as an orange amorphous solid (0.198 g, 50 %). Mp: 299-301 ºC, decomposition without melting. ^{1}H NMR (300.08 MHz, DMSO-d_6): δ (ppm) = 7.46-7.59 (m, 15H, PPh_3), 7.16 (s, H_e), 7.02 (s, NH_2), 6.19 (s, 2H, H_b, ^3J(Pt-H): 25.5 Hz), 2.35 (s, 3H, H_h). ^{13}C NMR (100.65 MHz, DMSO-d_6): δ (ppm) = 177.5 (C_i), 167.1 (C_g), 155.2 (C_a), 152.7 (C_f), 134.4-134.3 (PPh_3), 131.8 (C_c and C_d), 129.05 (PPh_3), 130.3 (C_e), 125.5 (C_b), 13.6 (C_h). ^{31}P NMR (162.00 MHz, DMSO-d_6): δ (ppm) = 25.70 (PPh_3, ^1J(Pt-P): 1888 Hz). IR (KBr, cm^{-1}) υ = 3472 (m, N-H), 3340 (s, N-H), 1598 (s, C=N), 1579 (m, C=N), 1497 (s, C=C aromatics). Elemental Analysis for $C_{27}H_{22}Cl_2N_3PPtS$: found C, 45.47; H, 3.15; N, 5.63 %; calculated C, 45.20; H, 3.09; N, 5.86 %. EI-MS: *m/z* 716.85 $[M-H]^+$, 100%.

*2.4.4.2. [Pt(3,4-Dichloro-acetophenone thiosemicarbazone)(PTA)] (**2.4**)*

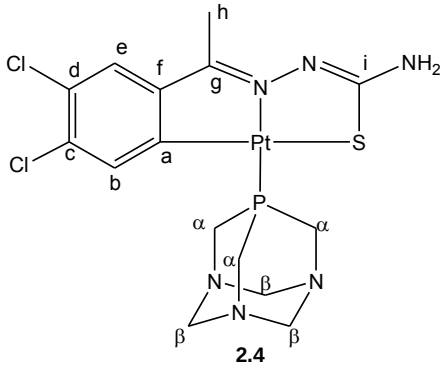

2.4

1,3,5-Triaza-7-phosphaadamantane (0.0383 g, 0.244 mmol) was reacted with complex **2.2** (0.102 g, 0.0558 mmol). The product (**2.4**) was isolated as an orange amorphous solid (0.102 g, 74 %.). Mp: 303-304 ºC, decomposition without melting. ^{1}H NMR (400.22 MHz, DMSO-d_6): δ (ppm) = 7.19-7.20 (m, 4H, H_e, NH_2, H_b), 4.51 (q, 6H, $^{1}J(H_{\beta(axial)}H_{\beta(equatorial)})$: 13.10 and 13.48 Hz, H_β), 4.20 (s, 6H, H_α), 2.28 (s, 3H, H_h). ^{13}C NMR (100.65 MHz, DMSO-d_6): δ (ppm) = 177.7 (C_i), 166.7 (C_g), 154.8 (C_a), 152.6 (C_f), 135.3 (C_c), 133,15 (C_d), 127.9 (C_e), 125.7 (C_b), 72.43 (C_α), 51.0 (C_β), 13.6 (C_h). ^{31}P NMR (162.00 MHz, DMSO-d_6): δ (ppm) = -65.70 (PPh_3, ^{1}J(Pt-P): 1680 Hz). IR (KBr, cm^{-1}) υ = 3413 (s, N-H), 3257 (s, N-H), 1621 (s, C=N), 1563 (m, C=N), 1501 (s, C=C aromatics). Elemental Analysis for $C_{15}H_{19}Cl_2N_6PPtS$: found C, 29.63; H, 3.23; N, 13.91 %; calculated C, 29.42; H, 3.13; N, 13.72. ESI-MS: *m/z* 613.0 $[M+H]^+$, 100%.

*2.4.4.3. [Pt_2(3,4-Dichloroacetophenone thiosemicarbazone)$_2$(dppf)] (**2.5**)*

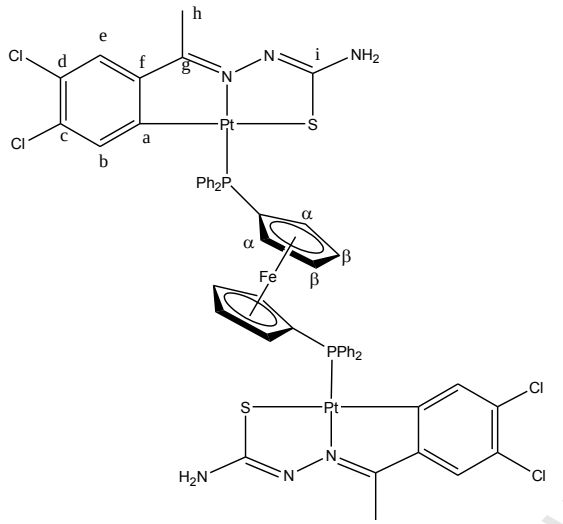

2.5

Bis(diphenylphosphinoferrocene) (0.0657 g, 0.118 mmol) was reacted with complex **2.2** (0.106 g, 0.0580 mmol). The product (**2.5**) was isolated as an orange amorphous solid (0.120 g, 70 %). Mp: 225-227 ºC. ^{1}H NMR (400.22 MHz, DMSO-d_6): δ (ppm) = 7.42-7.54 (m, 20H, PPh_2), 7.17 (s, 2H, H_e), 7.15 (s, 4H, NH_2), 6.13(s, 2H, H_b, ^{3}J(Pt-H): 20.0 Hz), 5.04 (br s, 4H, $H_α$), 4.23 (br s, 4H, $H_β$), 2.36 (s, 6H, H_h). ^{13}C NMR (75.46 MHz, DMSO-d_6): δ (ppm) = 177.1 (C_i), 166.5 (C_g), 154.1 (C_a), 152.0 (C_f), 132.9 (PPh_2), 131.0 (C_c and C_d), 128.0 (PPh_2) 126.7 (C_e), 124.8 (C_b), 73.5 – 74.9 ($C_α$ and $C_β$), 13.1 (C_h). ^{31}P NMR (162.00 MHz, DMSO-d_6): δ (ppm) = 11.62 (PPh_2, ^{1}J(Pt-P): 1881.8 Hz). IR (KBr, cm^{-1}) υ = 3475 (s, N-H), 3383 (s, N-H), 1595 (s, C=N), 1573 (m, C=N), 1499 (s, C=C aromatics). Elemental Analysis for $C_{52}H_{42}Cl_4FeN_6P_2Pt_2S_2$: found C, 42.36; H, 2.71; N, 5.53 %; calculated C, 42.64; H, 2.89; N, 5.74. ESI-MS: *m/z* 1465.0 $[M+H]^+$, 100%.

*2.4.4.4. [Pt_2(3,4-Dichloroacetophenone thiosemicarbazone)$_2$(dppe)] (**2.6**)*

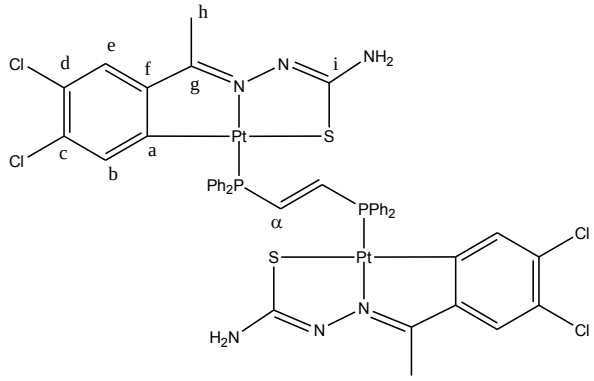

2.6

Trans-bis(diphenylphosphino)ethylene (0.0468 g, 0.118 mmol) was reacted with complex **2.2** (0.102 g, 0.0557 mmol). The product (**2.6**) was isolated as an orange amorphous solid (0.0976g, 67 %). Mp: 312-314 ºC. ^{1}H NMR (400.22 MHz, DMSO-d_6): δ (ppm) = 7.31-7.52 (m, 22H, $H_α$, PPh_2), 7.13(s, 2H, H_e), 7.12 (s, 4H, NH_2), 6.30 (s, 2H, H_b, ^{3}J(Pt-H): 24.1 Hz), 2.33 (s, 6H, H_h). ^{13}C NMR (100.65 MHz, DMSO-d_6): δ (ppm) = 177.3 (C_i), 167.4 (C_g), 154.6 (C_a), 152.4 (C_f), 135.0 ($C_α$), 134.0 (PPh_2), 132.11 (C_c and C_d), 129.3 (PPh_2) 127.5 (C_e), 125.7 (C_b), 13.7 (C_h). ^{31}P NMR (162.00 MHz, DMSO-d_6): δ (ppm) = 16.25 (t, PPh_2, ^{3}J(P-P): 22.80 Hz, ^{1}J(Pt-P): 1870.0 Hz). IR (KBr, cm^{-1}) υ = 3456 (s, N-H), 3324 (s, N-H), 1627 (s, C=N), 1606 (m, C=N), 1492 (s, C=C aromatics). Elemental Analysis for $C_{44}H_{36}Cl_4N_6P_2Pt_2S_2$: found C, 40.67 %; H, 2.95; N, 6.65; calculated C, 40.44; H, 2.78; N, 6.43 %. ESI-MS: *m/z* 1307.0 $[M+H]^+$, 100%.

*2.4.4.5. [Pt_2(3,4-Dichloroacetophenone thiosemicarbazone)$_2$(dppp)] (**2.7**)*

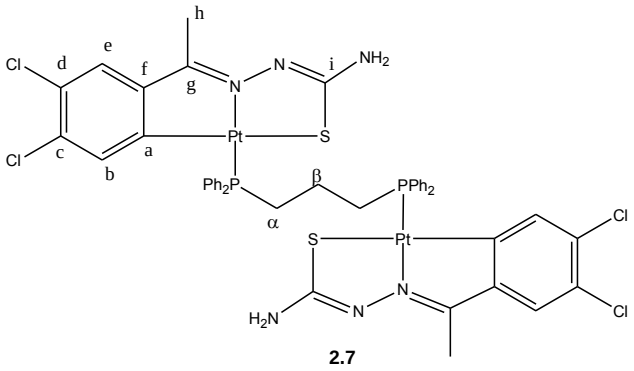

2.7

1,3-bis(diphenylphosphino)propane (0.0493 g, 0.120 mmol) was reacted with complex **2.2** (0.107 g, 0.0589 mmol). The product (**2.7**) was isolated as an orange amorphous solid (0.0988g, 63 %). Mp: 307-310 ºC, decomposition without melting. ^{1}H NMR (400.22 MHz, DMSO-d_6): δ (ppm) = 7.90-7.60 (m, 8H, PPh_2) 7.60-7.30 (m, 12H, PPh_2), 7.12 (s, 2H, H_e), 7.05 (s, 4H, NH_2), 6.16 (s, 2H, H_b, ^{3}J(Pt-H): 22.95 Hz), 2.81 (m, 4H, H_α), 2.32 (s, 6H, H_h), 1.76 (br s, 2H, H_β). ^{13}C NMR (100.65 MHz, DMSO-d_6): δ (ppm) = 177.2 (C_i), 166.1 (C_g), 154.3 (C_a), (C_f), 132.6 (PPh_2), (C_c and C_d), 128.3 (PPh_2) (C_e), (C_b), 29.3 (C_α), 20.66 (C_β), (C_h). ^{31}P NMR (162.00 MHz, DMSO-d_6): δ (ppm) = 16.55 (PPh_2, ^{1}J(Pt-P): 1845.9 Hz). Elemental Analysis for $C_{45}H_{40}Cl_4N_6P_2Pt_2S_2$: found C 41.02, H 3.41, N 6.24 %; calculated C, 40.86; H, 3.05; N, 6.35; S, 4.85%. ESI-MS: *m/z* 1323.0 $[M+H]^+$, 100%.

2.4.5. Reactivity Studies: Oxidative Addition Reaction

*2.4.5.1. [Pt(3,4-Dichloro-acetophenone thiosemicarbazone)(C_7H_7)(PTA)I] (**2.8**)*

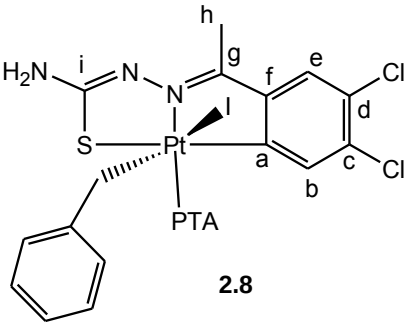

2.8

Complex **2.4** (0.1006 g, 0.1643 mmol) was suspended in DCM (10 cm^3) and the appropriate iodomethylbenzene (0.0361 g, 0.1656 mmol) was added. The reaction mixture was refluxed for 18 hours, cooled to room temperature and the product (**2.8**) was isolated as a pale orange solid (0.0873 g, 64 % crude yield) by vacuum filtration, washed with DCM (2 x 5 cm^3) and dried.

^{1}H NMR (400.22 MHz, DMSO-d_6): δ (ppm) = 7.55 (s, 5H, Ar-H), 7.20-7.23 (m, 3H, H_e and NH_2), 7.11 (s, 1H, H_b), 4.00 – 5.50 ppm (m, 14H, PTA-H and Ar-CH_2), 2.31 (s, 3H, H_h). ^{31}P NMR (162.00 MHz, DMSO-d_6): δ (ppm) = -39.80 (PPh_2, ^1J(Pt-P): 1778 Hz). IR (KBr, cm^{-1}) υ = 1601 (s, C=N), 1574 (m, C=N). ESI-MS: *m/z* 704 $[M-I]^+$, 100%.

2.4.6. X-ray Structure Analysis

Crystals suitable for single-crystal X-ray diffraction of complexes **2.2·3DMSO**, **2.3·2DMSO** and **2.4** were grown from the DMSO-d_6 NMR samples by exposure of the solutions to air. X-ray single crystal intensity data were collected on a Nonius Kappa-CCD diffractometer using graphite monochromated MoKα radiation (λ = 0.71073 Å). Temperature was controlled by an Oxford Cryostream cooling system (Oxford Cryostat). The strategy for the data collections was evaluated using the Bruker Nonius "Collect" program. Data were scaled and reduced using DENZO-SMN software.[106] Absorptions corrections were performed using SADABS.[107] The structure was solved by direct methods and refined employing full-matrix least-squares with the program SHELXL-97[108] refining on F^2.Packing diagrams were produced using the program PovRay and graphic interface X-seed.[109] For complex **2.2·3DMSO**, all non-hydrogen atoms, except the carbon and oxygen atoms on one of the DMSO molecules, were

refined anisotropically. All hydrogen atoms were positioned geometrically with distance of N-H being 0.88 Å and C-H distances ranging from 0.95 Å to 0.98 Å and refined as riding on their parent atoms, with U_{iso} (H) = 1.2 - 1.5 U_{eq} (C or N). In the asymmetric unit, one DMSO molecule is on general positions. Another one is on twofold rotation axis and it is disordered and shows high thermal motions, therefore the carbon and oxygen atoms were refined isotropically and the hydrogen atoms were not placed. The complex **2.2** main molecule is located at special positions on twofold rotation axis. The structure was refined successfully to R factor of 0.0204. For complex **2.3·2DMSO**, all non-hydrogen atoms were refined anisotropically. All the hydrogen atoms, except those on the N3 atom, were placed in idealised positions in a riding model with U_{iso} set at 1.2 or 1.5 times those of their parent atoms and fixed C-H bond lengths ranging from 0.95 Å to 0.98 Å. The hydrogen atoms H3A and H3B on N3 were located in the difference electron density maps and refined with simple bond lengths constraints. One DMSO molecule was disordered over two positions with site occupancy of 0.5 each. For complex **2.4**, All non-hydrogen atoms were refined anisotropically. All the hydrogen atoms were placed in idealised positions in a riding model with U_{iso} set at 1.2 or 1.5 times those of their parent atoms and restrained with fixed bond lengths ranging from 0.95 Å to 0.99 Å for C-H and 0.88 Å for N-H.

2.5. References

1. X. Du, C. Guo, E. Hansel, P. S. Doyle, C. R. Caffery, T. P. Holler, J. H. McKerrow and F. E. Cohen, *J. Med. Chem.*, **2002**, *45*, 2695.
2. R. B. De Oliveira, E. M. De Souza-Fagundes, R. P. P. Soares, A. A. Andrade, A. U. Krettli and C. L. Zani, *Eur. J. Med. Chem.*, **2008**, *43*, 1983.
3. K. J. Duffy, A. N. Shaw, E. Delorme, S. B. Dillon, C. Erickson-Miller, L. Giampa, Y. Huang, R. M. Keenan, P. Lamb, N. Liu, S. G. Miller, A. T. Price, J. Rosen, H. Smith, K. J. Wiggall, L. Zhang and J. I. Luengo, *J. Med. Chem.*, **2002**, *45*, 3573.
4. M. Abid, S. M. Agarwal and A. Azam, *Eur. J. Med. Chem.*, **2008**, *43*, 2035.
5. A. Walcourt, M. Loyevsky, D. B. Lovejoy, V. R. Gordeuk and D. R. Richardson, *Int. J. Biochem. Cell Biol.*, **2004**, *36*, 401.
6. N. Fujii, J.P. Mallari, E.J. Hansell, Z. Mackey, P. Doyle, Y.M. Zhou, J. Gut, P.J. Rosenthal, J.H. Mckerrow and R.K. Guy, *Bioorg. Med. Chem. Lett.*, **2005**, *15*, 121.
7. C. Costello, T. Karpanen, P. A. Lambert, P. Mistry, K. J. Parker, D. L. Rathbone, J. Ren, L. Wheeldon and T. Worthington, *Bioorg. Med. Chem. Lett.*, **2008**, *18*, 1708.
8. S. A. Khan and M. Yusuf, *Eur. J. Med. Chem.*, **2009**, *44*, 2597.
9. S. A. Khan, P. Kumar, R. Joshi, P. F. Iqbal and K. Saleem, *Eur. J. Med. Chem.*, **2008**, *43*, 2029.
10. I. Dilovic, M. Rubcic, V. Vrdoljak, S.K. Pavelic, M. Kralj, I. Piantanida and M. Cindric, *Bioorg. Med. Chem*, **2008**, *16*, 5189.
11. M.-C. Liu, T.S. Lin and A.C. Sartorelli, *J. Med. Chem.*, **1992**, *35*, 3672.
12. H. G. Petering, H. H. Buskirk and G. E. Underwood, *Cancer Res.*, **1964**, *24*, 367.
13. J. M. Kolesar, W. R. Schelman, P. G. Geiger, K. D. Holen, A. M. Traynor, D. B. Alberti, J. P. Thomas, C. R. Chitambar, G. Wilding and W. E. Antholine, *J. Inorg. Biochem.*, **2008**, *102*, 693.
14. D. Kovala-Demertzi, M.A. Demertzis, E. Filou, A.A Pantazaki, P.N. Yadav, J.R. Miller, Y. Zheng and D.A. Kyriakidis,, *Biometals*, **2003**, *16*, 411.
15. K. C. Agrawal, B. A. Booth, E. C. Moore and A. C. Sartorelli, *J. Med. Chem.*, **1972**, *15* (11), 1154.
16. J. H. McKerrow, E. Sun, P. J. Rosenthal and J. Bouvier, *Annu. Rev. Microbiol.*, **1993**, *47*, 821.
17. P. J. Rosenthal, *Int J Parasitol.*, **2004**, *34*, 1489.

18. S. E. Francis, D. J. Sullivan Jr and D. E. Goldberg, *Annu. Rev. Microbiol.*, **1997**, *51*, 97.
19. D. Sweeney, M. L. Raymera and T. D. Lockwood, *Biochem. Pharm.*, **2003**, *66*, 663.
20. A. Chipeleme, J. Gut, P. J. Rosenthal and K. Chibale, *Biorganic and Medicinal Chemistry*, **2007**, *15*, 273.
21. V. L. Lew, T. Tiffert and H. Ginsburg, *Blood*, **2003**, *101*, 4189.
22. M. N. Hughes; *The Inorganic Chemistry of Biological Processes*; John Wiley: Chichester, 1981.
23. H. Beraldo and D. Gambino, *Mini-reviews in Medicinal Chemistry*, **2004**, *4*, 31.
24. N. Farrel, *Coord. Chem. Rev.*, **2002**, *232*, 1.
25. B. Lippert; *Cisplatin. Chemistry and Biochemistry of a Leading Anticancer Drug*; VCHA & Wiley-VCH: Zurich, 1999.
26. C. G. Hartinger, A. D. Phillips and A. A. Nazarov, *Curr. Top. Med. Chem.*, **2011**, *11*, 2688.
27. A. Garoufis, S. K. Hadjikakou and N. Hadjiliadis, *Coord. Chem. Rev.,* , **2009**, *253*, 1384.
28. A. Garoufis, S. K. Hadjikakou and N. Hadjiliadis, In *Metallotherapeutic Drugs and Metal-based Diagnostic Agents: The Use of Metals in Medicine*; Eds. M. Gielen and E.R.T Tiekink, Ed.; Chichester: John Wiley & Sons Ltd, 2005.
29. Z. Guo and P.J. Sadler, *Angew. Chem. Int. Ed.*, **1999**, *38*, 1512.
30. P. C. A. Bruijnincx and P. J. Sadler, *Curr. Opin. Chem. Biol.*, **2008**, *12*, 197.
31. M. A. Jakupec, M. Galanski, V. B. Arion, C. G. Hartinger and B. K. Keppler, *Dalton Trans.*, **2008**, 183.
32. W. -H. Zhang, S. W. Chien and T. S. A. Hor, *Coord. Chem. Rev.*, **2011**, *255*, 1991.
33. T. S. Lobana, R. Rekha, R. J. Butcher, A. Castineiras, E. Bermejo and P. V. Bharatam, *Inorg. Chem.*, **2006**, *45*, 1535.
34. T. S. Lobana, S. Khanna and R. J. Butcher, *Z. Anorg. Allg. Chem.*, **2007**, *633*, 1820.
35. T. S. Lobana, S. Khanna, R. J. Butcher, A. D. Hunter and M. Zeller, *Inorg. Chem.*, **2007**, *46*, 5826.
36. E. M. Jouad, A. Riou, M. Allain, M. A. Khan and G. M. Bouet,, *Polyhedron*, **2001**, *20*, 67.
37. S. Lhuachan, S. Siripaisarnpipat and N. Chaichit, *Eur. J. Inorg. Chem.*, **2003**, 263.
38. E. Bermejo, R. Carballo, A. Castineiras, R. Domınguez, C. M. Mossmer, J. Strahle and D. X. West,, *Polyhedron*, **1999**, *18*, 3695.

39. Z. Lu, C. White, A. L. Rheingold and R. H. Crabtree, *Inorg. Chem.*, **1993**, *32*, 3991.

40. T. S. Lobana, R. Sharma, G. Bawa and S. Khanna, *Coord. Chem. Rev.*, **2009**, *253*, 977.

41. M. A. Ali and S. E. Livingstone, *Coord. Chem. Rev.*, **1974**, *13*, 115.

42. M. Cindric, M. Rubcic, I. Dilovic, G. Giester and B. Kamenar, *Croat. Chem. Acta*, **2007**, *80* (3-4), 583.

43. N. A. Mangalam and M. R. P. Kurup, *Spectrochim. Acta, Part A*, **2009**, *71*, 2040.

44. P. Ren, T. Liu, J. Qin and C. Chen, *Spectrochim. Acta, Part A*, **2003**, *59*, 1095.

45. R. M. El-Shazly, G.A.A Al-Hazmi, S.E. Ghazy, M.S. El-Shahawi and A.A. El-Asmy, *J. Coord. Chem.*, **2006**, *59*, 845.

46. J. S. Casas, M. V. Castano, M. C. Cifuentes, J. C. Garcia-Monteagudo, A. Sanchez, J. Sordo and U. Abram, *J. Inorg. Biochem.*, **2004**, *98*, 1009.

47. V. M. Leovac, L. S. Jovanovic, V. S. Jevtovic, G. Pelosi and F.Bisceglie, *Polyhedron*, **2007**, *26*, 2971.

48. Z. Afrasiabi, E. Sinn, W. Lin, Y. Ma, C. Campana and S. Padhye,, *J. Inorg. Biochem.*, **2005**, *99*, 1526.

49. S. Laly and G. Parameswaran, *Asian J. Chem.*, **1993**, *5* (3), 712.

50. B. Garcia, J. Garcia-Tojal, R. Ruiz, R. Gil-Garcia, S. Ibeas, B. Donnadieu and J. M. Leal, *J. Inorg. Biochem.*, **2008**, *102*, 1892.

51. M. B. Ferrari, S. Capacchi, G. Pelosi, G. Reffo, P. Tarasconi, R. Albertini, S. Pinelli and P. Lunghi, *Inorg. Chim. Acta*, **1999**, *286*, 134.

52. J. P. Scovill, D. L. Klayman and C. F. Franchino, *J. Med. Chem.*, **1982**, *25* (10), 1261.

53. J. Patole, S. Padhye, M. S. Moodbidri and N. Shirsat, *Eur. J. Med. Chem.*, **2005,**, *40*, 1052.

54. D. Pandiarajan and R. Ramesh, *Inorg. Chem. Commun.*, **2011**, *14*, 686.

55. B. Demoro, C. Sarniguet, R. Sánchez-Delgado, M. Rossi, D. Liebowitz, F. Caruso, C. Olea-Azar, V. Moreno, A. Medeiros, M. A. Comini, L. Otero and D. Gambino, *Dalton Trans.*, **2012**, *41*, 1534.

56. D. Kovala-Demertzi, P. N. Yadav, M. A. Demertzi, J. P. Jasiski, F. J. Andreadaki and I. D. Kostas, *Tet. Lett.*, **2004**, *45*, 2923.

57. I. D. Kostas, F. J. Andreadaki, D. Kovala-Demertzi, C. Prentjas and M. A. Demertzis, *Tet. Lett.*, **2005**, *46*, 1967.

58. K. S. O. Ferraz, L. Ferandes, D. Carrilho, M .C. X. Pinto, M. D. F. Leite, E. M. Souza–Fagundes, N. L. Speziali, I. C. Mendes and H. Beraldo, *Bioorg. Med. Chem.*, **2009**, *17*, 7138.

59. M. Vieites, P. Smircich, M. Pagano, L. Otero, L.L. Fischer, H. Terenzi, M.J. Prieto, V. Moreno, B. Garat and D. Gambino, *J. Inorg. Biochem.*, **2011**, *105*, 1704.

60. P. Kalaivani, R. Prabhakaran, F. Dallemer, P. Poornima, E. Vaishnavi, E. Ramachandran, V. V. Padma, R. Renganathan and K. Natarajan, *Metallomics*, **2012**, *4*, 101.

61. F. Beckford, D. Dourth, M. Shaloski Jr., J. Didion, J. Thessing, J. Woods, V. Crowell, N. Gerasimchuk, A. Gonzalez-Sarrías and N.P. Seeram, *J. Inorg. Biochem.*, **2011**, *105*, 1019.

62. F.A. Beckford, G. Leblanc, J. Thessing, M. Shaloski Jr, B.J. Frost, L. Li and N.P. Seeram, *Inorg. Chem. Commun.*, **2009**, *12*, 1094.

63. G. Raja, N. Sathya and C. Jayabalakrishnan, *J. Coord. Chem.*, **2011**, *64* (5), 817.

64. S. Grguric-Sipka, C.R. Kowol, S.-M. Valiahdi, R. Eichinger, M.A. Jakupec, A. Roller, S. Shova, V.B. Arion, B.K. Keppler, *Eur. J. Inorg. Chem.*, **2007**, (18), 2870.

65. P. Chellan, N. Shunmoogam-Gounden, D. T. Hendricks, J. Gut, P. J. Rosenthal, C. Lategan, P. J. Smith, K. Chibale and G. S. Smith, *J. Eur. Med. Chem.*, **2010**, 3520.

66. P. Chellan, S. Nasser, L. Vivas, K. Chibale and G. S. Smith, *J. Organomet. Chem.*, **2010**, *695*, 2225.

67. G. Xie, P. Chellan, J. Mao, K. Chibale, and G. S. Smith, *Adv. Synth. Catal.*, **2010**, *352* (10), 1641.

68. T. Stringer, B. Therrien, D.T. Hendricks, H. Guzgay and G. S. Smith, *Inorg. Chem. Comm.*, **2011**, *14* (6), 956.

69. P. Pelagatti, A. Venturini, A. Leporat, M. Carcelli, M. Costa, A. Bacchi, G. Pelizzi and C. Pelizzi, *J. Chem. Soc., Dalton Trans.*, **1998**, 2715.

70. A. G. Quiroga and C. N. Ranninger, *Coordination Chemistry Reviews*, **2004**, *248*, 119.

71. J. S. Casas, E. E. Castellano, J. Ellena, M. S. García-Tasende, M. L. Pérez-Parallé, A. Sánchez, Á. Sánchez-González, J. Sordo and Á. Touceda, *J. Inorg. Biochem.*, **2008**, *102*, 33.

72. G. A. Al-Hazmi, N. M. El-Metwally, O. A. El-Gammal and A. A. El-Asmy, *Spectrochim. Acta A* **2008**, *69*, 56.

73. D. Kovala-Demertzi, P. N. Yadav, M. A. Demertzis and M. Coluccia, *J. Inorg. Biochem.*, **2000** *78*, 347.

74. A. I. Matesanz, J. Perles and P. Souza, *Dalton Trans.*, **2012**, *41*, 12538.

75. D. Santos, B. Parajón-Costa, M. Rossi, F. Caruso, D. Benítez, J. Varela, H. Cerecetto, M. González, N. Gómez, M. E. Caputto, A. G. Moglioni, G. Y. Moltrasio, L. M. Finkielsztein and D. Gambino, *J. Inorg. Biochem.*, **2012**, *117*, 270.

76. S. Halder, P. Paul, S. -M. Peng, G. -H. Lee, A. Mukherjee, S. Dutta, U. Sanyal and S. Bhattacharya, *Polyhedron*, **2012**, *45*, 177.

77. J. P. Scovill, D. L. Klayman and D. G. Franchino, *J. Med. Chem.*, **1982**, *25*, 1261.

78. J. S. Lewis, J. M. Connet, J. R. Garbow, T. L. Buettner, Y. Fujibayashi, J. W. Fleshman and M. J. Welch, *Cancer Res.*, **2002**, *62*, 445.

79. R. I. Maurer, P. J. Blower, J. R. Dilworth, C. A. Reynolds, Y. Zheng and G. E. Mullen, *J. Med. Chem.*, **2002**, *45*, 1420.

80. C. Navarro-Ranninger, I. López-Solera, J. M. Pérez, J. H. Rodriguez-Ramos, J. L. García-Ruano, P. R. Raithby, J. R. Masaguer and C. Alonso, *J. Med. Chem.*, **1993**, *36*, 3795.

81. C. Navarro-Ranninger, I. López-Solera, V. González, J. M. Pérez, A. Alvarez-Valdés, A. Martín, P. R. Raithby, J. R. Masaguer and C. Alonso, *Inorg. Chem.*, **1996**, *35*, 5181.

82. J. Reedijk, *J. Chem. Soc., Chem. Commun.*, **1996**, 801.

83. A. G. Quiroga, J. M. Pérez, C. Alonso and C. Navarro-Ranninger *App. Organomet. Chem.*, **1998**, *12*, 809.

84. A. G. Quiroga, J. M. Perez, I. Lopez-Solera, J. R. Masaguer, A. Luque, P. Roman, A. Edwards, C. Alonso and C. Navarro-Ranninger, *J. Med. Chem.*, **1998**, *41*, 1399.

85. A. I. Matesanz, C. Herńandez, A. Rodríguez, and P. Souza, *Dalton Trans.*, **2011**, *40*, 5738.

86. J. A. Castillo-Garit, M. C. Vega, M. Rolón, Y. Marrero-Ponce, A. Gómez-Barrio, J. A. Escario, A. A. Bello, A. Montero, F. Torrens, F. Pérez-Giménez, V. J. Arán and C. Abad, *Eur. J. Med. Chem.*, **2011** *46*, 3324

87. R. V. C. Guido, G. H. G. Trossini, M. S. Castilho, G. Oliva, E. I. Ferreira and A. D. Andricopulo, *J. Enzym. Inhib. Med. Chem.*, **2008**, *23* (6), 964.

88. S. Komeda, *Metallomics*, **2011**, *3*, 650.

89. S. Ahmad, *Chem. Biodivers.*, **2010**, *7*, 543.

90. T. S. Lobana, G. Bawa, R. J. Butcher, B. -J. Liaw and C.W. Liu, *Polyhedron*, **2006**, *25*, 2897.

91. T. S. Lobana, A. Sánchez, J. S. Casas, A. Castiñeiras, J. Sordo, M. S. García-Tasende and E. M. Vázquez-López, *J. Chem. Soc. Dalton Trans.*, **1997**, 4289.

92. T. S. Lobana, S. Khanna, R. J. Butcher, A. D. Hunter and M. Zeller, *Polyhedron*, **2006**, *25*, 2755.

93. D. Vazquez-Garcıa, A. Fernandez, J. J. Fernandez, M. Lopez-Torres, A. Suarez, J. M. Ortigueira, J. M. Vila and H. Adams, *J. Organomet. Chem.*, **2000**, *595*, 199.

94. T. G. Appleton and J. R. Hall, *Inorg. Chem.*, **1971**, *10* (8), 1717.

95. G. Natile, L. Maresca and L. Cattalini, *J. Chem. Soc, Chem. Commun.*, **1976**, 24.

96. P. Smolenski and A. J. L. Pombeiro, *Dalton Trans.*, **2008**, 87.

97. P. Smolenski, C. Dinoi, M. Fatima, C. G. da Silva and A. J. L. Pombeiro, *J. Organomet. Chem.*, **2008**, *693*, 2338.

98. A. G. Quiroga, J. M. Perez, I. Lopez-Solera, J. R. Masaguer, A. Luque, P. Roman, A. Edwards, C. Alonso, C. Navarro-Ranninger, *J. Med. Chem.*, **1998**, *41*, 1399.

99. L. E. Shutton; *Tables of Interatomic Distances and Configurations in Molecules and Ions (Supplement);*; The Chemical Society: London, 1965.

100. Z. Afrasiabi, E. Sinn, W. Lin, Y. Ma, C. Campana and S. Padhye, *J. Inorg. Biochem.*, **2005**, *99*, 1526.

101. T. S. Lobana, G. Bawa, G. Hundal and M. Zeller, *Z. Anorg. Allg. Chem.*, **2008**, *634*, 931.

102. D. Vazquez-Garcıa, A. Fernandez, J. J. Fernandez, M. Lopez-Torres, A. Suarez, J. M. Ortigueira, J. M. Vila and H. Adams, *J. Organomet. Chem.*, **2000**, *595*, 199.

103. S. Achar, J. J. Vittal and R. J. Puddephatt, *Organometallics*, **1996**, *15*, 43.

104. S. Achar and R. J. Puddephatt, *J. Chem. Soc., Chem. Commun.*, **1994**, *1985-1986*,

105. G. Natile, L. Maresca and L. Cattalini, *J. Chem. Soc., Chem. Commun.*, **1976**, 24.

106. Z. Otwinowski and W. Minor; *Methods in Enzymology, Macromolecular Crystallography*; Academic Press New York, 1997.

107. G. M. Sheldrick, *SADABS*; University of Göttingen, Germany, 1997.

108. G. M. Sheldrick, SHELXL-97 and SHELXS-97, *Program for Crystal Structure Refinement*; University of Göttingen, Germany, 1997.

109. L. J. Barbour, *J. Supramol. Chem.*, **2001**, *1*, 189.

CHAPTER 3

In vitro Pharmacological Evaluation of Mono-, Di- and Tetranuclear Cycloplatinated Thiosemicarbazone Complexes

3.1. Introduction

The study of platinum-based cancer therapeutics is a well-established area of research. The most well-known clinically used drugs today are cisplatin and its analogues (Figure 3.1).[1,2] As discussed in Chapter 1, while these drugs have proven effective for the treatment of several cancers, there are several drawbacks to their use. In the case of cisplatin, patients tend to develop tumor resistance overtime and systemic side effects such as ototoxicity, neurotoxicity and nephrotoxicity are common. Additionally, a large portion of the intravenously administered dose of cisplatin is deactivated before it can reach its target.[3] These serious shortcomings have bred a need for the design of platinum complexes that are more robust; compounds that can maintain their structural integrity during transport and then deliver the bioactive species to its intended target.

Complexes containing ligands that can chelate to platinum in a bi- or tridentate manner may be less susceptible to decomposition and thus more likely to reach their cancer targets intact. Thiosemicarbazones are well-known for their ability to chelate to a variety of metals in a polydentate fashion.[4] These compounds have also exhibited biological activity *in vitro* as antiparasitics,[5-10] and antitumoral agents.[11-15] Their antiproliferative activities are believed to arise from their ability to arrest DNA synthesis through inhibition of ribonucleotide reductase.

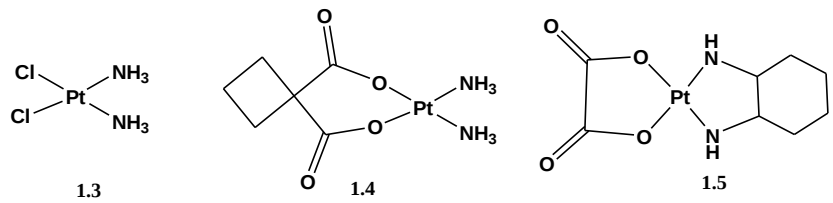

1.3 **1.4** **1.5**

Figure 3.1. Structures of cisplatin (**1.3**), carboplatin (**1.4**) and oxaliplatin (**1.5**).[1,2]

Examples of platinum thiosemicarbazone complexes as *in vitro* antitumoral agents have been reported. The tetraplatinum complex **I** and mononuclear complex **II** (Figure 3.2.) have both

been screened against several antitumoral cell lines.[16,17] In most cases, they exhibited *in vitro* cytotoxicities that were significantly better than cisplatin.

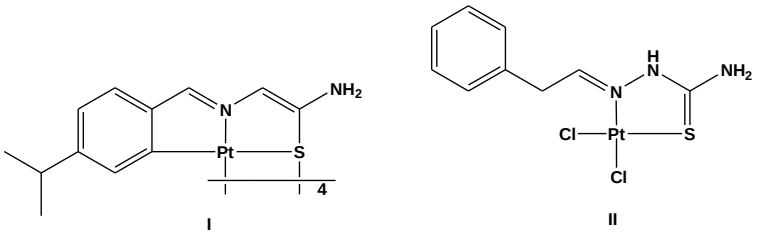

Figure 3.2. The tetranuclear and mononuclear platinum complexes **I** and **II**.[16,17]

A series of di- and trinuclear platinum thiosemicarbazone complexes (**III** - **XI**, Figure 3.3.) where each thiosemicarbazone moieity coordinates to the metal as a tridentate donor have shown moderate to low cytotoxicities against the oesophageal cancer cell line WHCO1.[18]

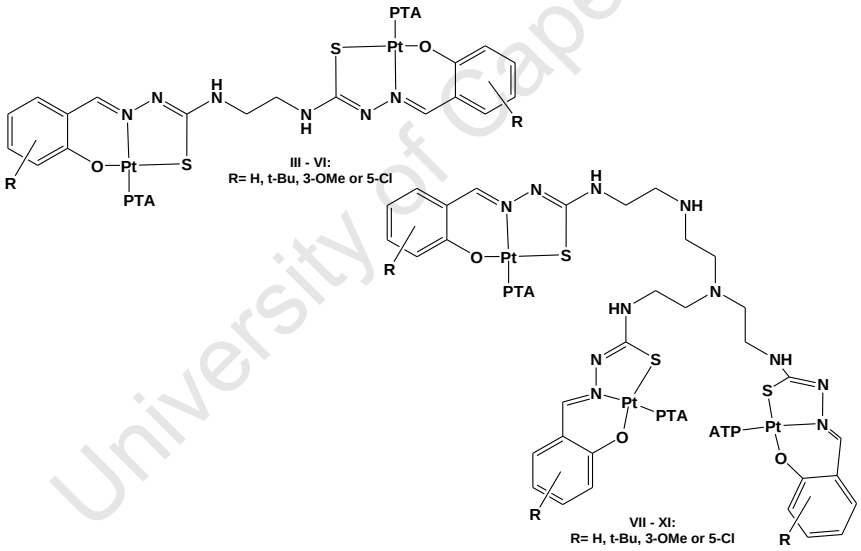

Figure 3.3. Di- (**III-VI**) and trinuclear (**VII-XI**) thiosemicarbazone Pt(II) complexes screened for antitumor activity against WHCO1 cell line.[18]

In the study of thiosemicarbazones as biological agents, these compounds have also emerged as promising candidates for the treatment of parasitic diseases.[5-10] Their *in vitro* antiparasitic activities have been studied extensively and their modes of action are believed to arise from several possible inhibitory mechanisms. Thiosemicarbazones may affect processes associated with hemoglobin (Hb) digestion in the food vacuole of the parasite. Their ability to chelate endogenous metals such as Fe(III) can inhibit parasite growth by withholding it from metal dependent enzymes such as ribonucleotide reductase and enzymes in the heme biosynthetic

pathway.[9,19] Alternatively, the resulting chelate complexes could inhibit cysteine proteases, effectively enhancing the natural inhibitory effect of endogenous metals on the protease catalytic site.[20] Another possible mechanism of cysteine protease inhibition could be through covalent modification of the cysteine thiol groups within the parasite via the electrophilic centers (the thione carbon and/or imine carbon) of the thiosemicarbazone moiety. All of the above inhibitory mechanisms would compromise the parasite's ability to degrade host hemoglobin required for parasite protein synthesis.[21-24]

The study of thiosemicarbazone complexes containing metals from the Platinum Group series as antiparasitic agents is still a relatively new area of research. An extensive series of mononuclear [O,N,S] tridentate Pd(II) and Pt(II) thiosemicarbazone complexes (**3.12-3.23**, Figure 3.3.) have been reported to exhibit moderate activity as antiparasitics against *P. falciparum* strains and *T. vaginalis*. Against the *Trichomonas vaginalis* parasite strain T1, the palladium and platinum complexes containing the 4-picoline ancillary ligand showed high % inhibitions of parasite growth.[25]

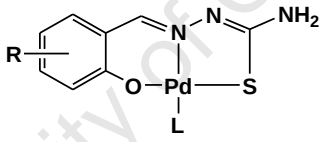

R = H, L = PPh_3 (**XII**), PTA (**XIII**), 4-picoline (**XIV**)
R = 3-OMe, L = PPh_3, (**XV**) PTA (**XVI**), 4-picoline (**XVII**)
R = 3-^{t}Bu, L = PPh_3 (**XVIII**), PTA (**XIX**), 4-picoline (**XX**)
R = 5-Cl, L = PPh_3 (**XXI**), PTA (**XXII**), 4-picoline (**XXIII**)

Figure 3.3. Library of Pd(II) thiosemicarbazone complexes studied for *in vitro* activity against *T. vaginalis.*[25]

We have recently reported on the synthesis and antiplasmodial activity of cyclopalladated mono-, di- and tetranuclear thiosemicarbazone complexes (Complexes **1.96**-**1.105**, Figure 3.4.).[26] These compounds exhibited moderate to low antiparasitic activity *in vitro*.

Based on the moderate activities displayed by these Pd(II) complexes, we wanted to evaluate how changing the metal to platinum would affect the bioactivies of the cyclometalated compounds. In this chapter, the *in vitro* evaluation of the mono-, di- and tetranuclear cycloplatinated thiosemicarbazone complexes **2.2**-**2.6** as antitumoral and antiparasitic agents will be discussed. An NMR study of the stability of these complexes in the presence of certain short peptides and an amino acid will also be presented. Preliminary studies into their

potential mechanism of action with respect to inhibition of β-hematin formation were also completed.

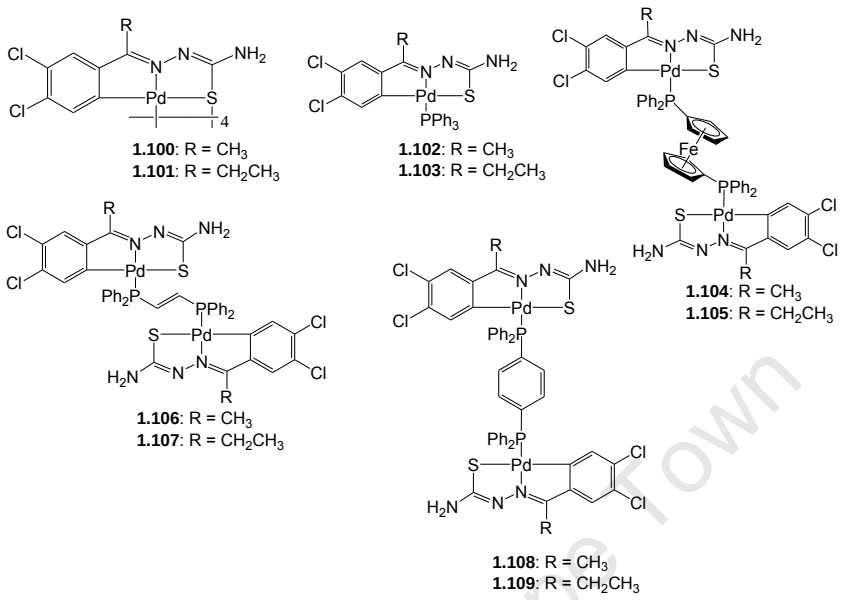

Figure 3.4. Cyclopalladated thiosemicarbazone complexes **1.96** – **1.105**.[26]

3.2. *In vitro* Screening of Thiosemicarbazone Complexes

3.2.1. In Vitro Antitumour Activity

The *in vitro* antiproliferative effect of compounds **2.1**- **2.6** (Figure 3.5) was evaluated against the cisplatin sensitive (A2780) and cisplatin resistant (A2780*cis*R) ovarian cancer cell lines. Table 3.1 lists the IC_{50} data ascertained for **2.1**-**2.6**. Ligand **2.1** exhibited the highest activity out of all the compounds tested against both cell lines [IC_{50} = 11.3 μM (A2780) and 13.8 μM (A2780*cis*R)]. Cyclometalation of ligand **2.1** led to a decrease in *in vitro* activity against both cell lines which is in contrast to previous reports where cycloplatination had a beneficial effect on activity.[17,27-30] However, most of these published accounts of an increase in activity were determined in other tumor cell lines. In order to confirm that the cycloplatinated complexes **2.2**-**2.6** are less active than **2.1** as antitumor agents in general, all of the compounds (**2.1**-**2.6**) need to be screened against several cancer cell lines.

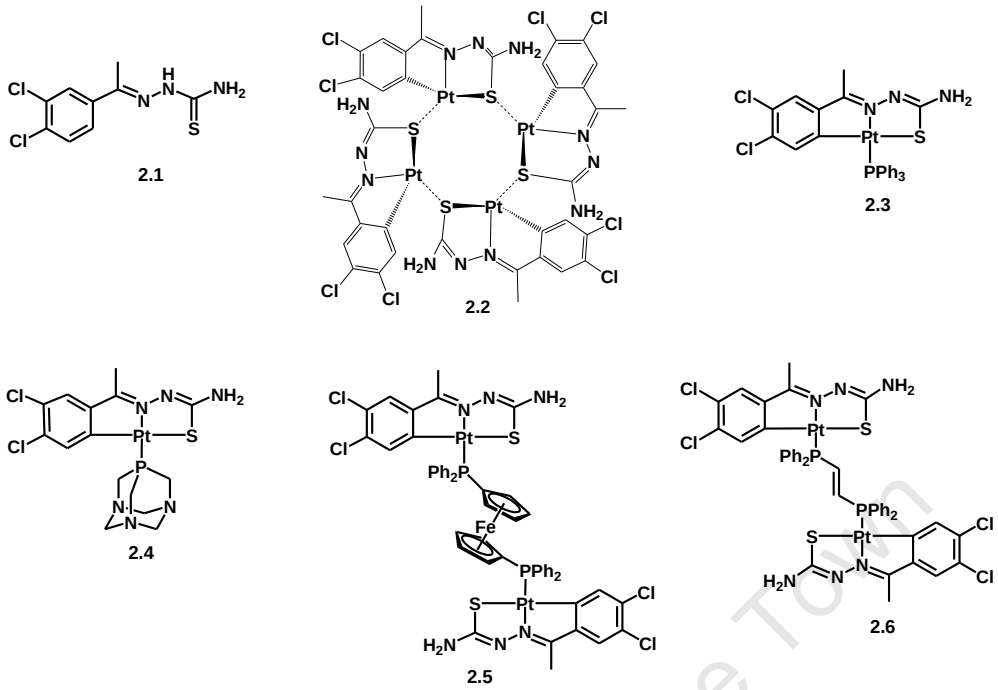

Figure 3.5. Compounds **2.1** – **2.6** that have been screened for *in vitro* pharmacological activity.

Complexes **2.2**-**2.5** are moderately cytotoxic against both cell lines with complex **2.4** showing the lowest IC_{50} values [IC_{50} = 21.20 μM (A2780) and 32.00 μM (A2780*cis*R)]. Complexes **2.2**, **2.4** and **2.5** are less active against the cisplatin resistant (A2780*cis*R) cell line, while complex **2.3** is more active in this cell line (IC_{50} = 99 μM) compared to A2780 (IC_{50} = 129 μM). While none of the compounds tested showed activities comparable to cisplatin against the A2780 cell line, ligand **2.1** shows a markedly better activity than cisplatin against the A2780*cis*R line. Despite having lower IC_{50} values compared to cisplatin, the calculated resistance indices for **2.1**-**2.6** are much lower than that of cisplatin suggesting that these types of complexes are markedly less susceptible to the same resistance mechanisms that inhibit cisplatin's activity against the A2780*cis*R cell line.[31]

Metalation of the thiosemicarbazone ligand seems to have an adverse effect on cytotoxicity and no direct correlation between the number of platinum-thiosemicarbazone moieties and pharmacological activity can be discerned. Against the A2780 cell line, the tetranuclear complex **2.2** (IC_{50} = 51.5 μM) is more active than complex **2.6** (IC_{50} = >200 μM) but is less active than the dppf containing complex **2.5** (IC_{50} = 36.5 μM). Instead, the type of ancillary ligand used in the design of platinum thiosemicarbazone chemotherapeutics may play a key

role in enhancing activity. The lipophilic nature of the phosphane in each complex could rationalize the trend in antiproliferative activity observed for **2.3**-**2.6**. Table 3.2 shows the calculated logP (ClogP) values of each phosphane used to prepare complexes **2.3**-**2.6**. These values were calculated using the ChemDraw Ultra 2010 version 12.0.2.1076 program.

Table 3.1. IC_{50}[a] determinations for **2.1**-**2.6** against A2780 and A2780*cis*R cancer cell lines

Compound	IC_{50} in A2780 (μM)	IC_{50} in A2780*cis*R (μM)	RI
2.1	11.3 ± 2.7	13.8 ± 2.6	1.22
2.2	51.5 ± 1.0	67.0 ± 10	1.11
2.3	129 ± 31	99.0 ± 4.7	0.76
2.4	21.2 ± 1.2	32.0 ± 7	1.51
2.5	36.5 ± 3.6	>200	--
2.6	> 200	175 ± 1.7	--
Cisplatin[b]	1.5	25.0	16.67

[a] IC_{50}: lowest compound concentration that inhibits 50 % of cell growth.
[b] IC_{50} values for cisplatin were determined using the same experimental assay and protocol as for **1**-**6** but were not determined at the same time as compounds **1**-**6**.

A logP value can be used as general guide to a compound's ability to enter a cell by passive diffusion.[32] High logP values indicate an affinity for lipids and suggest a compound is able to enter the lipid bilayer that surrounds cells.[32] However, a balance between lipophilicity and hydrophilicity is essential; if a compound is too lipophilic (high ClogP) then poor absorption or permeation from the lipid bilayer into the cytoplasm may be likely. The bis(diphenylphosphino)ethylene spacer displays the highest ClogP value (7.17) and most likely increases the lipophilic nature of complex **2.6** to such a degree that it cannot enter the cell and thus displays no significant activity against either cell line. Complex **2.3** and **2.5** have values of 5.68 and 5.01 respectively and complex **2.5** shows a much lower IC_{50} (36.5 μM) compared to **2.3** (129 μM) against the A2780 cell line. The improved activity of **2.5** compared to **2.3** may also be due to the presence of the ferrocenyl moiety. Incorporation of ferrocene into a molecule has been shown to increase antiproliferative activity.[33]

Table 3.2. Calculated ClogP values of each phosphane and the IC_{50} data of the corresponding complex

Phosphane	ClogP of Phosphane[a]	Complex	IC_{50} of Complex A2780 (μM)	IC_{50} in A2780*cis*R (μM)
PPh_3	5.68	**2.3**	129 ± 31	99.0 ± 4.7
PTA	-1.43	**2.4**	21.2 ± 1.2	32.0 ± 7
dppf	5.01	**2.5**	36.5 ± 3.6	>200
dppe	7.17	**2.6**	> 200	175 ± 1.7

[a] ClogP values were determined using the ChemDraw Ultra 2010 version 12.0.2.1076 program.

Complex **2.4** demonstrated the best IC_{50} out of all compounds tested against both cell lines and its ancillary ligand, PTA, has the lowest ClogP value (-1.43) indicating that this phosphane has a high hydrophilic nature. While PTA is not very lipophilic, its hydrophilic nature adds the right counter balance to the lipophilic nature of the Pt-TSC moiety (ClogP = 2.77) and may account for why this mononuclear complex has the best activity. This positive increase in activity has also been observed for other thiosemicarbazone complexes where replacement of the triphenylphosphane ligand with PTA led to higher activity.[18,34] The solubility of complex **2.4** in aqueous media could also be much higher compared to the other complexes as evidenced by Grguric-Sipka and co-workers who reported that changing the triphenylphosphane ligand in their ruthenium thiosemicarbazone complex to PTA yielded a water soluble derivative.[35]

Ultimately, *in vitro* assessment of compounds **2.1**-**2.6** revealed that the free ligand **2.1** was the best inhibitor of cell growth. However, the lower IC_{50} values observed for the complexes may likely be due to the phosphane ligands used for the preparation of **2.3**-**2.6**. Structural modification of the phosphanes, such as adding water soluble groups, to give added hydrophilicity to the cycloplatinated complex could very likely improve the pharmacological effect of these complexes as was observed for complex **2.4**. Replacement of the phosphane with another type of ancillary ligand such as a monodentate nitrogen ligand such as 4-picoline could also yield better antiproliferative activities.[36]

3.2.2. In Vitro Antiparasitic Activity

3.2.2.1. In vitro P. falciparum Activity

The antiparasitic activity of complexes **2.1** – **2.6** *in vitro* against two *Plasmodium falciparum* strains, D10 (chloroquine sensitive) and Dd2 (chloroquine resistant) and the *Trichomonas vaginalis* parasite strain T1 was determined. Table 3.3 shows the antiplasmodial data ascertained for compounds **2.1** – **2.6**. Ligand **2.1** did not exhibit significant activity against the D10 strain (IC_{50} = 95.8 μM). However, its cycloplatinated derivatives **2.2**-**2.4** do show much higher activity, suggesting the incorporation of platinum does influence the antiplasmodial activity of the thiosemicarbazone ligand. The tetranuclear complex **2.2** (IC_{50} = 32.29 μM) is 3 times more active than ligand **2.1**. Complexes **2.3** (IC_{50} = 19.93 μM) and **2.4** (IC_{50} = 21.42 μM) are respectively 5 and 4.5 times more active than ligand **2.1**. An increase

in antiplasmodial activity upon metalation has been observed for other thiosemicarbazone metal complexes. The cyclopalladated derivatives of **2.1** (complexes **1.96**, **1.98**, **1.100**, **1.102** and **1.104**, Figure 3.4, section 3.1) also displayed improved inhibition compared to **2.1** in the 3D7 (CQ sensitive) and K1 (CQ and pyrimethamine resistant) *P. falciparum* strains.[26] Gold(III) and gold(I) coordination complexes of **2.1** and other similar thiosemicarbazones have also demonstrated improved antiplasmodial activities over the free ligands.[37,38] Mononuclear arene-ruthenium complexes containing bidentate [N,S] aryl-thiosemicarbazone ligands were found to have enhanced inhibitory effects on the NF54 (CQ-sensitive) and Dd2 (CQ-resistant) *P. falciparum* strains[39] and the same trend was observed of bidentate Pd(II) and Pt(II) furfuryl-thiosemicarbazone complexes when tested against the W2 strain.[40]

Table 3.3. Antiplasmodial Data obtained for complexes **2.1**-**2.6**

Complex	D10: IC_{50}[a] (µM)	Dd2: IC_{50}[a] (µM)	RI[b]
2.1	95.8[c]	Not tested	--
2.2	32.29 ± 2.28	Not tested	--
2.3	19.93 ± 3.74	14.47 ± 1.98	0.72
2.4	21.42 ± 1.22	24.90 ± 3.24	1.16
2.5	Not active[d]	Not tested	--
2.6	Not active[d]	Not tested	--
Chloroquine diphosphate	0.012 ± 0.001	0.146 ± 2.08	12.17

[a] The minimum compound concentration required for 50 % inhibition *in vitro*.
[b] resistance index: determined as [IC_{50} Dd2]/[IC_{50} D10].
[c] IC_{50} value for **2.1** were determined in a previous experiment using the same assay.
[d] Up to the highest compound concentration tested (100 µg/cm^3).

Complexes **2.2**-**2.4** show only moderate activity compared to chloroquine diphosphate while **2.5** and **2.6** show no activity at the highest compound concentration tested. The inactivity of complexes **2.5** and **2.6** can be attributed to the presence of the diphosphane ligands which, as described for the antitumor studies (section 3.2.1.), could adversely affect the lipophilic nature of the Pt-TSC moieties. Complex **2.2** was not as active as the mononuclear complexes **2.3** and **2.4** and this may very likely be due to decreased hydrophilicity of the tetranuclear complex (Table 3.4). Lipophilicity and hydrophilicity have been put forth as important determinants of the accumulation of a drug within the acidic food vacuole of the malaria parasite.[41-44]

As discussed in section 3.2.1, the calculated logP value is a parameter that is used to estimate the lipophilic nature of a compound and can be used to explain the differences in *in vitro* activities observed. Complex **2.2** is highly lipophilic (ClogP = 14.96) and thus not very hydrophilic suggesting that **2.2** may not be able to accumulate within the acidic food vacuole efficiently and thus only displays moderate inhibitory effect. Complexes **2.3** and **2.4** have lower ClogP values of 9.46 and 6.32 respectively and show better antiplasmodial activities compared to **2.2**. They are still quiet lipophilic and this could account for their lower activity compared to chloroquine.

Table 3.4. Calculated logP values for **2.2**-**2.4** and their antiplasmodial data for the D10 strain

Complex	D10: IC_{50} (μM)	ClogP
2.2	32.29 ± 2.28	14.96
2.3	19.93 ± 3.74	9.459
2.4	21.42 ± 1.22	6.318
Chloroquine	0.012 ± 0.001	5.06

Complex **2.3** [IC_{50} = 19.98 μM (D10) and 14.47 μM (Dd2)], which contains the triphenylphosphane ancillary ligand, was more active compared to **2.4** [IC_{50} = 21.42 μM (D10) and 24.90 μM (Dd2)] against both *P. falciparum* strains. This is in contrast to the antitumor studies of **2.3** and **2.4**, however a strict comparison of the data ascertained against parasite strains and tumor cell lines is not possible as these are very different illnesses that operate under different mechanisms and thus compounds **2.1**-**2.6** most likely have completely different inhibitory targets against *P. falciparum* and tumor cell lines. It can be said that complex **2.3** appears to display selectivity toward *P. falciparum* over the tumor cell lines A2780 and A2780*cis*R. Further *in vitro* screening of **2.3** against other *P. falciparum* strains and tumor cell lines need to be investigated to confirm this. Complex **2.3** was more active against the Dd2 strain compared to the D10 strain but complex **2.4** showed the opposite trend. Nevertheless, complexes **2.3** and **2.4** displayed resistance indices of 0.72 and 1.16 respectively that are much lower than chloroquine diphosphate. In fact RI values of less than or close to 1 is seen as favourable for potential antiplasmodial drug candidates.[41] This suggests that mononuclear cycloplatinated thiosemicarbazones may very likely not be susceptible to the same resistance mechanisms experienced by chloroquine.

3.2.2.2. In vitro T. vaginalis Activity

Compounds **2.1** – **2.6** were investigated for further antiparasitic effects against the *Trichomonas vaginalis* strain T1. *Trichomonas vaginalis* is a flagellated facultative anaerobic protozoan, which causes the sexually transmitted infection trichomoniasis in humans and is reported to infect more than 170 million people worldwide, mainly in industrialized countries.[45] Infection can have serious implications like premature birth and increased risk of acquiring HIV, cervical cancer and aggressive prostate cancer.[45-48] Metronidazole is the current FDA-approved treatment[49] but approximately 5% of all cases reported display resistance to this compound and this percentage is increasing.[50] There is therefore a need to find alternative forms of treatment due to this increase in resistance.

The effect of compounds **2.1**-**2.6** on parasite viability was determined at a single dose concentration if 100 μM on the *T. vaginalis* strain T1. In contrast to the inhibitory studies for *P. falciparum*, complex **2.4** is the only compound that showed a significant percentage inhibition (92.5 %) of the *T. vaginalis* parasite (Table 3.5). Metronidazole, the current FDA approved treatment, exhibited a 100 % inhibition at this concentration (100 μM), comparable to **2.4**. The tetranuclear complex **2.2** showed a moderate percent inhibition of 68.7% while ligand **2.1** and the complexes **2.3**, **2.5** and **2.6** displayed only mild effects on parasite viability (42.3, 24.5 and 42.3 % respectively). Since **2.4** was deemed to be the most potent inhibitor out of all compounds tested, its IC_{50} value was determined. Although this compound is not as potent as metronidazole, complex **2.4** represents a potential new chemotype.

Table 3.5. Percent inhibition data of compounds **2.1**-**2.6** against *T. vaginalis*

COMPOUND	% INHIBITION (100μM)	IC_{50} T1 Strain (μM)
1	51.3	Not determined
2	68.7	Not determined
3	42.3	Not determined
4	92.5	21.1
5	24.5	Not determined
6	42.3	Not determined
Metronidazole[a]	100	0.79

[a] Current FDA approved treatment for *T. Vaginalis* infections

Cysteine proteases are integral to the parasitic life cycle. They are involved in several parasite functions including host invasion, nutrition and protein processing.[51] Thiosemicarbazones are believed to inhibit parasite growth through reversible interactions with cysteine proteases in

the parasite and a recent study of the interactions of Pt(II) complexes and cysteine proteases revealed that Pt(II) complexes can bind to the active site cysteine of different cysteine proteases.[52]

Furthermore, it was found that the presence of an aromatic ring enhanced the inhibitory activity of these complexes compared to clinical drugs, cisplatin and carboplatin. However, the type and rate of active site cysteine binding was unique for each cysteine protease. Different cysteine proteases have structurally different folds and this can sterically influence how the complex binds to the cysteine protease targets within each parasite.[52] This could account for the contrasting activities observed for complexes **2.3** and **3.4** against the *P. falciparum* and *T. vaginalis* parasite strains. Moreover, it has been shown that the PTA ligand forms specific interactions within the active site of a cysteine protease when bound to a different metal center.[53]

3.2.3. β-Hematin Inhibition Assay.

In the life cycle of the *Plasmodium falciparum* parasite, degradation of the infected host's hemoglobin to provide essential amino acids for its growth and nutrition is a vital step.[54] A side product of this hemoglobin digestion is free heme which is toxic to the parasite. The parasite removes this threat by conversion of the free heme into a crystalline solid known as hemozoin which is nontoxic to the parasite. Thus, this process is one potential target in the design of possible antiplasmodial therapeutics. Clinically used drugs, amodiaquine and chloroquine are believed to inhibit the formation of hemozoin.[55]

The ability of a potential drug to inhibit formation of hemozoin can be measured using a β-hematin (synthetic hemozoin) inhibition assay. Complex **2.3** exhibits the best antiplasmodial activity against the two malarial strains tested [IC_{50} = 19.98 μM (D10) and 14.47 μM (Dd2)] and was thus chosen, along with ligand **2.1** [IC_{50}: 95.8 μM (D10)], for β-hematin inhibition studies. Compounds **2.1** and **2.3** were tested using a modified NP-40 detergent mediated hematin formation screen.[56] Evidence suggests that neutral lipid particles within the digestive food vacuole act as the site of nucleation and crystal growth of hemozoin.[57] NP-40 is a low cost, lipophilic detergent that can mediate the formation of synthetic hemozoin (β-hematin). The NP-40 mediated assay attempts to mimic the conditions of the acidic food vacuole in the parasite to give a better measure of hemozoin formation.

Figure 3.6 shows the dose-response curves obtained for the compounds **2.1** and **2.3** along with amodiaquine and chloroquine. Neither ligand **2.1** nor complex **2.3** were found to hinder β-hematin formation at the concentrations tested compared to amodiaquine and chloroquine. This result suggests that arylthiosemicarbazones and their cycloplatinated complexes target other processes within the *Plasmodium falciparum* parasite.

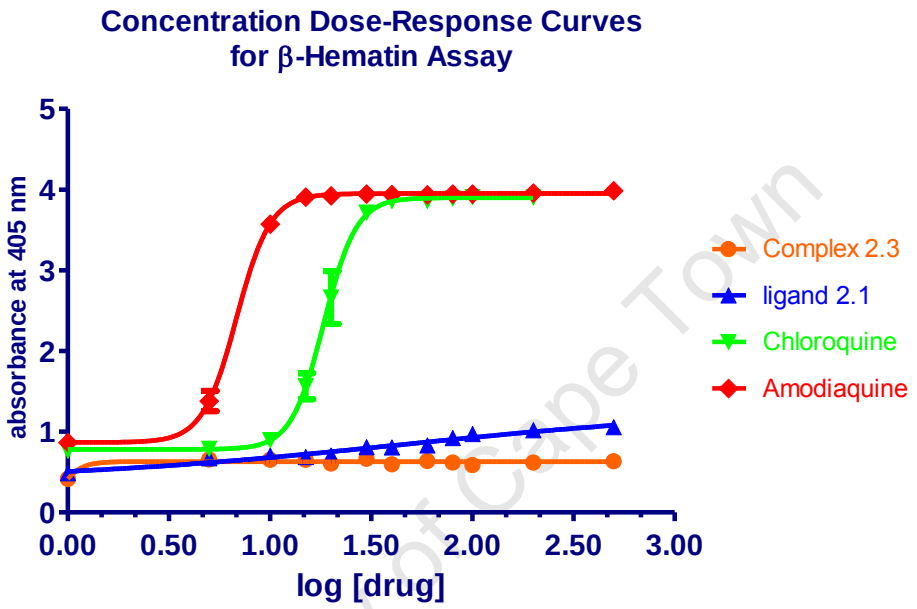

Figure 3.6. Concentration Dose Response Curves for NP-40 detergent mediated β-Hematin Assays of **2.1**, **2.3,** amodiaquine and chloroquine.

3.3. Stability Studies

As mentioned earlier, one of the drawbacks of using cisplatin as a chemotherapeutic agent is the fact that very little of the administered dose reaches its intended target. It has been found that up to 98 % of the intravenously administered dose of cisplatin is deactivated before it can reach its target.[3] This may occur either by cisplatin undergoing aquation in the extracellular membranes leading to formation of adducts with proteins such as serum albumin[3] or through binding of cisplatin to intracellular sulfur donors such as glutathione in the cytoplasm.[58,59] Thus, it is important that potential platinum metallotherapeutics exhibit stability in the presence of different biomolecules.

Previous spectroscopic studies of the interaction of cisplatin and an excess of methionine (Met) showed the formation of the [Pt(H-Met-OH-κ^2-N,S]$^{2+}$ metabolite.[60,61] It was also found to form adducts with cysteine.[60-62] These findings suggest that cisplatin may be deactivated by sulfur containing residues in the extracellular membranes. Further to this, the interaction of cisplatin with amino acids such as histidine, arginine, aspartic acid and glutamic acid have also been investigated to determine if further deactivation of cisplatin occurs through interaction with nitrogen donors.[61-66]

A preliminary NMR study of compounds **2.1** – **2.6** in the presence of one amino acid and four different short peptides was carried out in deuterated DMSO. Table 3.6 lists the amino acid and peptide sequences. Methionine was chosen based on previous studies of cisplatin with this amino acid.[60,61] Short peptides were used as cisplatin is believed to interact with the amino acid side-chains on the surface of proteins within cells.[67,68] A solution of each compound and the appropriate amino acid or peptide in DMSO-d_6 was heated to 37 °C and the ^{1}H NMR spectra recorded. For all of the experiments, compounds **2.1** – **2.6** remain stable in the presence of the different peptides and methionine up to 10 days.

Table 3.6. Definition of amino acid and peptide sequences

Code	Definition
Met	Methionine
Ala-Gly-His-Gly-Ala	Alanine-glycine-histidine-glycine-alanine
Ala-Gly-Lys-Gly-Ala	Alanine-glycine-lysine-glycine-alanine
Ala-Gly-Arg-Gly-Ala	Alanine-glycine-arginine-glycine-alanine
Ala-Gly-Trp-Gly-Ala	Alanine-glycine-tryptophan-glycine-alanine

Figures 3.7 - 3.9 show the spectra obtained for the ligand **2.1** and complex **2.4** after 10 days in the presence of methionine and the peptide Ala-Gly-Lys-Gly-Ala. No changes in the resonances assigned to the thiosemicarbazone compounds were observed.

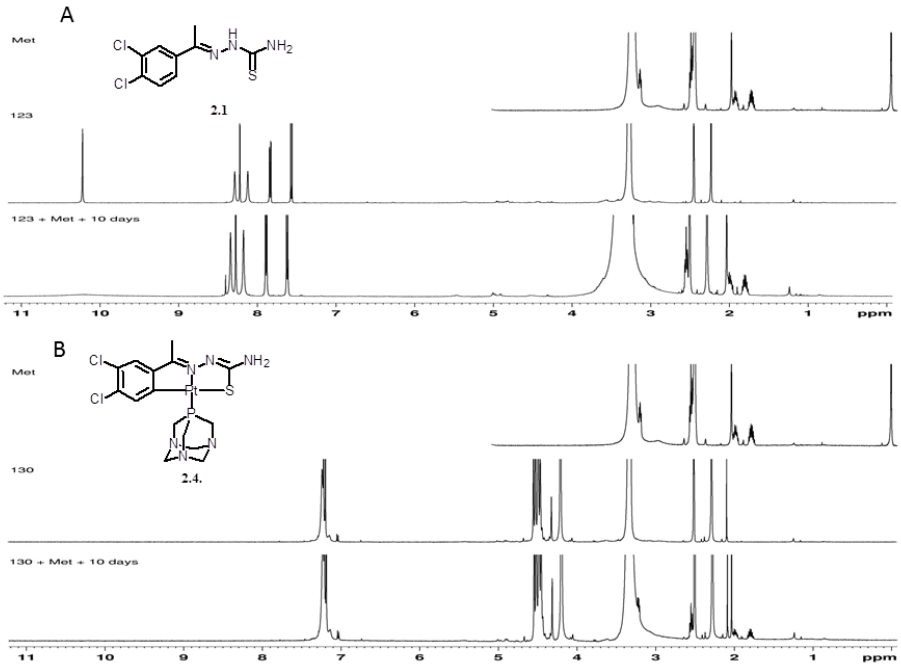

Figure 3.7. ^{1}H NMR spectra for A: Ligand **2.1**; Met; 2.1 + Met after 10 days at 37 °C and B: Complex **2.4**; Met; **2.4** + Met after 10 days at 37 °C

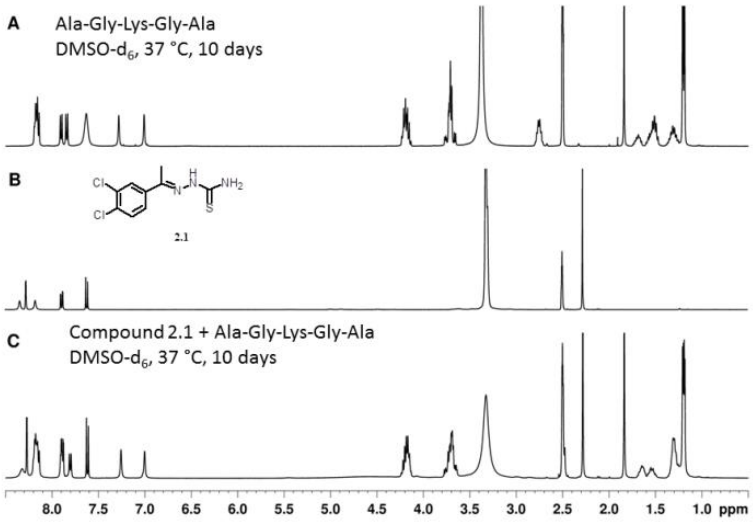

Figure 3.8. ^{1}H NMR spectra of A: Ala-Gly-Lys-Gly-Ala; B: ligand **2.1**; C: **2.1** + peptide

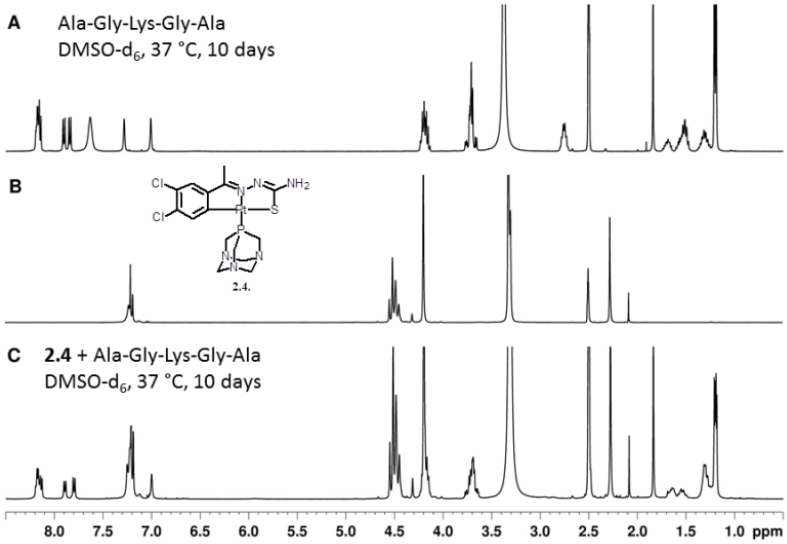

Figure 3.9. ^{1}H NMR spectra of A: Ala-Gly-Lys-Gly-Ala; B: complex **2.4**; C: **2.4** + peptide

The lack of interaction observed between each complex and the corresponding molecule may imply that thiosemicarbazone ligand (**2.1**) and its cycloplatinated analogues (**2.2**-**2.6**) may remain intact in the blood and cytoplasm. This result suggests that cycloplatinated thiosemicarbazones may be able to reach their antitumoral target intact. However, it is important to note that these NMR studies were carried out in DMSO-d_6 and are only a preliminary screen. Since the compounds have shown stability in the presence of certain simple peptides, the next step is stability studies of compounds **2.1**-**2.6** with different biomolecules in biological media at physiological pH (7.3) and temperature in order to ascertain if these compounds do indeed remain intact under physiological conditions.

3.4. Summary

The thiosemicarbazone complex **2.1** and its mono-, di- and tetraplatinum complexes **2.2**-**2.6** were screened for antiparasitic activity against *Plasmodium falciparum* and *Trichomonas vaginalis* strains and for antitumor activity against cisplatin-sensitive and cisplatin-resistant human ovarian carcinoma cell lines. They were found to exhibit moderate to low parasite growth inhibition and antiproliferative activities. The *in vitro* activities obtained for **2.1**-**2.8** against the A2780 and A2780*cis*R cell lines revealed that cyclometalation of ligand **2.1** led to a decrease in *in vitro* activity. This is in contrast to previous reports where cycloplatination had a beneficial effect on activity.

The lipophilic nature of the phosphane in each complex may influence the antiproliferative activities of **2.3**-**2.6**. Complex **2.4** demonstrated the best IC_{50} out of all compounds tested against both cell lines and its ancillary ligand, PTA, has a high hydrophilic nature providing the right counter balance to the high lipophilicity of the platinum-thiosemicarbazone moiety. Complex **2.5** had a better activity than complex **2.3** and can be attributed to the presence of the ferrocenyl group which is known to enhance biological activity. Overall, the moderate activities observed could be improved through structural modification of the phosphanes to increase the hydrophilicity of the cycloplatinated complexes or by replacement of the phosphane with another type of ancillary ligand such as a monodentate nitrogen ligand.

Against the D10 and Dd2 *P. falciparum strains*, complexes **2.2**-**2.4** were much more active than their free ligand **2.1** and the inactivity of complexes **2.5** and **2.6** may be attributed to the presence of the diphosphane ligand. The highly lipophilic nature of complex **2.2** may result in the complex being unable to enter the acidic food vacuole of the parasite efficiently thus accounting for moderate antiplasmodial activity. Complex **2.3** displayed the best inhibitory activity against both strains yet was much less active against the A2780 and A2780*cis*R cell lines suggesting that complex **2.3** may be selective for *P. falciparum* over tumor cell lines. Further *in vitro* screening of **2.3** against other *P. falciparum* strains and tumor cell lines need to be investigated to confirm this. All of the compounds (**2.1** – **2.6**) with the exception of **2.4** displayed moderate to low effects on parasite viability in the T. vaginalis strain T1.

When ligand **2.1** and complex **2.3** were evaluated for their ability to inhibit β-hematin formation *in vitro*, it was found that these compounds do not target this process at the concentrations used in the assay. Thiosemicarbazones and their metal complexes may act upon cysteine protease functions within the parasite, and a study of their interaction with different cysteine protease enzymes must be carried out to validate this hypothesis. Preliminary stability studies of compounds **2.1** – **2.6** experiments with different short peptides and the amino acid methionine using ^{1}H NMR imply that these compounds may be stable in the blood and plasma and they may reach their antitumoral target intact. Further studies of these compounds under physiological conditions must be carried out to confirm this deduction.

3.5. Experimental

3.5.1. P. falciparum in vitro assay.

The test samples were tested in triplicate on one occasion against chloroquine-sensitive (CQS) D10 strain and chloroquine-resistant (CQR) Dd2 strain of Plasmodium falciparum. Continuous *in vitro* cultures of asexual erythrocyte stages of P. falciparum were maintained using a modified method.[69] Quantitative assessment of antiplasmodial activity *in vitro* was determined via the parasite lactate dehydrogenase assay using a modified method.[70] The test samples were prepared to a 20 mg/cm^3 stock solution in 100% DMSO and sonicated to enhance solubility. Samples were tested as a suspension if not completely dissolved. Stock solutions were stored at -20ºC. Further dilutions were prepared on the day of the experiment. Chloroquine (CQ) was used as the reference drug in all experiments. A full dose-response was performed for all compounds to determine the concentration inhibiting 50% of parasite growth (IC50–value). Test samples were tested at a starting concentration of 100 μg/cm^3, which was then serially diluted 2-fold in complete medium to give 10 concentrations; with the lowest concentration being 0.2 μg/cm^3. The same dilution technique was used for all samples. CQ was tested at a starting concentration of 100 ng/cm^3 against the CQR strain and 1000 ng/cm^3 against the CQS strain. The highest concentration of solvent to which the parasites were exposed to had no measurable effect on the parasite viability (data not shown). The IC50-values were obtained using a non-linear dose-response curve fitting analysis via Graph Pad Prism v.4.0 software.

3.5.2. T. vaginalis in vitro assay.

Cultures of T. vaginalis T1 strain were grown in 5 cm^3 completed TYM Diamond's media in a 37ºC incubator for 24h. One hundred millimolar stocks of the compounds were made by dissolving in DMSO, were screened against T1 stain of T. vaginalis. Samples were tested as a suspension if not completely dissolved. Cells untreated and inoculated with 5μL DMSO are used as controls. Five microliters of 100mM stocks of compound library were inoculated for a final concentration of 100μM. Results were calculated based on counts utilizing a hemocytometer after 24h. For IC_{50} values, increasing concentrations of the compound (0-100μM) were tested for inhibitory activity and concentrations that inhibited at approximately 50% were then obtained by linear regression analysis. These predicted IC_{50} values were then confirmed by direct testing on T. vaginalis strain T1 as described above.

3.5.3. A2780 and A2780R cancer in vitro assay.

The human A2780 and A2780*cis*R ovarian carcinoma cells were obtained from the European Collection of Cell Cultures (Salisbury,UK). Cells were grown routinely in RPMI-1640 medium with 10% foetal calf serum (FCS) and antibiotics at 37 ◦C and 5% CO_2. Cytotoxicity was determined using the MTT assay (MTT = 3(4,5-dimethyl-2-thiazolyl)-2,5-diphenyl-2H-tetrazolium bromide). Cells were seeded in 96-well plates as monolayers with 100 cm^3 of cell solution (approximately 20,000 cells) per well and pre-incubated for 24 h in medium supplemented with 10% FCS. Compounds were prepared as DMSO solution then dissolved in the culture medium and serially diluted to the appropriate concentration, to give a final DMSO concentration of 1%. 100 cm^3 of drug solution was added to each well and the plates were incubated for another 72 h. Subsequently, MTT (5 mg/cm^3 solution) was added to the cells and the plates were incubated for a further 2 h. The culture medium was aspirated, and the purple formazan crystals formed by the mitochondrial dehydrogenase activity of vital cells were dissolved in DMSO. The optical density, directly proportional to the number of surviving cells, was quantified at 540 nm using a multiwell plate reader and the fraction of surviving cells was calculated from the absorbance of untreated control cells. Evaluation is based on means from three independent experiments, each comprising three microcultures per concentration level.

3.5.4. Detergent mediated assay for β-hematin inhibitors.

The β-hematin formation assay method described by Carter et al.[55] was modified for manual liquid delivery. Stock solutions of the test compounds were prepared at 10 mM, 2 mM and 0.4 mM by dissolving each sample in DMSO with sonication. Test compounds were delivered to a 96 well plate in triplicate from 0-500 μM (final concentration) with a total DMSO volume of 10 μL in each well. Deionized H2O (70 μL) and NP-40 (20 μL; 30.55 μM) were then added. A 25 mM haematin stock solution was prepared by sonicating hemin in DMSO, for complete dissolution, and then suspending 177.76 μL of this in a 2M acetate buffer (pH 4.8). The homogenous suspension (100 μL) was then added to the wells to give final buffer and hematin concentrations of 1 M and 100 μM respectively. The plate was covered and incubated at 37°C for 5-6 hours in a water bath. Analysis of the assay was carried out using the pyridine-ferrichrome method developed by Ncokazi and Egan.[71] A solution of 50% (v/v) pyridine, 30% (v/v) H2O, 20% (v/v) acetone and 0.2 M HEPES buffer

(pH 7.4) was prepared and 32 µL added to each well to give a final pyridine concentration of ± 5% (v/v). Acetone (60 µL) was then added to assist with hematin dispersion. The UV-vis absorbance of the plate wells was read on a SpectaMax plate reader. Sigmoidal dose-response curves were fitted to the absorbance data using GraphPad Prism v3.02.

3.7. References

1. B. Rosenberg, L. Van Camp and T. Krigas, *Nature*, **1965**, *205*, 698.
2. A. Levina, A. Mitra and P.A. Lay, *Metallomics*, **2009**, *1*, 458.
3. J. Reedijk, *Macromol. Symp.*, **2008**, *270*, 193.
4. T. S. Lobana, R. Sharma, G. Bawa and S. Khanna, *Coord. Chem. Rev.*, **2009**, *253* (7-8), 977.
5. X. Du, C. Guo, E. Hansel, P. S. Doyle, C. R, Caffery, T. P. Holler, J. H. McKerrow and F. E. Cohen, *J. Med. Chem.*, **2002**, *45*, 2695.
6. R. B. De Oliveira, E. M. De Souza-Fagundes, R. P. P. Soares, A. A. Andrade, A. U. Krettli and C. L. Zani, *Eur. J. Med. Chem.*, **2008**, *43*, 1983.
7. K. J. Duffy, A. N. Shaw, E. Delorme, S. B. Dillon, C. Erickson-Miller, L. Giampa, Y. Huang, R. M. Keenan, P. Lamb, N. Liu, S. G. Miller, A. T. Price, J. Rosen, H. Smith, K. J. Wiggall, L. Zhang and J. I. Luengo, *J. Med. Chem.*, **2002**, *45*, 3573.
8. M. Abid, S. M. Agarwal and A. Azam, *Eur. J. Med. Chem.*, **2008**, *43*, 2035.
9. A. Walcourt, M. Loyevsky, D. B. Lovejoy, V. R. Gordeuk and D. R. Richardson, *Int. J. Biochem. Cell Biol.*, **2004**, *36*, 401.
10. N. Fujii, J. P. Mallari, E. J. Hansell, Z. Mackey, P. Doyle, Y. M. Zhou, J. Gut, P. J. Rosenthal, J. H. Mckerrow and R. K. Guy, *Bioorg. Med. Chem. Lett.*, **2005**, *15*, 121.
11. I. Dilovic, M. Rubcic, V. Vrdoljak, S.K. Pavelic, M. Kralj, I. Piantanida and M. Cindric, *Bioorg. Med. Chem*, **2008**, *16*, 5189.
12. M. -C. Liu, T. S. Lin and A.C. Sartorelli, *J. Med. Chem.*, **1992**, *35*, 3672.
13. H.G. Petering, H.H. Buskirk and G.E. Underwood *Cancer Res.*, **1964**, *24*, 367.
14. J. M. Kolesar, W. R. Schelman, P. G. Geiger, K. D. Holen, A. M. Traynor, D. B. Alberti, J. P. Thomas, C. R. Chitambar, G. Wilding and W.E. Antholine, *J. Inorg. Biochem.*, **2008**, *102*, 693.
15. D. Kovala-Demertzi, M. A. Demertzis, E. Filou, A. A. Pantazaki, P. N. Yadav, J. R. Miller, Y. Zheng and D. A. Kyriakidis, *Biometals*, **2003**, *16*, 411.
16. A. G. Quiroga, J. M. Perez, E. I. Montero, J. R. Masaguer, C. Alonso and C. Navarro-Ranninger, *J. Inorg. Biochem.*, **1998**, *70*, 117.
17. A. G. Quiroga, J. M. Perez, I. Lopez-Solera, J. R. Masaguer, A. Luque, P. Roman, A. Edwards, C. Alonso and C. Navarro-Ranninger, *J. Med. Chem.*, **1998**, *41*, 1399.
18. T. Stringer, D. T. Hendricks, H. Guzgay and G. S. Smith, *Polyhedron*, **2012**, *31*, 486.

19. A. Chipeleme, J. Gut, P. J. Rosenthal and K. Chibale, *Bioorg. Med. Chem. Lett.*, **2007**, *15*, 273.
20. D. Sweeney, M. L. Raymera and T. D. Lockwood, *Biochem. Pharm.*, **2003**, *66*, 663.
21. J. H. McKerrow, E. Sun, P. J. Rosenthal and J. Bouvier, *Annu. Rev. Microbiol.*, **1993**, *47*, 821.
22. P. J. Rosenthal, *Int J Parasitol*, **2004**, *34*, 1489.
23. S. E. Francis, D. J. Sullivan Jr. and D. E. Goldberg, *Annu. Rev. Microbiol.*, **1997**, *51*, 97
24. V. L. Lew, T. Tiffert and H. Ginsburg, *Blood*, **2003**, *101*, 4189.
25. P. Chellan, T. Stringer, A. Shokar, P.J. Dornbush, G. Vazquez-Anaya, K.M. Land, K. Chibale and G.S. Smith, *J. Inorg. Biochem.*, **2011**, *105* (11), 1562.
26. P. Chellan, S. Nasser, L. Vivas, K. Chibale and G. S. Smith,, *J. Organomet. Chem.*, **2010**, *695*, 2225.
27. D. Kovala-Demertzi, A. Domopoulou, M. Demertzi, J. Valdés-Martinez, S. Hernandez-Hortega, G. Espinosa-Pérez and D. W. West, *Polyhedron*, **1996**, *15*, 2587.
28. A. G. Quiroga, J. M. Pérez, E. I. Montero, C. Alonso and C. Navarro-Ranninger, *J. Inorg. Biochem.*, **1999**, *75*, 293.
29. A. A. Ali, H. Nimir, C. Aktas, V. Huch, U. Rauch, K. -H. Schäfer and M. Veith, *Organometallics*, **2012**, *31*, 2256−2262.
30. A. G. Quiroga, J. M. Pérez, C. Alonso and C. Navarro-Ranninger, *Appl. Organometal. Chem.*, **1998**, *12*, 809.
31. M. Yoshida, A. R. Khokhar and Z. H. Siddik, *Anticancer Drug Des*, **1994**, *9*, 425.
32. E. H. Kerns and L. Di; *Drug-like Properties: Concepts, Structure Design and Methods from ADME to Toxicity Optimization*; 1st ed.; Elsevier Academic Press: California, 2008.
33. C. Ornelas, *New J. Chem*, **2011**, *35*, 1973.
34. P. Chellan, N. Shunmoogam-Gounden, D. T. Hendricks, J. Gut, P. J. Rosenthal, C. Lategan, P. J. Smith, K. Chibale and G. S. Smith, *J. Eur. Med. Chem.*, **2010**, 3520.
35. S. Grguric-Sipka, C. R. Kowol, S. -M. Valiahdi, R. Eichinger, M. A. Jakupec, A. Roller, S. Shova, V. B. Arion and B. K. Keppler, *Eur. J. Inorg. Chem.*, **2007** 2870.
36. S. Halder, S. -M. Peng, G. -H. Lee, T. Chatterjee, A. Mukherjee, S. Dutta, U. Sanyal and S. Bhattacharya, *New J. Chem.*, **2008**, *32*, 105.
37. S. D. Khanye, B. Wan, S. G. Franzblau, J. Gut, P. J. Rosenthal, G. S. Smith and K. Chibale, *J. Organomet. Chem.*, **2011**, *696*, 3392.

38. S. D. Khanye, G. S. Smith, C. Lategan, P. J. Smith, J. Gut, P. J. Rosenthal and K. Chibale, *J. Inorg. Biochem.*, **2010**, *104*, 1079.

39. M. Adams, Y. Li, H. Khot, C. De Kock, P. J. Smith, K. Land, K. Chibale and G. S. Smith, *Dalton Trans*, **2013**, *42*, 4677.

40. D. Bahl, F. Athar, M. B. P. Soares, M. S. de Sá, D. R. M. Moreira, R. M. Srivastava, A. C. L. Leite and A. Azam, *Bioorg. Med. Chem*, **2010**, *18*, 6857.

41. P. F. Salas, C. Herrmann, J. F. Cawthray, C. Nimphius, A. Kenkel, J. Chen, C. de Kock, P. J. Smith, B. O. Patrick, M. J. Adam and C. Orvig *J. Med. Chem.*, **2013**, *56* (4), 1596.

42. P. Olliaro, *Pharmacol. Ther.*, **2001**, *89*, 207.

43. L. Tilley, P. Loria and M. Foley, Chloroquine and other Quinoline Antimalarials In *Antimalarial Chemotherapy: Mechanisms of Action, Resistance and New Directions in Drug Discovery*; Rosenthal, P. J., Ed.; Humana Press: Totowa, NJ, 2001.

44. P. N. Rangarajan and G. Padmanaban, *Expert. Opin. Ther. Targets*, **2001**, *5*, 423.

45. D. Petrin, K. Delgaty, R. Bhatt and G. Garber, *Clin. Microbiol. Rev.*, **1998**, *11*, 300.

46. D. Soper, *Am. J. Obstet. Gynecol.* , **2004**, *190*, 281.

47. G. L. Lloyd, J. R. Case, D. De Frias and R. E. Brannigan, *J. Urol.* , **2003**, *170*, 924.

48. S. Sutcliffe, E. Giovannucci, J. F. Alderete, T. H. Chang, C. A. Gaydos, J. M. Zenilman, A. M. de Marzo, W. C. Willett and E. A. Platz, *Cancer Epidemiol. Biomarkers Prev.* , **2006**, *15*, 939.

49. S.L. Cudmore, K.L. Delgaty, S.F. Hayward-McClelland, D.P. Petrin, G.E. Garber,, *Clin. Microbiol. Rev.*, **2004**, *17*, 783.

50. J.R. Schwebke, D. Burgess, *Clin. Microbiol. Rev.*, **2004**, *17*, 794.

51. S. P. Fricker, R. M. Mosi, B. R. Cameron, I. Baird, Y. Zhu, V. Anastassov, J. Cox, P. S. Doyle, E. Hansell, G. Lau, J. Langille, M. Olsen, L. Qin, R. Skerlj, R. S. Y. Wong, Z. Santucci and J. H. McKerrow, *J. Inorg. Biochem.*, **2008**, *102*, 1839.

52. Y. -C. Lo, W. -C. Su, T. -P. Ko, N. -C. Wang and A. H. -J. Wang *J. Biomol. Struct. Dyn.*, **2011**, *29* (2), 267.

53. A. Casini, C. Gabbiani, F. Sorrentino, M. P. Rigobello, A. Bindoli, T. J. Geldbach, A. Marrone, N. Re, C. G. Hartinger, P. J. Dyson and L. Messori, *J. Med. Chem.*, **2008**, *51*, 6773.

54. Goldberg, D. E.; Slater, A.F.; Cerami, A.; Henderson, G.B., *Proc. Natl. Acad. Sci. U. S. A.*, **1990**, *87*, 2931.

55. T. J. Egan and H. M. Marques, *Coord. Chem. Rev.*, **1999**, *190-192*, 493.

56. M. D. Carter, V. V. Phelan, R. D. Sandlin, B. O. Bachmann and D. W. Wright, *Comb. Chem. High Throughput Screen*, **2010**, *13* (3), 285.
57. R. D. Sandlin, M. D. Carter, P. J. Lee, J. M. Auschwitz, S. E. Leed, J. D. Johnson and D. W. Wright, *Antimicrob. Agents Chemother.*, *55* (7), 3363.
58. R.A. Alderden, M.D. Hall and T.W. Hambley, *J. Chem. Educ.*, **2006**, *83*, 728.
59. A.F.A. Peacock and P.J. Sadler, *Chem.-Asian J.*, **2008**, *3*, 1890.
60. P. del S. Murdoch, J. D. Ranford, P. J. Sadler and S. J. Berners-Price, *Inorg. Chem.*, **1993**, *32*, 2249.
61. M. Hahn, M. Kleine and W. S. Sheldrick, *J. Biol. Inorg. Chem.*, **2001**, *6*, 556.
62. T. Zimmermann, M. l. Zeizinger and J. V. Burda, *J. Inorg. Biochem.*, **2005**, *99*, 2184.
63. M. Beltran, G. B. Onoa, E. Pedroso, V. Moreno and A. Grandas, *J. Biol. Inorg. Chem.*, **1999**, *4*, 701.
64. T. G. Appleton, F. J. Pescb, M. Wienken, S. Menzer and B. Lippert, *Inorg. Chem.*, **1992**, *31*, 4410.
65. A. H. Talebian, D. Bensely, A. Ghiorghis, C. F. Hammer, P. S. Schein and D. Green, *Inorg. Chim. Acta*, **1991**, *179*, 281.
66. T. G. Appleton, J. R. Hall, D. W. Neale and C. S. M. Thompson, *Inorg. Chem.*, **1990**, *29*, 3985.
67. J. -M. Teuben and J. Reedijk, *J. Biol. Inorg. Chem.*, **2000**, *5*, 463.
68. T. Peleg-Shulman and D. Gibson, *J. Am. Chem. Soc.*, **2001**, *123*, 3171.
69. W. Trager and J. B. Jensen, *Science*, **1976**, *193* (4254), 673.
70. M. T. Makler, J. M. Ries, J. A. Williams, J. E. Bancroft, R. C. Piper, B. L. Gibbins and D. J. Hinrichs, *Am. J. Trop. Med. Hyg.*, **1993**, *48*, 739.
71. K. K. Ncokazi and T.J. Egan, *Anal. Biochem.*, **2005**, *338* (2), 306.

CHAPTER 4

Synthesis and Characterisation of Di- and Trinuclear Ruthenium, Rhodium and Iridium Functionalised Pyridyl Aromatic Ethers

4.1. Introduction

The use of metals such as rhodium, iridium and ruthenium for the preparation of polynuclear complexes is attractive since these metals are stable in several oxidation states giving rise to interesting metal complex architectures as well as physical and/or electronic properties.[1-9] Di- and polyaromatic or heteroaromatic ethers have been utilized for the preparation of homometallic complexes.[10-14] Poly aryl ethers are known to exhibit high thermal stability and have been studied as polymeric or dendritic supports in catalysis and biology.[14-17]

From a pharmacological standpoint, polyaryl ethers are believed to have potential as a drug delivery system. Conjugation of a bio-active moiety to a polyether scaffold may stabilize these compounds sufficiently to allow them to reach their biological target where they can be released.[16] While larger dendrimeric polyaryl ethers have been proposed as potential drug delivery agents, smaller di- or tri-aryl ethers could still have biologically relevant properties.

The study of diaryl ether containing molecules as pharmacological agents has become particularly pertinent since structure-activity relationship analyses of several biologically important natural products have shown that these compounds contain diaryl ether functionalities.[18] Some of these small molecule diaryl ethers have been proposed to act as tyrosine kinase inhibitors and have had some success for the treatment of metastatic non-small cell lung cancer and pancreatic cancer.[19] The aryl-ether containing compound, cis-tamoxifen (**I**, **Figure 4.1.**), is currently used clinically to treat early and advanced ER+ (estrogen receptor positive) breast cancer.[20] Furthermore, the organometallic analogue, ferrocifen (**II**), showed enhanced growth inhibition activity *in vitro* compared to cis-tamoxifen.[21-23] More recently, pentamethylcyclopentadienyl rhodium derivatives have also been found to exhibit biological effect *in vitro* against the MCF7 and the MDA-MB-231 breast cancer cell lines thus demonstrating the potential of aromatic ethers as antiproliferative agents.[20]

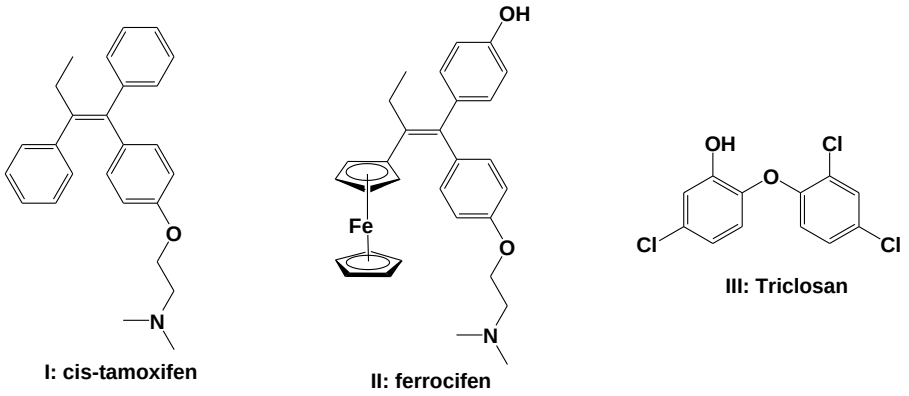

Figure 4.1. Aryl ether containing compounds with tumor growth inhibitory effects, cis-tamoxifen and ferrocifen and the diaryl ether compound Triclosan that is active *in vitro* against two strain of *P. falciparum*.

Apart from the potential pharmacological benefits of aryl ethers against cancer, these compounds may also be active against tropical diseases such as malaria. In fact, the diaryl ether, Triclosan (**III**, **Figure 4.1.**) along with its derivatives has demonstrated *in vitro* activity against a chloroquine sensitive and a chloroquine resistant strain of *P. falciparum*.[24,25] A library of 4-pyridone functionalized diaryl ethers have also been studied for *in vitro* and *in vivo* antiplasmodial activity against different strains of *P. falciparum* and all of the compounds were found to inhibit parasite growth in the low nanomolar range *in vitro*, exhibiting values that were either comparable or significantly lower than chloroquine.[26]

Mono- and polynuclear ruthenium-arene and pentamethylcyclopentadienyl rhodium and iridium pyridyl complexes have demonstrated promising pharmacological activities particularly as antiproliferative agents making them viable candidates for further study.[27-29] Thus, the coupling of metallated pyridyl functionalities to a simple aryl ether scaffold may lead to an enhanced biological effect whereby the aryl ether framework would stabilize the metal moieties allowing them to be delivered intact to their pharmacological target.

In this chapter, the synthesis and characterization of two new di- and tripyridyl aromatic ether compounds along with their Ru(II), Rh(III) and Ir(III) functionalized organometallic complexes is described.

The choice to prepare a simple dipyridyl ether ligand system is based on structure analyses of previously reported compounds that revealed simple diaryl ether derivatives to have biological activity.[18,19] For the preparation of the tripyridyl ether ligands, a tris-hydroxyphenyl-triazine scaffold was chosen since polyaryl functionalized triazine derivatives

and some of their metal complexes have been reported to exhibit *in vitro* cytotoxic effects as both antiparasitic and antitumoral agents.[30-36]

The design of these complexes aims to couple the biological properties of different functionalities to give an enhanced *in vitro* antiparasitic or antitumor effect; namely, the established *in vitro* pharmacological activities of half-sandwich Ru(II), Rh(III) and Ir(III) moieties and alkyl-pyridines as well as the lipophilic nature of aryl ethers. All of the compounds synthesized were evaluated *in vitro* as antitumor agents against two tumor cell lines of human ovarian cancer and as antiparasitic agents against the *P. falciparum* strains, NF54 (chloroquine sensitive) and Dd2 (chloroquine resistant), and the *T. vaginalis* strain G3 and the results of these studies are presented in Chapter 6.

4.2. Results and Discussion

4.2.1. Synthesis and characterisation of di- and tripyridyl aromatic ether ligands

The new di- and tripyridyl aromatic ether ligands, [3,5-Bis-(pyridin-4-ylmethoxy)-phenyl]-methanol (**4.1**) and 2,4,6-Tris-[4-(pyridin-4-ylmethoxy)-phenyl]-[1,3,5]triazine (**4.2**), were prepared using two typical Williamson-ether synthesis protocols (Scheme 4.1.).[37] For ligand **4.1**, the aromatic alcohol, 3,5-di(hydroxyl)benzylalcohol was reacted with 4-bromomethylpyridine hydrobromide in THF with 18-crown-6 as the phase transfer catalyst for the weak base, K_2CO_3. After purification by organic-aqueous solution extraction, the product (**4.1**) was isolated as an amorphous solid in 40 % yield.

This method (eqn 4.1.) proved unsuccessful for the preparation of the tripyridyl ligand (**4.2**) and instead tris(4-hydroxylphenyl)triazine was reacted with 4-bromomethylpyridine hydrobromide in DMF at 80 °C with K_2CO_3 as base yielding the ligand **4.2** as a yellow solid in 52 % yield.

Examination of the proton NMR spectra for ligands **4.1** and **4.2** gives convincing evidence for the formation of the aromatic ether functionalities. A singlet occurring at 5.18 and 5.21 ppm for **4.1** and **4.2** respectively is assigned to the alkyl ether protons H_d. This resonance shift is typical for aryl-alkyl ethers.[37,38] For both ligands, the pyridyl protons, H_a and H_b, resonate between 8.55 - 8.75 ppm (H_a) and 7.40 – 7.43 ppm (H_b) as doublets as a result of through-bond coupling to each other. Coupling constants of between 6 – 9 Hz are observed and agree with a ^3J *ortho* coupling for aromatic and heteroaromatic protons.

Eqn 4.1.

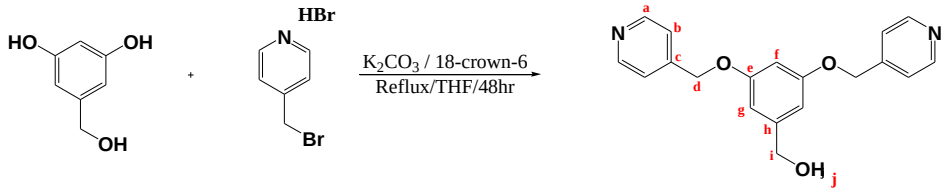

4.1: brown solid, 40 %

Eqn 4.2.

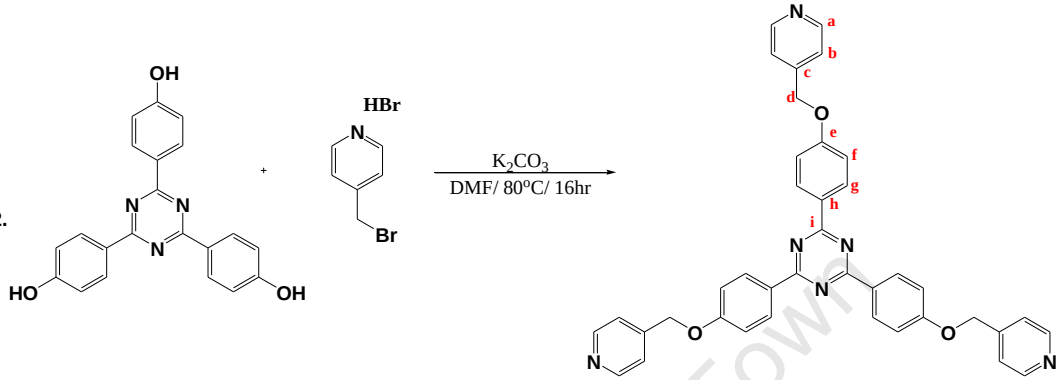

4.2: yellow solid, 52 %

Scheme 4.1.

For **4.1**, the benzyl protons H_i resonate at 4.58 ppm as a singlet and relatively upfield to this shift the hydroxyl proton resonates as a broad singlet at 4.22 ppm. Two singlets at 6.90 and 6.59 ppm are respectively assigned to the protons H_g and H_f of the tri-substituted benzene ring. In the triazine functionalized ligand **4.2**, the protons of the benzene rings are observed as doublets at 8.65 and 7.12 ppm. The more downfield resonance is assigned to H_g as these protons would experience a high deshielding effect due to their close proximity to the triazine ring.

Analysis of **4.1** and **4.2** with $^{13}C\{^1H\}$ NMR spectroscopy reveals that the *ortho* and *meta* carbons of the pyridyl rings resonate at approximately 150.0 (C_a) and 121.5 (C_b) ppm. The alkyl ether carbons occur at 67.8 and 67.9 ppm for **4.1** and **4.2** respectively. In the case of **4.1**, the benzyl carbon resonates at 63.4 ppm and the most deshielded carbon resonance of 158.1 ppm is due to the ether functionalized aromatic carbons C_e. For **4.2**, the carbons of the triazine ring resonate at 158.1 ppm. The unsubstituted carbons of the benzene rings of **4.2** are observed at 141.57 (C_f) and 128.3 (C_g) ppm. The alkyl-substituted carbon C_c of the pyridyl ring exhibits a resonance at 134.0 ppm.

Further evidence confirming that etherification had occurred was garnered from the infrared analyses of **4.1** and **4.2**. Both ligands show one strong absorption bands in the region of 1130-1170 cm^{-1} as a consequence of the C-O ether bond vibration. For **4.1**, the pyridyl imine C=N

stretching frequency is assigned to a strong absorption band at 1597 cm^{-1}; a similar frequency is observed for **4.2**. The triazine C=N bond present in **4.2** vibrates at a higher frequency compared to the pyridyl imine and is assigned to an absorption band at 1607 cm^{-1}. Electron-Impact (EI) mass spectrometry was used to analyse **4.1** and **4.2**. Both compounds exhibit at base peak corresponding to its ionized parent ion, $[M]^+$.

4.2.2. Synthesis and Characterisation of PGM Complexes

Ligands **4.1** and **4.2** were peripherally metalated using the precursors, dichloro(*p*-cymene)ruthenium(II) dimer, dichloro(pentamethylcyclopentadienyl)rhodium(III) dimer and dichloro(pentamethylcyclopentadienyl)iridium(III) dimer (Schemes **4.2.** and **4.3**.).

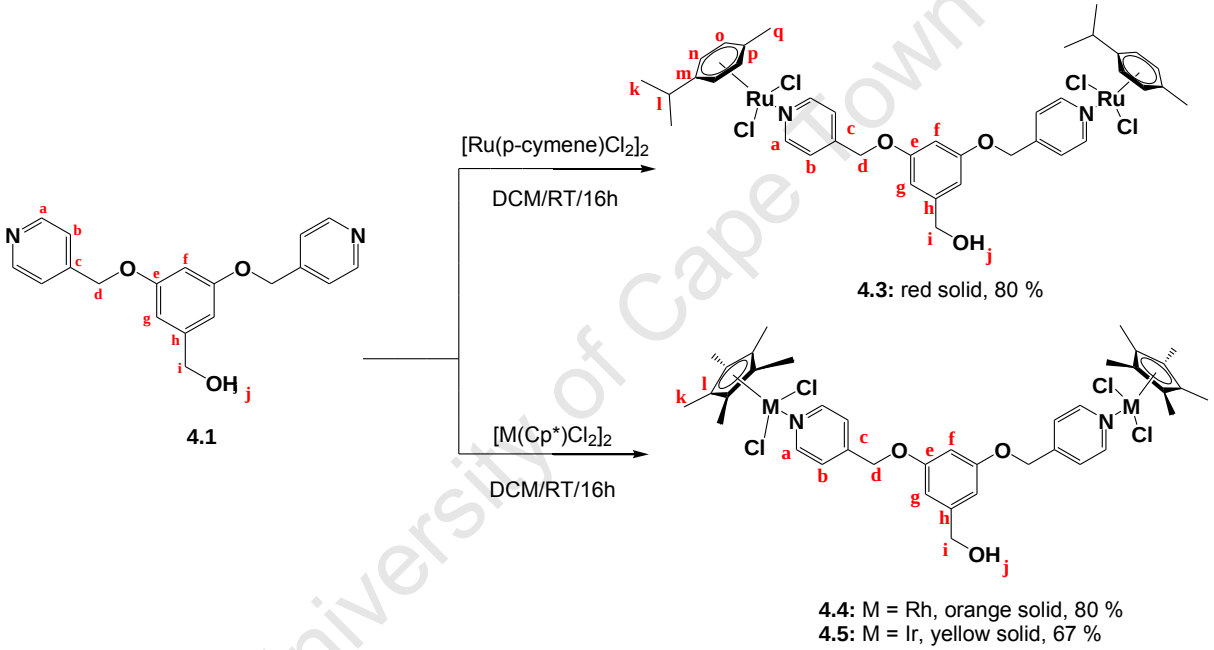

Scheme 4.2.

For complexes **4.3** – **4.6**, the appropriate ligands were reacted with the corresponding dimers in DCM at room temperature. This method proved unsuccessful for the synthesis of complexes **4.7** and **4.8**, most likely due to the fact that ligand **4.2** and the rhodium and iridium dimers are only partially soluble in DCM. These complexes (**4.7** and **4.8**) were therefore prepared by reaction of the corresponding dimer and **4.2** in refluxing methanol (Scheme **4.3.**). Complexes **4.3**- **4.8** were isolated as air-stable solids in moderate to high yields.

Metallation of the pyridyl nitrogens in ligands **4.1** and **4.2** was confirmed using both NMR and IR spectroscopies.

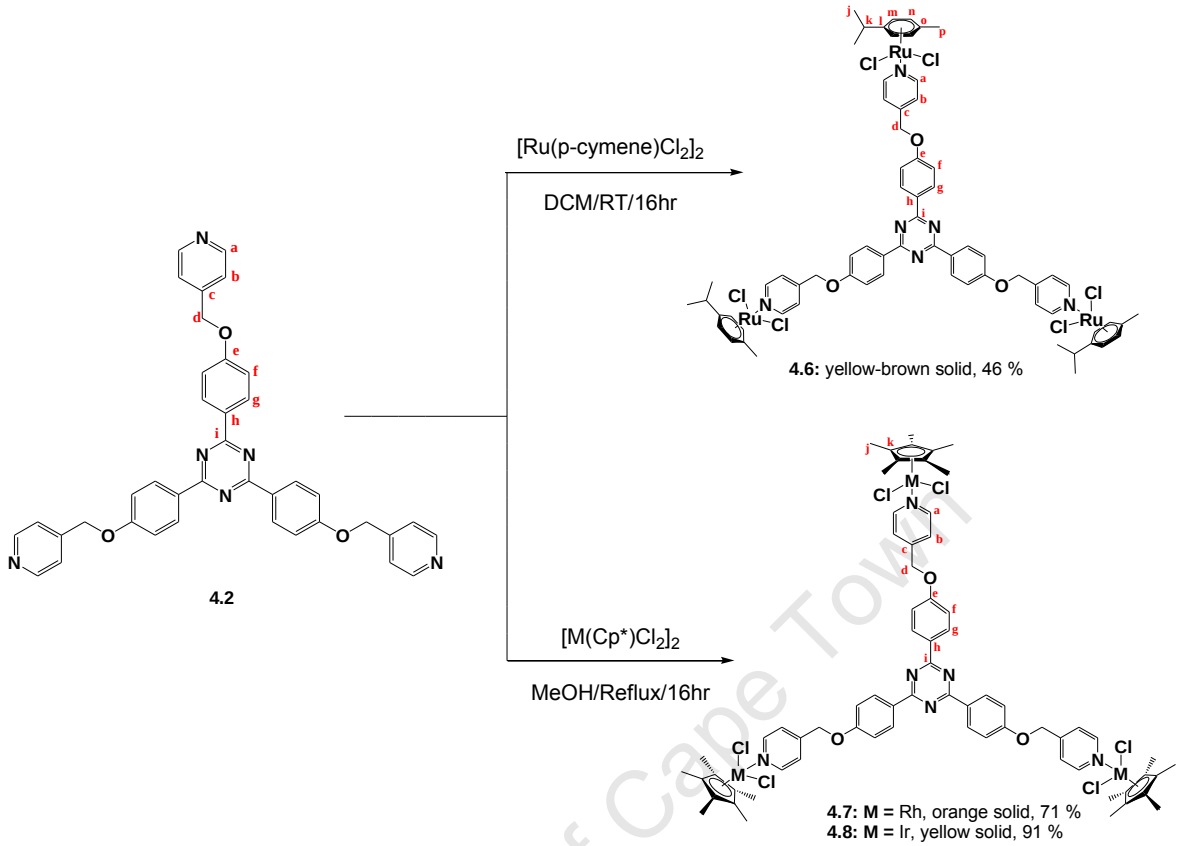

Scheme 4.3.

Comparison of the ^{1}H NMR spectra of **4.3** – **4.8** with their corresponding free ligands (**4.1** and **4.2**) reveals for all the complexes, a downfield shift of the doublet associated with the pyridyl protons *ortho* to nitrogen to around 9.00 ppm. Figures 4.2. and 4.3. show the proton NMR spectra for two dinuclear (**4.3** and **4.5**, **Figure 4.2.**) and two trinuclear (**4.6** and **4.8**, **Figure 4.3.**) complexes along with their corresponding free ligand. This deshielding of the H_a proton resonances is characteristic of metal coordination to nitrogen and arises from increased back-bonding between the metal and nitrogen causing reduced electron density in the *ortho* carbon-hydrogen bond. This effect has been reported for other mono- and multinuclear Ru(II), Rh(III) and Ir(III) complexes containing monodentate 4-pyridyl ligands.[27,29,39-44] A minimal change in the resonances associated with the other protons of the now metallated pyridyl ether ligands were observed confirming that coordination of the metal occurs only at the pyridyl nitrogens and that there was no coordination to the nitrogen atoms of the triazine core.

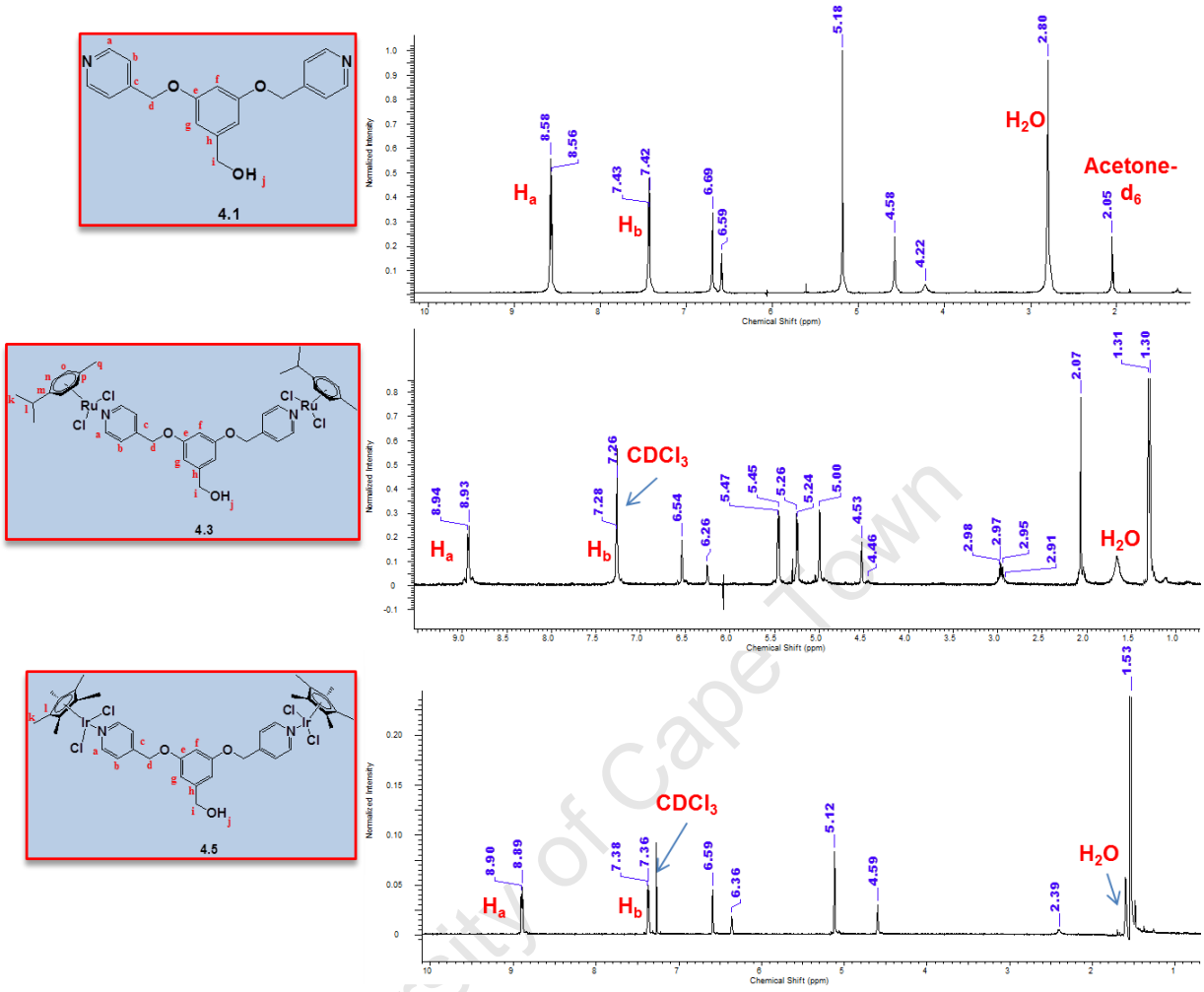

Figure 4.2. Proton NMR spectra for **4.1** (Acetone-d_6), **4.3** and **4.5** ($CDCl_3$)

For the Ru(II) complexes **4.3** and **4.6**, the proton resonances corresponding to the aromatic protons of the *p*-cymene ring are observed downfield compared to the alkyl ether protons at 5.47 and 5.26 ppm; with the lower frequency resonance assigned to the protons *ortho* to the methyl substituent. For complex **4.3** these resonances are observed as distinct doublets with the expected ^3J coupling of between 5.50 and 6.00 Hz. However, for complex **4.6** they are seen as broad singlets. This broadening of the proton signals is also observed for the other resonances associated with **4.6** (**Figure 4.3.**).

The trinuclear complexes, **4.6** – **4.8**, exhibit low solubility in the chlorinated solvents DCM and chloroform and are insoluble in other common organic solvents such as methanol, ethanol and acetone. Thus, the broadening of the proton NMR signals for **4.6** is attributed to the fairly dilute $CDCl_3$ NMR sample. The methyl protons of the isopropyl substituent of the

arene ring are observed at 1.30 and 1.56 ppm for complexes **4.3** and **4.6** respectively; the methyl protons resonate at *ca.* 2.10 ppm for both complexes. The rhodium and iridium functionalized complexes **4.4**-**4.5** and **4.7**-**4.8** display a singlet at approximately 1.55 ppm for the protons of the pentamethylcyclopentadienyl ring.

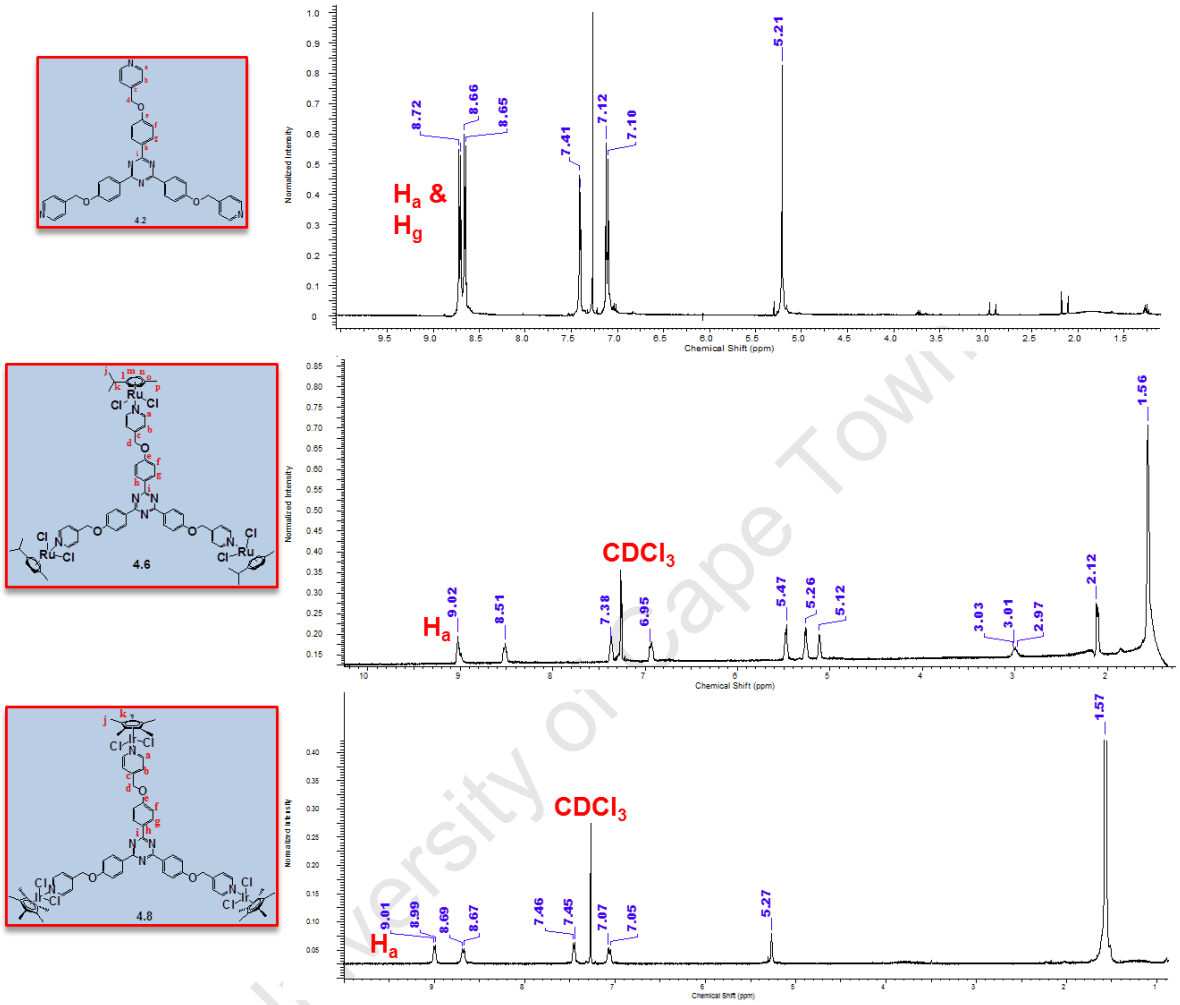

Figure 4.3. ^{1}H NMR Spectra for **4.2**, **4.6** and **4.8** in $CDCl_3$.

Analysis of complexes **4.3** – **4.5** using $^{13}C\{^{1}H\}$ NMR spectroscopy reveals a high frequency shift of the resonance assigned to C_a compared to the free ligand (**4.1**) to between 155.0 and 153.0 ppm (**Table 4.1.**). As was observed in the proton NMR spectra for complexes **4.3**-**4.5**, little to no effect is observed on the other carbon resonances assigned to the metal-coordinated ligand. The resonances assigned to the alkyl ether carbons (C_d) occur at approximately the same shift of between 67.5 - 67.8 ppm. The benzyl carbon (C_i) also occurs at essentially the same resonance in the complexes (**4.3** – **4.5**) compared to the free ligand (**4.1**) confirming that complexation to the hydroxyl oxygen had not occurred.

The *p*-cymene moieties of complex **4.3** show a singlet at 82.9 and 82.0 ppm due to the resonances of the unsubstituted aromatic carbons of the ring. The isopropyl substituted aromatic carbon (C_m) and the methyl substituted carbon (C_p) resonates at 97.2 and 103.2 ppm respectively. These resonances agree with similar mononuclear 4-pyridyl complexes.[27] For complexes **4.4** and **4.5**, the carbons of the pentamethylcyclopentadienyl ring occur at 94.1 and 85.8 ppm respectively. The carbon of the methyl substituents (C_k) are seen at approximately 8.5 ppm.

Table 4.1. Selected $^{13}C\{^1H\}$ NMR shifts for Compounds **4.1** and **4.3-4.5**

	$^{13}C\{^1H\}$ NMR shift (ppm)				
Compound	**C_a**	**C_c**	**C_d**	**C_e**	**C_i**
4.1	149.7	159.5	67.8	146.3	63.4
4.3	154.5	159.9	67.5	148.7	64.1
4.4	153.1	159.2	67.8	148.7	64.5
4.5	153.2	159.2	67.6	149.1	64.6

Due to the low solubility of complexes **4.6** – **4.8** in most common deuterated solvents, ascertaining decent ^{13}C NMR spectra proved difficult. Even NMR experiments run overnight at 30 °C in a mixture of DMSO-d_6 and $CDCl_3$ failed to give spectra with good resolution.

Metallation of the pyridyl nitrogens was further confirmed for complexes **4.3** - **4.8** using IR spectroscopy. For all complexes, a high energy shift of the absorption band associated with the pyridyl C=N vibration was observed compared to the corresponding free ligand. For the dinuclear complexes a shift to approximately 1615 cm^{-1} compared to **4.1** (where it is observed at 1597 cm^{-1}) was noted and for the trinuclear complexes the $C{=}N_{pyridyl}$ vibration is observed between 1613 and 1623 cm^{-1}. The C=N vibration associated with the triazine functionality in complexes **4.6** – **4.8** shows no change compared to the free ligand (**4.2**) and is still observed at approximately 1606 cm^{-1}, providing further evidence that no complexation to the triazine nitrogens had occurred .

High resolution Electrospray Ionisaton Mass Spectrometry was used to determine the molecular ions for each complex (**Table 4.2.**). Complexes **4.3** and **4.4** exhibited a base peak corresponding to a triply charged complex; with **4.4** forming an acetonitrile adduct. The trinuclear complexes **4.6**-**4.8** also form adducts with either sodium (**4.6**), methanol (**4.7**) or water (**4.8**).

Table 4.2. Mass Spectral Data for Complexes **4.3** – **4.8**

Complex	Base peak *m/z*	Assignment
4.3	312.01	$[M + 3H]^{3+}$
4.4	351.01	$[M + 3H + 3CH_3CN]^{3+}$
4.5	1083.2	$[M - Cl]^{+}$
4.6	270.6	$[M + 3Na^{+} + 3H^{+}]^{6+}$
4.7	810.2	$[M + 2H + 2CH_3OH]^{2+}$
4.8	441.1	$[M - 4Cl^{-} + 4H_2O]^{4+}$

4.2.3. Electronic Spectral Analysis

The electronic properties of compounds **4.1** – **4.8** were analyzed using UV-vis Spectroscopy. Figures 4.4. and 4.5. show the UV-vis spectra for the dipyridyl (**4.1** and **4.3**-**4.5**) and tripyridyl compounds (**4.2** and **4.6**-**4.8**) respectively. Table 4.3 lists the energy absorptions observed. All of the complexes were analysed at a concentration of 0.5 μM in DCM (dipyridyl compounds) or DMSO (tripyridyl compounds). Assignment of the absorption bands were made based on similar complexes reported in the literature.[42,45,46]

Table 4.3. Spectral Data for compounds **4.1** – **4.8** ascertained using UV-vis Spectrometry

Compound	λ_{max} (nm)[a]		
4.1	358 (π-π*)		
4.3	343 (π-π*)	383-471 (MLCT, $d–\pi_{ligand}$)	
4.4	336 (π-π*)	369-469 (MLCT, $d_{metal} –\pi_{ligand}$)	
4.5	323 (π-π*)	415-465 (MLCT, $d_{metal} –\pi_{ligand}$)	
4.2	345 (π-π*)	409 (π–π*)	
4.6	343 (π-π*)	405 (MLCT, $d_{metal} –\pi_{ligand}$)	482 (LMCT, $\pi_{ligand}–d_{metal}$)
4.7	345 (π-π*)	410 (MLCT, $d_{metal} –\pi_{ligand}$)	
4.8	368 (π-π*)	374 (MLCT, $d_{metal} –\pi_{ligand}$)	446 (LMCT, $\pi_{ligand}–d_{metal}$)

[a] transitions are given in parentheses.

All of the complexes exhibit a hyperchromic shift in the absorption bands compared to their corresponding free ligand. In the visible region, the absorption bands are fairly broad which is characterisitic of highly conjugated aromatic systems. Ligand **4.1** shows a broad soret band in the UV region at 345 nm and is attributed to the intraligand π-π* transitions of the aromatic and heteroaromatic rings. This intraligand transition shows a hypsochromic shift in the

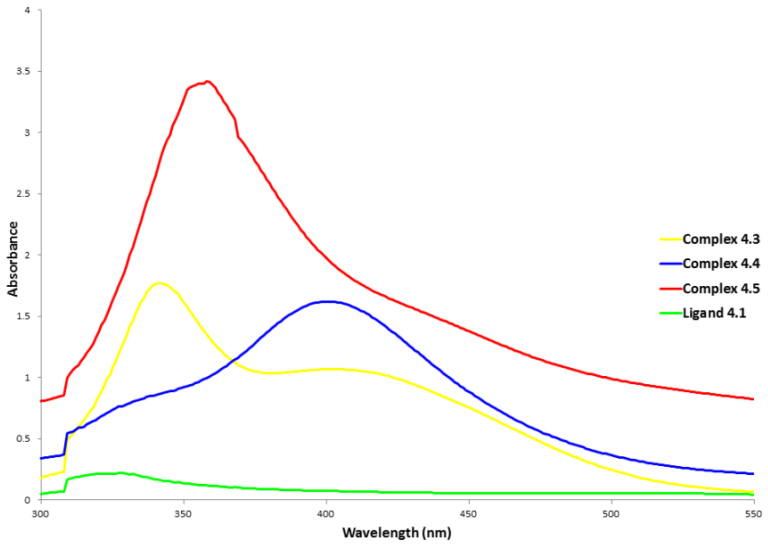

Figure 4.4. UV-vis Spectra for compounds **4.1** and **4.3**-**4.5**. The compounds were analysed at ambient temperature using a 0.5 µM solution of each compound in DCM in a 1 cm glass cuvette.

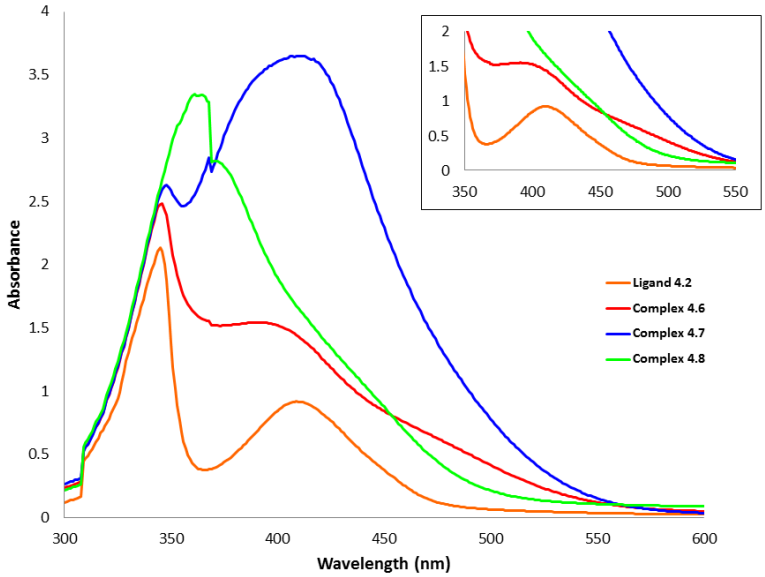

Figure 4.5. UV-vis Spectra for compounds **4.2** and **4.6**-**4.8**; with expansion of the visible region inset. The compounds were analysed at ambient temperature using a 0.5 µM solution of each compound in DMSO in a 1 cm glass cuvette.

complexes (**4.3**-**4.5**). Compared to corresponding dinuclear complexes, the absorption spectra of **4.1** is much less intense. The complexes (**4.3**-**4.5**) are intensely coloured and the metal to ligand and ligand to metal charge transfer (MLCT and LMCT) bands thus absorb strongly in the visible region while the free ligand is a pale beige colour and shows no absorption in the visible region.

The tripyridyl functionalized triazine ligand **4.2** is a bright yellow solid and shows a strongly absorbing soret band in the visible region at 409 nm due to the intraligand π-π* transitions. The MLCT bands for the complexes (**4.6**-**4.8**) absorb strongly in this region and most likely mask the intraligand absorptions in the visible region. Complexes **4.6** and **4.8** show shoulders to their MLCT bands at 482 and 446 nm respectively and these absorptions are most likely due to ligand to metal charge transfers (LMCT).

4.2.4. Single Crystal X-ray Diffraction Analysis

Singles crystals of complex **4.5** suitable for single crystal X-ray analysis were grown from a mixture of methanol and hexane. Complex **4.5** crystallized in monoclinic space group Pn with one molecule of methanol and three molecules of water in the asymmetric unit. The molecular structure of **4.5** validates the proposed structures of **4.3** - **4.8** put forth by the spectroscopic and spectrometric characterizations discussed earlier. Figure 4.5 shows the complex structure of **4.5**·$\mathbf{C_{0.5}H_5O_2}$ with the solvent molecules omitted and the crystal data is listed in Table 4.4. Tables 4.5 and 4.6 list selected bond lengths and angles for the molecular structure of **4.5**.

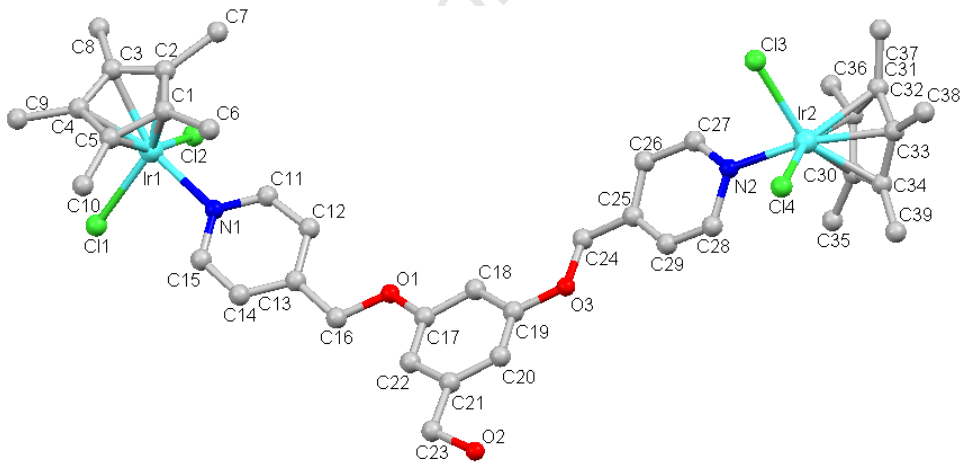

Figure **4.5.** Molecular structure of **4.5** with hydrogen atoms and solvent molecules omitted.

Each iridium metal center adopts a typical 'piano-stool' conformation with the two chlorido and the pyridyl ring as the three legs and a pseudo-tetrahedral coordination geometry. Comparison of the Ir-C bond lengths between the metal and each bonded carbon of the pentamethylcyclopentadienyl ring reveal them to be similar indicating that the ring is

symmetrically bound to iridium. The Ir-Cl, Ir-C and Ir-N bond lengths observed in **4.5** are approximately 2.41 Å (Ir-Cl), 2.12 Å (Ir-C) and 2.10 Å (Ir-N).

Table **4.4.** Crystal Data for **Complex 4.5·$C_{0.5}H_5O_2$**

Complex 4.5·$C_{0.5}H_5O_2$	
Formula	$C_{39.5}H_{53}Cl_4Ir_2N_2O_5$
Formula weight	1162.04
Crystal system	Monoclinic
Space group	Pn
a (Å)	8.9586(19)
b (Å)	20.905(5)
c (Å)	12.436(3)
β (deg.)	90.550(5)
V (Å^3)	2329.0(9)
Z	2
D_c (g.cm^{-3})	1.614
μ (mm^{-1})	5.972
θ range for data collection (deg.)	2.47 to 25.80
Limiting indices	-10 < h < 10
	-25 < k < 25
	-15 < l < 15
no. of reflns meads	12247
no. of reflns used (Rint)	7998 (0.0000)
no. of params	429
R1	0.0343
wR2	0.0871
goodness of fit on F2	1.029

These values agree with those observed for similar complexes in the literature[39,43,47,48] as well as the expected length calculated from the covalent radii of iridium, chlorine (Ir-Cl: 2.40 Å), carbon (Ir-C: 2.09 Å) and nitrogen (Ir-N: 2.09 Å).[49] In the coordinated pyridyl-ether ligand, the C-N bond lengths in the pyridyl ring are found to be between 1.25 – 1.40 Å and the alkyl C-O bond lengths of the ether functionalities between 1.41 and 1.43 Å, comparing favourably to the interatomic distances typical of pyridines and ethers (C=N: 1.34 Å and C-O: 1.43 Å).[50]

In **4.5**, the bond angles observed for Cl-Ir-Cl and N-Ir-Cl are all close to 90 ° and the bond angles formed between the bonded carbons of the Cp* ligand, iridium and chloride ligand vary from 90 to 150 °. This trend has also been observed within the molecular structures of similar Cp*Ir(III) pyridyl complexes.[39,43,47,48]

Table **4.5.** Selected bond lengths observed for complex **4.5·$C_{0.5}H_5O_2$**

Bond Length (Å)			
Ir1-N1	2.095(12)	**Ir2-N2**	2.067(11)
Ir1-C1	2.122(14)	**Ir2-C30**	2.090(18)
Ir1-C2	2.120(17)	**Ir2-C31**	2.171(17)
Ir1-C3	2.146(14)	**Ir2-C32**	2.238(19)
Ir1-C4	2.158(11)	**Ir2-C33**	2.141(19)
Ir1-C5	2.120(17)	**Ir2-C34**	2.11(3)
Ir1-Cl1	2.408(4)	**Ir2-Cl3**	2.418(7)
Ir1-Cl2	2.405(4)	**Ir2-Cl4**	2.419(5)
N1-C11	1.303(19)	**N2-C27**	1.25(2)
N1-C15	1.343(18)	**N2-C28**	1.43(2)
O1-C16	1.408(18)	**O3-C24**	1.429(19)
O1-C17	1.381(16)	**O3-C19**	1.399(18)

Table 4.6. Selected bond lengths observed for complex **4.5· $C_{0.5}H_5O_2$**

Bond Angles (°)			
C4-Ir1-Cl1	93.0(5)	**C33-Ir2-Cl3**	110.9(5)
C3-Ir1-Cl1	118.3(5)	**C32-Ir2-Cl3**	91.9(6)
C1-Ir1-Cl1	138.3(6)	**C30-Ir2-Cl3**	145.5(5)
C2-Ir1-Cl1	155.8(5)	**C31-Ir2-Cl3**	107.8(5)
C5-Ir1-Cl1	100.5(5)	**C34-Ir2-Cl3**	149.9(6)
N1-Ir1-Cl1	87.5(3)	**N2-Ir2-Cl3**	86.1(4)
C4-Ir1-Cl2	127.7(4)	**C33-Ir2-Cl4**	100.8(5)
C3-Ir1-Cl2	99.4(5)	**C32-Ir2-Cl4**	133.4(5)
C1-Ir1-Cl2	132.2(6)	**C30-Ir2-Cl4**	128.1(5)
C2-Ir1-Cl1	100.7(5)	**C31-Ir2-Cl4**	161.2(5)
C5-Ir1-Cl2	163.8(4)	**C34-Ir2-Cl4**	97.6(7)
N1-Ir1-Cl2	87.4(3)	**N2-Ir2-Cl4**	87.5(4)
Cl2-Ir1-Cl1	89.43(16)	**Cl3-Ir2-Cl4**	86.4(3)

4.3. Summary

Two new pyridyl ether ligands have been synthesised and peripherally metallated with ruthenium, rhodium and iridium precursors to give the corresponding di- and trinuclear complexes. All of the compounds were isolated as air and moisture stable solids and were

characterised using a variety of analytical and spectroscopic techniques. The molecular structure of **4.5** confirms the monodentate coordination of the pyridyl ether ligands to each metal put forth by the spectroscopic and spectrometric characterisations of complexes **4.3** - **4.8**.

A study of their *in vitro* antiparasitic and antitumor activity has been undertaken and the results are discussed in Chapter 6.

4.4. Experimental

4.4.1. Chemicals and General Methods

1,2,3,4,5-Pentamethylcyclopentadiene, α-phellandrene, 4-bromomethylpyridine hydrobromide, 3,5-dihydroxybenzylalcohol and 4-cyanophenol were purchased from Sigma-Aldrich and used without further purification. Ruthenium trichloride trihydrate, rhodium trichloride trihydrate and iridium trichloride trihydrate were kindly donated by AngloAmerican Platinum Limited. All solvents used were analytical grade and dried over molecular sieves. All reactions were carried out in air unless otherwise stated. The precursors, 2,4,6-Tris(*p*-hydroxyphenyl)triazine,[51] dichloro(*p*-cymene)ruthenium(II) dimer,[52] dichloro(pentamethyl-cyclopentadienyl)rhodium(III) dimer[53] and dichloro(pentamethylcyclopentadienyl)-iridium(III) dimer[53] were synthesised using literature methods.

4.4.2. Spectroscopic and Analytical Methods

Nuclear Magnetic Resonance (NMR) Spectra were recorded on a Varian Unity XR400 MHz (^{1}H at 399.95 MHz, ^{13}C at 100.58 MHz), Varian Mercury XR300 (^{1}H at 300.08 MHz, ^{13}C at 75.46 MHz) or Bruker Biospin GmbH (^{1}H at 400.22 MHz, ^{13}C at 100.65 MHz) spectrometer at ambient temperature. Chemical shifts for ^{1}H and ^{13}C{1H} NMR shifts are reported using tetramethylsilane (TMS) as the internal standard and ^{31}P{1H} NMR spectra were measured relative to H_3PO_4 as the external standard. NMR spectra were recorded in either deuterated dimethylsulfoxide (DMSO-d_6) or deuterated chloroform ($CDCl_3$-d_1) unless otherwise stated. Infrared (IR) absorptions were measured on Perkin-Elmer Spectrum 100 FT-IR Spectrometer as either KBr pellets or using a Universal Diamond Attenuated Total Reflection (ATR) accessory. Microanalyses for C, H, and N were carried out using a Thermo Flash 1112 Series CHNS-O Analyser and melting points were determined using a Büchi Melting Point Apparatus B-540. Mass Spectrometry determinations were carried out on all new compounds using either electron impact (EI) on a JEOL GC Matell instrument or electrospray ionisation (ESI) on a Waters API Quattro Micro instrument in either the positive or negative mode.

4.4.3. Synthesis of Pyridyl-ether Ligands

*4.4.3.1. [3,5-Bis-(pyridin-4-ylmethoxy)-phenyl]-methanol (**4.1**)*

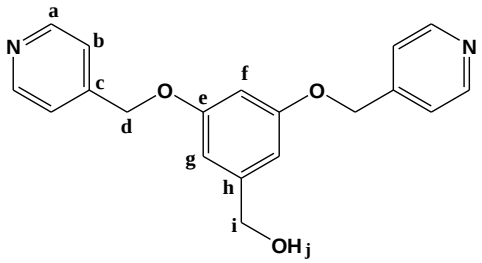

4.1

To a solution of 3,5-dihydroxybenzylalcohol (0.0659 g, 0.474 mmol) in acetone (30 cm^3), potassium carbonate (0.3903 g, 2.82 mmol) and 18-crown-6 (0.0248 g, 0.0942 mmol) was added. The mixture was stirred at room temperature for 15 minutes before 4-bromomethylpyridine hydrobromide (0.250 g, 0.989 mmol) was added and the reaction mixture heated to reflux for 48 hours. The reaction solvent was then evaporated under reduced pressure and the crude brown residue was extracted with DCM (50 cm^3). The organic layer was washed with deionized water (4 x 20 cm^3) and brine (1 x 20 cm^3), dried over magnesium sulfate, filtered and the solvent evaporated under reduced pressure to afford the product (**4.1**) as a brown amorphous solid. Yield: 0.0618 g, 41 %. Mp: 194-196 °C, . ^{1}H NMR (400 MHz, Acetone-d_6): δ (ppm) = 8.58 (d, ^3J(H_a-H_b): 6.39 Hz, 4H, H_a), 7.42 (d, ^3J(H_b-H_a): 5.59 Hz, 4H, H_b), 6.90 (s, 2H, H_g), 6.59 (s, 1H, H_f), 5.18 (s, 4H, H_d), 4.58 (s, 2H, H_i), 4.22 (br s, 1H, H_j). ^{13}C NMR (400 MHz, Acetone-d_6): δ (ppm) = 159.5 (C_e), 149.7 (C_a), 146.3 (C_c), 145.5 (C_h), 121.45 (C_b), 105.5 (C_g), 100.4 (C_f), 67.8 (C_d), 63.4 (C_i). IR (atr, cm^{-1}) υ = 3184 (br w, O-H), 1597 (s, C=N), 1166 (s, -C-<u>O-CH$_2$</u>-). Elemental Analysis for $C_{19}H_{18}O_3N_2$: found C, 67.89; H, 5.73; N, 8.03 %; calculated for $C_{19}H_{18}O_3N_2 \cdot 0.5CH_4O$: C, 67.44; H, 5.36; N, 8.28 %. EI-MS: *m/z* 322.11 ($[M]^+$, 100%).

*4.4.3.2. 2,4,6-Tris-[4-(pyridin-4-ylmethoxy)-phenyl]-[1,3,5]triazine (**4.2**)*

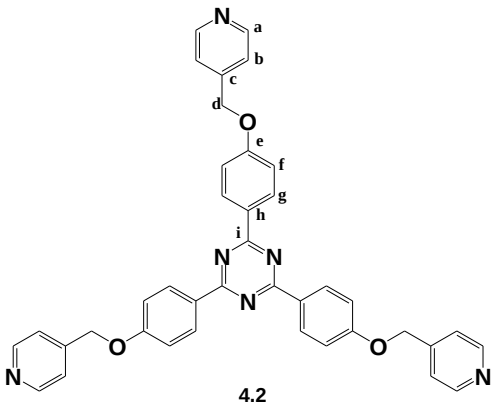

4.2

2,4,6-Tris(4-hydroxyphenyl)triazine (0.100 g, 0.280 mmol) and potassium carbonate (0.232 g, 1.68 mmol) was added to DMF (30 cm^3) and stirred for 5 minutes at room temperature. 4-Bromomethylpyridine hydrobromide (0.234 g, 0.924 mmol) was then added and the reaction mixture was heated to 80 °C for 18 hours with stirring. Upon cooling to room temperature, the reaction mixture was diluted with ethyl acetate (100 cm^3) and washed with deionized water (3 x 50 cm^3) and brine (1 x 50 cm^3). The organic layer was then dried over magnesium sulfate, filtered and the solvent evaporated under reduced pressure to afford the product (**4.2**) as a bright yellow amorphous solid. Yield: 0.0924 g, 52 %. Mp: 253-254 °C, .^{1}H NMR (400 MHz, $CDCl_3$-d_1): δ (ppm) = 8.71 (d, $^3J(H_a\text{-}H_b)$: 9.19Hz, 6H, H_a), 8.65 (d, $^3J(H_g\text{-}H_f)$: 5.99 Hz, 6H, H_g), 7.41 (d, $^3J(H_b\text{-}H_a)$: 4.80 Hz, 6H, H_b), 7.12 (d, $^3J(H_f\text{-}H_g)$: 8.80 Hz, 6H, H_f), 5.21 (s, 6H, H_d). ^{13}C NMR (400 MHz, Acetone-d_6): δ (ppm) = 158.1 (C_i), 149.8 (C_a), 141.57 (C_e), 134.0 (C_c), 128.3 (C_g), 123.3 (C_h), 121.5 (C_b), 115.12 (C_f), 67.9 (C_d). IR (atr, cm^{-1}) υ = 1607(w, $C{=}N_{triazine}$), 1592 (w, $C{=}N_{pyridyl}$), 1131 (s, -C-O-CH_2-). Elemental Analysis for $C_{39}H_{30}O_3N_6$: found C, 72.07; H, 5.10; N, 12.52 %; calculated for $C_{39}H_{30}O_3N_6 \cdot 0.5C_4H_8O_2$: C, 74.26; H, 4.79; N, 13.33. EI-MS: *m/z* 630.21 ($[M]^+$, 100%)

4.4.4. Synthesis of Dinuclear Ru(II), Rh(III) and Ir(III) Pyridyl-ether Complexes

4.4.4.1. General Synthetic Method for Dinuclear Complexes

The ligand [3,5-Bis-(pyridin-4-ylmethoxy)-phenyl]-methanol (**4.1**) (1 molar equivalent) was dissolved in DCM (15 cm^3) and the appropropriate ruthenium, rhodium or iridium dimer (1.1 molar equivalent) was added and the reaction solution was stirred for 16 hours at room temperature. The reaction solvent was then reduced under reduced pressure to approximately a third of its original volume. The product was then precipitated from solution by addition of diethyl ether and isolated by vacuum filtration, washed with diethyl ether and dried.

*4.4.4.2 {([3,5-Bis-(pyridin-4-ylmethoxy)-phenyl]-methanol)di[dichloro(p-cymene)Ru(II)]} (**4.3**)*

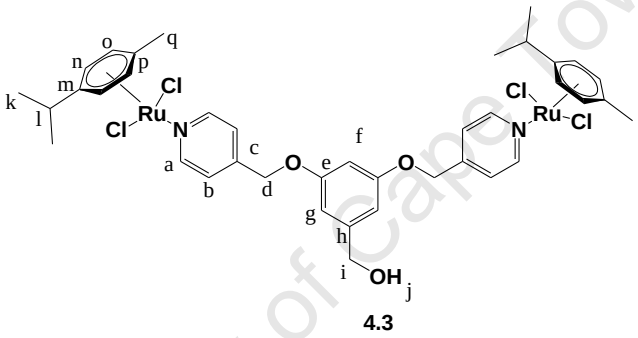

4.3

[3,5-Bis-(pyridin-4-ylmethoxy)-phenyl]-methanol (**4.1**) (0.0400 g, 0.124 mmol) was reacted with dichloro(*p*-cymene)ruthenium(II) dimer (0.0833 g, 0.136 mmol). The product (**4.3**) was isolated as dark red amorphous solid. Yield: 0.0931 g, 80 %. Mp: 141 °C, decomposition without melting. ^{1}H NMR (400 MHz, $CDCl_3$-d_1): δ (ppm) = 8.93 (d, $^3J(H_a\text{-}H_b)$: 5.11 Hz, 4H, H_a), 7.26 (d, $^3J(H_b\text{-}H_a)$: 4.39 Hz,4H, H_b), 6.54 (s, 2H, H_g), 6.26 (s, 1H, H_f), 5.44 (d, $^3J(H_o\text{-}H_n)$: 5.99 Hz, 4H, H_o), 5.25(d, $^3J(H_n\text{-}H_o)$: 5.59 Hz, 4H, H_n), 5.00 (s, 4H, H_d), 4.53 (s, 2H, H_i), 4.46 (br s, 1H, H_j), 2.00-2.90 (m, 2H, H_l), 2.03 (s, 6H, H_q), 1.30 (d, $^3J(H_k\text{-}H_l)$: 6.79 Hz, 12H, H_k). ^{13}C NMR (400 MHz, $CDCl_3$-d_1): δ (ppm) = 159.9 (C_e), 154.5 (C_a), 148.7 (C_c), 144.8 (C_h), 122.2 (C_b), 106.2 (C_g), 103.2 (C_p), 100.8 (C_f), 97.2 (C_m), 82.9 (C_o), 82.0 (C_n), 67.5 (C_d), 64.1 (C_i), 30.6 (C_l), 22.2 (C_k), 18.2 (C_q). IR (atr, cm^{-1}) υ = 3435(br s, O-H), 1598 (s, C=N), 1595 (s, $C{=}C_{aromatics}$), 1160 (s, -C-O-CH_2-). Elemental Analysis for $C_{39}H_{46}Cl_4N_2O_3Ru_2$: found C 47.92; H, 5.40; N, 2.46 %; calculated for $C_{39}H_{46}Cl_4N_2O_3Ru_2 \cdot 0.5CH_2Cl_2$: C, 47.93; H, 4.74; N, 2.87. ESI-MS: *m/z* 312.01 ($[M + 3H]^{3+}$, 100%).

4.4.4.3. {([3,5-Bis-(pyridin-4-ylmethoxy)-phenyl]-methanol)di[dichloro(pentamethyl-cyclopentadienyl)Rh(III)]} ***(4.4)***

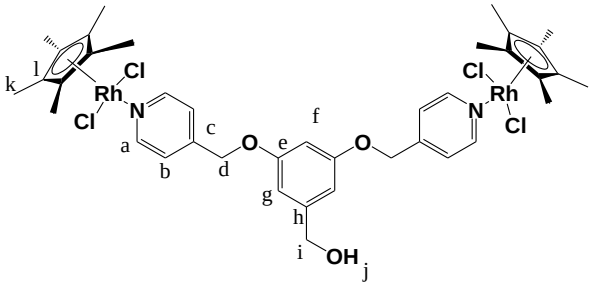

4.4

[3,5-Bis-(pyridin-4-ylmethoxy)-phenyl]-methanol (**4.1**) (0.0473 g, 0.147 mmol) was reacted with dichloro(pentamethylcyclopentadienyl)rhodium(III) dimer (0.1006 g, 0.163 mmol). The product (**4.4**) was isolated as a bright orange amorphous solid. Yield: 0.1104 g, 80 %. Mp: 228 - 230 °C. ^{1}H NMR (400 MHz, $CDCl_3$-d_1): δ (ppm) = 8.91 (br s, 4H, H_a), 7.38 (d, ^{3}J(H_a-H_b): 6.39 Hz, 4H, H_b), 6.57 (s, 2H, H_g), 6.33 (s, 1H, H_f), 5.07 (s, 4H, H_d), 4.58 (s, 2H, H_i), 2.61 (br s, 1H, H_j), 1.58 (s, 30H, H_k). ^{13}C NMR (400 MHz, $CDCl_3$-d_1): δ (ppm) = 159.2 (C_e), 153.1 (C_a), 148.7 (C_c), 144.8 (C_h), 122.9 (C_b), 106.6 (C_g), 101.3 (C_f), 94.1 (C_l), 67.8 (C_d), 64.5 (C_i), 8.8 (C_k). IR (atr, cm^{-1}) υ = 3443(br w, O-H), 1615 (s, C=N), 1152 (s, -C-O-CH_2-). Elemental Analysis for $C_{39}H_{48}Cl_4N_2O_3Rh_2$: found C, 47.13; H, 5.42; N, 2.04 %; calculated for $C_{39}H_{48}Cl_4N_2O_3Rh_2 \cdot C_3H_7Cl_2O_{0.5}$: C, 47.48; H, 5.21; N, 2.63. ESI-MS: *m/z* 351.01 ([M + 3H + $3CH_3CN$]$^{3+}$, 100%).

*4.4.4.4. {([3,5-Bis-(pyridin-4-ylmethoxy)-phenyl]-methanol)di[dichloro(pentamethyl-cyclopentadienyl)Ir(III)]} (**4.5**)*

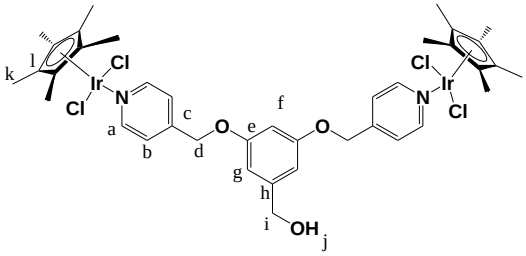

4.5

[3,5-Bis-(pyridin-4-ylmethoxy)-phenyl]-methanol (**4.1**) (0.0372 g, 0.115 mmol) was reacted with dichloro(pentamethylcyclopentadienyl)iridium(III) dimer (0.1013 g, 0.127 mmol). The product (**4.5**) was isolated as a bright yellow amorphous solid. Yield: 0.0865 g, 67 %. Mp: 195 °C, decomposition without melting. ^{1}H NMR (400 MHz, $CDCl_3$-d_1): δ (ppm) = 8.89 (d, $^{3}J(H_a\text{-}H_b)$: 5.60 Hz, 4H, H_a), 7.38 (d, $^{3}J(H_a\text{-}H_b)$: 4.80 Hz, 4H, H_b), 6.59 (s, 2H, H_g), 6.36 (s, 1H, H_f), 5.12 (s, 4H, H_d), 4.59 (s, 2H, H_i), 2.39 (br s, 1H, H_j), 1.54 (s, 30H, H_k). ^{13}C NMR (400 MHz, $CDCl_3$-d_1): δ (ppm) = 159.2 (C_e), 153.2 (C_a), 149.1 (C_c), 144.6 (C_h), 123.0 (C_b), 106.7 (C_g), 101.3 (C_f), 85.8 (C_l), 67.6 (C_d), 64.6 (C_i), 8.5 (C_k). IR (atr, cm^{-1}) υ = 3458 (br w, O-H), 1615 (s, C=N), 1152 (s, -C-O-CH_2-). Elemental Analysis for $C_{39}H_{48}Cl_4N_2O_3Ir_2$: found C 39.14; H, 4.49; N, 1.80 %; calculated for $C_{39}H_{48}Cl_4N_2O_3Ir_2 \cdot C_6H_{12}Cl_3O$: C, 39.65; H, 4.52; N, 2.05. ESI-MS: *m/z* 1083.2 ($[M - Cl]^+$, 100%).

4.4.5. Synthesis of Trinuclear Ru(II), Rh(III) and Ir(III) Pyridyl-ether Complexes

4.4.5.1. General Synthetic Method for Trinuclear Complexes

The ligand 2,4,6-Tris-[4-(pyridin-4-ylmethoxy)-phenyl]-[1,3,5]triazine (**4.2)** (2 molar equivalent) was dissolved in DCM (15 cm^3) and the appropropriate ruthenium, rhodium or iridium dimer (3.1 molar equivalent) was added and the reaction solution was stirred for 16 hours at room temperature. The reaction solvent was then reduced under reduced pressure to approximately a third of its original volume. The product was then precipitated from solution by addition of diethyl ether and isolated by vacuum filtration, washed with diethyl ether and dried.

*4.4.5.2. {([2,4,6-Tris-[4-(pyridin-4-ylmethoxy)-phenyl]-[1,3,5]triazine]tri[dichloro(p-cymene)Ru(II)]} (**4.6**)*

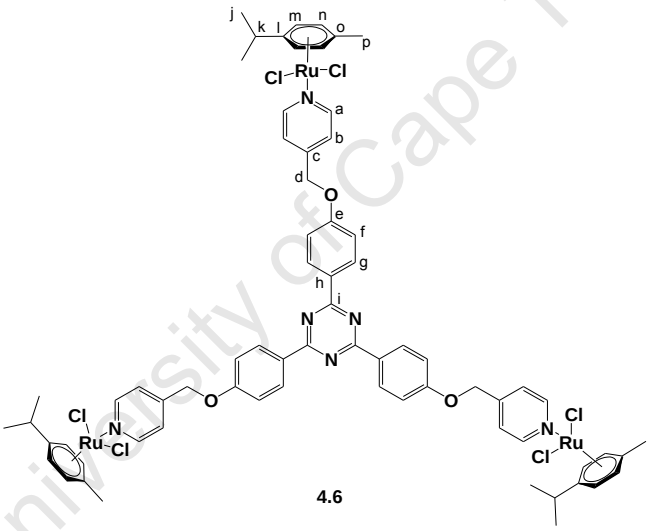

4.6

2,4,6-Tris-[4-(pyridin-4-ylmethoxy)-phenyl]-[1,3,5]triazine (**4.2**) (0.0675 g, 0.107 mmol) was added to stirred solution of dichloro(*p*-cymene)ruthenium(II) dimer (0.102 g, 0.167 mmol) in DCM (15 cm^{-3}). The reaction was allowed to stir at room temperature for 16 hours at which time the volume of the solvent was reduced to approximately 5 cm^{-3} and an excess of diethyl ether was added; precipitating the product (**4.6**). The product (**4.6**) was isolated as a yellow brown amorphous solid by filtration under reduced pressure, washed with diethyl ether and dried. Yield: 0.0767 g, 46 %. Mp: 207-211 °C, decomposition without melting. ^{1}H NMR (400 MHz, $CDCl_3$-d_1): δ (ppm) = 9.02 (br s, 6H, H_a), 8.53 (br s, 6H, H_g), 7.36 (br s, 6H, H_b), 6.95 (br s, 6H, H_f), 5.48 (br s, 6H, H_o), 5.27 (br s, 6H, H_n), 5.12 (br s, 6H, H_d), 3.01 (m, 3H, H_k), 2.12 (s, 9H, H_p), 1.56 (br s, 18H, H_j). IR (atr, cm^{-1}) υ = 1623 (w, $C{=}N_{pyridyl}$), 1607 (w,

C=$N_{triazine}$), 1149 (s, -C-<u>O-CH$_2$</u>-). Elemental Analysis for $C_{69}H_{72}Cl_6N_6O_3Ru_3$: found C 52.11; H, 5.03; N, 4.62 %; calculated for $C_{69}H_{72}Cl_6N_6O_3Ru_3 \cdot CH_6O_2$: C, 51.98; H, 5.05; N, 5.19. ESI-MS: *m/z* 270.6 ($[M + 3Na^+ + 3H^+]^{6+}$, 100%)

*4.4.5.3. {([2,4,6-Tris-[4-(pyridin-4-ylmethoxy)-phenyl]-[1,3,5]triazine]tri[dichloro(penta-methylcyclopentadienyl)Rh(III)]} (**4.7**)*

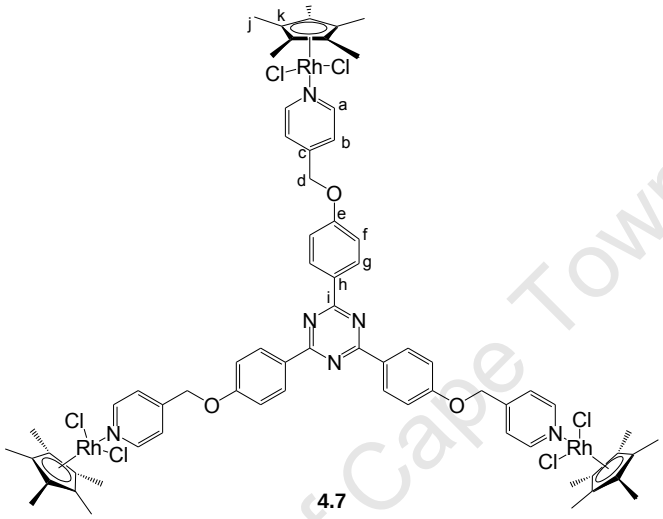

4.7

2,4,6-Tris-[4-(pyridin-4-ylmethoxy)-phenyl]-[1,3,5]triazine (**4.2**) (0.0614 g, 0.0974 mmol) was suspended in a stirred solution of dichloro(pentamethylcyclopentadienyl)rhodium(III) dimer (0.101 g, 0.162 mmol) in methanol (20 cm^{-3}). The reaction mixture was stirred at reflux for 16 hours and then cooled to room temperature. The product (**4.3**) was isolated as dark orange amorphous solid by filtration under reduced pressure, washed with methanol (10 cm^{-3}) and diethyl ether (10 cm^{-3}) and dried. Yield: 0.108 g, 71 %. Mp: 267 °C, decomposition without melting.^{1}H NMR (400 MHz, $CDCl_3$-d_1): δ (ppm) = 9.02 (d, ^3J(H_a-H_b): 6.00 Hz, 6H, H_a), 8.66 (d, ^3J(H_g-H_f): 8.79 Hz, 6H, H_g), 7.47 (d, ^3J(H_b-H_a): 6.40 Hz, 6H, H_b), 7.06 (d, ^3J(H_f-H_g): 8.80 Hz, 6H, H_f), 5.23 (s, 6H, H_d), 1.56 (s, 45H, H_j). IR (atr, cm^{-1}) υ = 1613 (w, C=$N_{pyridyl}$), 1606 (w, C=$N_{triazine}$), 1146 (s, -C-<u>O-CH$_2$</u>-). Elemental Analysis for $C_{69}H_{75}Cl_6N_6O_3Rh_3$: found C, 52.00; H, 4.72; N, 5.10 %; calculated for $C_{69}H_{75}Cl_6N_6O_3Rh_3 \cdot CH_4O$: C, 52.13; H, 4.75; N, 5.29. ESI-MS: *m/z* 810.2 ($[M + 2H + 2CH_3OH]^{2+}$, 100%).

*4.4.5.4. {([2,4,6-Tris-[4-(pyridin-4-ylmethoxy)-phenyl]-[1,3,5]triazine]tri[dichloro(penta-methylcyclopentadieny)Ir(III)]} (**4.8**)*

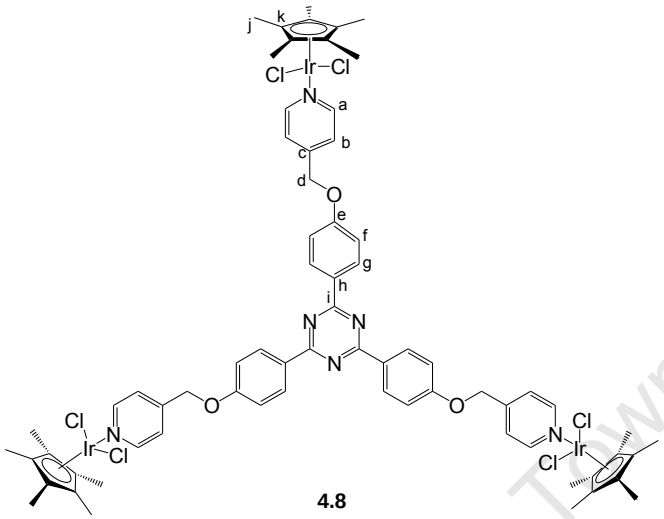

4.8

2,4,6-Tris-[4-(pyridin-4-ylmethoxy)-phenyl]-[1,3,5]triazine (**4.2**) (0.0496 g, 0.0786 mmol) was suspended in a stirred solution of dichloro(pentamethylcyclopentadienyl)iridium(III) dimer (0.103 g, 0.129 mmol) in methanol (20 cm^{-3}). The reaction mixture was stirred at reflux for 16 hours and then cooled to room temperature. The product (**4.3**) was isolated as yellow amorphous solid by filtration under reduced pressure, washed with methanol (10 cm^{-3}) and diethyl ether (10 cm^{-3}) and dried. Yield: 0.131 g, 91 %. Mp: 257 °C, decomposition without melting. ^{1}H NMR (400 MHz, $CDCl_3$-d_1): δ (ppm) = 8.99 (d, $^{3}J(H_a\text{-}H_b)$: 6.40 Hz, 6H, H_a), 8.65 (d, $^{3}J(H_g\text{-}H_f)$: 8.80 Hz, 6H, H_g), 7.45 (d, $^{3}J(H_b\text{-}H_a)$: 4.00 Hz, 6H, H_b), 7.04 (d, $^{3}J(H_f\text{-}H_g)$: 8.80 Hz, 6H, H_f), 5.24 (s, 6H, H_d) 1.56 (s, 45H, H_j). IR (atr, cm^{-1}) υ = 1619 (w, $C{=}N_{pyridyl}$), 1606 (w, $C{=}N_{triazine}$), 1146 (s, -C-O-CH_2-). Elemental Analysis for $C_{69}H_{75}Cl_6N_6O_3Ir_3$: found C, 45.10; H, 4.31; N, 4.81 %; calculated: C, 45.40; H, 4.14; N, 4.60. ESI-MS: *m/z* 441.1 ($[M - 4Cl^- + 4H_2O]^{4+}$, 100%)

4.4.6. X-Ray Structure Analysis

Single-crystal X-ray diffraction data were collected on a Bruker KAPPA APEX II DUO diffractometer using graphite-monochromated Mo-Kα radiation (χ = 0.71073 Å). Data collection was carried out at 173(2) K. Temperature was controlled by an Oxford Cryostream cooling system (Oxford Cryostat). Cell refinement and data reduction were performed using the program SAINT.[54] The data were scaled and absorption correction performed using SADABS[2]. The structure was solved by direct methods using SHELXS-97[55] and refined by full-matrix least-squares methods based on F^2 using SHELXL-97[55] and using the graphics interface program X-Seed.[56,57] The programs X-Seed and POV-Ray[58] were both used to prepare molecular graphic images. There are three water and one methanol molecules in the asymmetric unit and all were refined with half site occupancy factors. One water oxygen atom was refined anisotropically and all other non-hydrogen atoms of the solvents were refined with isotropic displacement parameters. The carbon atoms from C30 to C39 on the main molecule were restrained geometrically to a reasonable shape and were refined isotropically. All other non-hydrogen atoms on the main molecule were refined anisotropically. All hydrogen atoms, except those of the solvent molecule and the hydroxyl hydrogen H2 on O2, were placed in idealised positions and refined with geometrical constraints. The hydrogen atom H2 was located in the difference electron density map and refined with distance of O2-H2 set to 0.97 Å. The structure was refined to R factor of 0.0563. The highest peak is 3.01e/Å^3, 1.01 Å from IR1; the deepest hole is -1.95 e/Å^3, 0.78 Å from IR2.

4.5. References

1. V. Balzani, A. Juris and M. Venturi, *Chem. Rev.*, **1996**, *96*, 759.
2. L. Cuesta, E. Tomat, V. M. Lynch and J. L. Sessler, *Chem. Commun.*, **2008**, 3744.
3. J. Setsune, M. Toda and T. Yoshida, *Chem. Commun.*, **2008**, 1425.
4. A. J. Atkins, D. Black, A. J. Blake, A. Marin-Becerra, S. Parsons, L. Ruiz-Ramirez and M. Schröder, *Chem. Commun.*, **1996**, 457.
5. A. -Q. Jia, Y. -F. Han, Y. -J. Lin and G. -X. Jin, *Organometallics*, **2010**, *29*, 232.
6. E. Mas-Marza, E. Peris, I. Castro-Rodriguez and K. Meyer, *Organometallics*, **2005**, *24*, 3158.
7. C. Ganesamoorthy, M. S. Balakrishna and J. T. Mague, *J. Organomet. Chem.*, **2009**, *694*, 3390.
8. E. Zangrando, M. Casanova and E. Alessio, *Chem. Rev.*, **2008**, *108*, 4979.
9. P. Aguirre-Etcheverry and D. O'Hare, *Chem. Rev.*, **2010**, *110*, 4839.
10. A. S. Abd-El-Aziz, E. K. Todd and T. H. Afifi, *Macromol. Rapid Commun.*, **2002**, *23*, 113.
11. Y. -H. Liao and J. R. Moss, *Organometallics*, **1996**, *15*, 4307.
12. A. S. Abd-El-Aziz and C. R. de Denus, *J. Chem. Soc, Chem. Commun.*, **1994**, 663.
13. A. S. Abd-El-Aziz, C. R. de Denus, E. K. Todd and S. A. Bernardin, *Macromolecules*, **2000**, *33*, 5000.
14. B. Natarajan and N. Jayaraman, *J. Organomet. Chem.*, **2011**, *696*, 722.
15. E. Bonaplata, H. Ding, B. E. Hanson and J. E. McGrath, *Polym. Commun.*, **1995**, *36* (15), 3035.
16. M. Liu and J. M. J. Fréchet, *Pharm. Sci. Technol. To.*, **1999**, *2* (10), 393.
17. J. Nithyanandhan and N. Jayaraman, *Tetrahedron*, **2005**, *61*, 11184.
18. F. Bedos-Belval, A. Rouch, C. Vanucci-Bacque and M. Baltas, *Med. Chem. Commun.*, **2012**, *3*, 1356.
19. X. -F. Wang, X. -T. Tian, E. Ohkoshi, B. Qin, Y. -N. Liu, P. -C. Wub, M. -J. Hour, H .-Y. Hung, K. Qian, R. Huang, K. F. Bastow, W. P. Janzen, J. Jin, S. L. Morris-Natschke, K. -H. Lee and L. Xie, *Bioorg. Med. Chem. Lett.*, **2012**, *22*, 6224.
20. S. Top, I. Efremenko, M. N. Rager, A. Vessières, P. Yaswen, G. Jaouen and R. H. Fish, *Inorg. Chem.*, **2011**, *50*, 271.

21. S. Top, A. Vessières, G. Leclercq, J. Quivy, J. Tang, J. Vaissermann, M. Huché, and G. Jaouen, *Chem. - Eur. J.*, **2003**, *9*, 5223.

22. H. E. Amouri, A. Vessiéres, D. Vichard, S. Top, M. Gruselle and G. Jaouen, *J. Med. Chem.*, **1992**, *35*, 3130.

23. G. Jaouen, S. Top, A. Vessiéres, G. Leclercq, J. Quivy, L. Jin and A. Croisy, *C. R. Acad. Sci., Paris*, **2000**, *3*, 89.

24. J. S. Freundlich, J. W. Anderson, D. Sarantakis, H. -M. Shieh, M. Yu, J. -C. Valderramos, E. Lucumi, M. Kuo, W. R. Jacobs Jr., D. A. Fidock, G. A. Schiehser, D. P. Jacobus and J. C. Sacchettini, *Bioorg. Med.Chem. Lett.*, **2005**, *15* 5247.

25. J. S. Freundlich, M. Yu, E. Lucumi, M. Kuo, H. -C. Tsai, J. -C. Valderramos, L. Karagyozov, W. R. Jacobs Jr., G. A. Schiehser, D. A. Fidock, D. P. Jacobus and J. C. Sacchettini, *Bioorg. Med. Chem. Lett.*, **2006**, *16*, 2163.

26. C. L. Yeates, J. F. Batchelor, E. C. Capon, N. J. Cheesman, M. Fry, A. T. Hudson, M. Pudney, H. Trimming, J. Woolven, J. M. Bueno, J. Chicharro, E. Fernández, J. M. Fiandor, D. Gargallo-Viola, F. G. las Heras, E. Herreros and M. L. León, *J. Med. Chem.*, **2008**, *51*, 2845.

27. K. -G. Liu, X. -Q. Cai, X. -C. Li, D. -A. Qin and M. -L. Hu, *Inorg. Chim. Acta*, **2012**, *388*, 78.

28. F. Schmitt, P. Govindaswamy, O. Zava, G. Suss-Fink, L. Juillerat-Jeanneret and B. Therrien, *J. Biol. Inorg. Chem.*, **2009**, *14*, 101.

29. F. Schmitt, P. Govindaswamy, G. Süss-Fink, W.H. Ang, P.J. Dyson, L. Juillerat-Jeanneret and B. Therrien, *J. Med. Chem.*, **2008**, *51*, 1811.

30. S. S. Machakanur, B. R. Patil, D. S. Badiger, R. P. Bakale, K. B. Gudasi and K. W. A. Bligh, *J. Mol. Struct.*, **2012**, *1011* (121),

31. H. R. Bhat, S. K. Gupta and U. P. Singh, *RSC Advances*, **2012**, *2*, 12690.

32. K. Abdi, H. Hadadzadeh, M. Salimi, J. Simpson and A. D. Khalaji, *Polyhedron*, **2012**, *44*, 101.

33. N. Kumar, S. I. Khan and D. S. Rawat, *Helvetica Chim. Acta*, **2012**, *95*, 1181.

34. L. E. H. Paul , B. Therrien and J. Furrer, *J. Biol. Inorg. Chem.*, **2012**, *17*, 1053.

35. S. S. Machakanur, B. R. Patil, A. H. Pathan, G. N. Naik, S. G. Ligade and K. B. Gudasi, *Der. Pharma. Chemica.*, **2012**, *4* (2), 600.

36. M. Sharma, K. Chauhan, S. S. Chauhan, A. Kumar, S. V. Singh, J. K. Saxena, P. Agarwal, K. Srivastava, S. R. Kumar, S. K. Puri, P. Shah, M. I. Siddiqi and P. M. S. Chauhan, *Med. Chem. Commun.*, **2012**, *3*, 71.

37. I. N. Nnamani, G. S. Joshi, R. Danso-Danquah, O. Abdulmalik, T. Asakura, D. J. Abraham, and M. K. Safo, *Chem Biodivers.*, **2008**, *5* (9), 1764.
38. Y. Liu, P.-F. Yan, Y.-H. Yu, G.-F. Hou, J.-S. Gao and J.Y. Lu, *Cryst. Growth Des.*, **2010**, *10* (4), 1559.
39. Y. Yamamotoa, H. Suzuki, N. Tajima and K. Tatsumi, *Chem. Eur. J.*, **2002**, *8* (2), 372.
40. P. Govindaswamy, G. Süss-Fink and B. Therrien, *Organometallics*, **2006**, *26*, 915.
41. A. Bacchi, G. Cantoni, P. Pelagatti and S. Rizzato, *J. Organomet. Chem.*, **2012**, *714*, 81.
42. J. Grau, V. Noe, C. Ciudad, M. J. Prieto, M. Font-Bardia, T. Calvet, V. Moreno, *J. Inorg. Biochem.*, **2012** *109*, 72.
43. M. Yadav, A. K. Singh, R. Pandey and D. S. Pandey, *J. Organomet. Chem.*, **2010**, *695* 841.
44. P. Govender, N. C. Antonels, J. Mattsson, A. K. Renfrew, P. J. Dyson, J. R. Moss, B. Therrien and G. S. Smith, *J. Organomet. Chem.*, **2009**, *694*, 3470.
45. J. G. Małecki, M. Jaworska and R. Kruszynski, *Polyhedron*, **2006**, *25*, 2519.
46. S. K. Singh, M. Trivedi, M. Chandra and D. S. Pandey, *J. Organomet. Chem.*, **2005**, *690*, 647.
47. J. -Q. Wang, C. -X. Ren and G. -X. Jin *Organometallics*, **2006**, *25*, 74.
48. Y. -F. Han, J. -S. Zhang, Y. -J. Lin, J. Dai, and G. -X. Jin, *J. Organomet. Chem.*, **2007**, *692*, 4545.
49. L. Pauling; *The Nature of the Chemical Bond*; third ed.; Cornell University Press: New York, 1960.
50. L. E. Shutton; *Tables of Interatomic Distances and Configurations in Molecules and Ions (Supplement)*; The Chemical Society: London, 1965.
51. B. P. Dash, R. Satapathy, J. A. Maguire and N. S. Hosmane, *Organometallics*, **2010**, *29*, 5230.
52. M. A. Bennett, T. N. Huang, T. W. Matheson and A. K. Smith, *Inorg. Synth.*, **1982**, *21*, 74.
53. C. White, A. Yates and P. M. Maitlis, *Inorg. Synth.*, **1992**, *29*, 228.
54. SAINT Version 7.60a, Bruker AXS Inc., Madison, WI, USA, 2006.
55. G. M. Sheldrick, SHELXS-97 and SHELXL-97, University of Göttingen, Germany, 1997.
56. L. J. Barbour, *J. Supramol. Chem.*, **2001**, *1*, 189.

57. J. L. Atwood and L. J. Barbour, *Cryst. Growth Des.*, **2003**, *3*, 3.

58. http://www.povray.org.

CHAPTER 5

Synthesis and Characterisation of Di- and Trinuclear Ruthenium, Rhodium and Iridium Functionalised Pyridyl Aromatic Esters

5.1. Introduction

The synthesis and biological study of molecules containing aromatic ester functionalities is not uncommon. In fact, the inclusion of this type of moiety when considering the design of potential new chemotherapeutics is important as they are highly lipophilic groups and thus, may enhance diffusion of the drug through cell membranes.[1,2] There are numerous examples of aromatic esters with a variety of bioactivities in the literature. A series of lipophilic esters prepared from 4-acetyl-2-(2-hydroxyethyl)-5,6-bis(4-chlorophenyl)-2H-pyridazin-3-one (**I**, **Figure 5.1.**) have shown *in vivo* efficacy as antihypertensive agents.[3] A library of aromatic esters derived from cinnamic acid (**II**) have demonstrated anti-inflammatory effects *in vitro*[4] and ester functionalized analogues of bezafibrate (**III**) have also been investigated as orally active hypolipidemic agents.[5] Tyrosyl (2-(4-hydroxyphenyl)ethanol) is a known antioxidant and its ester derivatives have been assessed as antimicrobial and antileishmania agents.[6]

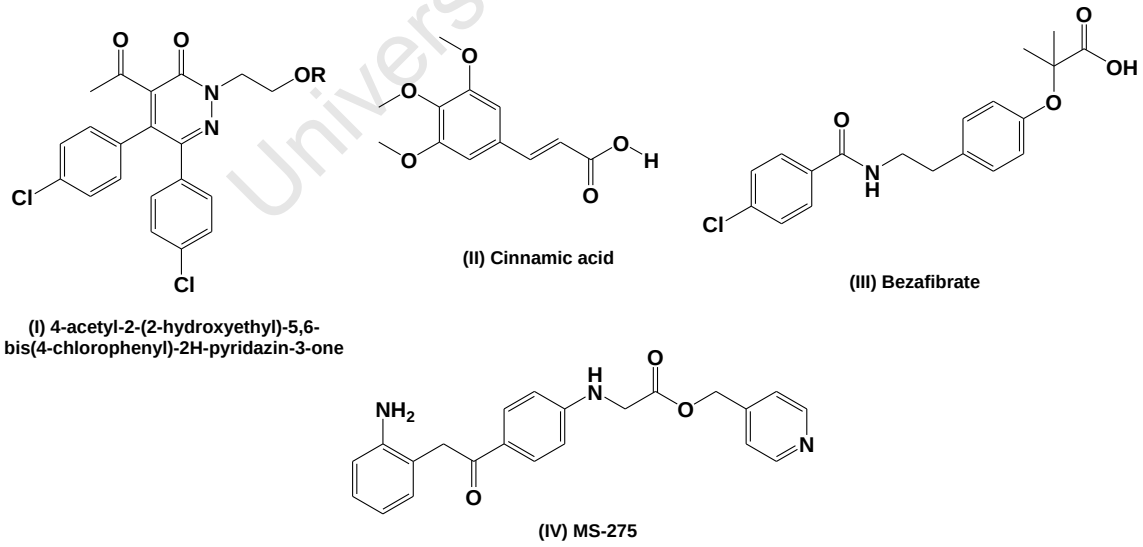

Figure 5.1. Examples of aromatic ester derivatives studied for different bioactivities.

As cancer chemotherapeutics, the pyridyl ester containing compound MS-275 (**IV**) is currently undergoing phase II clinical trials.[7] Larger polyester scaffolds have also gained considerable attention for tumor targeting either as micelles or via conjugation of the potential drug molecule onto the polyester scaffold.[8-12] Polyester dendrimers have been found to be less toxic and exhibit better biodegradability compared to polyamine and polyamide derivatives.[13] Thus, the premise of these studies is that these macromolecular scaffolds act as drug delivery vehicles, allowing preferential uptake by tumors through endocytosis. Once in the tumor cell, the ester bonds are hydrolyzed by esterases and the active drug moieties are released.

Mono- and polynuclear ruthenium-arene and pentamethylcyclopentadienyl rhodium and iridium pyridyl complexes have demonstrated promising pharmacological activities particularly as antiproliferative agents making them viable candidates for further study.[14-16] There have been several reports of the conjugation of the ruthenium arene moieties to mono- and di-aryl esters to give antitumoral agents with encouraging activities. An ethacrynic acid derivatized RAPTA complex (**V**, Figure 5.2) was found to inhibit glutathione-S-transferases with an activity that was better than the free acid while the RAPTA-C complex was completely inactive.[17-19] Mono- and dipyridyl ester containing ruthenium arene complexes (**VI** and **VII**) have demonstrated similar *in vitro* activities against both the cisplatin sensitive (A2780) and resistant (A2780*cis*R) human ovarian tumor cell line.[20] The pyridyl ester containing complex, 5-fluorouracil-1-methyl isonicotinate ruthenium arene (**VIII**), showed a moderate increase in activity against human BEL-7402 hepatocellular carcinoma cells compared to 5-fluorouracil.[14]

These examples demonstrate the viability of platinum group metal (PGM) functionalized pyridyl ester complexes as *in vitro* pharmacological agents. The pyridyl ester groups may increase the lipophilic nature of these complexes thereby allowing the active metal moieties to reach its target.

In this chapter, the synthesis and characterization of two di- and tripyridyl aromatic ester compounds along with their new Ru(II), Rh(III) and Ir(III) functionalized organometallic complexes is described. The rationale for the use of these ligands is to increase the lipohilic nature of the complexes by having more than one ester functionality. Further to this, the preparation of these complexes aims to couple the established *in vitro* pharmacological activities of half-sandwich Ru(II), Rh(III) and Ir(III) moieties with that of alkyl-pyridines. All

of the compounds synthesized have been evaluated *in vitro* as antitumor agents against the A2780 (cisplatin-sensitive) and A2780*cis*R (cisplatin-resistant) human ovarian carcinoma cell lines and as antiparasitic agents against the *P. falciparum* strains, NF54 (chloroquine sensitive) and Dd2 (chloroquine resistant), and the *T. vaginalis* strain G3 and the results of these studies are presented in Chapter 6.

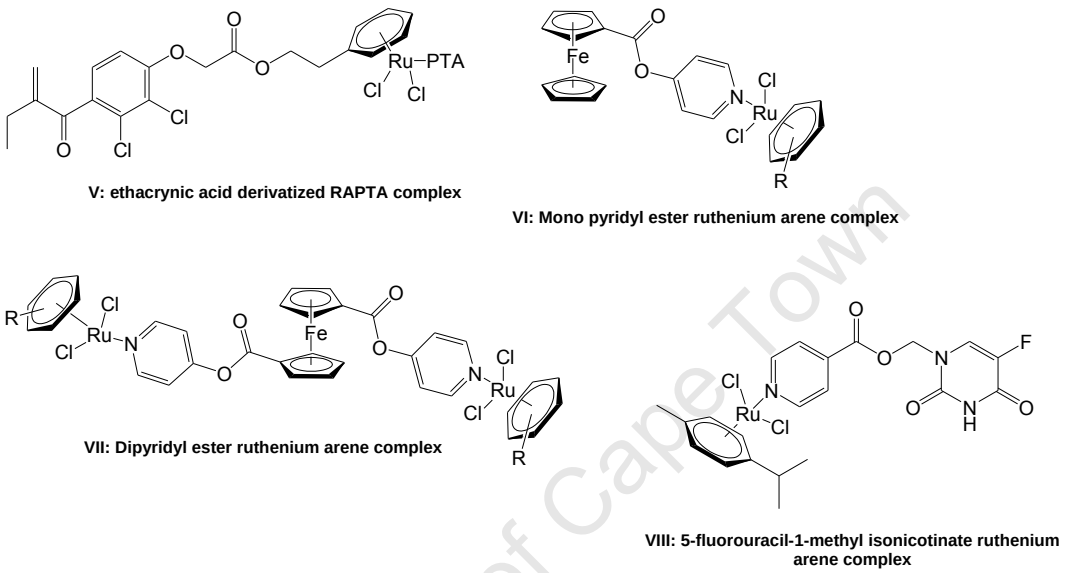

Figure 5.2. Examples of arene ruthenium ester complexes studied for activity as *in vitro* antitumor agents.

5.2. Results and Discussion

5.2.1. Synthesis and characterization of di- and tripyridyl ester ligands

Before the di- and tripyridyl ester ligands **5.1** and **5.2** were successfully prepared, two known reaction methods were initially attempted to synthesize compound **5.2** (Routes (i) and (ii), Scheme 5.1.) in order to establish a route that could be used for the preparation of both ligands. The Steglich Esterification method was first employed. 4-Pyridine carbinol was reacted with 1,3,5-benzene-tricarboxylic acid using N,N'-dicyclohexylcarbodiimide (DCC) as a coupling reagent and 4-dimethylaminopyridine (DMAP) as a catalyst. However, proton NMR analysis of the crude solid isolated revealed it to be unreacted DCC. Repeating this synthetic route but at reflux yielded the same result.

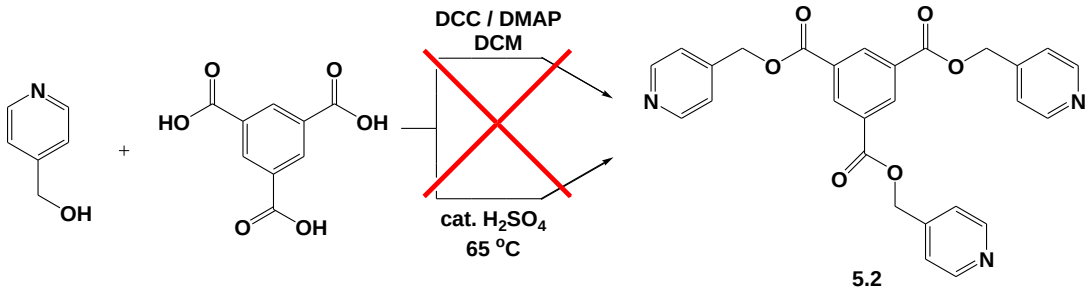

Scheme 5.1.

This route may not have been successful due to the poor solubility of the triacid precursor in DCM. The acid, 1,3,5-benzene-tricarboxylic acid, displayed better solubility in the alcoholic solvents methanol and ethanol but alcoholic solvents are not ideal as they would also undergo esterification.

The second route was then attempted, where a mixture of the tricarboxylic acid and a large excess of 4-pyridine carbinol along with a few drops of sulfuric acid was heated (without solvent) to a temperature slightly higher (65 °C) than the melting point of the alcohol for 16 hours. As with the previous method, a white solid was isolated but analysis using proton NMR revealed the solid to be unreacted tricarboxylic acid. Ligands **5.1** and **5.2** were finally successfully prepared by alkylation of the carboxylic acid.

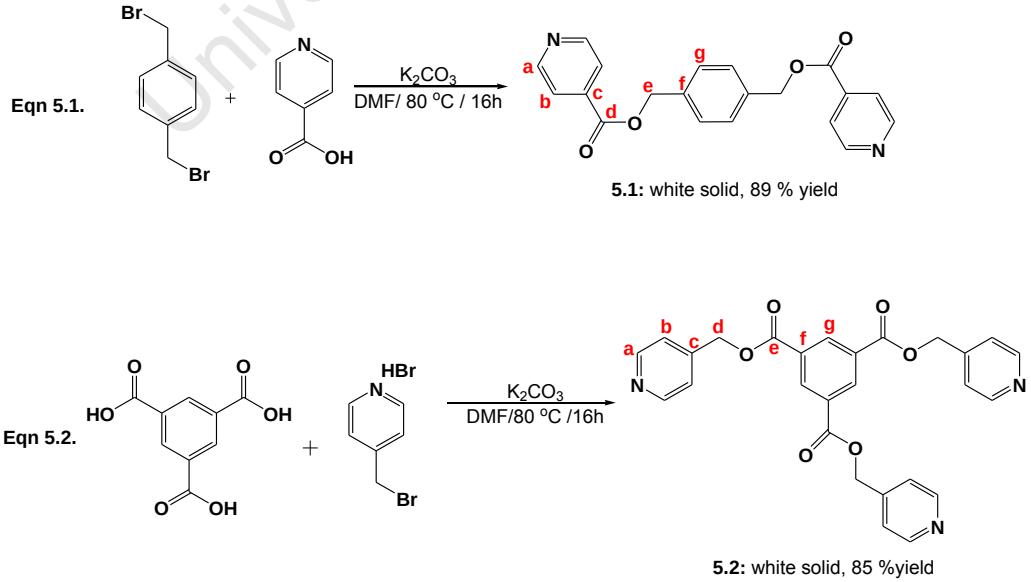

Scheme 5.2.

Ligand **5.1** was prepared by reaction of isonicotinic acid with 1,4-(bromomethyl)benzene in the presence of potassium carbonate in DMF (Eqn. **5.1**, Scheme **5.2**). The same reaction method was used for the preparation of ligand **5.2** which was obtained by reaction of 4-(bromomethyl)benzene with 1,3,5-benzene-tricarboxylic acid. Both ligands were isolated in high yields as air and moisture stable white solids. Both of these ligands have been reported in the literature and characterization of **5.1** and **5.2** agrees with the data previously reported.[21,22]

Analysis of the ^{1}H NMR spectra for **5.1** and **5.2** revealed that the pyridyl protons *ortho* and *meta* to nitrogen resonate between 8.60 - 8.90 and 7.35 – 7.50 ppm respectively as doublets due to through-bond coupling to each other. The coupling constants observed are typical of *para*-substituted 4-pyridyl rings. Compared to the tripyridyl ligand **5.2**, the protons H_a of the pyridyl rings in **5.1** are slightly more deshielded. This can be attributed to the ester functionalities that are bonded in the *para* position of the pyridyl rings giving rise to a much higher electron withdrawing effect on the H_a protons compared to ligand **5.2** where a methylene CH_2 spacer separates the ester functionalities from the pyridyl rings.

In the case of both ligands, a singlet observed at 5.41 and 5.45 ppm for **5.1** and **5.2** respectively confirmed esterification had occurred as these resonances correspond to the presence of the alkyl (-CH_2) ester protons and agree with the resonances observed for other aromatic alkyl ester compounds.[21-23] For ligand **5.1**, the aromatic protons of the central benzene core is observed as a singlet at 7.49 ppm whereas for ligand **5.2**, the three protons of the benzene ring are observed at 8.98 ppm due to the strongly electron withdrawing nature of the ester functionalities bonded to the ring in the 1, 3 and 5 positions.

This deshielding effect is also observed in the $^{13}C\{^{1}H\}$ NMR spectrum of **5.2** where the ester functionalized carbons (C_f) of the phenyl ring resonate at 144.2 ppm. The most deshielded resonance observed in the $^{13}C\{^{1}H\}$ NMR spectra of **5.1** and **5.2** is seen at approximately 164.5 ppm and is assigned to the carbonyl carbon of the ester substituents. The carbons, H_a and H_b, of the pyridyl rings resonate at approximately 150.0 and 122.0 ppm respectively. For **5.1**, the *para*-substituted carbon (C_c) of the pyridyl rings is observed further downfield at 137.3 ppm compared to **5.2** (131.1 ppm) as a consequence of the deshielding effect of the ester functional groups. For **5.2**, the ester functionalities are situated one carbon away from the pyridyl ring and their electron withdrawing effect is less strong.

Further spectroscopic analysis of ligands **5.1** and **5.2** using infrared (IR) spectroscopy reveals that the ester C=O bond vibration is observed in the expected region at approximately 1720 cm^{-1}. A single absorption band is observed at 1605 and 1611 cm^{-1} for **5.1** and **5.2** respectively due to the C=N stretching of the pyridyl rings. The O-CH_2 bond vibration of the ester functionalities is assigned to a strong absorption band observed in the region of 1230 and 1280 cm^{-1} for both ligands.

5.2.2. Synthesis and Characterisation of PGM Complexes

Ligands **5.1** and **5.2** were reacted with the precursors, dichloro(*p*-cymene)ruthenium(II) dimer, dichloro(pentamethylcyclopentadienyl)rhodium(III) dimer or dichloro(pentamethyl-cyclopentadienyl)iridium(III) dimer to yield the corresponding di- or trinuclear complexes **5.3** - **5.8** (Schemes 5.3 and 5.4) in moderate to high yields. All of the complexes were prepared using the same method. The appropriate ligand and dimer were stirred in DCM at room temperature for 16 hours and the resulting product was precipitated from the reaction solution using diethyl ether.

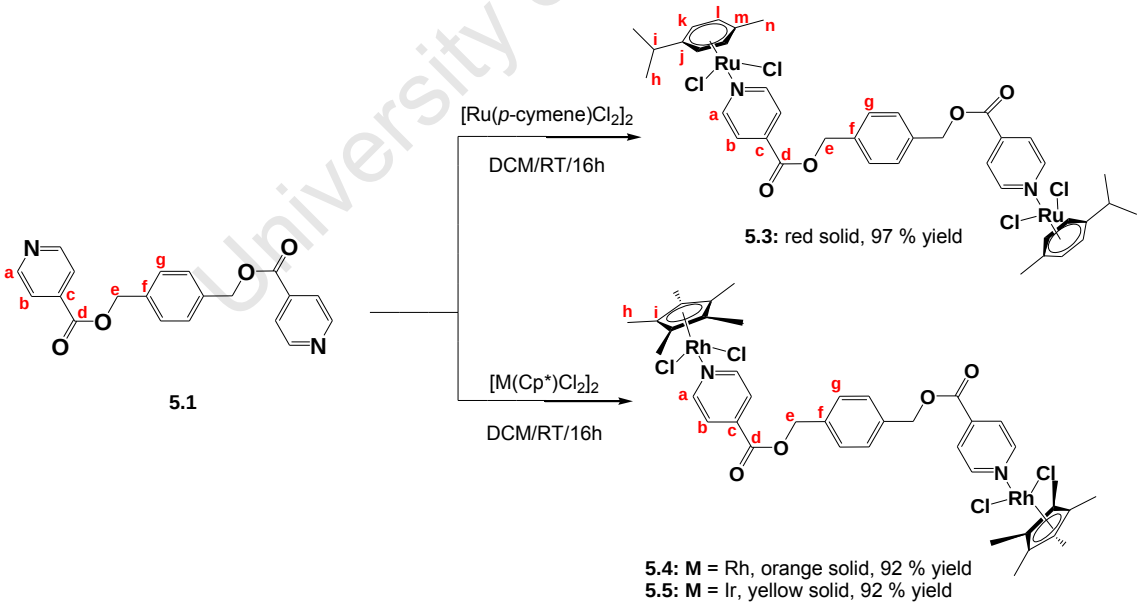

Scheme 5.3.

Complexes **5.3** – **5.8** are new compounds and were fully characterized using several analytical and spectroscopic techniques including NMR, UV-vis and X-ray crystallography.

Spectroscopic evidence confirming peripheral metalation of ligands **5.1** and **5.2** via the pyridyl nitrogens was garnered from the NMR and IR spectral analyses.

The proton NMR spectra for complexes **5.3** – **5.8** all show a downfield shift of the protons *ortho* to nitrogen compared to their corresponding free ligands (**5.1** and **5.2**, Figures 5.3. and 5.4.) which is typical for monodentate 4-pyridyl ligands coordinated to Ru(II), Rh(III) or Ir(III) metal centers.[14,16,24-31] This deshielding of the protons H_a would be expected upon metal coordination to the nitrogen as it leads to less electron density in the *ortho* carbon-hydrogen bond due to strong back-bonding between an empty π^*-orbital of nitrogen and a filled d-ordital of the transition metal.

Similar to the free ligands (**5.1** and **5.2**), in the dinuclear complexes (**5.3** - **5.5**) this deshielding of the doublet associated with the *ortho* protons (H_a) of the pyridyl ring is much more pronounced compared to the trinuclear complexes **5.6** – **5.8** due to the proximity of the ester groups to the pyridyl rings. For all of the complexes (**5.3** - **5.8**), the resonances assigned to the ester methylene protons display minimal change compared to the free ligands confirming that no metal coordination occurs to the oxygen atoms.

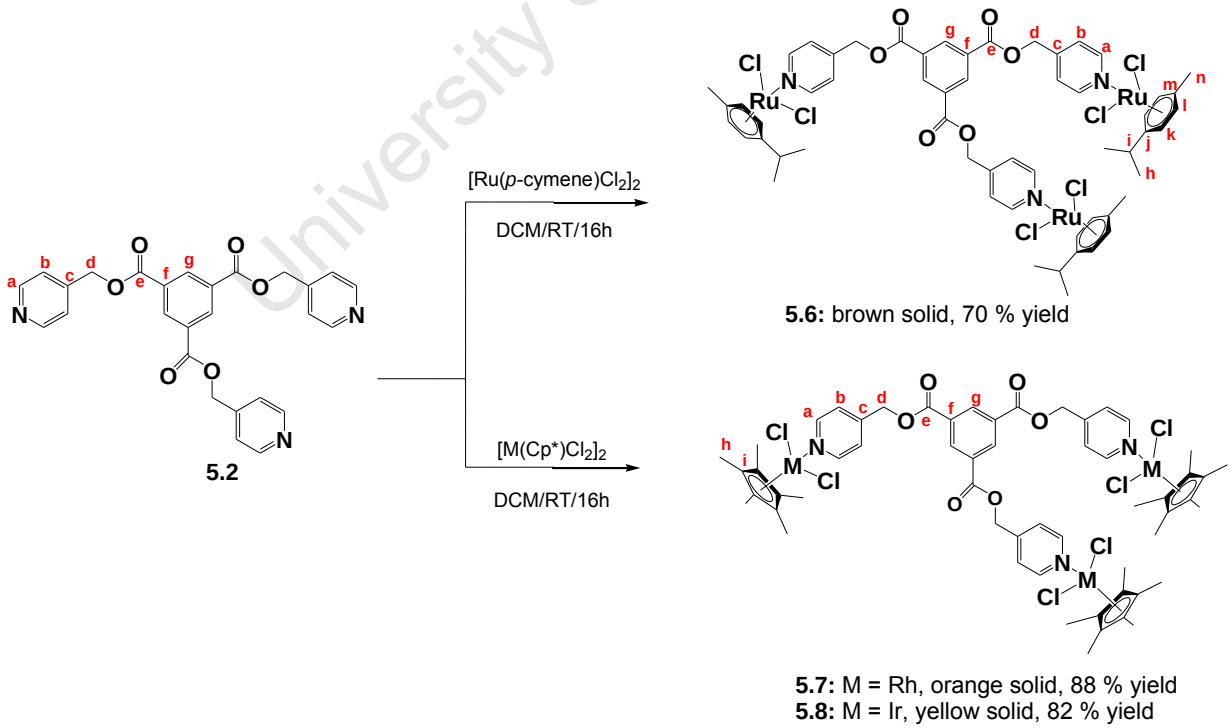

Scheme 5.4.

For the di- and tri-ruthenium complexes, **5.3** and **5.6**, the *p*-cymene ligand displays proton resonances characteristic of similar neutral piano-stool dichloro ruthenium complexes.[16,24,27,29-31] The methyl protons of the isopropyl group (H_h) are observed at *ca.* 1.30 ppm, resonating as a doublet due to coupling to the proton H_i and the proton H_i is observed as a multiplet between 2.90 and 3.00 ppm. The methyl protons H_n resonate as a singlet at 2.10 ppm. The aromatic protons, H_k and H_m, of the *p*-cymene ligand resonate as two doublets between 5.00 and 5.50 ppm. The methyl protons of the pentamethylcyclopentadienyl ligands of the rhodium (**5.4** and **5.7**) and iridium (**5.5** and **5.8**) complexes are seen as a singlet between 1.50 and 1.60 ppm in the proton NMR spectra for these complexes.

Analysis of complexes **5.3** – **5.8** using $^{13}C\{^1H\}$ NMR spectroscopy reveals a high frequency shift of the resonance assigned to C_a compared to the free ligand (**5.1** and **5.2**) (Table 5.1) confirming metal coordination to the pyridyl nitrogens. For complexes **5.3**-**5.5**, a shift downfield of approximately 5.0 ppm is noted compared to **5.1**. In comparison to the free ligand **5.2**, a shift of approximately 5.0 ppm for C_a is observed for the triruthenium complex **5.6** and around 3.0 ppm for the rhodium and iridium analogues (**5.7** and **5.8**).

Similar to the proton NMR spectra for complexes **5.3**-**5.8**, little to no effect is observed on the other carbon resonances assigned to the metal-coordinated ester ligands. The resonances assigned to the carbonyl carbon (C_d in **5.3**-**5.5** and C_e in **5.6**-**5.8**) as well as the alkyl ester carbon (C_e in **5.3**-**5.5** and C_d in **5.6**-**5.8**) occur at approximately the same shift compared to the free ligand. This serves as further evidence that coordination to the ester oxygens does not occur.

For the rhodium (**5.4** and **5.7**) and iridium (**5.5** and **5.8**) complexes, the carbon resonance associated with the methyl substituents (C_h) of the pentametylcyclopentadienyl ligand are observed between 8.5 and 9.0 ppm. The aromatic carbons (C_i) of the ring are observed at approximately 95.0 ppm for the rhodium complexes and in the iridium complexes these carbons resonate further upfield at approximately 86.0 ppm. These shifts are similar to other piano-stool Cp* rhodium and iridium complexes.[32-35] The *p*-cymene moieties of complexes **5.3** and **5.6** show two singlets between 82.0 and 83.0 ppm due to the resonances of the unsubstituted aromatic carbons of the ring. The isopropyl substituted aromatic carbon (C_j) and the methyl substituted aromatic carbon (C_m) resonates at approximately 97.0 and 104.0 ppm respectively. These resonances agree with similar mononuclear 4-pyridyl complexes.[14,27,31]

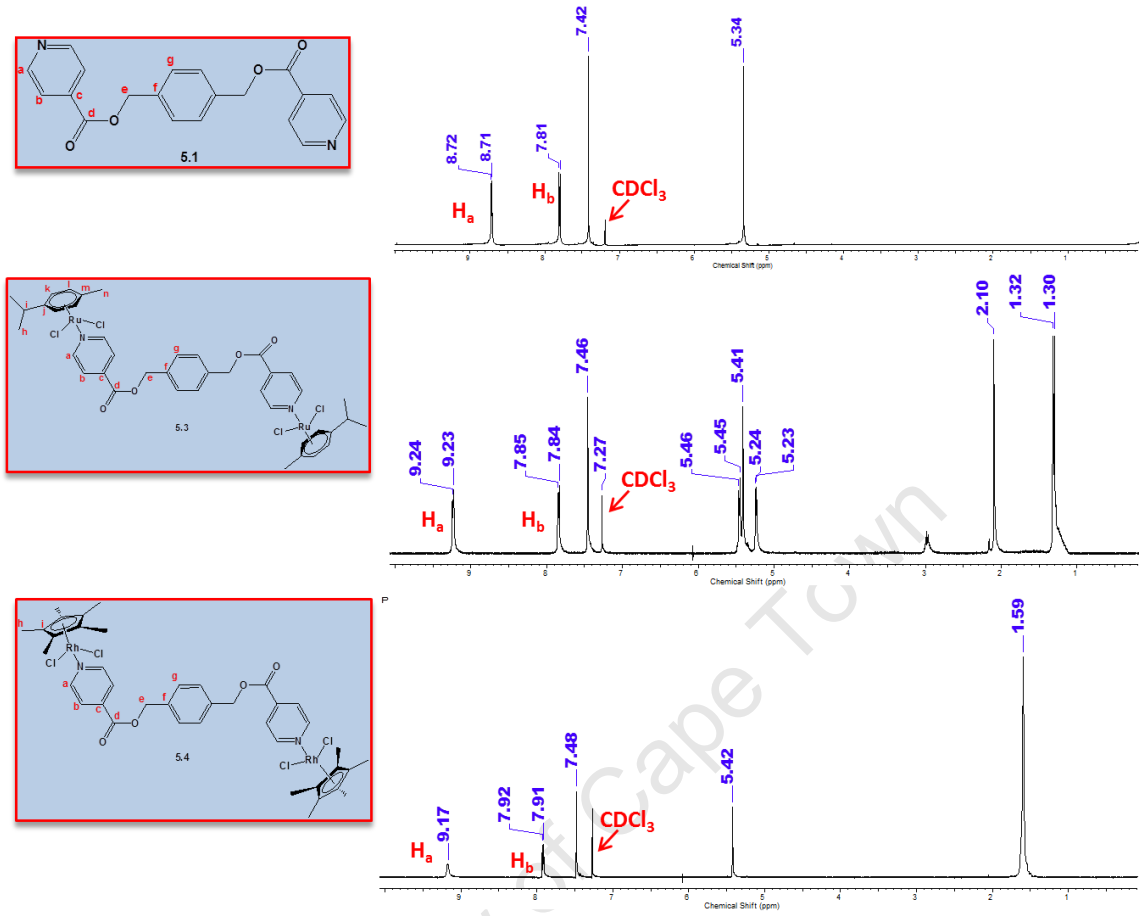

Figure 5.3. Proton NMR spectra for compounds **5.1**, **5.3** and **5.4** run in $CDCl_3$.

Further analysis of the complexes **5.3** – **5.8** using infrared spectroscopy reveals no shift in the absorption band associated with the C=O bond vibration of the now metalated ligands, supportive of the evidence gleaned from the NMR analyses that metal coordination to the ester oxygen atoms does not occur. The C=N bond vibration of the pyridyl functionalities do exhibit an expected shift to higher frequency as a consequence of metal complexation to nitrogen. A high frequency increase of 15 – 20 cm^{-1} is noted and agrees with literature examples.[36-39] For all of the complexes, a strong absorption band in the region of 1200 – 1300 cm^{-1} is observed and is assigned to the C-O bond stretching of the ester functionalities.[14,27,30,40]

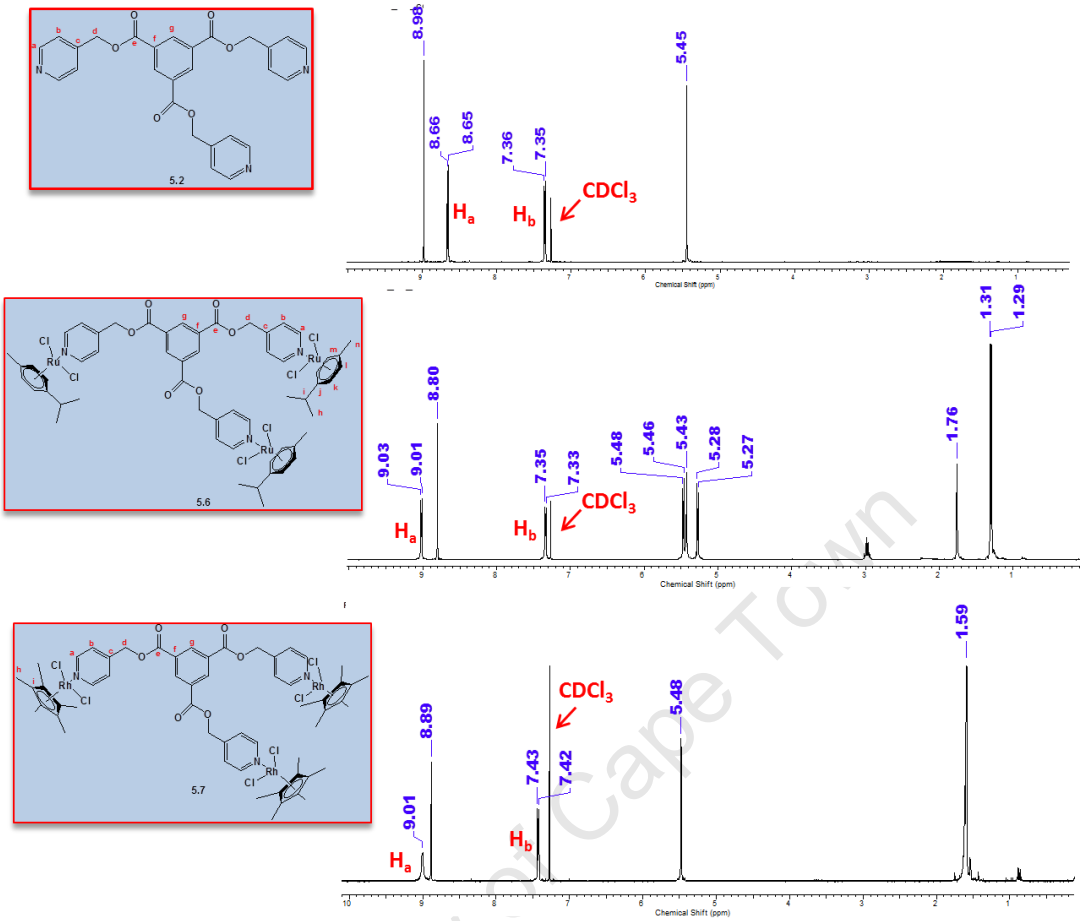

Figure 5.4. Proton NMR spectra for compounds **5.2, 5.6** and **5.7** run in $CDCl_3$.

Table 5.1. Selected $^{13}C\{^1H\}$ NMR shifts for Compounds **5.1-5.8**

	$^{13}C\{^1H\}$ NMR shift (ppm)			
Compound	**C_a**	**C_c**	**C_d**	**C_e**
5.1	150.6	137.3	164.9	67.0
5.3	155.9	138.5	163.6	67.5
5.4	154.0	138.7	163.8	67.4
5.5	154.4	138.7	163.4	67.5
5.2	150.3	131.1	65.5	164.3
5.6	155.1	130.8	64.7	163.8
5.7	153.6	130.8	64.7	163.9
5.8	153.6	130.8	64.6	163.9

Mass spectral analysis of complexes **5.3** – **5.8** using ESI-MS reveals molecular ion fragments corresponding to the molecular weights of the proposed structures (Table 5.2). Complexes **5.4** and **5.7** exhibit base peaks corresponding to the sodium adduct and complexes **5.3** and **5.8** form adducts with methonal upon either protonation or loss of chlorido ligands. Complexes **5.5** and **5.6** show *m/z* peaks corresponding to the loss of a chlorido ligand. Within these complexes, there are several potential sites of ionization, thus mass fragments corresponding to multiply charged species is possible.

Table 5.2. Mass Spectral Data for Complexes **5.3** – **5.8**

Complex	*m/z*	Assignment (Intensity)
5.3	312.01	$([M - 3Cl + 3CH_3OH]^{3+}$ (100 %)
5.4	989.02	$([M - H + Na]^{+}$ (100 %)
5.5	1100.21	$([M - Cl]^{+}$ (100 %)
5.6	1367.03	$[M – Cl]^{+}$ (20%)
5.7	1432.01	$[M - H + Na]^{+}$ (100%)
5.8	363.05	$[M + 5H + 4CH_3OH]^{5+}$ (100%)

5.2.3. Electronic Spectral Analysis

The electronic properties of compounds **5.1** – **5.8** were analyzed using UV-vis Spectroscopy. Figures 5.5. and 5.6. show the UV-vis spectra for the dipyridyl ester (**5.1** and **5.3**-**5.5**) and tripyridyl ester compounds (**5.2** and **5.6**-**5.8**) respectively. Table 5.3 lists the energy absorptions observed. All of the complexes were analysed at a concentration of 0.1 mM in chloroform and assignment of the absorption bands were made based on similar complexes reported in the literature.[27,28,33,37]

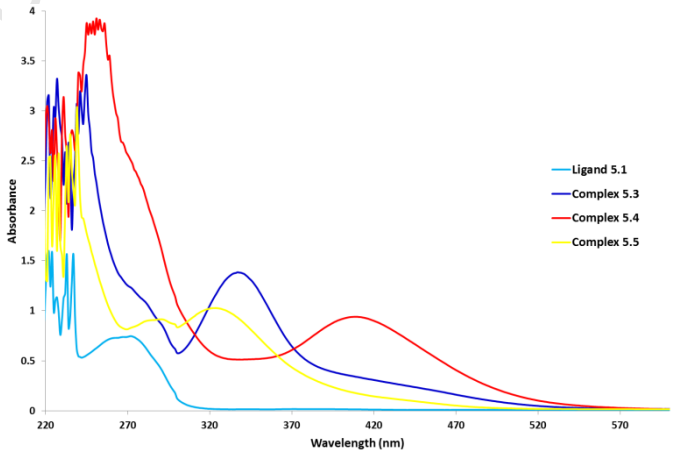

Figure 5.5. UV-vis Spectra for compounds **5.1** and **5.3**-**5.5**. The compounds were analysed at ambient temperature using a 0.1 mM solution of each compound in chloroform in a 1 cm quartz cuvette

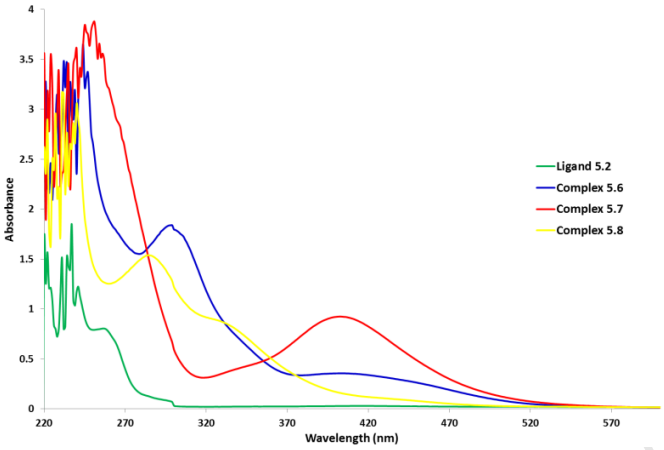

Figure 5.6. UV-vis Spectra for compounds **5.2** and **5.6**-**5.8**. The compounds were analysed at ambient temperature using a 0.1 mM solution of each compound in chloroform in a 1 cm quartz cuvette.

A hyperchromic shift in the intensity of the spectra for the complexes **5.3**-**5.8** is noted in comparison to their free ligands. The ligands, **5.1** and **5.2**, are white solids and thus show no absorption in the visible region of the spectrum. For all of the compounds, the absorption band observed between 200-300 nm is assigned to the intraligand n-π* and π-π* transitions of the aromatic and ester groups. These transitions exhibit a red shift upon complexation; the metal moieties effectively act as an auxochrome causing the intraligand transitions to shift to longer wavelength. In general, the absorption spectra for all of the compounds exhibit fairly broad bands, which is characterisitic of highly conjugated aromatic systems. Charge transfer bands observed between 300-350 and 400-450 nm are characteristic of the MLCT dπ-π* transitions between the metal and ligand.

Table 5.3. Spectral Data for compounds **5.1** – **5.8** ascertained using UV-vis Spectrometry

Compound	λ_{max} (nm)[a]		
5.1	272 (n-π*/π-π*$_{intraligand}$)		
5.3	280 (n-π*/π-π*$_{intraligand}$)	337 (MLCT dπ$_{metal}$–π*$_{ligand}$)	400-450 (MLCT dπ$_{metal}$–π*$_{ligand}$)
5.4	280 (n-π*/π-π*$_{intraligand}$)		410 (MLCT dπ$_{metal}$–π*$_{ligand}$)
5.5	290 (n-π*/π-π*$_{intraligand}$)	324 (MLCT dπ$_{metal}$–π*$_{ligand}$)	400-450 (MLCT dπ$_{metal}$–π*$_{ligand}$)
5.2	257 (n-π*/π-π*$_{intraligand}$)		
5.6	260 (n-π*/π-π*$_{intraligand}$)	299 (MLCT dπ$_{metal}$–π*$_{ligand}$)	405 (MLCT dπ$_{metal}$–π*$_{ligand\ d}$)
5.7	250 (n-π*/π-π*$_{intraligand}$)	335 (MLCT dπ$_{metal}$–π*$_{ligand}$)	402 (MLCT dπ$_{metal}$–π*$_{ligand}$)
5.8	284 (n-π*/π-π*$_{intraligand}$)	334 (MLCT dπ$_{metal}$–π*$_{ligand}$)	400-450 (MLCT dπ$_{metal}$–π*$_{ligand}$)

[a] transitions are given in parentheses.

5.2.4. Single Crystal X-ray Diffraction (XRD) Analysis

The molecular structures of complexes **5.4** and **5.5** were elucidated using single crystal XRD. Crystals were grown from a solution of chloroform and hexane. Both complexes crystallize with two complex molecules and four chloroform molecules in the asymmetric unit with a monoclinic system and $P2_1$ space group. Figures 5.6 and 5.7 show the molecular structures of **5.4** and **5.5** and Tables 5.4 – 5.6 list the crystal data and selected bond lengths and angles.

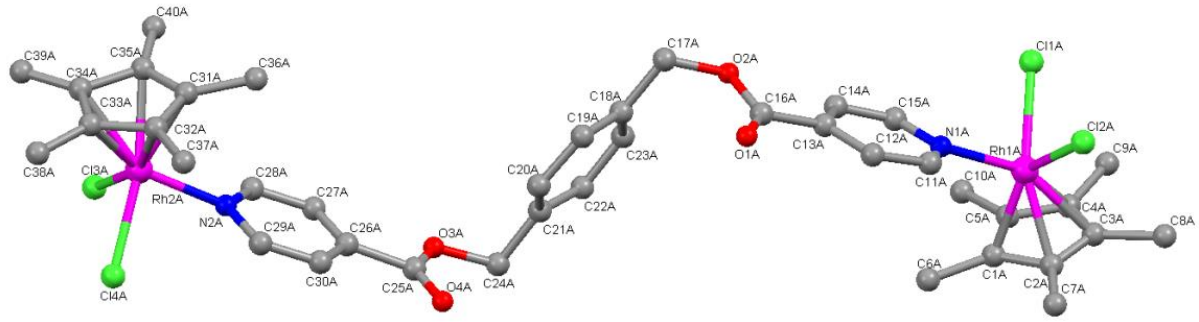

Figure 5.6. Molecular structure of Complex **5.4** with hydrogen atoms omitted for clarity

The determined molecular structures of complexes **5.4** and **5.5** validate the structures of **5.3** - **5.8** evidenced by the spectroscopic and spectrometric characterizations discussed earlier. In the structures of both dinuclear complexes, each metal center adopts a typical 'piano-stool' conformation with the two chlorido and the pyridyl ring as the three legs and a *pseudo*-tetrahedral coordination geometry. The pentamethylcyclopentadienyl ring is bound to the metal in the expected η^5 manner. The pyridyl ester ligand is coordinated to each metal center in a monodentate fashion as suggested by the spectroscopic characterizations. Comparison of the Rh-C and Ir-C bond lengths between the metal and each bonded carbon of the pentamethylcyclopentadienyl ring reveal them to be similar indicating that the ring is symmetrically bound to rhodium (**5.4**) or iridium (**5.5**). The bond lengths observed in **5.4** and **5.5** between the metal and the coordinated atoms are approximately 2.40 Å (M-Cl), 2.10 Å (M-C) and 2.10 Å (M-N). These values agree with those observed for similar complexes in the literature[16,24,28,34,35,38,39,41] as well as the expected length calculated from the covalent radii of iridium or rhodium, chlorine (M-Cl: 2.40 (Ir); 2.41 (Rh) Å), carbon (M-C: 2.09 (Ir); 2.10 (Rh) Å) and nitrogen (M-N: 2.09 (Ir); 2.10 (Rh) Å).[42]

Table **5.4.** Crystal Data for **5.4·2CHCl$_3$ and 5.5·2CHCl$_3$**

	Complex **5.4·2CHCl$_3$**	Complex **5.5·2CHCl$_3$**
Formula	$C_{42}H_{48}Cl_{10}N_2O_4Rh_2$	$C_{42}H_{48}Cl_{10}Ir_2N_2O_4$
Formula weight	1205.14	1383.72
Crystal system	Monoclinic	Monoclinic
Space group	$P2_1$	$P2_1$
a (Å)	11.5800(6)	11.572(2)
b (Å)	20.4163(11)	20.505(4)
c (Å)	21.4575(11)	21.518(4)
β (deg.)	102.7920(10)	103.65(3)
V (Å^3)	4947.1(4)	4961.9(17)
Z	4	4
D_c (g.cm^{-3})	1.618	1.852
μ (mm^{-1})	1.249	5.938
θ range for data collection (deg.)	1.80 to 27.56	1.84 to 27.46
Limiting indices	-15 < h < 7	0 < h < 14
	-26 < k < 26	0 < k < 26
	-23 < l < 27	-27 < l < 27
no. of reflns meads	36455	11634
no. of reflns used (Rint)	22713	10862
no. of params	1001	1021
R1	0.1052	0.0404
wR2	0.2009	0.0942
goodness of fit on F2	1.023	1.040

In the coordinated pyridyl-ester ligand of both complexes **5.4** and **5.5**, the C-N bond lengths in the pyridyl ring are found to be between 1.30 – 1.35 Å. The alkyl C-O bond lengths of the ester functionalities are between 1.30 and 1.36 Å and the C=O bond lengths are shorter (1.16 – 1.20 Å), comparing favourably to the interatomic distances typical of pyridines and aromatic esters (C=N: 1.34 Å, C-O: 1.43 Å and C=O: 1.23 Å).[43]

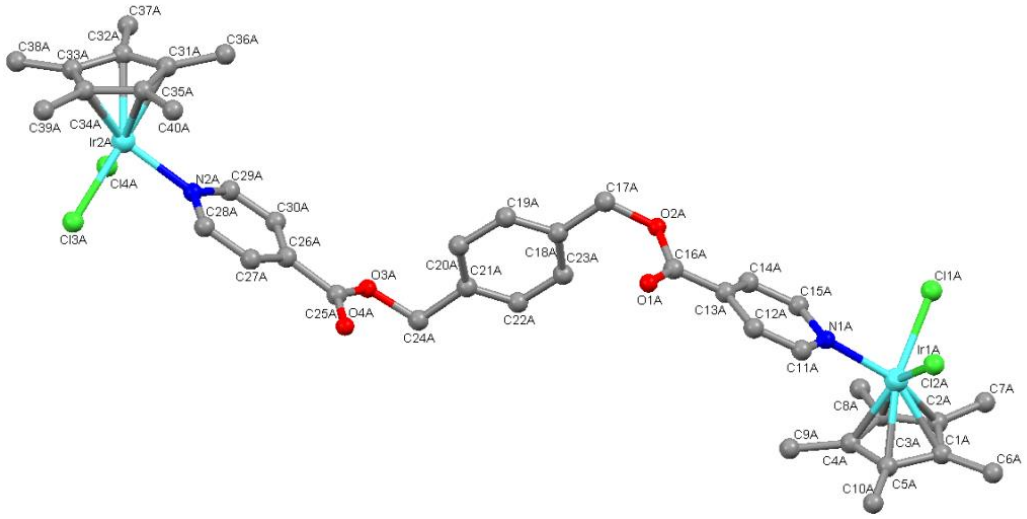

Figure 5.7. Molecular structure of Complex **5.5** with hydrogen atoms omitted for clarity.

Table 5.5. Selected bond lengths observed for complexes **5.4·2CHCl$_3$** and **5.5·2CHCl$_3$**

	Complex **5.4·2CHCl$_3$** M = Rh	Complex **5.5·2CHCl$_3$** M = Ir		Complex **5.4·2CHCl$_3$** M = Rh	Complex **5.5·2CHCl$_3$** M = Ir
M1-N1	2.119(8)	2.095(8)	**M2-N2**	2.116(8)	2.114(8)
M1-C1	2.054(14)	2.160(9)	**M2-C31**	2.137(9)	2.143(10)
M1-C2	2.099(11)	2.161(9)	**M2-C32**	2.143(8)	2.157(10)
M1-C3	2.146(12)	2.162(9)	**M2-C33**	2.169(9)	2.163(11)
M1-C4	2.203(16)	2.132(11)	**M2-C34**	2.154(9)	2.193(12)
M1-C5	2.093(13)	2.130(10)	**M2-C35**	2.139(8)	2.136(11)
M1-Cl1	2.412(2)	2.401(3)	**M2-Cl3**	2.399(2)	2.415(3)
M1-Cl2	2.399(2)	2.415(3)	**M2-Cl4**	2.416(2)	2.394(3)
N1-C11	1.321(12)	1.361(13)	**N2-C28**	1.323(12)	1.344(13)
N1-C15	1.337(11)	1.342(14)	**N2-C29**	1.362(12)	1.379(13)
O1-C16	1.160(12)	1.198(14)	**O3-C25**	1.291(12)	1.312(13)
O2-C16	1.332(13)	1.364(14)	**O4-C25**	1.218(12)	1.196(14)

Table 5.6. Selected bond angles observed for complexes **5.4·2CHCl$_3$** and **5.5·2CHCl$_3$**

	Complex **5.4·2CHCl$_3$** M = Rh	Complex **5.5·2CHCl$_3$** M = Ir		Complex **5.4·2CHCl$_3$** M = Rh	Complex **5.5·2CHCl$_3$** M = Ir
C4-M1-Cl1	92.8(4)	136.9(4)	**C34- M2-Cl3**	94.4(3)	93.2(3)
C3-M1-Cl1	117.0(3)	101.8(4)	**C33- M2-Cl3**	124.8(3)	109.6(3)
C1- M1-Cl1	138.6(4)	121.5(3)	**C31- M2-Cl3**	135.8(3)	152.3(4)
C2- M1-Cl1	153.0(3)	94.7(3)	**C32- M2-Cl3**	160.4(3)	148.2(3)
C5- M1-Cl1	100.9(4)	158.8(3)	**C35- M2-Cl3**	100.3(3)	112.5(4)
N1- M1-Cl1	88.4(2)	87.2(3)	**N2- M2-Cl3**	89.3(2)	86.0(2)
C4- M1-Cl2	123.7(3)	135.8(4)	**C34- M2-Cl4**	123.7(3)	137.9(4)
C3- M1-Cl2	96.1(3)	161.0(3)	**C33- M2-Cl4**	95.6(3)	103.0(3)
C1- M1-Cl2	131.7(4)	96.7(3)	**C31- M2-Cl4**	133.9(3)	120.7(4)
C2- M1-Cl2	97.0(3)	125.1(3)	**C32- M2-Cl4**	100.4(3)	94.2(3)
C5- M1-Cl2	156.5(4)	101.2(3)	**C35- M2-Cl4**	160.3(3)	159.3(4)
N1- M1-Cl2	88.8(2)	87.0(2)	**N2- M2-Cl4**	87.2(2)	86.7(2)
Cl2- M1-Cl1	89.44(8)	87.31(10)	**Cl3- M2-Cl4**	90.28(9)	86.94(10)
C25-O3-C24-C21	-96.1(10)	-92.9(12)	**C16-O2-C17-C18**	-78.5(11)	-84.3(12)

With respect to the bond angles, the values observed between Cl-M-Cl and N-M-Cl are all close to 90 ° and the bond angles formed between the bonded carbons of the Cp* ligand, the metal and the chlorido ligand vary from 90 to 150 °. This trend has also been observed within the molecular structures of similar Cp*Ir(III) and Cp*Rh(III) pyridyl complexes.[16,24,28,38,39] Within the pyridyl ester ligands of both **5.4** and **5.5**, the dihedral angles formed between the

central phenyl ring and each ester functionality is close to 90 ° indicating that the pyridyl rings orientate themselves almost perpendicular to the phenyl spacer thereby minimizing electrostatic interactions within the complex molecules.

5.3. Summary

Two di- and tri-pyridyl ester ligands (**5.1** and **5.2**) have been synthesised by alkylation of the carboxylic acid. These ligands were functionalized with either [(p-cymene)$RuCl_2$], [(pentamethylcyclopentadienyl)$RhCl_2$] or [(pentamethylcyclopentadienyl)$IrCl_2$] moieties to give a series of new di- (**5.3**-**5.5**) and trinuclear (**5.6**-**5.8**) complexes. All of the compounds were isolated as air- and moisture-stable solids and were characterised using a variety of analytical and spectroscopic techniques. Proton NMR analyses of compounds **5.1**-**5.8** revealed that the proximity of the ester functionalities to the pyridyl ring influences the deshielding effect on the protons *ortho* to nitrogen. Minimal change in the ester methylene proton resonances confirmed no metal coordination occurs to the oxygen atoms.

The molecular structures of **5.4** and **5.5** confirms the monodentate coordination of the pyridyl ester ligands to each metal put forth by the spectroscopic and spectrometric characterisations of complexes **5.3** - **5.8**. The elucidated molecular structures of the complexes **5.4** amd **5.5** revealed a typical ‘piano-stool’ geometry around the metal and analysis of the dihedral angles formed between the central phenyl ring and the ester functionalities indicate that the pyridyl metal moieties position themselves almost perpendicular to the phenyl spacer thus minimizing electrostatic interactions.

A study of their *in vitro* antiparasitic and antitumor activity has been undertaken and the results are discussed in Chapter 6.

5.4. Experimental

5.4.1. Chemicals and General Methods

1,2,3,4,5-Pentamethylcyclopentadiene, α-phellandrene, 4-bromomethylpyridine hydrobromide, isonicotinic acid, 1,3,5-benzenetricarboxylic acid and 1,4-bis(bromomethyl)benzene were purchased from Sigma-Aldrich and used without further purification. Ruthenium trichloride trihydrate, rhodium trichloride trihydrate and iridium trichloride trihydrate were kindly donated by AngloAmerican Platinum Limited. All solvents used were analytical grade and dried over molecular sieves. All reactions were carried out in air unless otherwise stated. The precursors, dichloro(*p*-cymene)ruthenium(II) dimer,[44] dichloro(pentamethylcyclopentadienyl)rhodium(III) dimer[45] and dichloro(pentamethylcyclopentadienyl)iridium(III) dimer[45] were synthesised using literature methods.

5.4.2. Spectroscopic and Analytical Methods

Nuclear Magnetic Resonance (NMR) Spectra were recorded on a Varian Unity XR400 MHz (^{1}H at 399.95 MHz, ^{13}C at 100.58 MHz), Varian Mercury XR300 (^{1}H at 300.08 MHz, ^{13}C at 75.46 MHz) or Bruker Biospin GmbH (^{1}H at 400.22 MHz, ^{13}C at 100.65 MHz) spectrometer at ambient temperature. Chemical shifts for ^{1}H and ^{13}C{1H} NMR shifts are reported using tetramethylsilane (TMS) as the internal standard and ^{31}P{1H} NMR spectra were measured relative to H_3PO_4 as the external standard. NMR spectra were recorded in deuterated chloroform ($CDCl_3$-D_1) unless otherwise stated. Infrared (IR) absorptions were measured on Perkin-Elmer Spectrum 100 FT-IR Spectrometer using a Universal Diamond Attenuated Total Reflection (ATR) accessory. Microanalyses for C, H, and N were carried out using a Thermo Flash 1112 Series CHNS-O Analyser and melting points were determined using a Büchi Melting Point Apparatus B-540. Mass Spectrometry determinations were carried out on all new compounds using electrospray ionisation (ESI) on a Waters API Quattro Micro instrument in either the positive or negative mode.

5.4.3. Synthesis of Pyridyl-ester Ligands

*5.4.3.1. Diisonicotinic Acid 1,4-Xylylene Diester (**5.1**)[22]*

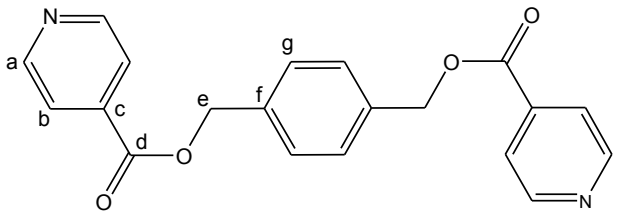

5.1

To a solution of 1,4-bis(bromomethyl)benzene (0.204 g, 0.772 mmol) in DMF (20 cm^3), potassium carbonate (0.262 g, 1.89 mmol) and isonicotinic acid (0.197 g, 1.60 mmol) was added. The reaction mixture was stirred at 80 °C for 18 hours. Upon cooling to room temperature, the reaction mixture was diluted with ethyl acetate (100 cm^3) and washed with deionized water (2 x 50 cm^3) and brine (1 x 30 cm^3). The organic layer was then dried over magnesium sulfate, filtered and the solvent evaporated to yield the product (**5.1**) as an off-white amorphous solid. Yield: 0.239 g, 89 %. Mp: 223-225 °C. ^{1}H NMR (400 MHz, $CDCl_3$-d_1): δ (ppm) = 8.80 (d, $^3J(H_a\text{-}H_b)$: 7.99 Hz, 4H, H_a), 7.89 (d, $^3J(H_b\text{-}H_a)$: 8.00 Hz, 4H, H_b), 7.49 (s, 4H, H_g), 5.41 (s, 4H, H_e). ^{13}C NMR (400 MHz, $CDCl_3$-d_1): δ (ppm) = 164.9 (C_d), 150.6 (C_a), 137.3 (C_c), 135.7 (C_f), 128.7 (C_g), 122.9 (C_b), 67.0 (C_e). IR (atr, cm^{-1}) υ = 1719 (s, C=O), 1597 (s, C=N), 1270(s, =C-O-CH_2-). Elemental Analysis for $C_{20}H_{16}O_4N_2$: found C, 68.58; H, 5.16; N, 6.86 %; calculated C, 68.95; H, 4.63; N, 8.04 %.

*5.4.3.2. Benzene-1,3,5-tricarboxylic acid tripyridin-4-ylmethyl ester (**5.2**)*[21]

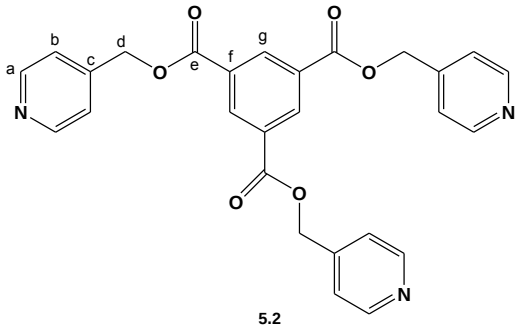

5.2

To a solution of 1,3,5-benzenetricarboxylic acid (0.200 g, 0.952 mmol) in DMF (20 cm^3), potassium carbonate (0.8161 g, 5.90 mmol) and 4-bromomethylpyridine hydrombromide (0.748 g, 2.96 mmol) was added. The reaction mixture was stirred at 80 °C for 18 hours. Upon cooling to room temperature, the reaction mixture was diluted with ethyl acetate (100 cm^3) and washed with deionized water (2 x 50 cm^3) and brine (1 x 30 cm^3). The organic layer was then dried over magnesium sulfate, filtered and the solvent evaporated to yield the product (5.2) as an off-white amorphous solid. Yield: 0.392 g, 85 %. Mp: 125-127 °C. ^{1}H NMR (400 MHz, $CDCl_3$-d_1): δ (ppm) = 8.98 (s, 3H, Hg), 8.66 (d, ^3J(H_a-H_b): 5.80 Hz, 6H, H_a), 7.36 (d, ^3J(H_b-H_a): 6.13 Hz, 6H, H_b), 5.45 (s, 6H, H_d). ^{13}C NMR (400 MHz, $CDCl_3$-d_1): δ (ppm) = 164.3 (C_e), 150.3 (C_a), 144.2 (C_f), 135.1 (C_g), 131.1 (C_c), 122.1 (C_b), 65.5 (C_d). IR (atr, cm^{-1}) υ = 1726 (s, C=O), 1605 (s, C=N), 1237 (s, =C-O-CH_2-). Elemental Analysis for $C_{27}H_{21}O_6N_3$: found C, 64.64; H, 5.00; N, 7.38 %; calculated for $C_{27}H_{21}O_6N_3 \cdot C_2H_4O$: C, 64.38; H, 5.40; N, 6.83 %.

5.4.4. Synthesis of Dinuclear Ru(II), Rh(III) and Ir(III) Pyridyl-ether Complexes

5.4.4.1. General Synthetic Method for Dinuclear Complexes

The ligand (**5.1**) (1 molar equivalent) was dissolved in DCM (15 cm^3) and the appropriate ruthenium, rhodium or iridium dimer (1.1 molar equivalent) was added and the reaction solution was stirred for 16 hours at room temperature. The reaction solvent was then reduced to approximately a third of its original volume. The product was then precipitated from solution by addition of diethyl ether and isolated by vacuum filtration, washed with diethyl ether and dried.

*5.4.4.2 {([(Diisonicotinic Acid 1,4-Xylylene Diester)di[dichloro(p-cymene)Ru(II)]} (**5.3**)*

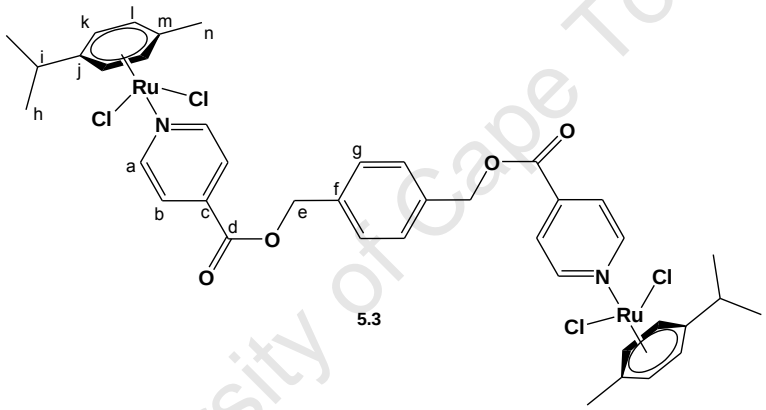

5.3

Diisonicotinic Acid 1,4-Xylylene Diester (**5.1**) (0.0536 g, 0.154 mmol) was reacted with dichloro(*p*-cymene)ruthenium(II) dimer (0.101 g, 0.163 mmol). The product (**4.3**) was isolated as dark red amorphous solid. Yield: 0.148 g, 97 %. Mp: 226-228 °C, decomposition without melting).^{1}H NMR (400 MHz, $CDCl_3$-d_1): δ (ppm) = 9.24 (d, $^3J(H_a\text{-}H_b)$: 6.41 Hz, 4H, H_a), 7.85 (d, $^3J(H_b\text{-}H_a)$: 6.59 Hz,4H, H_b), 7.46 (s, 4H, H_g), 5.46 (d, $^3J(H_l\text{-}H_k)$: 5.68 Hz, 4H, H_l), 5.41 (s, 4H, H_e), 5.24 (d, $^3J(H_k\text{-}H_l)$: 5.86 Hz, 4H, H_k), 3.00-2.96 (m, 2H, H_i), 2.10 (s, 6H, H_n), 1.32 (d, $^3J(H_h\text{-}H_i)$: 6.96 Hz, 12H, H_h). ^{13}C NMR (400 MHz, $CDCl_3$-d_1): δ (ppm) = 163.6 (C_d), 155.9 (C_a), 138.5 (C_c), 135.5 (C_f), 128.8 (C_g), 123.5 (C_b), 103.8 (C_m), 97.4 (C_j), 83.1 (C_l), 82.4 (C_k), 67.5 (C_e), 30.7 (C_i), 22.3 (C_h), 18.2 (C_n). IR (atr, cm^{-1}) υ = 1719 (s, C=O), 1611 (s, C=N), 1271 (s, =C-<u>O-CH$_2$</u>-). Elemental Analysis for $C_{39}H_{46}Cl_4N_2O_3Ru_2$: found C, 48.34; H, 4.92; N, 1.89 %; calculated $C_{39}H_{46}Cl_4N_2O_3Ru_2 \cdot C_{4.5}H_{11}ClO$: C, 50.01; H, 4.61; N, 2.92. ESI-MS: *m/z* 312.01 ($[M - 3Cl + 3CH_3OH]^{3+}$, 100%)

*5.4.4.3 {([(Diisonicotinic Acid 1,4-Xylylene Diester) di[dichloro(pentamethylcyclo-pentadienyl)Rh(III)]} (**5.4**)*

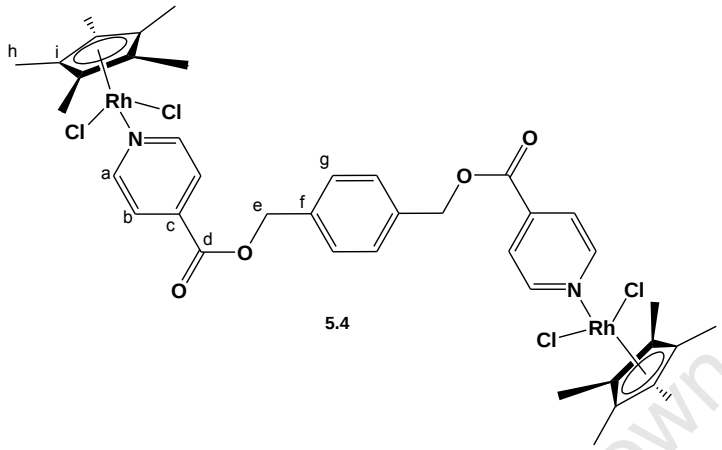

5.4

Diisonicotinic Acid 1,4-Xylylene Diester (**5.1**) (0.0538 g, 0.154 mmol) was reacted with dichloro(pentamethylcyclopentadienyl)rhodium(III) dimer (0.0954 g, 0.154 mmol). The product (**5.4**) was isolated as a bright orange amorphous solid. Yield: 0.141 g, 92 %. Mp: 169-171 °C, decomposition without melting. ^{1}H NMR (400 MHz, $CDCl_3$-d_1): δ (ppm) = 9.16 (br s, 4H, H_a), 7.92 (d, ^{3}J(H_b-H_a): 6.59 Hz, 4H, H_b), 7.47(s, 4H, H_g), 5.42 (s, 4H, H_e), 1.59 (s, 30H, H_h). ^{13}C NMR (400 MHz, $CDCl_3$-d_1): δ (ppm) = 163.8 (C_d), 154.0 (C_a), 138.7 (C_c), 135.6 (C_f), 128.77 (C_g), 124.1 (C_b), 94.2 (C_i), 67.4 (C_e), 8.9 (C_h). IR (atr, cm^{-1}) υ = 1739 (s, C=O), 1613 (s, C=N), 1278 (s, =C-O-CH_2-).Elemental Analysis for $C_{40}H_{46}Cl_4N_2O_4Rh_2$: found C, 44.62; H, 5.20; N, 1.36 %; calculated: C, 49.71; H, 4.79; N, 2.89. ESI-MS: *m/z* 989.02 ($[M - H + Na]^+$, 100%)

*5.4.4.4 {([(Diisonicotinic Acid 1,4-Xylylene Diester) di[dichloro(pentamethyl-cyclopentadienyl)Ir(III)]} (**5.5**)*

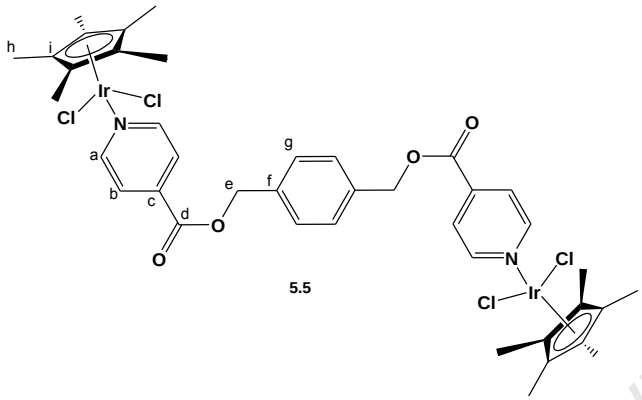

5.5

Diisonicotinic Acid 1,4-Xylylene Diester (**5.1**) (0.0426 g, 0.122 mmol) was reacted with dichloro(pentamethylcyclopentadienyl)iridium (III) dimer (0.101 g, 0.127 mmol). The product (**5.4**) was isolated as a bright yellow amorphous solid. Yield: 0.136 g, 92 %. Mp: 295 - 296 °C.^{1}H NMR (400 MHz, $CDCl_3$-d_1): δ (ppm) = 9.17 (d, ^{3}J(H_a-H_b): 6.78 Hz, 4H, H_a), 7.90 (d, ^{3}J(H_b-H_a): 7.99 Hz, 4H, H_b), 7.48 (s, 4H, H_g), 5.43 (s, 4H, H_e), 1.55(s, 30H, H_h). ^{13}C NMR (400 MHz, $CDCl_3$-d_1): δ (ppm) = 163.4 (C_d), 154.4 (C_a), 138.7 (C_c), 135.6 (C_f), 128.8 (C_g), 124.5 (C_b), 86.1 (C_i), 67.5 (C_e), 8.5 (C_h). IR (atr,cm^{-1}) υ = 1739 (s, C=O), 1613 (s, C=N), 1278 (s, =C-O-CH_2-). Elemental Analysis for $C_{40}H_{46}Cl_4N_2O_4Ir_2$: found C, 37.91; H, 4.16; N, 2.44 %; calculated: C, 41.95; H, 3.20; N, 2.44. ESI-MS: *m/z* 1100.21 ([M -Cl]$^{+}$, 100%)

5.4.5. Synthesis of Trinuclear Ru(II), Rh(III) and Ir(III) Pyridyl-ether Complexes

5.4.5.1. General Synthetic Method for Trinuclear Complexes

The ligand (**5.2**) (2 molar equivalent) was dissolved in DCM (15 cm^3) and the appropriate ruthenium, rhodium or iridium dimer (3.1 molar equivalent) was added and the reaction solution was stirred for 16 hours at room temperature. The reaction solvent was then reduced to approximately a third of its original volume. The product was then precipitated from solution by addition of diethyl ether and isolated by vacuum filtration, washed with diethyl ether and dried.

*5.4.5.2. {[Benzene-1,3,5-tricarboxylic acid tripyridin-4-ylmethyl ester]tri[dichloro(p-cymene)Ru(II)]} (**5.6**)*

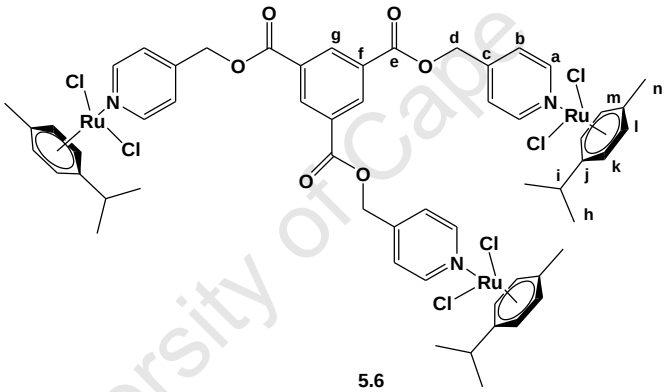

5.6

Benzene-1,3,5-tricarboxylic acid tripyridin-4-ylmethyl ester (**5.2**) (0.0519 g, 0.107 mmol) was reacted with dichloro(*p*-cymene)ruthenium(II) dimer (0.106 g, 0.174 mmol). The product (**5.6**) was isolated as a yellow brown amorphous solid. Yield: 0.109 g, 70 %. Mp: 215-216 °C. ^{1}H NMR (400 MHz, $CDCl_3$-d_1): δ (ppm) = 9.03 (d, ^3J(H_a-H_b): 6.41 Hz, 6H, H_a), 8.80 (s, 3H, H_g), 7.35 (d, ^3J(H_b-H_a): 6.41 Hz,6H, H_b), 5.47 (d, ^3J(H_l-H_k): 5.86 Hz, 6H, H_l), 5.43 (s, 6H, H_d), 5.27 (d, ^3J(H_k-H_l): 6.04 Hz, 6H, H_k), 2.80-3.10 (m, 3H, H_i), 2.09 (s, 9H, H_n), 1.31 (d, ^3J(H_h-H_i): 6.96 Hz, 18H, H_h). ^{13}C NMR (400 MHz, $CDCl_3$-d_1): δ (ppm) = 163.8 (C_e), 155.1 (C_a), 146.6 (C_g), 135.1 (C_f), 130.8 (C_c), 123.0 (C_b), 103.6 (C_m), 97.2 (C_j), 82.8 (C_l), 82.2 (C_k), 64.7 (C_d), 30.7 (C_n), 22.3 (C_h), 18.2 (C_i). IR (atr, cm^{-1}) υ = 1728 (s, C=O), 1617 (s, C=N), 1232 (s, =C-O-CH_2-). Elemental Analysis for $C_{57}H_{63}Cl_6N_3O_6Ru_3$: found C, 48.30; H, 5.23; N, 2.28 %; calculated: C, 48.83; H, 4.53; N, 2.99. ESI-MS: *m/z* 1367.03 ($[M - Cl]^+$, 20%); 312.01 ($[M - 4Cl]^{4+}$, 100%).

*5.4.5.3. {[Benzene-1,3,5-tricarboxylic acid tripyridin-4-ylmethyl ester]tri[dichloro(penta-methylcyclopentadienyl)Rh(III)]} (**5.7**)*

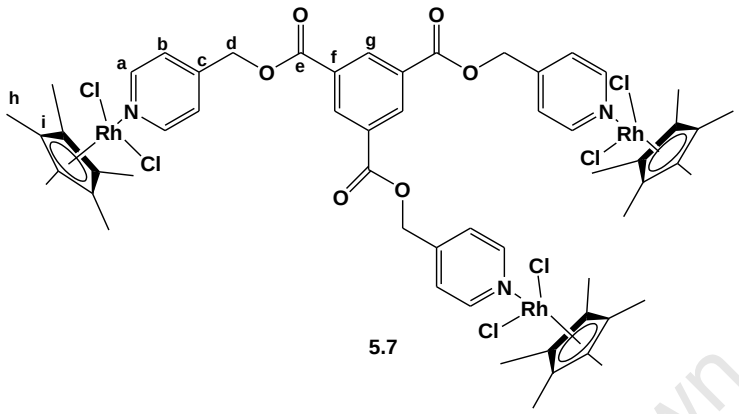

5.7

Benzene-1,3,5-tricarboxylic acid tripyridin-4-ylmethyl ester (**5.2**) (0.0513 g, 0.106 mmol) was dichloro(pentamethylcyclopentadienyl)rhodium(III) dimer (0.101 g, 0.163 mmol). The product (**5.7**) was isolated as dark orange amorphous solid. Yield: 0.132 g, 88 %. Mp: 209-210 °C.^{1}H NMR (400 MHz, $CDCl_3$-d_1): δ (ppm) = 9.00 (br s, 6H, H_a), 8.89 (s, 3H, Hg), 7.43 (d, ^{3}J(H_b-H_a): 6.59 Hz, 6H, H_b), 5.48 (s, 6H, H_d), 1.59 (s, 45H, H_h). ^{13}C NMR (300 MHz, DMSO-d_6): δ (ppm) = 163.9 (C_e), 153.6 (C_a), 146.9 (C_g), 135.2 (C_f), 130.8 (C_c), 123.6 (C_b), 94.22 (C_i), 64.7 (C_d), 8.9 (C_h). IR (KBr, cm^{-1}) υ = 1723 (s, C=O), 1616 (m, C=N), 1225 (s, -C-O-CH_2-). Elemental Analysis for $C_{57}H_{66}Cl_6N_3O_6Rh_3$: found C, 47.45; H, 5,80; N, 0.94 %; calculated: C, 48.53; H, 4.72; N, 2.99. ESI-MS: *m/z* 1432.01 ($[M - H + Na]^+$, 100%).

*5.4.5.4. {[Benzene-1,3,5-tricarboxylic acid tripyridin-4-ylmethyl ester]tri[dichloro(penta-methylcyclopentadienyl)Ir(III)]} (**5.8**)*

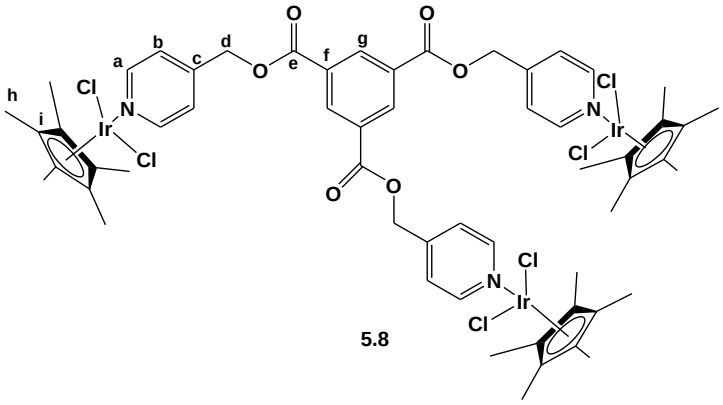

5.8

Benzene-1,3,5-tricarboxylic acid tripyridin-4-ylmethyl ester (**5.2**) (0.0397 g, 0.0821 mmol) was dichloro(pentamethylcyclopentadienyl)iridium(III) dimer (0.100 g, 0.125 mmol). The product (**4.3**) was isolated as a bright yellow amorphous solid. Yield: 0.113 g, 82 %. Mp: 227-230 °C, decomposition without melting. ^{1}H NMR (400 MHz, $CDCl_3$-d_1): δ (ppm) = 9.01 (d, 6H, $^{3}J(H_a\text{-}H_b)$: 6.78 Hz, H_a), 8.90, (s, 3H, Hg), 7.42 (d, $^{3}J(H_b\text{-}H_a)$: 6.78 Hz, 6H, H_b), 5.43 (s, 6H, H_d), 1.47 (s, 45H, H_h). ^{13}C NMR (300 MHz, DMSO-d_6): δ (ppm) = 163.9 (C_e), 153.6 (C_a), 146.9 (C_g), 135.2 (C_f), 130.8 (C_c), 123.8 (C_b), 85.9 (C_i), 64.6 (C_d), 8.6 (C_h). IR (KBr, cm^{-1}) υ = 1729 (s, C=O), 1612 (m, C=N), 1230 (s, -C-O-CH_2-). Elemental Analysis for $C_{57}H_{66}Cl_6N_3O_6Ir_3$: found C, 38.80; H, 4.28 ; N, 1.57 %; calculated: C, 40.78; H, 3.96; N, 2.50. ESI-MS: *m/z* 363.05 ($[M + 5H + 4CH_3OH]^+$, 100%).

5.4.5. X-Ray Structure Analysis

Single-crystal X-ray diffraction data were collected on a Bruker KAPPA APEX II DUO diffractometer using graphite-monochromated Mo-Kα radiation (χ = 0.71073 Å). Data collection was carried out at 173(2) K. Temperature was controlled by an Oxford Cryostream cooling system (Oxford Cryostat). Cell refinement and data reduction were performed using the program SAINT.[46] The data were scaled and absorption correction performed using SADABS.[36] The structure was solved by direct methods using SHELXS-97[47] and refined by full-matrix least-squares methods based on F^2 using SHELXL-97[47] and using the graphics interface program X-Seed.[48,49] The programs X-Seed and POV-Ray[50] were both used to prepare molecular graphic images.

For complex **5.4**, there are four chloroform molecules in the asymmetric unit. Two of them were modelled with the chlorine atoms disordered over two positions with each having site occupancy 0.50. All non-hydrogen atoms of the main molecule, except the carbon atoms C1A-C10A and C36B-C40B, were refined anisotropically. C1A-C10A and C36B-C40B were refined with isotropic temperature factors and were restrained to a reasonable geometry. All hydrogen atoms were placed in idealised positions and refined with geometrical constraints. The structure was refined to R factor of 0.072. The highest peak is 2.89 e/Å3, 0.92 Å from Rh2B and the deepest hole is -0.71 e/Å3, 0.57 Å from CL4X. The Flack x parameter was refined with BASF and TWIN commands to be 0.54936 with esd 0.03821.

For complex **5.5**, there are four chloroform molecules in the asymmetric unit. Two of them were modelled with the chlorine atoms disordered over two positions with each having site occupancy 0.50. All non-hydrogen atoms of the main molecule, except the carbon atoms C6A-C10A and C6B-C10B, were refined anisotropically. C6A-C10A and C6B-C10B were refined with isotropic temperature factors and were restrained to a reasonable geometry. All hydrogen atoms were placed in idealised positions and refined with geometrical constraints. The structure was refined to R factor of 0.0360. The highest peak is 3.12e/Å3, 0.86 Å from IR1A and the deepest hole is -1.30 e/Å3, 0.56 Å from CL1Z.

5.5. References

1. T. J. Ritchie and S. J. F. Macdonald, *Drug Discov. Today*, **2009**, *14* (21-22), 1011.
2. T. J. Ritchie and S. J. F. Macdonald, S. Peace, S. D. Pickett and C. N. Luscombe, *Med. Chem. Commun.*, **2012**, *3*, 1062.
3. S. W. Fogt, J. A. Scozzie, R. D. Heilman and L. J. Powers, *J. Med. Chem.*, **1980**, *23*, 1445.
4. S. Kumar, P. Arya, C. Mukherjee, B. K. Singh, N. Singh, V. S. Parmar, A. K. Prasad and B. Ghosh, *Biochemistry*, **2005**, *44*, 15944.
5. B. P. Bandgar, R. J. Sarangdhar, K. Fruthous, J. Mookkan, S. Chaudhary, H. V. Chavan, S. B. Bandgar and V. Y. Kshirsagar, *Eur. J. Med. Chem.*, **2012**, *57*, 217.
6. I. Aissa, R. M. Sghair, M. Bouaziz, D. Laouini, S. Sayadi and Y. Gargouri, *Lipids Health Dis.*, **2012**, *11:13*,
7. H. Hess-Stumpp, T. U. Bracker, D. Henderson and O. Politz, *Int. J. Biochem. Cell Biol.*, **2007**, *39*, 1388.
8. O. L. P. De Jesús, H. R. Ihre, L. Gagne, J. M. J. Fréchet and F. C. Szoka, Jr., *Bioconjugate Chem.*, **2002**, *13*, 453.
9. A. L. Acton, C. Fante, B. Flatley, S. Burattini, I. W. Hamley, Z. Wang, F. Greco and W. Hayes *Biomacromolecules*, **2013**, *14* (2), 564.
10. X. Ma, Z. Zhou, E. Jin, Q. Sun, B. Zhang, J. Tang and Y. Shen, *Macromolecules*, **2013**, *46* (1), 37.
11. C. Gong, S. Deng, Q. Wu, M. Xiang, X. Wei, L. Li, X. Gao, B. Wang, L. Sun, Y. Chen, Y. Li, L. Liu, Z. Qian, Y. Wei, *Biomaterials*, **2013**, *34*, 1413.
12. Y. Xiao, H. Hong, A. Javadi, J. W. Engle, W. Xu, Y. Yang, Y. Zhang, T. E. Barnhart, W. Cai and S. Gong, *Biomaterials*, **2012**, *33*, 3071.
13. N. Feliu, M. V. Walter, M. I. Montañez, A. Kunzmann, A. Hult, A. Nyström, M. Malkoch and B. Fadeel, *Biomaterials*, **2012**, *33*, 1970.
14. K. -G. Liu, X. -Q. Cai, X. -C. Li, D. -A. Qin, M. -L. Hu, *Inorg. Chim. Acta*, **2012**, *388*, 78.
15. F. Schmitt, P. Govindaswamy, O. Zava, G. Suss-Fink, L. Juillerat-Jeanneret and B. Therrien, *J. Biol. Inorg. Chem.*, **2009**, *14*, 101.
16. F. Schmitt, P. Govindaswamy, G. Süss-Fink, W. H. Ang, P. J. Dyson, L. Juillerat-Jeanneret and Bruno Therrien, *J. Med. Chem.*, **2008**, *51*, 1811.

17. W. H. Ang, E. Daldini, L. Juillerat-Jeanneret and P. J. Dyson, *Inorg. Chem.*, **2007**, *46* (22), 9048.

18. W. H. Ang, A. De Luca, C. Chapuis-Bernasconi, L. Juillerat-Jeanneret, M. Lo Bello, P. J. Dyson, *Chem. Med. Chem.*, **2007**, *2* (12), 1799.

19. W. H. Ang, L. J. Parker, A. De Luca, L. Juillerat-Jeanneret, C. J. Morton, M. Lo Bello, M. W. Parker, P. J. Dyson, *Angew. Chem. Int. Ed.*, **2009**, *48* (21), 3854.

20. M. Auzias, B. Therrien, G. Süss-Fink, Pet. Štěpnička, W. H. Ang and P. J. Dyson, *Inorg. Chem.*, **2008**, *47*, 578.

21. S. Ghosh and P. S. Mukherjee, *J. Org. Chem.*, **2006**, *71*, 8412.

22. X. -B. Shao, X. -K. Jiang, X. Zhao, C. -X. Zhao, Y. Chen and Z. -T. Li, *J. Org. Chem.*, **2004**, *69*, 899.

23. E. H. Kim, S. Hong, J. M. Lee, D. N. Lee, Y. M. Jun, W. -Y. Lee and B. H. Kim, *Inorg. Chim. Acta*, **2009**, *362*, 1577.

24. Y. Yamamotoa, H. Suzuki, N. Tajima and K. Tatsumi, *Chem. Eur. J.*, **2002**, *8* (2), 372.

25. P. Govindaswamy, G. Süss-Fink and B. Therrien, *Organometallics*, **2006**, *26*, 915.

26. A. Bacchi, G. Cantoni, P. Pelagatti and S. Rizzato, *J. Organomet. Chem.*, **2012**, *714*, 81.

27. J. Grau, V. Noe, C. Ciudad, M.J. Prieto, M. Font-Bardia, T. Calvet, V. Moreno, *J. Inorg. Biochem.*, **2012** *109*, 72.

28. M. Yadav, A. K. Singh, R. Pandey and D. S. Pandey, *J. Organomet. Chem.*, **2010**, *695* 841.

29. P. Govender, N. C. Antonels, J. Mattsson, A. K. Renfrew, P. J. Dyson, J. R. Moss, B. Therrien and G. S. Smith, *J. Organomet. Chem.*, **2009**, *694*, 3470.

30. G. Süss-Fink, F. -A. Khan, L. Juillerat-Jeanneret, P. J. Dyson and A. K. Renfrew, *J. Clust. Sci.*, **2010**, *21*, 313.

31. S. Grgurić-Šipka, I. Ivanović, G. Rakić, N. Todorović, N. Gligorijević, S. Radulović, V. B. Arion, B. K. Keppler and Ž. L. Teši, *Eur. J. Med. Chem.*, **2010**, *45*, 1051.

32. N. Mézailles, P. E. Fanwick and C. P. Kubiak, *Organometallics*, **1997**, *16* (8), 1526.

33. S. K. Singh, M. Trivedi, M. Chandra and D. S. Pandey, *J. Organomet. Chem.*, **2005**, *690*, 647.

34. P. Govindaswamy, Y. A. Mozharivskyj and M. R. Kollipara, *Polyhedron*, **2005**, *24*, 1710.

35. M. Chandra, A. N. Sahay, S. M. Mobin and D. S. Pandey, *J. Organomet. Chem.*, **2002**, *658*, 43.
36. G. M. Sheldrick, SADABS version 2.05, University of Göttingen, Germany, 1997.,
37. J. G. Małecki, M. Jaworska and R. Kruszynski, *Polyhedron*, **2006**, *25*, 2519.
38. Y. -F. Han, J. -S. Zhang, Y. -J. Lin, J. Dai and G. -X. Jin, *J. Organomet. Chem.*, **2007**, *692*, 4545.
39. J. -Q. Wang, C. -X. Ren and G. -X. Jin *Organometallics*, **2006**, *25*, 74.
40. R. Schobert, S. Seibt, K. Effenberger-Neidnicht, C. Underhill, B. Biersack and G. L. Hammond, *Steroids*, **2011**, *76*, 393.
41. M. Gras, B. Therrien, G. Süss-Fink, A. Casini, F. Edafe and P. J. Dyson, *J. Organomet. Chem.*, **2010**, *695* (8), 1119.
42. L. Pauling; *The Nature of the Chemical Bond*; third ed.; Cornell University Press: New York, 1960.
43. L. E. Shutton; *Tables of Interatomic Distances and Configurations in Molecules and Ions (Supplement)*; The Chemical Society: London, 1965.
44. M. A. Bennett, T. N. Huang, T. W. Matheson and A. K. Smith, *Inorg. Synth.*, **1982**, *21*, 74.
45. C. White, A. Yates and P.M. Maitlis, *Inorg. Synth.*, **1992**, *29*, 228.
46. SAINT Version 7.60a, Bruker AXS Inc., Madison, WI, USA, 2006,
47. G. M. Sheldrick, SHELXS-97 and SHELXL-97, University of Göttingen, Germany, 1997.,
48. L. J. Barbour, *J. Supramol. Chem.*, **2001**, *1*, 189.
49. J. L. Atwood and L. J. Barbour, *Cryst. Growth Des.*, **2003**, *3*, 3.
50. E. Mas-Marza, E. Peris, I. Castro-Rodriguez and K. Meyer, *Organometallics*, **2005**, *24*, 3158.

CHAPTER 6

In Vitro Pharmacological Evaluation of Di- and Trinuclear Ruthenium, Rhodium and Iridium Pyridyl Ethers and Esters

6.1. Introduction

The clinical success of cisplatin and its analogues for the treatment of different cancers has had a profound effect on establishing the use of metal complexes in medicine. Lately, increasing drug resistance and the emergence of unwanted side effects to currently available therapies have bred a need for novel pharmacological agents. Thus, the design and study of metal-chemotherapeutics complexes as potential pharmaceuticals may potentially identify new drug candidates. Apart from platinum, ruthenium(II), rhodium(III) and iridium(III), have been identified as biologically relevant metals and their complexes are gaining attention as alternatives to platinum-containing compounds. The design and study of these complexes as potential drug candidates has been the subject of numerous reviews.[1-13]

Ruthenium is able to access a range of oxidation states [Ru(II), Ru(III) and Ru(IV)] under physiological conditions and its compounds may be less toxic than those of platinum.[14-18] This reduced toxicity is believed to be a consequence of ruthenium being able to mimic iron in the binding to biological molecules like albumin and transferrin.[14] Cancer cells rapidly divide and so exhibit a greater demand for iron causing transferrin receptors to be over-expressed thus leading to ruthenium based drugs to be more effectively delivered to cancer cells.[17,18]

As detailed in Chapter 1 (section 1.2.1.2.), the discovery of the antimetastatic activity of NAMI-A (**1.21**, Figure 6.1)[19-21] and the antineoplastic ability of KP-1019 (**1.22**)[22,23] has effectively established the biological relevance of ruthenium. Both these compounds have recently completed Phase I clinical trials[24-28] and are currently undergoing preliminary Phase II evaluation.[29-31]

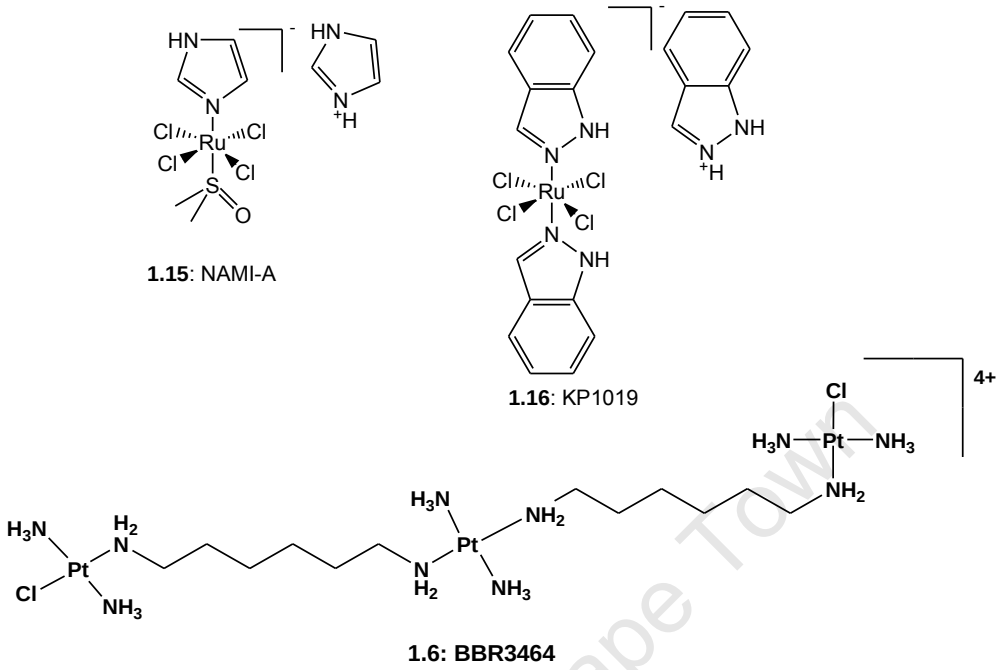

Figure 6.1. Structures of the Ru(III) metallotherapeutics currently in Phase II evaluation[19-23,32,33] and BBR3464.

NAMI-A acts as an anti-metastatic agent by either inhibiting metastasis formation[34] or reducing metastases size[35] while KP1019 is an antineoplastic agent that has demonstrated activity against a wide range of preclinical tumor models.[18,36,37] KP1019 exerts its cytotoxic effect through induction of apoptosis via the intrinsic mitochondrial pathway.

Since their discovery, the study of organoruthenium complexes for antiprolifeartive activities has rapidly gained momentum and most of the examples found in the literature are largely made up of Ru(II) arene complexes which were first developed by two distinct research groups, Dyson and co-workers[14,38,39] and Sadler and co-workers.[27,40] The basis for the design and study of these arene-ruthenium(II) complexes was the suggestion that the previously studied Ru(III) complexes **1.21** and **1.22** were precursors from which the active Ru(II) species was generated *in vivo*.[27,40] The amphilic nature of the arene-ruthenium moiety is also believed to enhance the antiproliferative activities of the overall complex.[41]

While there are fewer reports on the application of Rh(III) and Ir(III) organometallic complexes as biological agents, they are slowly garnering more attention. An account of the anti-tumor properties of $RhCl_3 \cdot 3H_2O$ actually predates the discovery of cisplatin[42] but the

cytotoxic abilities of Rh(III) and Ir(III) were not seriously considered until recently.[1,43] This lack of interest has been attributed to the kinetic inertness of these metal ions.[1,43-45] However, it has been proposed that this lack of reactivity can be overcome using one of two rational approaches, (i) the use of one or more ligands that provide a strong *trans* effect to improve the rate of substitution and (ii) complexation of these metals to ligands that display independent cytotoxic activities and can thus interact with specific biological targets.[1]

The antitumor efficacy of BBR3464 demonstrated the validity of the concept of multinuclearity for the development of potential metallo-chemotherapeutics.[46,47] Since the development of BBR3464, the study of polynuclear complexes containing other PGM metals has emerged as an area of great potential.[3,48-50] A series of tetranuclear iridium, rhodium and ruthenium porphyrin complexes (Figure 6.2) have also been studied for activity as dual photosensitizers and chemotherapeutics in human melanoma Me300 cells.[51,52]

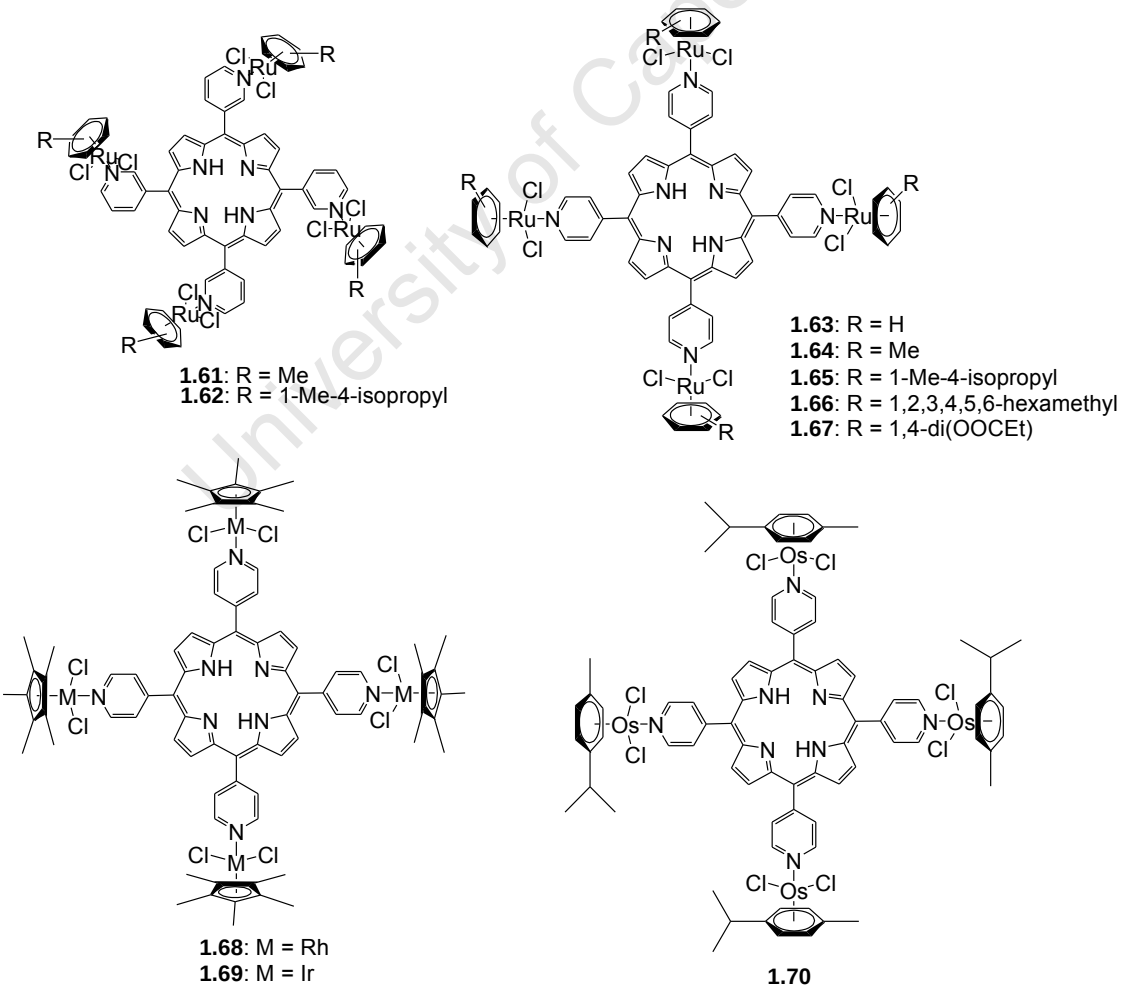

Figure 6.2. Structure of tetranuclear-organometallic complexes studied for activity against Me300 cell line.

Against parasitic diseases, metal complexes are emerging as potential metallo-antiparasitics. Malaria is amongst the deadliest and most widespread parasitic diseases found today. Currently, the standard first line therapy for uncomplicated *P. falciparum* malaria infections is artemisinin-based combined therapy (ACT).[53,54] Despite the effectiveness of ACT treatments, the emergence of resistance to these drugs is a very real possibility and is under intense monitoring.[54] Recent reports of resistance and suspected resistance of *P. falciparum* to artemisinins highlight the importance of developing alternative drug candidates since most of the currently developed drugs are mainly artemisinin derivatives and may eventually become susceptible to parasite resistance as well.[55-59]

Published accounts of the study of PGM complexes as antiplasmodial agents are largely made up of chloroquine or other amino-quinoline metal-conjugates.[53,60,61] Sánchez-Delgado *et al* reported that a [Ru(II)-chloroquine]$_2$ dimer and mononuclear Rh(I) complex (Figure 6.3) proved active against *P. falciparum* strains *in vitro*.[62] The dinuclear ruthenium complex (**1.85**) is 4.5 times more active than chloroquine diphosphate against two chloroquine resistant *P. falciparum* strains, FcB1 and FcB2. The rhodium complex (**1.86**) exhibited activities similar to chloroquine diphosphate.

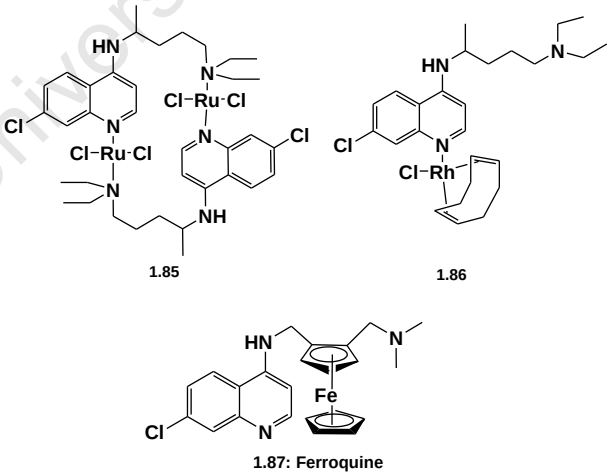

Figure 6.3. Structure of ruthenium (**1.85**) and rhodium (**1.86**) chloroquine metalloconjugates and ferroquine (**1.87**).[61-63]

Consequent to the initial chloroquine metal conjugate work pioneered by Sánchez-Delgado *et al*, came the discovery of the chloroquine analogue, Ferroquine (**1.87**).[64] The metallocene

containing complex has shown impressive antiplasmodial activity and is even active in chloroquine resistant strains.[61,64-66] It has completed Phase I clinical trials and is expected to complete Phase II clinical trials against uncomplicated malaria soon. Iridium-chloroquine analogues (**1.92** – **1.94**) have also been studied for *in vitro* antiplasmodial activity on cultures of *P. Berghei* (Figure 6.4).[67] These complexes were able to inhibit parasite growth at nanomolar concentrations.

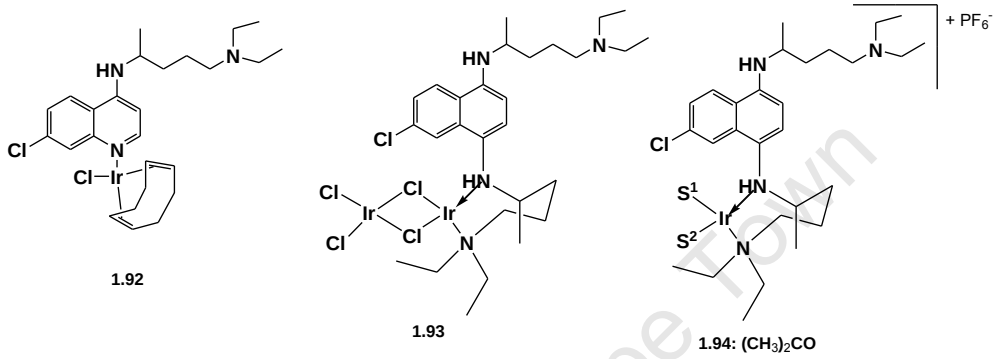

Figure 6.4. Iridium-CQ conjugates displaying nanomolar activity against *P. berghei*.[67]

Ruthenium-arene chloroquine conjugates (Figure 6.5) have been extensively studied for their *in vitro* antiplasmodial against three chloroquine resistant (W2, Dd2 and K1) and four chloroquine sensitive (FcB1, 3D7, PFB and F32) *P. falciparum* strains.[68]

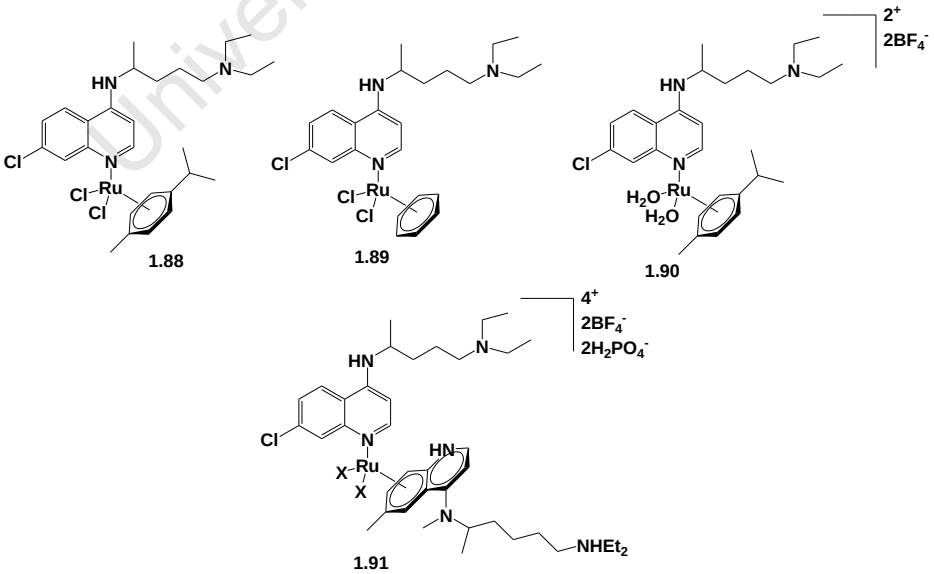

Figure 6.5. Ruthenium arene chloroquine conjugates **1.88** – **1.91**.

There are fewer examples of antiplasmodial PGM metal complexes that are non-quinolone based. A series of cationic platinum complexes containing substituted bipyridyl and phenanthroline ligands were tested for antiplasmodial activity against the D10 (chloroquine sensitive) and K1 (chloroquine resistant) strains.[69] They inhibited parasite growth at concentrations in the nanomolar range. Several examples of mononuclear ruthenium and palladium thiosemicarbazone complexes (Figure 6.6) were reported to show antiplasmodial activity in the micromolar range against NF54 (chloroquine sensitive),[70] Dd2 (chloroquine resistant),[70] W2 (chloroquine resistant)[71] and D10 (chloroquine sensitive)[71] P. falciparum strains. Polynuclear cyclopalladated thiosemicarbazone derivatives have also been found to demonstrate mild inhibition of parasite growth on the 3D7 (chloroquine sensitive) and K1 (chloroquine resistant) strains.[72]

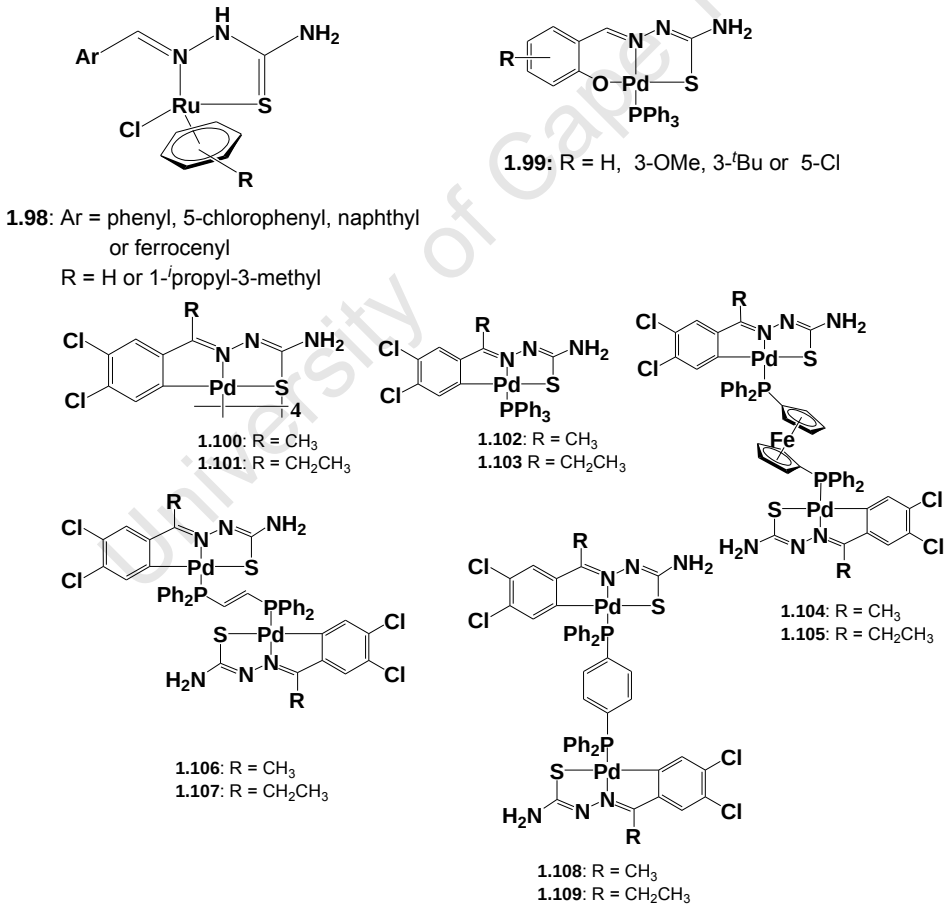

Figure 6.6. Ruthenium and Palladium thiosemicarbazone complexes that have been studied for antiplasmodial activity.[70-73]

In this chapter, the *in vitro* pharmacological evaluation of the pyridyl ether (**4.3** - **4.5** and **4.6**-**4.8**, Figure 6.7) and pyridyl ester (**5.3** - **5.5** and **5.6** - **5.8**, Figure 6.8) complexes and their free ligands (**4.1**, **4.2**, **5.1** and **5.2**) for antitumor and antiparasitic activity will be discussed. Selections of the compounds were screened for antiparasitic activity against a Chloroquine sensitive (CQS) *Plasmodium falciparum* strain and the *Trichomonas vaginalis* parasite strain G3. Antitumor activity was investigated by *in vitro* assay against a cisplatin sensitive and a cisplatin resistant human ovarian carcinoma cell line.

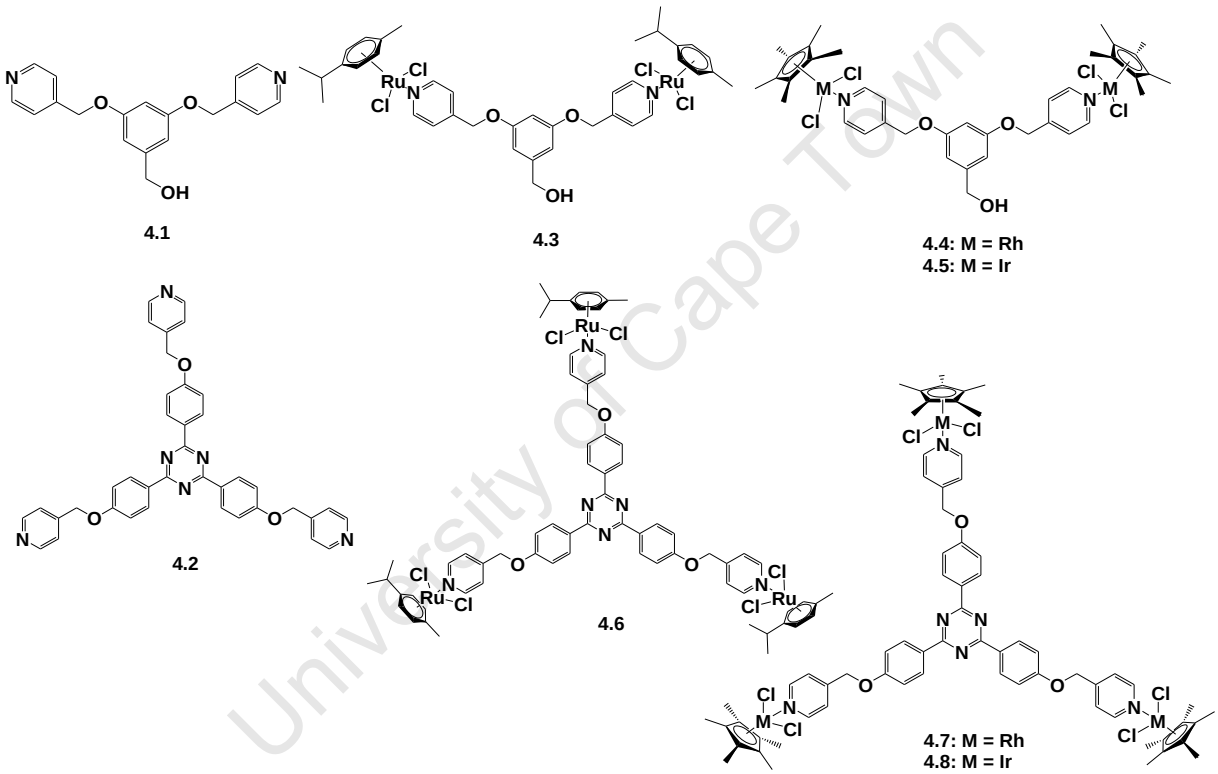

Figure 6.7. Di- and trinuclear PGM pyridyl ether complexes (**4.3**-**4.5** and **4.6**-**4.8**) and their corresponding free ligands (**4.1** and **4.2**).

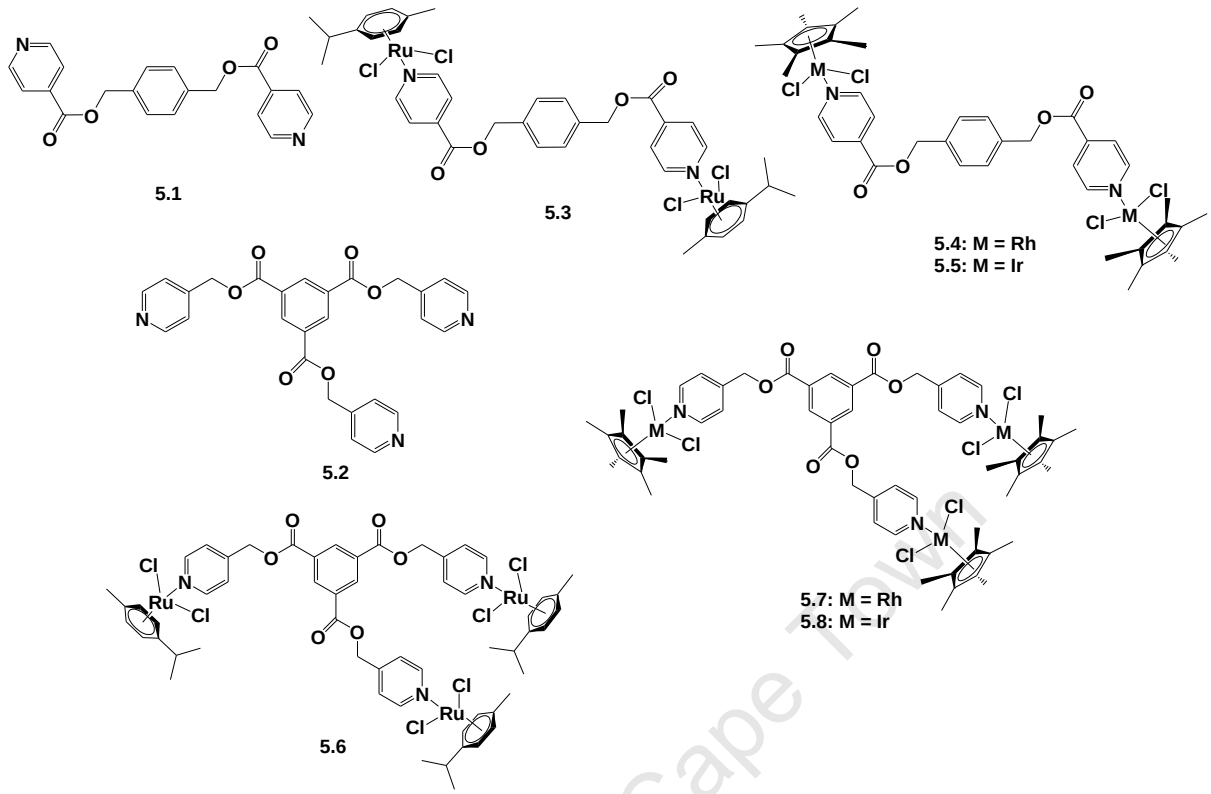

Figure 6.8. Di- and trinuclear PGM pyridyl ester complexes (**5.3**-**5.5** and **5.6**-**5.8**) and their corresponding free ligands (**5.1** and **5.2**).

6.2. Turbidimetric Solubility Assay

There are four cornerstones to early drug discovery; Absorption, Distribution, Metabolism and Excretion (ADME). The first step in evaluation of potential drug candidates for *in vitro* activity is analysis of their solubility in aqueous medium. This is an important property because it has a bearing on a compound's bioavailability since it impacts on absorption. Solubility also validates the *in vitro* assay data obtained. In general, based on their solubility range (Table 6.1.); compounds can be classed into three different categories. If a compound displays solubility greater than 100 μg/ml, then it should have good absorption. With respect to metal complexes, often polynuclear complexes display poor solubility in aqueous-based *in vitro* assays and are sometimes screened as suspensions in the assay thus casting doubt on the *in vitro* activities observed. One method used to validate aqueous solubility during early drug discovery is the Turbidimetric (kinetic) Solubility Assay.[74-77]

For compounds **4.1** – **4.8** and **5.1** – **5.8** and the dimers $[(p\text{-cymene})RuCl_2]_2$, $[Cp^*RhCl_2]_2$ and $[Cp^*IrCl_2]_2$, a solution of the test compound (in DMSO) was serially diluted with aqueous

PBS buffer to give a range of concentrations and allowed to equilibrate. A solubility range of the test compound was then determined from the concentration at which the compound began to precipitate from solution causing turbidity. This turbidity was detected by assessing the light scatter caused by the suspended particles using UV-vis spectroscopy.

Table 6.1. The three solubility categories used to class compounds

Solubility Range	
< 10 µg/ml	Sparingly soluble
10 – 60 µg/ml	Partially soluble
> 60 µg/ml	Soluble

Table 6.2 lists the solubility ranges of compounds **4.1**-**4.8** and **5.1**-**5.8** and the [(p-cymene)$RuCl_2]_2$, [Cp*$RhCl_2]_2$, [Cp*$IrCl_2]_2$ dimers. In micromolar concentration, most of the compounds were soluble in the PBS buffer up to the maximum concentration tested. Converting this data to µg/ml shows that all of the compounds had solubility greater than > 60 µg/ml. Reserpine and Hydrocortisone were used as controls for the solubility assays. Complex **4.6** showed the lowest solubility but it is still displayed good solubility in the buffer. All of the free ligands (**4.1**, **4.2**, **5.1** and **5.2**) as well as the trinuclear rhodium and iridium ester complexes **5.7** and **5.8** and the ruthenium, rhodium and iridium dimers display no turbidity up to the highest concentration tested.

Overall, the data ascertained implies that the di- and tripyridyl ether and ester compounds are good candidates for *in vitro* biological testing. Precipitation of these compounds from the various *in vitro* assays would be unlikely and thus the activities observed for these compounds are a true reflection of their *in vitro* activity since all of the compounds should remain in solution.

Table 6.2. Turbidimetric Solubility Data for Compounds **4.1**-**4.8** and **5.1**-**5.8**

Compound	Determined Turbidimetric Solubility (µM)	Determined Turbidimetric Solubility (µg/ml)
4.1	>200	> 64.27
4.2	> 200	> 126.14
4.3	160 - 200	149.35 - 186.70
4.4	80 - 120	75.15 - 112.73
4.5	160 - 200	178.89 - 223.61
4.6	40 - 80	61.97 - 123.94
4.7	80 - 120	124.62 - 186.94
4.8	80 - 120	146.06 - 219.09
5.1	> 200	> 69.67
5.2	> 200	> 96.69
5.3	160 - 200	153.72 - 192.15
5.4	160 - 200	154.63 - 193.28
5.5	80 - 120	91.05 - 137.41
5.6	> 200	> 280.41
5.7	> 200	> 282.12
5.8	> 200	> 335.71
[(*p*-cymene)$RuCl_2$]$_2$	> 200	> 122.48
[Cp*$RhCl_2$]$_2$	> 200	> 103.62
[Cp*$IrCl_2$]$_2$	> 200	> 159.34
Reserpine	20 - 40	12.17 - 24.34
Hydrocortisone	> 200	> 72.49

6.3. *In Vitro* Screening

6.3.1. In vitro Antiparasitic Activity

The pyridyl ether compound series (**4.1**-**4.8**) and pyridyl ester compound series (**5.1**-**5.8**) were evaluated for antiparasitic activity against the CQS NF54 *P. falciparum* strain and the *T. vaginalis* parasite strain G3. *Trichomonas vaginalis* is a flagellated facultative anaerobic protozoan, which causes the sexually transmitted infection trichomoniasis in humans and is reported to infect more than 170 million people worldwide, mainly in industrialized countries.[78] Infection can have serious implications like premature birth and increased risk of acquiring HIV, cervical cancer and aggressive prostate cancer.[78-81] Metronidazole is the current FDA-approved treatment[82] but approximately 5% of all cases reported display resistance to this compound and this percentage is increasing.[83] There is therefore a need to find alternative forms of treatment due to this increase in resistance.

6.3.1.1. In vitro P. falciparum Activity

The *in vitro* antiplasmodial activity of all compounds was first ascertained against the chloroquine sensitive (CQS) NF54 *P. falciparum* strain. Compounds exhibiting the best activities were then screened for inhibitory effects on the chloroquine resistant (CQR) *P. falciparum* strain Dd2. The IC_{50} values determined with standard error of the mean (SEM) values are shown in Table 6.3. The compounds showing the best activities are highlighted in red. The ruthenium, rhodium and iridium dimers, $[(p\text{-cymene})RuCl_2]_2$, $[Cp^*RhCl_2]_2$, $[Cp^*IrCl_2]_2$ and the organometallic chloroquine analogue, Ferroquine, were also screened for activity. Chloroquine diphosphate was screened as a control for the *in vitro* experiments.

Table 6.3. *In vitro* IC_{50}[a] data for compounds **4.1** – **4.8** and **5.1** – **5.8** against the chloroquine sensitive *P. falciparum* strain **NF54**

Compound	Ligand type	Metal Moiety	No of metal moieties	NF54 (μM)	SEM[b] (μM)
4.1	pyridyl ether	none	none	36.36	3.91
4.2	pyridyl ether	none	none	0.39	0.06
5.1	pyridyl ester	none	none	48.42	0.62
5.2	pyridyl ester	none	none	22.18	3.46
4.3	pyridyl ether	$(p\text{-cymene})RuCl_2$	2	10.68	1.41
4.4	pyridyl ether	Cp^*RhCl_2	2	13.67	1.51
4.5	pyridyl ether	Cp^*IrCl_2	2	56.79	9.95
5.3	pyridyl ester	$(p\text{-cymene})RuCl_2$	2	7.04	0.72
5.4	pyridyl ester	Cp^*RhCl_2	2	25.16	2.23
5.5	pyridyl ester	Cp^*IrCl_2	2	42.63	1.01
4.6	pyridyl ether	$(p\text{-cymene})RuCl_2$	3	0.24	0.01
4.7	pyridyl ether	Cp^*RhCl_2	3	0.23	0.03
4.8	pyridyl ether	Cp^*IrCl_2	3	1.64	0.25
5.6	pyridyl ester	$(p\text{-cymene})RuCl_2$	3	5.87	0.58
5.7	pyridyl ester	Cp^*RhCl_2	3	10.84	2.55
5.8	pyridyl ester	Cp^*IrCl_2	3	10.27	2.04
$[(p\text{-cymene})RuCl_2]_2$	-		2	16.80	2.94
$[Cp^*RhCl_2]_2$	-	-	2	20.90	0.87
$[Cp^*IrCl_2]_2$	-	-	2	59.40	19.45
Ferroquine	-	-	1	0.03	0.01
Chloroquine diphosphate	-	-	-	0.02	0.01

[a] concentration inhibiting 50% of parasite growth
[b] SEM: standard error of the mean

With respect to the free ligands (**4.1**, **4.2**, **5.1** and **5.2**), the tripyridyl ether ligand (**4.2**) was the most active (IC_{50} = 0.39 μM). Between the two dipyridyl ligands (**4.1** and **5.1**), the dipyridyl

ether ligand was more active (**4.1**, IC_{50} = 36.36 μM) and the tripyridyl ester ligand (**5.2**) shows better activity than both the dipyridyl ligands. The significantly greater activity observed for **4.2** compared to the other ligands may be attributed to the central triazine core. The incorporation of a triazine moiety into potential antimalarials has been previously reported.[84,85] Some substituted s-triazines have shown *in vitro* activities against D6 (CQS),[84] W2 (CQR),[84] 3D7 (CQS)[85] and K1 (CQR)[85] *P. falciparum* strains similar to the IC_{50} value determined for **4.2**. Substituted *s*-triazine compounds are believed to target dihydrofolate reductase (DHFR) in the *P. falciparum* parasite.[84,86] DHFR is an enzyme that catalyzes the nicotinamide adenine dinucleotide phosphate (NADPH) dependent reduction of dihydrofolate to tetrahydrofolate. Further to this, functionalization of ligand **4.2** with ruthenium (**4.6**) and rhodium (**4.7**) led to an enhancement of the *in vitro* antiplasmodial activity [IC_{50} = 0.24 μM (**4.6**) and 0.23 μM (**4.7**)]. The iridium derivative **4.8** (IC_{50} = 1.64 μM) was less active but inspection of all compounds tested reveal that ligand **4.2** and its trinuclear organometallic complexes (**4.6**-**4.8**) displayed significantly greater activity.

While the other compounds tested displayed only moderate activities, a trend in activities could be observed. For the pyridyl ether series (**4.1**-**4.8**), the presence of the Cp^*IrCl_2 moieties (**4.5** and **4.8**) seems to have a detrimental effect on inhibitory activities. Both these complexes were less active than the corresponding free ligand; complex **4.5** is 0.64 times less active than **4.1** and complex **4.8** is 0.24 times less active than **4.2**. This is not observed for the pyridyl ester series (**5.1**-**5.8**) where the iridium derivatives show enhanced activity compared to the corresponding free ligands. In fact, the tripyridyl ester complex **5.8** (IC_{50} = 10.27 μM) is twice as active compared to **5.2** (IC_{50} = 22.18 μM). This contrast in activity may be due to the differences in structural orientation within the complexes brought about by the ester functionality compared to the ether group. Based on the molecular structures determined for complexes **4.5**, **5.4** and **5.5** (Chapter 4 and Chapter 5), the pyridyl and phenyl rings in the ligands of the pyridyl ether complexes (**4.3**-**4.8**) are almost co-planar while for the pyridyl ester complexes (**5.3**-**5.8**) the pyridyl and aromatic rings reside in different planes most likely to minimize steric and electronic effects between the pentamethylcyclopentadienyl-metal moieties.

Consideration of the antiplasmodial data obtained for the dipyridyl ester complex series (**5.3**-**5.5**) showed that these complexes were much more active than their corresponding free ligand **5.1** (IC_{50} = 48.42 μM). However, there was a great difference in the antiplasmodial

activity as the metal moiety was varied. Complex **5.3** (IC_{50} = 7.04 μM) was the most active, followed by **5.4** (IC_{50} = 25.16 μM) and then **5.5** (IC_{50} = 42.63 μM) was the least active of the three complexes (**5.3**-**5.5**). For all of the dinuclear complexes (**4.3**-**4.5** and **5.3**-**5.5**) it is clear that activity decreased with a change in metal moiety in the order of (*p*-cymene)$RuCl_2$ > Cp*$RhCl_2$ > Cp*$IrCl_2$.

For both the pyridyl ether and pyridyl ester series, functionalization of the free ligands (**4.1**, **4.2**, **5.1** and **5.2**) with either the (*p*-cymene)$RuCl_2$ (**4.3**, **4.6**, **5.4** and **5.6**) or Cp*$RhCl_2$ (**4.4**, **4.7**, **5.4** and **5.7**) moieties led to a strong increase in antiplasmodial activity suggesting that these metal moieties play a role in activity. Comparison of the activities of the dimers, [(*p*-cymene)$RuCl_2]_2$, [Cp*$RhCl_2]_2$ and [Cp*$IrCl_2]_2$, to the corresponding ether (**4.3**-**4.8**) and ester (**5.3**-**5.8**) complexes reveals that the dimers are less active than the di- and trinuclear complexes with the exception of complex **5.4**. However, this observation coupled with the fact that the complexes (**4.3**-**4.8** and **5.3**-**5.8**) are more active than the free ligands suggests that there is a cooperative effect between metal moiety and ligand on antiplasmodial activity. Both the ligands (**4.1**, **4.2**, **5.1** and **5.2**) and the dimers were only moderately active on their own but conjugation of the different metal moieties onto the corresponding ligand led to a beneficial increase in activity.

Overall, from the *in vitro* data determined on the NF54 CQS strain several key trends for the design of better organometallic antimalarials can be discerned. The incorporation of a triazine moiety into the complex structure (**4.6**-**4.8**) has a profound effect on activity. The trinuclear complexes display better activities compared to the dinuclear derivatives when strictly compared within each compound series (pyridyl ether and pyridyl ester) thus proposing that an increase in metal moieties leads to an increase in activity *in vitro*. All of the complexes showed better activity than the corresponding free ligand. The pyridyl ether series (**4.1**-**4.8**) displayed better activity against the *P. falciparum* CQS strain NF54 compared to the pyridyl ester series (**5.1**-**5.8**). However, the tripyridyl ester complexes (**5.6**-**5.8**) were more active than the dipyridyl ether (**4.3**-**4.5**) complexes and the dipyridyl ester complexes showed the least promising activity. The order of activity of the complexes can be summarized as follows; tripyridyl ether complexes (**4.6**-**4.8**) > tripyridyl ester complexes (**5.6**-**5.8**) > dipyridyl ether complexes (**4.3**-**4.5**) > dipyridyl ester complexes (**5.3**-**5.5**).

Since the triazine containing complexes **4.3** and **4.4** along with their free ligand **4.2** showed enhanced activities compared to the other complexes screened against CQS NF54 strain, they were screened for *in vitro* antiplasmodial activity against the chloroquine resistant (CQR) *P. falciparum* strain Dd2 (Table 6.4). All three compounds were less active against the Dd2 strain compared to the NF54 strain. The complexes **4.6** (IC_{50} = 0.64 μM) and **4.7** (IC_{50} = 0.44 μM) were more active than the free ligand **4.2** (IC_{50} = 0.86 μM) indicating functionalization of **4.2** with the metal moieties enhances antiplasmodial activity. Complex **4.7** was more active than complex **4.6**. Against the NF54 strain, the ruthenium complexes were more active than the rhodium complexes when strictly compared within each class (ligand type and number of metal moieties) but against the Dd2 strain, it may be that the rhodium complexes might have better activity. Screening of all the other ruthenium (**4.3**, **5.3** and **5.6**) and rhodium (**4.4**, **5.4** and **5.7**) against the Dd2 strain must be carried out to confirm if complexes of rhodium will be better than ruthenium derivatives against this chloroquine resistant strain.

Their resistance index (RI) was determined based on the IC_{50} values observed for each P. falciparum strain. The RI value is an important implement when analysing potential drug candidates. A low RI value may suggest that the compound is likely to exhibit activity against resistant parasite strains.[87,88] A RI value of 1 or less is ideal. Chloroquine has a very high RI value (6.65) and compounds **4.2** and **4.7** have a much lower RI value (2.22 and 1.89 respectively) suggesting that these compounds are likely to be active against chloroquine-resistant strains of the parasite.

Table 6.4. *In vitro* IC_{50} data for most active compounds against the **NF54** (CQ sensitive) and **Dd2** (CQ resistant) *P. falciparum* strains

Compound	NF54 (μM)	Dd2 (μM)[a]	Resistance Index[b]
4.2	0.39	0.86 (0.07)	2.22
4.6	0.24	0.64 (0.03)	2.67
4.7	0.23	0.44 (0.06)	1.89
Chloroquine diphosphate	0.02	0.133	6.65

[a] standard errors are given in parentheses

[b] Resistance Index (RI) = IC_{50} Dd2/IC_{50} NF54

6.3.1.2. β-Hematin Inhibiton Assay

The mechanism of hemozoin formation is currently a target for antiplasmodial drug discovery. In the life cycle of the *Plasmodium falciparum* parasite, degradation of the infected host's hemoglobin to provide essential amino acids for parasite growth and nutrition is a vital step.[89] The *P. falciparum* trophozoite ingests large quantities of the host's hemoglobin (Figure 6.9).[61] Within the acidic digestive food vacuole, the hemoglobin (Hb) is then degraded using several endopeptidases and the metalloprotease falcilysin to produce peptides which are further broken down to amino acids.[61] A side product of this hemoglobin digestion is free heme which if toxic to the parasite. Free heme is reported to induce lipid peroxidation, oxygen-derived radical formation as well as protein and DNA oxidation.[90-93] Furthermore it can hinder phospholipid membrane stability.[94]

Thus, to circumvent these effects, the parasite initiates a detoxification mechanism and removes the threat by conversion of the free heme into a crystalline solid known as hemozoin (also known as malaria pigment) which is nontoxic to the parasite. Clinically used drugs, amodiaquine and chloroquine are believed to inhibit the formation of hemozoin.[95] The ability of a potential drug to inhibit formation of hemozoin can be measured using the NP-40 mediated β-hematin (synthetic hemozoin) inhibition assay.

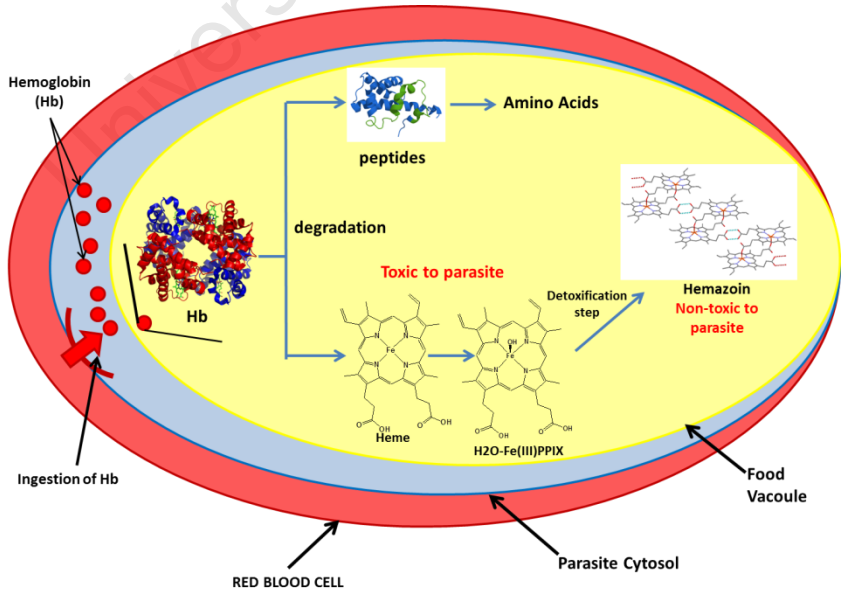

Figure 6.9. Graphical depiction of the hemoglobin degradation and heme detoxification process that occurs within the malaria parasite.

There is evidence suggesting that neutral lipid particles act as the site of nucleation and crystal growth of hemozoin within the digestive food vacuole.[96] NP-40 is a low cost, lipophilic detergent that can mediate the formation of synthetic hemozoin (β-hematin). The NP-40 mediated assay seeks to mimic the conditions of the acidic food vacuole in the parasite to give a better measure of hemozoin formation. Test compounds were screened at a range of concentrations between 0 – 500 μM in quadruplicate.

The amount of hematin not converted to β-hematin was then assessed by addition of a pyridine solution which causes formation of a pyridine-ferrichrome complex which is detected by UV-vis spectroscopy.[97] Figure 6.10A shows a prepared 96-well plate before incubation and Figure 6.10B shows the same plate after incubation and addition of the pyridine solution. The wells that have turned orange denote inhibition of β-hematin formation at that specific compound concentration. The absorbance data obtained is used to plot a sigmoidal dose-response curve from which the concentration for 50 % inhibition of β-hematin formation (IC_{50}) can be determined.

Figure 6.10. Images of (**A**) β-Hematin NP-40 Assay of compounds before incubation and (**B**) β-Hematin NP-40 Assay of compounds after 16 h incubation at 37 °C followed by addition of pyridine solution. Note: Wells that have turned orange represent β-hematin inhibition at that particular compound concentration.

From all of the compounds (**4.1**-**4.8** and **5.1**-**5.8**) screened for *in vitro* antiplasmodial activity against the NF54 CQS *P. falciparum* strain, the compounds showing cytotoxicities of approximately 10 μm or less (**4.2**, **4.3**, **4.6**-**4.8**, **5.3** and **5.6**-**5.8**) were assayed for β-Hematin inhibition (Table 6.5). The dimers, $[(p\text{-cymene})RuCl_2]_2$, $[Cp^*RhCl_2]_2$ and $[Cp^*IrCl_2]_2$, as well as the ligand **5.2** were also assayed for comparison. The tri-ruthenium pyridyl ester complex **5.6** showed the best inhibitory effect (IC_{50} = 7.76 uM) which was comparable to amodiaquine (IC_{50} = 6.83 μM) and the tripyridyl ether triazine ligand **4.2** was the second most active compound (IC_{50} = 9.93 μM). Complex **4.8**, the iridium functionalized tripyridyl ether

complex, was the least active (IC_{50} = 64.64 μM). Neither ligand **5.1** or **5.2** were able to inhibit β-hematin formation, yet their corresponding complexes (**5.3** and **5.6**-**5.8**) showed inhibitory effects suggesting that the overall complex structure is needed to stop formation of synthetic hemozoin. The fact that the dimers did not show activity also highlights the importance of the interaction between the metal and ligand for complexes **5.3** and **5.6**-**5.8**.

Table 6.5. IC_{50} Data for Compounds Screened for β-Hematin Inhibitory Activity Using NP-40 mediated β-Hematin Assay[a]

Compound	IC_{50} (μM)	95 % Confidence Interval
4.2	9.93	9.61-10.25
4.3	37.16	36.30-38.04
4.6	20.72	19.46-22.07
4.7	20.56	18.75-22.55
4.8	64.64	61.70-67.72
5.1	No inhibition	-
5.2	No inhibition	-
5.3	29.19	28.09-30.34
5.6	7.76	7.19-8.37
5.7	24.99	21.47-29.90
5.8	12.48	11.76-13.24
[(*p*-cymene)$RuCl_2$]$_2$	No inhibition	-
[Cp*$RhCl_2$]$_2$	No inhibition	-
[Cp*$IrCl_2$]$_2$	No inhibition	-
Ferroquine	14.51	13.72-15.34
Chloroquine	18.43	17.56-19.34
Amodiaquine	6.83	6.57-7.10

[a] Only compounds showing *in vitro* cytotoxic values of approximately 10 μM or less were screened.

The tri-ruthenium and tri-rhodium pyridyl ether complexes (**4.6** and **4.7**) exhibited the best *in vitro* parasite growth inhibition against the NF54 strain. These complexes were found to have β-hematin inhibitory activities [IC_{50} = 20.72 μM (**4.6**) and 20.56 μM (**4.7**)] similar to chloroquine (IC_{50} = 18.43 μM). The tripyridyl ester rhodium complex (**5.7**) displayed moderate inhibition (IC_{50} = 24.99 μM) while the iridium derivative (**5.8**) was very active (IC_{50} = 12.48 μM). Overall, the best inhibitor of β-hematin formation were the triruthenium pyridyl ester complex (**5.6**), the ligand **4.2** and the complex **5.8**; which were better at inhibiting formation of synthetic hemozoin than ferroquine and chloroquine.

All of the compounds screened using the NP-40 mediated assay are polyaromatic in nature making them capable of intermolecular π-π interactions. Thus, it is possible that these compounds can inhibit formation of hemozoin through π-π stacking with hematin. Most of the compounds screened using this assay were able to inhibit β-hematin formation in a lipidic atmosphere to some degree. Should these compounds be able to enter the acidic food vacuole of the parasite intact, then they may very likely inhibit parasite growth through inhibition of hemozoin.

A direct correlation between the activities observed for the β-hematin inhibition assays and the activities obtained for the compounds in the parasite is not possible as the β-hematin inhibition assays are carried out in a parasite free medium.

6.3.1.3. In vitro T. vaginalis Activity

The effect on parasite viability of a selection of the pyridyl ether (**4.2**-**4.8**) and all the pyridyl ester (**5.1**-**5.8**) compound series were evaluated on the *T. vaginalis* strain G3 (Figures 6.11A and 6.11B). Cells were inoculated with 50 and 25 μM doses of compounds. All of the compounds were able to influence parasite viability in a dose dependent manner. For the pyridyl ether series (**4.2**-**4.8**) at 50 μM, the best percent inhibitions were observed for complexes **4.4** (92.4 %) and **4.8** (89.4 %). Moderate inhibitory effects were observed for complexes **4.5**-**4.7** (81.8, 65.2 and 83.3 % respectively). The tripyridyl ether ligand (**4.2**) demonstrated only 72.7 % inhibition while its rhodium and iridium complexes (**4.7** and **4.8**) displayed much better inhibitions; the ruthenium derivative (**4.6**) showed decreased inhibition (65.2 %) compared to **4.2**. The dinuclear rhodium and iridium complexes (**4.4** and **4.5)** also displayed better % inhibitions (92.4 and 81.8 % respectively) than the ruthenium analogue (**4.3**, 63.6 %).

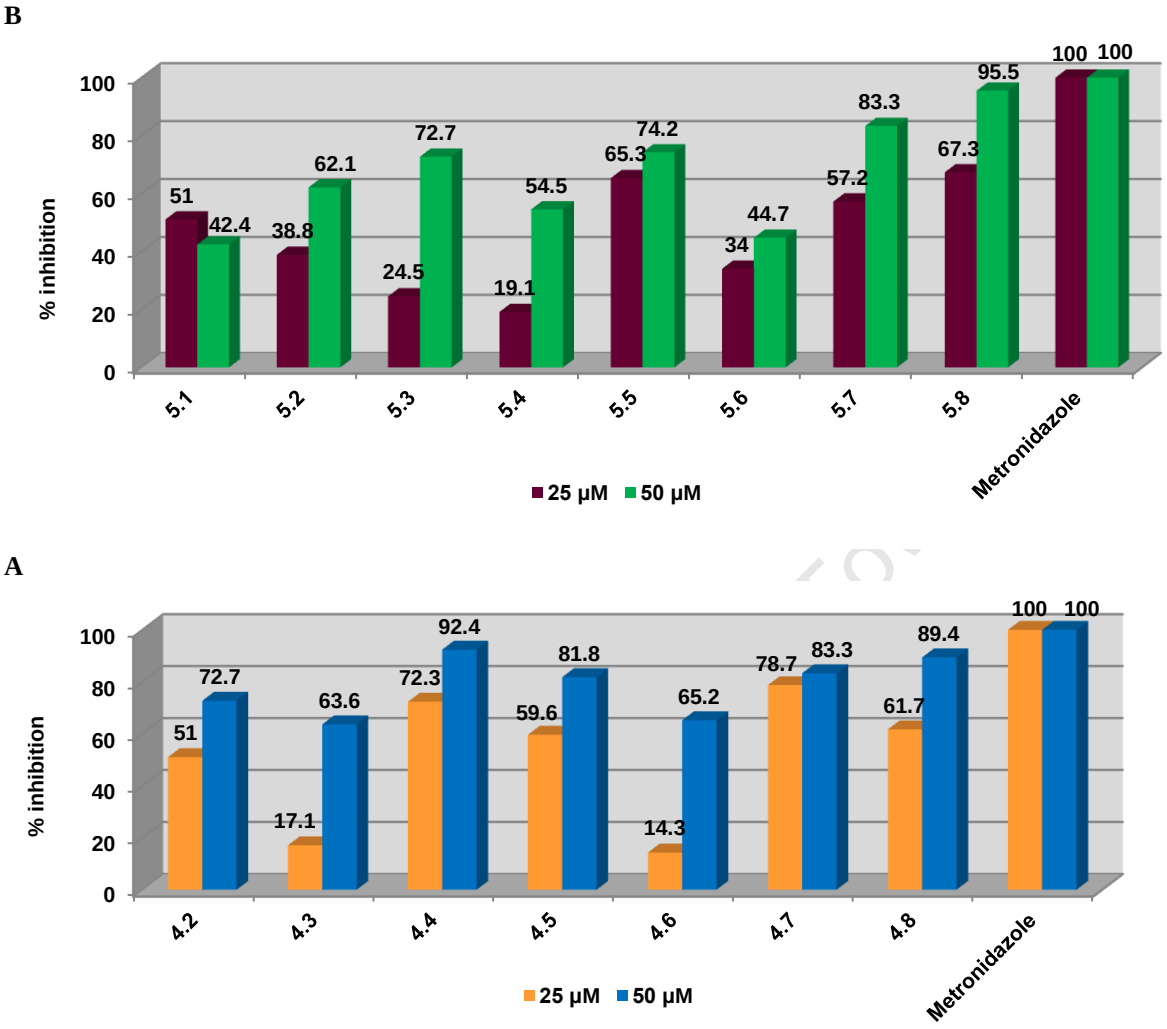

Figure 6.11. Graphical Representation of % inhibition data ascertained for compounds **4.2** – **4.8** (Chart A) and **5.1** – **5.8** against *T. vaginalis* strain G3

When comparing the dinuclear (**4.3**-**4.5**) and trinuclear (**4.6**-**4.8**) pyridyl ether complexes, it can be discerned that with respect to the type of metal moiety, the dinuclear complexes display similar inhibitory effects to their trinuclear analogues. This seems to imply that in the case of the pyridyl ether series, there is no increase in activity with an increase in the number of metal moieties. Furthermore, the incorporation of the triazine core does not appear to result in enhanced inhibitory effects as the dinuclear and trinuclear complexes show similar activity as evidenced by their percent inhibitions. At the lower concentration of 25 µM, a decrease in the percent inhibitions is observed for all of the compounds. Ligand **4.3** and complex **4.6** display the highest decrease in activity (17.1 and 14.3 % respectively) while complex **4.7** showed the slightest change in % inhibition. The rhodium complexes **4.4** and **4.7** have similar

similar inhibitions at 25 μM (72.3 and 78.7 %) and the same trend can be seen for the iridium complexes **4.5** and **4.8**. Out of all the pyridyl ether complexes, the rhodium complexes (**4.4** and **4.7**) have shown the best *in vitro* activity against G3.

In contrast, the pyridyl ester series (**5.1**-**5.8**) were not as active as the pyridyl ether series (**4.2**-**4.8**). At 50 μM, the tripyridyl ester ligand (**5.2**) displayed better inhibitory activity (62.1 %) than the dipyridyl ester ligand **5.1** (42.4 %) but a decrease in compound concentration to 25 μM resulted in ligand **5.2** displaying a much lower activity than **5.1** (38.8 vs 51.1 %). At both 25 and 50 μM concentrations, the dinuclear ruthenium (**5.3**) and iridium (**5.5**) complexes exhibited better activities than the dinuclear rhodium complex **5.4**. At 25 μM, complexes **5.3** and **5.5** were not as active (24.5 and 19.1 % respectively) as their corresponding free ligand **5.1** (51 %). The iridium derivative **5.5** had better activity than the free ligand at both concentrations (65.3 % at 25 μM and 74.2 % at 50 μM). The trinuclear complexes **5.7** and **5.8** displayed better inhibitory activity compared to the free ligand **5.2** at both 25 and 50 μM concentrations. At 50 μM, the tri-ruthenium complex **5.6** showed similar inhibition (44.7 %) to ligand **5.2** (42.4 %) and is less active than **5.2** at 25 μM (51 % vs 34 %). Complex **5.8** exhibited the best activity out of all the pyridyl ester complexes tested at both compound concentrations. At 25 μM, the iridium complexes, **5.5** and **5.8**, exhibit similar inhibitory activities of 65.3 and 67.3 % respectively. Complexes **5.3** and **5.4** display the weakest activity out of the all the pyridyl ester compounds (**5.1**-**5.8**).

Comparison of the pyridyl ether complexes (**4.3**-**4.8**) to the pyridyl ester complexes (**5.3**-**5.8**) reveals that the tripyridyl ether iridium complex **4.8** has similar activity to the tripyridyl ester iridium complex **5.8** at both compound concentrations. The dinuclear pyridyl ether complexes (**4.3**-**4.5**) showed superior activity than the dipyridyl ester complexes. At 25 μM, the pyridyl ether rhodium complexes **4.4** and **4.7** are more active than the pyridyl ester rhodium complexes **5.4** and **5.7**. In contrast, the pyridyl ether ruthenium complexes **4.3** and **4.6** were less active than the pyridyl ester ruthenium complexes **5.3** and **5.6**.

Overall, complex **5.8** displayed the best inhibitory effect out of all complexes tested but taken as a whole, the pyridyl ether series (**4.2**-**4.8**) are much better inhibitors of the *T. vaginalis* strain G3 with the tri-rhodium complex **4.7** showing the slightest decrease in activity with a decrease in compound concentration. None of the compounds (**4.1**-**4.8** and **5.1**-**5.8**) were not as active as the FDA-approved treatment for T. vaginalis infections, metronidazole. This drug

displayed 100 percent inhibition at both concentrations. Nevertheless, these complexes represent a new chemotype for the inhibition of the *T. vaginalis* strain G3. Modification of the ligand structure and/or the metal moieties may increase the activity of these compounds. For example, pyridyl ether or pyridyl ester ligands that are able to chelate to the metal in a bidentante manner may lead to the formation of complexes that are more stable in the biological medium. Modification of the arene or cyclopentadienyl ligands to give added water solublility to the metal moieties could also enhance activity.

6.3.2. In vitro Antitumor Activity

The pyridyl ether series (**4.1**-**4.8**) and the pyridyl ester series (**5.1**-**5.8**) were evaluated for antiproliferative activity on the A2780 (cisplatin sensitive) and A2780*cis*R (cisplatin resistant) human ovarian carcinoma cell line. The toxicity of the pyridyl ester series on healthy cells was also assessed using the human embryonic kidney (HEK) cell line. Cells were incubated with each compound at different concentrations up to a maximum concentration of 200 μM. The IC_{50} determinations are shown in Table 6.6 and a graphical respresentation of the most active compounds' activities is depicted in figure 6.12.

None of the compounds in the pyridyl ether series (**4.1**-**4.8**) demonstrated inhibitory activities on either the A2780 or A2780*cis*R cell lines up to the highest concentration tested (200 μM). In the pyridyl ester series (**5.1**-**5.8**), the dinuclear iridium complex **5.5** and the trinuclear complexes (**5.6**-**5.8**) were the only compounds to show antiproliferative activity implying that the role played by the number of aryl ester groups and the type of metal moiety in the complex influences inhibitory activity. Complexes **5.6** and **5.7** showed comparable activity to each other (IC_{50} = 53.0 and 52.4 μM respectively) in the A2780 cell line. The di- and trinuclear iridium complexes **5.5** (IC_{50} = 101.9 μM) and **5.8** (IC_{50} = 97.0 μM) also displayed similar weak activities.

Table 6.6. IC_{50}[a] Determinations for Compound **4.1** – **4.8** and **5.1** – **5.8** against cisplatin sensitive (**A2780**) and cisplatin resistant (**A2780*cis*R**) human ovarian carcinoma and Human Embryonic Kidney (**HEK**) cell lines[b]

Compound	Ligand type	Metal Moiety	No of metal moieties	A2780 (μM)[c]	A2780 *cis*R (μM)[c]	RI[d]	HEK (μM)[c]
4.1	pyridyl ether	none	none	> 200[e]	> 200		Not tested
4.2	pyridyl ether	none	none	> 200	> 200		Not tested
5.1	pyridyl ester	none	none	> 200	> 200		> 200
5.2	pyridyl ester	none	none	> 200	> 200		> 200
4.3	pyridyl ether	(p-cymene)$RuCl_2$	2	> 200	> 200		Not tested
4.4	pyridyl ether	Cp*$RhCl_2$	2	> 200	> 200		Not tested
4.5	pyridyl ether	Cp*$IrCl_2$	2	> 200	> 200		Not tested
5.3	pyridyl ester	(p-cymene)$RuCl_2$	2	> 200	> 200		> 200
5.4	pyridyl ester	Cp*$RhCl_2$	2	> 200	> 200		> 200
5.5	pyridyl ester	Cp*$IrCl_2$	2	101.9 (8.2)	> 200	-	118.8 (9.8)
4.6	pyridyl ether	(p-cymene)$RuCl_2$	3	> 200	> 200		Not tested
4.7	pyridyl ether	Cp*$RhCl_2$	3	> 200	> 200		Not tested
4.8	pyridyl ether	Cp*$IrCl_2$	3	> 200	> 200		Not tested
5.6	pyridyl ester	(p-cymene)$RuCl_2$	3	53.0 (3.0)	84.4 (5.2)	1.59	98.1 (2.0)
5.7	pyridyl ester	Cp*$RhCl_2$	3	52.4 (0.4)	58.7 (4.1)	1.12	68.9 (6.4)
5.8	pyridyl ester	Cp*$IrCl_2$	3	97.0 (4.0)	45.5 (5.7)	0.46	148.5 (24.7)
cisplatin	-	-	1	1.5	25	16.66	7

[a] IC_{50}: concentration inhibiting 50% of cell growth
[b] Error values are given in parentheses.
[c] Resistance Index = IC_{50} A2780*cis*R/IC_{50} A2780
[d] No activity was observed up to the highest concentration of compound, 200 μM.

All of the active complexes (**5.5** – **5.8**) were less toxic to healthy cells with the tri-iridium complex **5.8** showing the greatest difference in toxicities between the carcinoma cells (A2780 and A2780*cis*R) and healthy cells (HEK). Complexes **5.5** – **5.8** were also less toxic than cisplatin toward the HEK cell line. This suggests that ruthenium, rhodium and iridium complexes of pyridyl ester complexes may likely show better uptake into cancer cells compared to healthy cells. Complex **5.8** was more active against the A2780*cis*R cell line (IC_{50} = 45.5 μM) than the A2780 cell line. The ruthenium complex **5.6** was 1.6 times less active on the A2780*cis*R cell line (IC_{50} = 84.4 μM) compared to the A2780 cell line (IC_{50} =

53.0 μM). None of the complexes were as active as cisplatin against either carcinoma cell line (IC_{50} = 1.5 (A2780) and 25 (A2780*cis*R) μM). Comparison of **5.6**-**5.8** to each other revealed that the ruthenium (**5.6**) and rhodium (**5.7**) complexes had better antiproliferative activity compared to the iridium complex **5.8**. Complex **5.7** displayed the best activity against both cell lines compared to **5.6** and **5.8** and it is the least toxic to healthy cells.

As mentioned earlier in (Section 6.3.1.1.), the resistance index (RI) for a compound is used as a tool to estimate whether a potential chemotherapeutic will develop or be susceptible to known resistance mechanisms.[98] This index has been used to assess other metal complexes studied for antitumor activity.[98,99] An RI index close to or less than one is ideal. Inspection of the resistance index for complexes **5.6**-**5.8** reveal that complexes of this type are less likely to be vulnerable to currently known resistance mechanisms compared to cisplatin. Complex **5.8** showed superior activity against the A2780*cis*R cell line compared to A2780 giving rise to a much lower RI value of 0.46 compared to the other active pyridyl ester complexes (**5.5**-**5.7**).

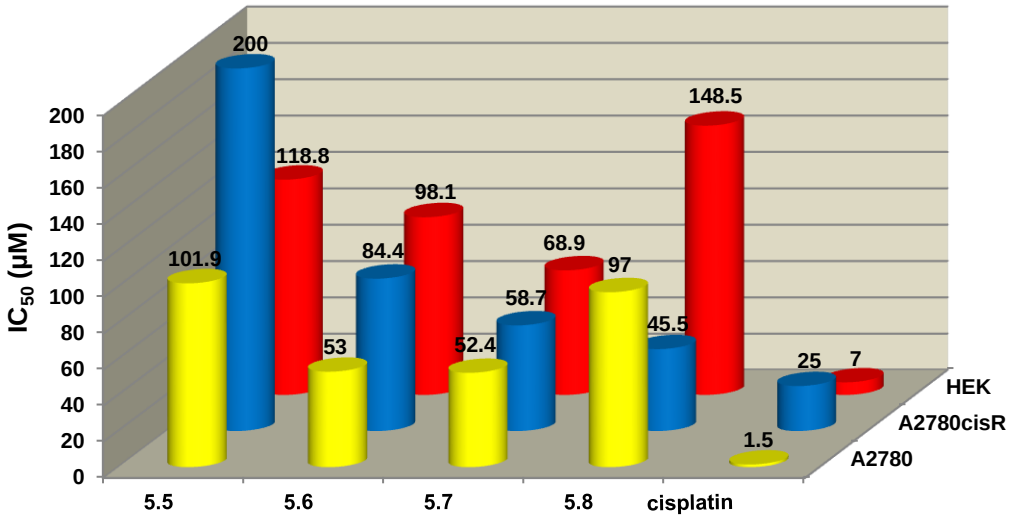

Figure 6.12. Graphical representation of the complexes showing activity against the **A2780**, **A2780*cis*R** and **HEK** cell lines.

Within the pyridyl ester series (**5.1**-**5.8**) it has been demonstrated that the dinuclear complexes (**5.3**-**5.5**) are not as active as the trinuclear complexes, implying that increasing the size and the number of metal centers of the overall complex increases antitumor activity. This effect has also been observed for other multinuclear arene-ruthenium complexes.[48,100,101] Other di-, tri-, tetra- and hexanuclear ruthenium arene complexes have been studied for *in vitro* cytotoxic activity against the A2780 and A2780*cis*R cell lines.[48,99,100,102,103] Most of these complexes demonstrated better activities than all of the complexes screened during this study (**4.3**-**4.8** and **5.3**-**5.8**). However, it is important to note that the complexes reported in the literature contain ligands that are not structurally similar to the pyridyl ether (**4.1** and **4.2**) and pyridyl ester (**5.1** and **5.2**) ligands used to prepare **4.3**-**4.8** and **5.3**-**5.8** and in some cases the coordination mode of the ligands to the metal are different to that of complexes **4.3**-**4.8** and **5.3**-**5.8**. In some of the reported complexes, the ligands chelate to the metal in a bidentate fashion.

Further to this, all of the compounds (**4.1**-**4.8** and **5.1**-**5.8**) must be screened for anti-tumor activity on a panel of other tumor cell lines. It is possible that these compounds may selectively inhibit cell growth against other tumor cell lines. Overall, in contrast to the antiparasitic studies, the tripyridyl ester complexes display better antiproliferative activities than the pyridyl ether series (**4.1**-**4.8**). It's possible that the pyridyl ether series are selective to parasitic cells but screening against other tumor cell lines need to be carried out to ascertain if this is true. The activity of the pyridyl ester series (**5.1**-**5.8**) could be enhanced by modification of the ligand system and the metal moieties.

6.4. Summary

Two new series of di- and trinuclear ruthenium, rhodium and iridium complexes have been evaluated for *in vitro* biological activity. All of the complexes and their free ligands (**4.1**-**4.8** and **5.1**-**5.8**) were found to exhibit moderate to high antiplasmodial activity against the NF54 CQS P. falciparum strain. The trinuclear pyridyl ether complexes (**4.6**-**4.8**) and their free ligand demonstrated significantly higher activities than the other complexes tested and this was attributed to the incorporation of a central triazine moiety into their structures. The trinuclear complexes display better activities compared to the dinuclear derivatives when strictly compared within each compound series (pyridyl ether and pyridyl ester) thus proposing that an increase in metal moieties leads to an increase in activity *in vitro*. All of the complexes showed better activity than the corresponding free ligand.

The most active compounds were assayed for inhibition of β-hematin formation and most of the compounds inhibited formation of synthetic hemozoin to some degree. This activity may be consequence of their polyaromatic structure. Should these compounds be able to enter the acidic food vacuole of the parasite intact, then they may very likely inhibit parasite growth through inhibition of hemozoin.

Against the Trichomonas vaginalis strain G3, both the pyridyl ether and pyridyl ester compound series decreased parasite viability in a dose dependent manner. The complex **5.8** displayed the best inhibitory effect out of all complexes tested but as a whole, the pyridyl ether series (**4.2**-**4.8**) were much better inhibitors of the *T. vaginalis* strain G3.

Antitumoral studies against the A2780 and A2780*cis*R cell lines revealed that the trinuclear pyridyl ester complexes were the only active complexes. The tri-iridium complex (**5.8**) was found to be twice as active against the cisplatin resistant cell line (A2780*cis*R) compared to the A2780 cell line and also demonstrated the lowest toxicity against human embryonic kidney (HEK) cells. The rhodium complex **5.7** displayed the best inhibitory effect compared to its ruthenium (**5.6**) and iridium (**5.8**) derivatives.

The activity of the pyridyl ether (**4.1**-**4.8**) and pyridyl ester (**5.1**-**5.8**) series could be improved through modification of the ligand structure and/or the metal moieties may increase the activity of these compounds. The design of pyridyl ether or pyridyl ester ligands that can to chelate to the metal in a polydentante manner may lead to the formation of complexes that are more stable and hence display better pharmacological activites. Modification of the arene or cyclopentadienyl ligands of the metal moieties to give added hydrophilicity could also enhance activity.

6.5. Experimental

6.5.1. P. falciparum in vitro assay.

The test samples were tested in triplicate on one occasion against chloroquine-sensitive (CQS) NF54 strain and chloroquine-resistant (CQR) Dd2 strain of Plasmodium falciparum. Continuous *in vitro* cultures of asexual erythrocyte stages of *P. falciparum* were maintained using a modified method.[104] Quantitative assessment of antiplasmodial activity *in vitro* was determined via the parasite lactate dehydrogenase assay using a modified method.[105] The test samples were prepared to a 20 mg/cm^3 stock solution in 100% DMSO and sonicated to enhance solubility. Stock solutions were stored at -20ºC. Further dilutions were prepared on the day of the experiment. Chloroquine (CQ) was used as the reference drug in all experiments. A full dose-response was performed for all compounds to determine the concentration inhibiting 50% of parasite growth (IC50–value). Test samples were tested at a starting concentration of 100 μg/cm^3, which was then serially diluted 2-fold in complete medium to give 10 concentrations; with the lowest concentration being 0.2 μg/cm^3. The same dilution technique was used for all samples. CQ was tested at a starting concentration of 100 ng/cm^3 against the CQR strain and 1000 ng/cm^3 against the CQS strain. The highest concentration of solvent to which the parasites were exposed to had no measurable effect on the parasite viability (data not shown). The IC_{50}-values were obtained using a non-linear dose-response curve fitting analysis via Graph Pad Prism v.4.0 software.

6.5.2. T. vaginalis in vitro susceptibility assay.

Trichomonas vaginalis strain G3 was cultured anaerobically in 15 mL conical centrifuge tubes containing 10 mL of Diamond's TYM media, pH 6.2. Dimethyl sulfoxide was used to dissolve compounds and generate 100 mM stock concentrations of each compound. Each compound was then tested at two concentrations, 25 uM and 50 uM, for *in vitro* inhibition of parasite growth. DMSO alone controls as well as tubes of untreated cells were carried along side-by-side. Test cultures were incubated for 24-hours at 37°C under anaerobic conditions. Cell densities were determined using a hemacytometer. Percentage inhibition was determined by comparing cell numbers in treatment tubes with the DMSO control tube. The results of these assays (n=6) were analyzed and standard errors were determined.

6.5.3. A2780 and A2780cisR cancer in vitro assay.

The human A2780 and A2780*cis*R ovarian carcinoma cells were obtained from the European Collection of Cell Cultures (Salisbury,UK). Cells in the log phase of growth were seeded at a densitiy of 2000-2500 per well into 96-well culture treated plates in 0.1 mL of complete media in all wells except for one column reserved for the media only control. The cells were allowed to attach during an overnight incubation at 37°C, 5% CO_2 prior to treating with test compounds. Test compounds were serially diluted in complete culture media and added to each well in a volume of 0.1 mL for a total final volume of 0.2 mL/well (max 0.1% DMSO final, where used). Cells were exposed to test compounds for 72 hours at 37°C, 5% CO_2. Then, the culture supernatant was carefully removed from all wells of each plate and 0.02 mL of MTT reagent was added to each well. The plates were returned to the incubator for 2 h. Following the incubation period, DMSO (0.1 mL) was added to all wells to dissolve the formazan crystals. The plates were allowed to shake on a table shaker at room temperature for 15 min and the absorbance at 590 nm was measured using a SpectraMAX e5 plate reader (Molecular Devices). The percentage of surviving cells was calculated from the ratio of absorbance of treated to untreated cells. The IC_{50} values for the inhibition of cell growth were determined by fitting the plot of the log of the ratio between the percentages of surviving cells, divided by the amount of dead cells, against the log of drug concentration using a linear threshold function.

6.5.4. Detergent mediated assay for β-hematin inhibitors.

The β-hematin formation assay method described by Carter et al.[95] was modified for manual liquid delivery. Stock solutions of the test compounds were prepared at 10 mM, 2 mM and 0.4 mM by dissolving each sample in DMSO with sonication. Test compounds were delivered to a 96 well plate in triplicate from 0-500 μM (final concentration) with a total DMSO volume of 10 μL in each well. Deionized H_2O (70 μL) and NP-40 (20 μL; 30.55 μM) were then added. A 25 mM hematin stock solution was prepared by sonicating hemin in DMSO, for complete dissolution, and then suspending 177.76 μL of this in a 2M acetate buffer (pH 4.8). The homogenous suspension (100 μL) was then added to the wells to give final buffer and hematin concentrations of 1 M and 100 μM respectively. The plate was covered and incubated at 37°C for 16 hours in a water bath. Analysis of the assay was carried out using the pyridine-ferrichrome method developed by Ncokazi and Egan.[97] A solution of 50% (v/v) pyridine, 30% (v/v) H_2O, 20% (v/v) acetone and 0.2 M HEPES buffer (pH 7.4)

was prepared and 32 µL added to each well to give a final pyridine concentration of ± 5% (v/v). Acetone (60 µL) was then added to assist with hematin dispersion. The UV-vis absorbance of the plate wells was read on a SpectraMax plate reader. Sigmoidal dose-response curves were fitted to the absorbance data using GraphPad Prism v5.00.

6.5.5. Turbidimetric Solubility Assay

Preparation of 0.01M pH 7.4 Phosphate Buffered Saline (PBS) involved dissolving 1 intact PBS buffer tablet (EC Diagnostics AB, Sweden) in sufficient distilled water to make 1000 mL of a solution comprising 0.14M NaCl, 0.003M KCl and 0.01M phosphate buffer. This solution was filtered through a 0.22 µm nylon filter to remove any particulate contaminants and the pH ascertained using a pH meter. The test compounds were prepared by making 10 mM stock solutions in DMSO from which, dilutions of the compounds in both DMSO and 0.01M pH 7.4 PBS were prepared in a 96-well plate, in triplicate. Wells in columns 1-6 contained compounds in DMSO and columns 7-12 contained the compounds in PBS at similar nominal concentrations as those in DMSO. The final volume of solvent in each assay plate well was 200 µL, prepared by pipetting 4 µL each of solution from the pre-dilution plate to the corresponding well into both DMSO and PBS (both 196 µL). This ensured that the final concentration of DMSO in the PBS aqueous buffer did not exceed 2 % v/v. The different concentrations in DMSO were prepared to serve as controls to determine potential false turbidimetric absorbance readings arising from the compounds in solution absorbing incident radiation at the analysis wavelength. After making the assay plate preparation, the plate was covered and left to equilibrate for 2 hours at ambient temperature. After incubation, UV-vis absorbance readings from the plate were measured at 620 nm. Corrected absorbance readings at different concentrations of test compounds were calculated by subtracting absorbance of the blank (DMSO and 1 % DMSO in PBS) from each subsequent concentration absorbance.

6.6. References

(1) Y. Geldmacher, M. Oleszak and W. S. Sheldrick, *Inorg. Chim. Acta* **2012**, *393*, 84.

(2) C. S. Allardyce and P. J. Dyson, *Top. Organomet. Chem.* **2006**, *17*, 177.

(3) C. G. Hartinger, A. D. Phillips and A. A. Nazarov, *Curr. Top. Med. Chem.* **2011**, *11* (21), 2688.

(4) A. Casini, C. G. Hartinger, A. A. Nazarov and P. J. Dyson, *Top. Organomet. Chem.* **2010**, *32*, 57.

(5) A. M. Pizarro and P. J. Dyson, *Biochimie* **2009**, *91*, 1198.

(6) H. -K. Liu and P. J. Sadler, *Acc. Chem. Res.* **2011**, *44* (5), 349.

(7) N. P. E. Barry and P. J. Sadler, *Chem. Soc. Rev.* **2012**, *41*, 3264.

(8) G. S. Smith and B. Therrien, *Dalton Trans.* **2011**, *40*, 10793.

(9) C. G. Hartinger, *Angew. Chem. Int. Ed.* **2010**, *49*, 8304

(10) W. H. Ang, A. Casini, G. Sava and P. J. Dyson, *J. Organomet. Chem.* **2011**, *696*, 989.

(11) C. G. Hartinger and P. J. Dyson, *Chem. Soc. Rev.* **2009**, *38*, 391.

(12) C. G. Hartinger, N. Metzler-Nolte and P. J. Dyson, *Organometallics* **2012**, *31*, 5677.

(13) K. J. Kilpin and P. J. Dyson, *Chem. Sci.* **2013**, *4*, 1410.

(14) W. H. Ang and P. J. Dyson, *Eur. J. Inorg. Chem.* **2006**, 4003

(15) C. S. Allardyce and P. J. Dyson, *Platinum Met. Rev.* **2001**, *45*, 62.

(16) I. Kostova, *Curr. Med. Chem.* **2006**, *13*, 1085.

(17) C. S. Allardyce, A. Dorcier, C. Scolaro and P. J. Dyson, *Appl. Organomet. Chem.* **2005**, *19*, 1.

(18) M. Galanski, V. B. Arion, M. A. Jakupec and B. K. Keppler, *Curr. Pharm. Des.* **2003**, *9*, 2078.

(19) I. Bratsos, S. Jedner, T. Gianferrara and E. Alessio, *Chimia* **2007**, *61*, 692.

(20) A. Bergamo and G. Sava, *Dalton Trans.* **2007**, 1267.

(21) G. Sava, I. Capozzi, K. Clerici, G. Gagliardi, E. Alessio and G. Mestroni, *Clin. Exp. Metastasis* **1998**, *16*, 371.

(22) C. G. Hartinger, M. A. Jakupec, S. Zorbas-Seifried, M. Groessl, A. Egger, W. Berger, H. Zorbas, P. J. Dyson and B. K. Keppler, *Chem. Biodiversity* **2008**, *5*, 2140.

(23) F. Lentz, A. Drescher, A. Lindauer, M. Henke, R. A. Hilger, C. G. Hartinger, M. E. Scheulen, C. Dittrich, B. K. Keppler and U. Jaehde, *Anti-Cancer Drugs* **2009**, *20*, 97.

(24) M. Groessl, E. Reisner, C. G. Hartinger, R. Eichinger, O. Semenova, A. R. Timerbaev, M. A. Jakupec, V. B. Arion and B. K. Keppler, *J. Med. Chem.* **2007**, *50*, 2185.

(25) S. Kapitza, M. Pongratz, M. A. Jakupec, P. Heffeter, W. Berger, L. Lackinger, B. K. Keppler and B. Marian, *J. Cancer Res. Clin. Oncol.* **2005**, *131*, 101.

(26) A. V. Vargiu, A. Robertazzi, A. Magistrato, P. Ruggerone and P. Carloni, *J. Phys. Chem. B* **2008**, *112*, 4401.

(27) E. Reisner, V. B. Arion, B. K. Keppler and A. J. L. Pombeiro, *Inorg. Chim. Acta* **2008**, *361*, 1569.

(28) B. K. Keppler, WO Application 2002059135, *Chem. Abstr.* **2002**, *vol. 137*, ref. 119658.

(29) P. J. Dyson and G. Sava, *Dalton Trans.* **2006**, (1929-1933),

(30) J. M. Rademaker-Lakhai, D. van den Bongard, D. Pluim, J. H. Beijnen and J. H. M. Schellens, *Clin. Cancer Res.* **2004**, *10*, 3717.

(31) A. Bergamo, C. Gaiddon, J. H. M. Schellens, J. H. Beijnen and G. Sava,, *J. Inorg. Biochem.* **2012**, *106*, 90.

(32) M. J. Clarke, *Coord. Chem. Rev.* **2002**, *232*, 69.

(33) M. J. Clarke, *Coord. Chem. Rev.* **2003**, *236*, 209.

(34) M. Cocchietto, S. Zorzet, A. Sorc and G. Sava, *Invest. New Drugs* **2003**, *21*, 55.

(35) G. Sava, S. Zorzet, C. Turrin, F. Vita, M. Soranzo, G. Zabucchi, M. Cocchietto, A. Bergamo, S. DiGiovine, G. Pezzoni, L. Sartor and S. Garbisa, *Clin. Cancer Res.* **2003**, *9*, 1898.

(36) B. K. Keppler, K. G. Lipponer, B. Stenzel and F. Kratz, In *Metal Complexes in Cancer Chemotherapy*; B. K. Keppler, Ed.; VCH, Weinheim,1993 Vol.,

(37) T. Pieper, K. Borsky and B. K. Keppler, *Top. Biol. Inorg. Chem.* **1999**, *1*, 171.

(38) P. J. Dyson, *Chimia* **2007**, *61*, 698.

(39) W. H. Ang, *Chimia* **2007**, *61*, 140.

(40) A .F. A. Peacock and P. J. Sadler, *Chem.-Asian J.* **2008**, *3*, 1890.

(41) G. Süss-Fink, *Dalton Trans.* **2010**, *371* (7), 1673.

(42) A. Taylor and N. Carmichael, *Cancer Studies* **1953**, *2*, 36.

(43) N. Katsaros and A. Anagnostopoulou, *Crit. Rev. Oncol.* **2002**, *42*, 297.

(44) L. Messori, G. Marcon, P. Orioli, M. Fontani, P. Zanello, A. Bergamo, G. Sava and P. Mura, *J. Inorg. Biochem.* **2003**, *95*, 37.

(45) G. Mestroni, E. Alessio, A. Sessanti o Santi, S. Geremia, A. Bergamo, G. Sava, A. Boccarelli, A. Schettino and M. Coluccia, *Inorg. Chim. Acta* **1998**, *273* 62.

(46) C. Manzotti, G. Pratesi, E. Menta, R. Di Domenico, E. Cavalletti, H. H. Fiebig, L. R. Kelland, N. Farrell, D. Polizzi, R. Supino, G. Pezzoni, and F. Zunino, *Clin. Cancer. Ress.* **2000**, *6*, 2626.

(47) J. D. Roberts, J. Peroutka and N. Farrell, *J. Inorg. Biochem.* **1999** *77*, 51.

(48) M. G. Mendoza-Ferri, C. G. Hartinger, A. A. Nazarov, R. E. Eichinger, M. A. Jakupec, K. Severin and B. K. Keppler, *Organometallics* **2009**, *28*, 6260.

(49) B. Therrien, W.H. Ang, F. Cherioux, L. Vieille-Petit, L. Juillerat-Jeanneret, G. Suess-Fink and P. J. Dyson, *J. Cluster Sci.* **2007**, *18*, 741.

(50) G. Gasser, I. Ott and N. Metzler-Nolte, *J. Med. Chem.* **2011**, *54*, 3.

(51) F. Schmitt, P. Govindaswamy, G. Süss-Fink, W. H. Ang, P. J. Dyson, L. Juillerat-Jeanneret and Bruno Therrien, *J. Med. Chem.* **2008**, *51*, 1811.

(52) F. Schmitt, P. Govindaswamy, O. Zava, G. Suss-Fink, L. Juillerat-Jeanneret and B. Therrien, *J. Biol. Inorg. Chem.* **2009**, *14*, 101.

(53) P. F. Salas, C. Herrmann and C. Orvig, *Chem. Rev.* **2013**, *113*, 3450.

(54) World Health Organization: Guidelines for the Treatment of Malaria, 2nd ed.; WHO Press: Geneva.

(55) M. Enserink, *Science* **2010**, *328*, 844.

(56) World Health Organization. Global plan for artemisinin resistance containment (GPARC), WHO Press: Geneva.

(57) H. Noedl, Y. Se, K. Schaecher, B. L. Smith, D. Socheat and M. M. N. Fukuda, *Engl. J. Med.* **2008**, *359*, 2619.

(58) A. M. Dondorp, F. Nosten, P. Yi, D. Das, A. P. Phyo, J. Tarning, K. M. Lwin, F. Ariey, W. Hanpithakpong, S. J. Lee, P. Ringwald, K. Silamut, M. Imwong, K. Chotivanich, P. Lim, T. Herdman, S. An, S. Yeung, P. Singhasivanon, N. P. J. Day, N. Lindegardh, D. Socheat and N. J. N. White, *Engl. J. Med.* **2009**, *361*, 455.

(59) N. Gargano, F. Cenci and Q. Bassat, *Trop. Med. Int. Health* **2011**, *16*, 1466.

(60) C. Biot, W. Castro, C. Y. Botte and M. Navarro, *Dalton Trans.* **2012**, *41*, 6335.

(61) M. Navarro, W. Castro and C. Biot, *Organometallics* **2012**, *31*, 5715.

(62) R. A. Sánchez-Delgado, M. Navarro, H. Perez, and J. A. Urbina, *J. Med. Chem.* **1996**, *39*, 1095.

(63) R. A. Sánchez-Delgado, A. Anzellotti and L. Suarez, Metal Complexes as Chemotherapeutic Agents Against Tropical Diseases In *Metal Ions in Biological Systems*; A. Sigel and H. Sigel, Ed.; CRC Press,2004 Vol., Chapter 12.

(64) C. Biot, G. Glorian, L. A. Maciejewski, J. S. Brocard, O. Domarle, G. Blampain, P. Millet, A. J. Georges, H. Abessolo, D. Dive, and J. Lebibi,, *J. Med. Chem.* **1997**, *40*, 3715.

(65) M. Henry, S. Briolant, A. Fontaine, J. Mosnier, E. Baret, R. Amalvict, T. Fusai, L. Fraisse, C. Rogier, and B. Pradines, *Antimicrob. Agents. Chem.* **2008**, *52*, 2755.

(66) C. Biot, F. Nosten, L. Fraisse, D. Ter-minassian, J. Khalife and D. Dive, *Parasite* **2011**, *18*, 207.

(67) M. Navarro, S. Pekerar and H. A. Perez, *Polyhedron* **2007**, *26*, 2420.

(68) C. S. K. Rajapakse, A. Martınez, B. Naoulou, A. A. Jarzecki, L. Suarez, C. Deregnaucourt, V. Sinou, J. Schrevel, E. Musi, G. Ambrosini, G. K. Schwartz and R. A. Sanchez-Delgado, *Inorg. Chem.* **2009**, *48* (1122-1131),

(69) T. J. Egan, K. R. Koch, P. L. Swan, D. A. Van Schalkwyk and P. J. Smith, *J. Med. Chem.* **2004**, *47*, 2926.

(70) M. Adams, Y. Li, H. Khot, C. De Kock, P. J. Smith, K. Land, K. Chibale and G. S. Smith, *Dalton Trans* **2013**, *42*, 4677.

(71) P. Chellan, N. Shunmoogam-Gounden, D. T. Hendricks, J. Gut, P. J. Rosenthal, C. Lategan, P. J. Smith, K. Chibale and G. S. Smith, *J. Eur. Med. Chem.* **2010**, 3520.

(72) P. Chellan, S. Nasser, L. Vivas, K. Chibale, and G. S. Smith,, *J. Organomet. Chem.* **2010**, *695*, 2225.

(73) P. Chellan, S. Nasser, L. Vivas, K. Chibale and G. S. Smith, *J. Organomet. Chem.* **2010**, *695*, 2225.

(74) E. H. Kerns and L. Di; *Drug-like Properties: Concepts, Structure Design and Methods from ADME to Toxicity Optimization*; 1st ed.; Elsevier Academic Press: California, 2008.

(75) C. A. Lipinski, F. Lombardo, B. W. Duminy and P. J. Feeney, *Adv. Drug Deliv. Rev.* **2001**, *46*, 3.

(76) J. Alsenz and M. Kansy, *Adv. Drug Deliv. Rev.* **2007**, *59*, 546.

(77) L. Pan, Q. Ho, K. Tsutsui and L. Takahashi, *J. Pharm. Sci.* **2001**, *4*, 521.

(78) D. Petrin, K. Delgaty, R. Bhatt and G. Garber, *Clin. Microbiol. Rev.* **1998**, *11*, 300.

(79) D. Soper, *Am. J. Obstet. Gynecol.* **2004**, *190*, 281.

(80) G. L. Lloyd, J. R. Case, D. De Frias and R. E. Brannigan, *J. Urol.* **2003**, *170*, 924.

(81) S. Sutcliffe, E. Giovannucci, J. F. Alderete, T. H. Chang, C. A. Gaydos, J. M. Zenilman, A. M. de Marzo, W. C. Willett and E. A. Platz, *Cancer Epidemiol. Biomarkers Prev.* **2006**, *15*, 939.

(82) S.L. Cudmore, K.L. Delgaty, S.F. Hayward-McClelland, D.P. Petrin, G.E. Garber,, *Clin. Microbiol. Rev.* **2004**, *17*, 783.

(83) J. R. Schwebke and D. Burgess, *Clin. Microbiol. Rev.* **2004**, *17*, 794.

(84) N. Kumar, S. I. Khan and D. S. Rawat, *Helvetica Chim. Acta* **2012**, *95*, 1181.

(85) M. Sharma, K. Chauhan, S. S. Chauhan, A. Kumar, S.V. Singh, J. K. Saxena, P. Agarwal, K. Srivastava, S. R. Kumar, S. K. Puri, P. Shah, M. I. Siddiqi and P. M. S. Chauhan, *Med. Chem. Commun.* **2012**, *3*, 71.

(86) A. Agarwal, K. Srivastava, S. K. Purib and P. M. S. Chauhan, *Bioorg. Med. Chem. Lett.* **2005**, *15*, 531.

(87) D. Dive and C. Biot, *ChemMedChem* **2008** *3*,383.

(88) P. F. Salas, C. Herrmann, J. F. Cawthray, C. Nimphius, A. Kenkel, J. Chen, C. de Kock, P. J. Smith, B. O. Patrick, M. J. Adam and C. Orvig *J. Med. Chem.* **2013**, *56* (4), 1596.

(89) D. E. Goldberg, A. F. Slater, A. Cerami and G. B. Henderson, *Proc. Natl. Acad. Sci. U. S. A.* **1990**, *87*, 2931.

(90) J. Van der Zee, D. P. Barr and R. P. Mason, *Free Radic. Biol. Med.* **1996**, *20*, 199−206.

(91) J. M. Gutteridge and A. Smith, *Biochem. J.* **1988**, *256*, 861−865.

(92) R. L. Aft and G. C. Mueller, *J. Biol. Chem.* **1984**, *259*, 301−305.

(93) R. L. Aft and G. C. Mueller, *J. Biol. Chem.* **1983**, *258*, 12069−12072.

(94) A. C. Chou and C. D. Fitch, *J. Clin. Invest.* **1981**, *68*, 672−677.

(95) T.J. Egan and, H.M. Marques, *Coord. Chem. Rev.* **1999**, *190-192*, 493.

(96) R. D. Sandlin, M. D. Carter, P. J. Lee, J. M. Auschwitz, S. E. Leed, J. D. Johnson and D. W. Wright, *Antimicrob. Agents Chemother.* *55* (7), 3363.

(97) K. K. Ncokazi and T. J. Egan, *Anal. Biochem.* **2005**, *338* (2), 306.

(98) J. Ruiz, V. Rodrıguez, N. Cutillas, G. Lopez and Delia Bautista, *Inorg. Chem.* **2008**, *47*, 10025.

(99) F. Linares, M. A. Galindo, S. Galli, M. A. Romero, J. A. R. Navarro and E. Barea, *Inorg. Chem.* **2009**, *48*, 7413.

(100) M. Auzias, B. Therrien, G. Süss-Fink, P. Štěpnička, W. H. Ang and P. J. Dyson, *Inorg. Chem.* **2008**, *47*, 578.

(101) P. Govender, N.C. Antonels, J. Mattsson, A.K. Renfrew, P.J. Dyson, J.R. Moss, B. Therrien and G.S. Smith, *J. Organomet. Chem.* **2009**, *694*, 3470.

(102) L. E. H. Paul, J. Furrer and B. Therrien, *J. Organomet. Chem.* **2012**, http://dx.doi.org/10.1016/j.jorgchem.2012.12.011.

(103) N. P. E. Barry, F. Edafe and B. Therrien, *Dalton Trans.* **2011**, *40*, 7172.

(104) W. Trager and J. B. Jensen, *Science* **1976**, *193* (4254), 673.

(105) M. T. Makler, J. M. Ries, J. A. Williams, J. E. Bancroft, R. C. Piper, B. L. Gibbins and D. J. Hinrichs, *Am. J. Trop. Med. Hyg.* **1993**, *48*, 739.

CHAPTER 7

Synthesis and Study of Cyclopalladated Thiosemicarbazone Complexes as Catalyst Precursors for the Suzuki-Miyaura Cross Coupling Reaction

7.1. Introduction

Cross-coupling reactions are a set of transition metal catalyzed reactions that are an essential synthetic tool and palladium containing complexes are the most extensively employed catalyst systems for these reactions. Some of the most well-known and widely used cross-coupling reactions are the Heck, Stille, Suzuki-Miyaura and Buchwald-Hartwig cross-couplings.[1,2] These types of reactions have proven useful for the syntheses of polymers,[3,4] natural products,[5] agrochemicals[6,7] and pharmaceuticals.[8,9] Thus, the search for a metal complex which can catalyze these types of reactions efficiently while maintaining high chemo- and regio-selectivity and recyclability is an ongoing process. In cross-coupling reactions, palladium(II) complexes are generally used as catalyst precursors from which the active Pd(0) species is generated *in situ*. One disadvantage of the current catalyst systems used is that the metal complex sometimes undergoes decomposition during the reaction leading to poor recyclability of the metal complex as well as impurities in the products making the process a costly one.[10]

Thiosemicarbazones are widely known for their metal chelating abilities to a large variety of metals.[11] These compounds can be classified as hybrid ligands as they are capable of acting as bi- or multidentate ligands through several donor atoms.[12] Studies into the biological applications of thiosemicarbazone metal complexes are prolific. Research into their role in catalysis however, is still a relatively new area of interest. One of the earliest reports of their catalytic abilities was published in 1998 by Pelagatti and co-workers; they found that tridentate [N,N,S] thiosemicarbazone palladium(II) complexes were able to catalyze chemoselective homogenous hydrogenation reactions.[13] More recently, a cyclometallated ruthenium(II) thiosemicarbazone complex was used for the catalytic transfer hydrogenation of substituted ketones with high efficiency.[14] Moderate activities were also observed for the Suzuki-Miyaura coupling of aryl halides and phenylboronic acids using tridentate [C,N,O] Ni(II) thiosemicarbazones.[15]

Tridentate pincer-type Pd(II) complexes are known to efficiently catalyze carbon-carbon coupling reactions.[16-19] Tridentate thiosemicarbazone Pd(II) complexes may exhibit similar behavior. The thiosemicarbazone ligand occupies three of the four coordination sites available on the metal and this may restrict how the olefinic or organo-halide substrates coordinate to the metal thus influencing the selectivity of the catalyst. These complexes are also known to exhibit high thermal stability, both in the solid state and in solution, making them good candidates for high temperature homogenous catalysis. Within our group, we have investigated the synthesis and application of tridentate [O,N,S] Pd(II) thiosemicarbazone complexes as anticancer and antimalarial agents.[20-22] To demonstrate the versatility of these complexes (Figure 7.1), we have also studied their catalytic activity as catalyst precursors for the Mizoroki-Heck coupling reaction and have recently published some of our findings.[23] For these reasons, four Pd(II) analogues of the cycloplatinated complexes discussed in Chapter 2 were prepared in order to undertake a preliminary investigation as catalyst precursors for the Suzuki-Miyaura cross couplings of a variety of aryl halides and aryl boronic acids.

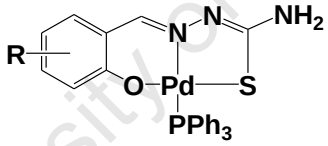

1.99: R = H, 3-OMe, 3-^{t}Bu or 5-Cl

Figure 7.1. Tridentate [O,N,S] Pd(II) thiosemicarbazone complexes that were investigated for activity as catalyst precursors for the Mizoroki-Heck coupling reaction.[23]

7.2. Results and discussion

7.2.1. Synthesis and Characterisation of Cyclopalladated complexes

The thiosemicarbazone ligands, 3,4-dichloroacetophenone thiosemicarbazone (**2.1**) was treated with a suspension of potassium tetrachloropalladate in deoxygenated ethanol and water gave the yield the tetranuclear complex **7.1** which was further reacted with the

appropriate phosphane to give the corresponding mono- (**7.2**) and dinuclear (**7.3** and **7.4**) complexes (Scheme 7.1).

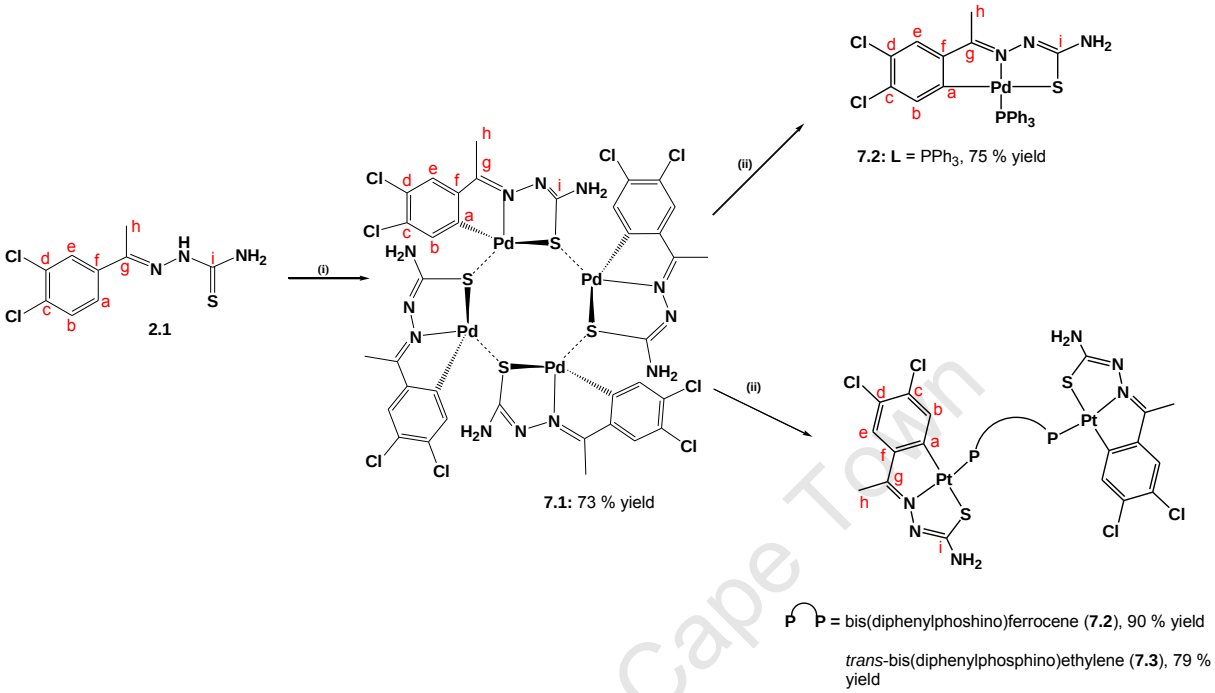

Scheme 7.1.

Each complex was isolated as an air- and moisture-stable amorphous yellow solid with high thermal stability. The ^{1}H NMR spectra for complex **7.1** showed only two singlets in the aromatic region and both integrated for one proton each, supporting palladation of the *ortho*-carbon upon loss of the proton. The absence of a signal corresponding to the hydrazinic proton corroborates coordination of sulfur to palladium in the thiolato form and formation of a new imine bond upon deprotonation of the hydrazinic nitrogen.[24,25] The amino (-NH_2) protons of the coordinated ligand **2.1** in each of the phosphane containing complexes **7.2**-**7.4** resonate as a singlet in each spectrum between 6.79 and 6.99 ppm. These resonances are slightly upfield compared to the tetranuclear precursor **7.1**, where these protons are observed as singlets at 7.17 and 7.11 ppm respectively. This slight shielding may be due to increased electron density around the metal and hence greater electron distribution over the ligand due to back-bonding between the metal and coordinated phosphorus.

The cyclopentadienyl (Cp) protons of the bis(diphenylphosphino)ferrocene (dppf) bridging ligand for compounds **7.3** as two broad singlets between 4.50 and 5.10 ppm, the downfield peak is assigned to the protons α to the carbon-phosphorus bond. For compound **7.4**, the alkene protons of the *trans*-bis(diphenylphosphino)ethylene (dppe) ligand are assigned to a multiplet occurring between 7.28 and 7.33 ppm. In the $^{13}C\{^{1}H\}$ NMR spectra for the tetranuclear complex **7.1**, coordination of the imine nitrogen to palladium is further supported by the assignment of the imine carbon (C_g) to a peak at 166.1 ppm, a downfield shift relative to the free ligand (**2.1**) where it resonates at 145.2 ppm. This is in accordance with resonances observed for similar complexes.[25,26] An upfield shift of approximately 10 ppm of the thiolato carbon (C_i) in the complex **7.1** is noted in comparison to the thione carbon of the free ligand (**2.1**) confirms coordination of sulfur in the thiolato form.[26] The *ortho*-carbon shows a large shift from approximately 128.0 ppm in the free ligand to 165.0 ppm. This extreme deshielding of the carbon nucleus is characteristic of palladation of the *ortho*-carbon and substantiates formation of the cyclopalladated complex **7.1**.[26,27] Compared to **7.1**, similar resonances are observed for the imine carbon in complexes **7.2** – **7.4**. A downfield shift is observed for the thiolato carbon (C_i) resonance from between 167.7 ppm for **7.1** to between 175.0 – 179.0 ppm for **7.2** – **7.4** is also noted.

All of the complexes (**7.2-7.4**) display one singlet in the $^{31}P\{^{1}H\}$ NMR spectra. The phosphorus nucleus of the mononuclear complex **7.2** resonates at 38 .75 ppm; the phosphorus nuclei of the dppf ligand of **7.3** occurs at a lower chemical shift of 29.19 ppm as a consequence of the electron-rich ferrocenyl moiety and the phosphorus singlet of the trans-dppe ligand in complex **7.4** occurs at 34.18 ppm. All of these resonances are consistent with those of similar complexes and further support coordination of phosphorus *trans* to the imine nitrogen.[25,28-32]

Only two absorption bands are observed in the N-H region of the infrared spectrum for all complexes (**7.1** – **7.4**), indicating that there are only two amine bonds in the complexes compared to that of the free ligands. The formation of the second imine bond is supported by the observation of two absorption bands between 1525 and 1620 cm^{-1}. The lower frequency band is assigned to the palladium coordinated imine. A shift to lower frequency compared to the free ligand is attributed to the loss of double bond character upon coordination of the nitrogen to the metal. The higher absorption band is hence assigned to the stretching vibration of the newly formed C=N and points to the existence of the metal coordinated to sulphur in

the thiolate form. ESI-mass spectrometry was used to further characterise the complexes (**7.1** – **7.4**) prepared. All of the compounds exhibit molecular ion peaks corresponding to each compound in its protonated form.

7.2.2. Preliminary Catalytic Activity in the Suzuki-Miyaura Cross Coupling Reaction

The four cyclopalladated thiosemicarbazone complexes (**7.1**-**7.4**) were evaluated for their ability to catalyze a series of Suzuki-Miyaura cross coupling reactions. The first step was to screen different catalytic conditions to optimize activity. Table 7.1 shows the data ascertained for these reactions. The palladium catalyst precursors (**7.1**-**7.4**) were first screened for the Suzuki-Miyaura cross coupling of 4-(methoxy)-iodobenzene and phenylboronic acid in dioxane using K_3PO_4 as the base (Entries 1-5, Table 7.1). The mononuclear complex **7.2** (1 mol %) gave a 95 % yield of the coupled product when the reaction was carried out at 100 °C. However, a decrease in the reaction temperature to 60 °C yielded only 20 % of the coupled product (Entry 2). At 60 °C, the tetranuclear complex **7.1** and dinuclear complex **7.3** also showed low activity while the bis(diphenylphosphino)ferrocene bridged complex **7.4** (0.5 mol %) showed a much more promising activity of 60 %. Thus, this complex was chosen for further screening of catalytic conditions.

With the aryl halide substrate changed to 4-(methoxy)-bromobenzene and using 0.5 mol % of **7.4** at 100 °C, it was found that the best yields were obtained when the cross coupling reactions were carried out in DMF or dioxane (Entries 6-10). Further catalytic reactions in DMF using different bases at 100 °C (Entries 11-15) showed a significant decrease in activity particularly when cesium carbonate or triethylamine are used as the base for the cross coupling reactions. Varying the temperature (Entries 16-18) and carrying out the reactions under argon (Entries 17 and 18) showed that better yields were obtained as the temperature was increased with a 94 % yield obtained at 130 °C. Screening these different conditions showed that complex **7.4** exhibited the best activity when a 0.5 mol % complex loading was used in DMF with K_3PO_4 as base at 130 °C under argon. Under the same conditions, $Pd(OAc)_2$ using PPh_3 as co-ligand afforded only 78 % of the coupled product (entry 19).

Using these optimal conditions, the complex **7.4** was then applied to the Suzuki-Miyaura cross-coupling of bromobenzene with different arylboronic acid substrates. Figure 7.2 shows a graphical representation of the product yields obtained for each substrate.

Table 7.1. Screening various catalytic conditions. [a]

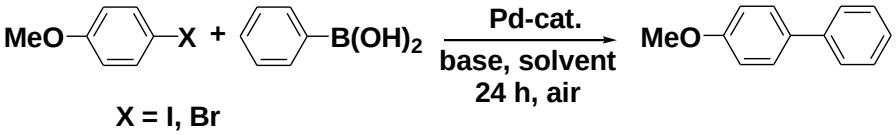

Entry	X	Pd-cat. (mol%)	Base	Solvent	T (^{o}C)	Yield (%)[b]
1	I	**7.2** (1)	K_3PO_4	Dioxane	100	95
2	I	**7.2** (1)	K_3PO_4	Dioxane	60	20
3	I	**7.1** (0.5)	K_3PO_4	Dioxane	60	19
4	I	**7.3** (0.25)	K_3PO_4	Dioxane	60	10
5	I	**7.4** (0.5)	K_3PO_4	Dioxane	60	60
6	Br	**7.4** (0.5)	K_3PO_4	Dioxane	100	44
7	Br	**7.4** (0.5)	K_3PO_4	DMF	100	43
8	Br	**7.4** (0.5)	K_3PO_4	DMSO	100	10
9	Br	**7.4** (0.5)	K_3PO_4	Toluene	100	34
10	Br	**7.4** (0.5)	K_3PO_4	NMP	100	30
11	Br	**7.4** (0.5)	K_2CO_3	DMF	100	25
12	Br	**7.4** (0.5)	Cs_2CO_3	DMF	100	5
13	Br	**7.4** (0.5)	^{t}BuOK	DMF	100	20
14	Br	**7.4** (0.5)	Et_3N	DMF	100	5
15	Br	**7.4** (0.5)	Na_2CO_3	DMF	100	22
16	Br	**7.4** (0.5)	K_3PO_4	DMF	120	58
17[c]	Br	**7.4** (0.5)	K_3PO_4	DMF	120	67
18[c]	Br	**7.4** (0.5)	K_3PO_4	DMF	130	94
19[c,d]	Br	Pd cat. (0.5)	K_3PO_4	DMF	130	78

[a] Reaction conditions: Aryl halide (0.3 mmol), phenylboronic acid (0.4 mmol), Pd-complex (0.25-1 mol%), base (2 equiv), solvent (2 mL), 60-130 ^{o}C, 24 h, air. [b] Isolated yield (based on aryl halide). [c] The reaction was performed under argon atmosphere. [d] $Pd(OAc)_2/PPh_3$ (1:2).

A product yield of 95 % was observed when the substrate 4-methoxy-phenylboronic acid was used (Entry 2, Figure 7.2) and 88 % yield was obtained when the 3-methoxy derivative was used (Entry 3). Allowing the reaction to proceed for 48 hours resulted in the product yield increasing to 90 % (Entry 4). Only a 31 % yield was obtained for the reaction using 2-methoxy-phenylboronic acid as substrate (Entry 5), this low yield could be due to steric hindrance from the methoxy substituent. The catalytic reactions using the phenylboronic acid (entry 1) and 4-methyl-phenylboronic acid (entry 6) substrates both resulted in a 93 % yield of coupled product. The complex **7.4** was also able to efficiently catalyze the coupling of the chlorido substituted phenylboronic acid with bromobenzene (Entry 7) but a slight decrease in activity was observed when the halide substituent is changed to fluorine (Entry 8). High activity was also observed for the naphthalenylboronic acid substrate (Entries 10 and 11).

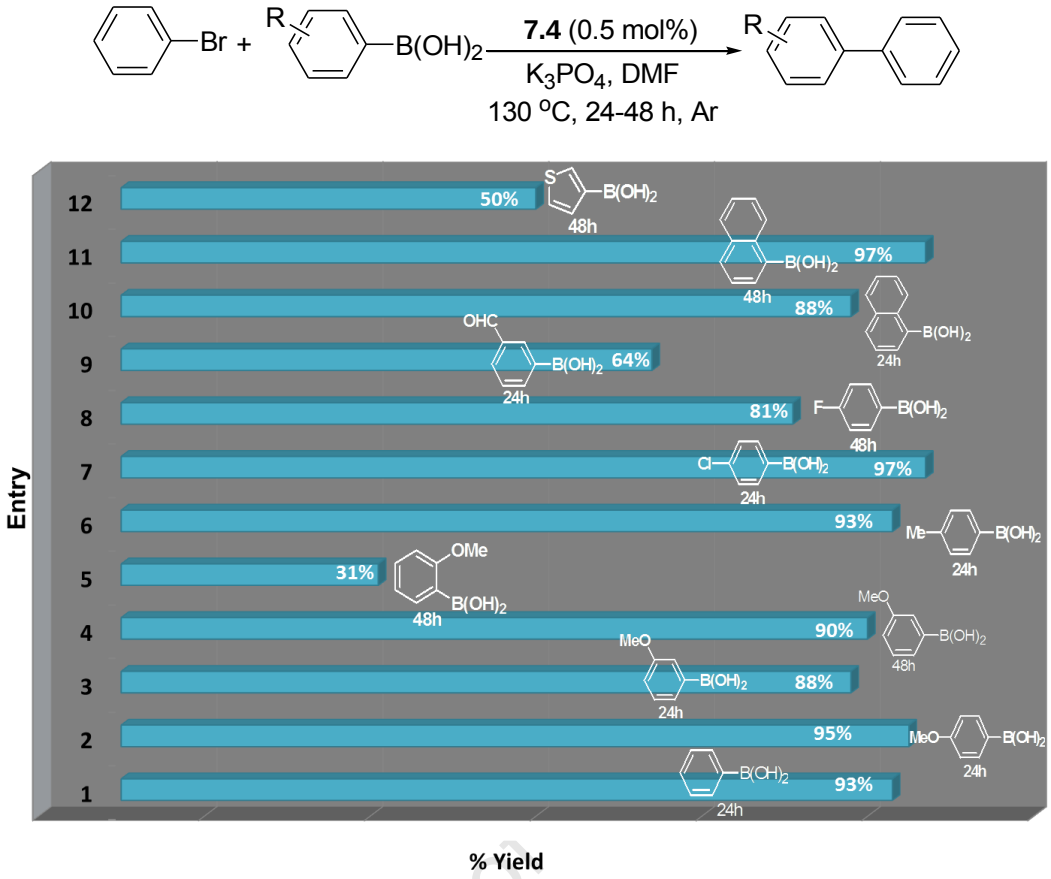

Figure 7.2. Suzuki-Miyaura coupling of bromobenzene and aryl boronic acids using **7.4.** The catalytic conditions: Bromobenzene (0.3 mmol), arylboronic acid (0.4 mmol), 7.4 (0.5 mol%), K_3PO_4 (2 equiv), DMF (2 mL), 130 °C, 24-48 h, Ar. [b] Isolated yield based on bromobenzene (average of two runs).

The Suzuki-Miyaura coupling reactions between phenylboronic acid and different aryl halides using **7.4** as pre-catalyst also displayed promising results (Figure 7.3). Yields of 99 % were obtained when the substrates 3-bromoacetophenone, 3-bromopyridine or 3-methoxy-bromobenzene were used (Entries 2, 4 and 10, Figure 7.3). The coupling reactions using aryl bromide substrates containing a chlorido or fluorido substituent also demonstrated high product yields (Entries 1 and 8). In contrast to the arylboronic acid derivative (Entry 5, Figure 7.2), a moderately good yield of 70 % was observed for the substrate 2-methoxy-bromobenzene (Entry 11, Figure 7.3).

When the reaction was allowed to proceed for 48 hours, a yield of 77 % was obtained for the less reactive 4-nitro-chlorobenzene (Entry 13). Much lower activity is observed for the coupling reactions of other chlorobenzenes (Entries 14 and 15). With the exception of entries

14 and 15, complex **7.4** efficiently catalyzed the coupling of phenylboronic acid and different aryl halides irrespective of the type of substituent (electron withdrawing or electron donating) with yields between 70 – 99 % being attained. This moderate to excellent activity was also upheld when the substituents were varied on the phenylboronic acid (Figure 7.3). This preliminary study has demonstrated the versatility of this complex as it is able to produce a wide variety of coupled products and its effectiveness does not seem to be dependent on the type of aryl substrate used.

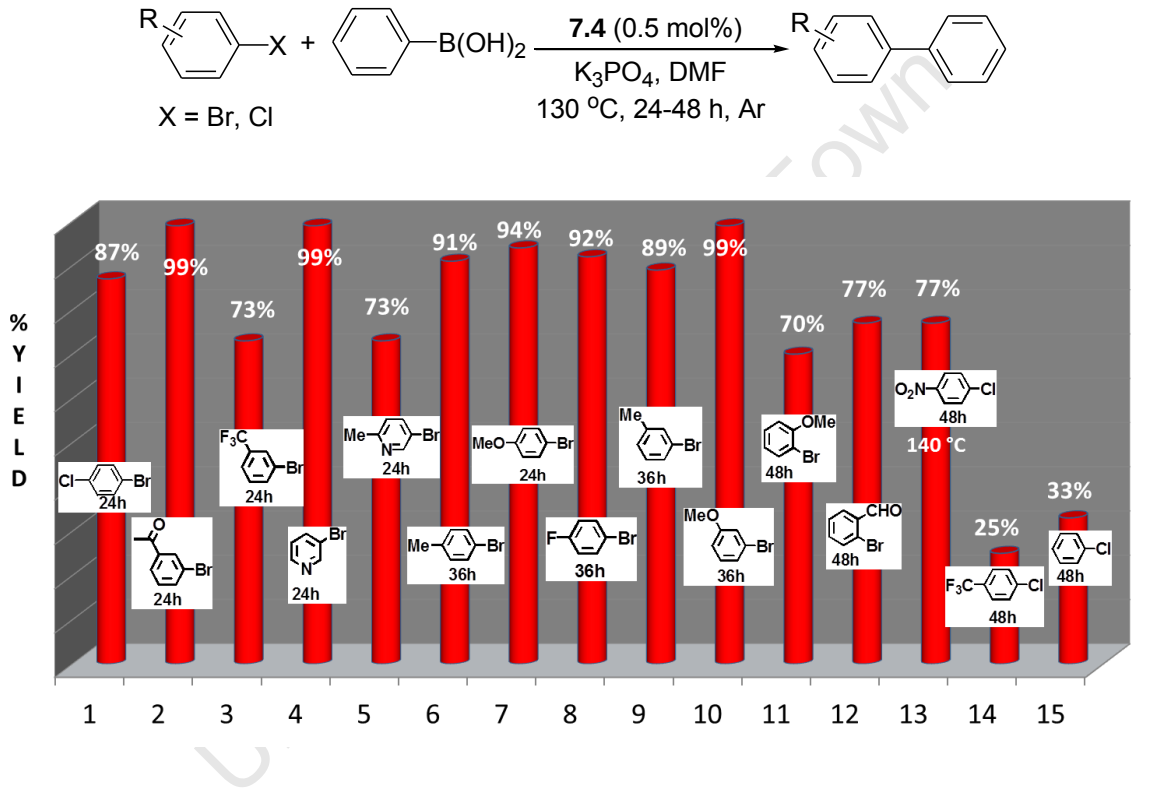

Figure 7.3. Suzuki-Miyaura coupling reactions between phenylboronic acid and various aryl halides. The catalytic conditions: aryl halide (0.3 mmol), phenylboronic acid (0.4 mmol), **7.4** (0.5 mol%), K_3PO_4 (2 equiv), DMF (2 mL), 130 ^oC, 24-48 h, Ar. Isolated yield based on aryl halide (average of two runs).

7.3. Summary

Four cyclopalladated complexes (**7.1**-**7.4**) of ligand **2.1** were prepared by reaction with potassium tetrachloropalladate and subsequent cleavage of the Pd-S bridging bonds with different mono- and diphosphines. Spectral characterization of complexes **7.1**-**7.4** confirm

that the ligand **2.1** acts as a tridentate dinegative [C,N,S] donor to palladium in the same manner as found in complexes **2.2**-**2.7** (Chapter 2).

A preliminary screening of complexes **7.1**-**7.4** for activity as catalyst precursors for the Suzuki-Miyaura cross coupling reaction revealed complex **7.4** to be a robust catalyst. It was able to efficiently catalyze the coupling of various aryl halides and aryl boronic acids, irrespective of the type of electron-withdrawing or electron-donating substituent on the aromatic ring. A more in-depth investigation of complex **7.4** for catalytic activity should be undertaken.

7.4. Experimental

7.4.1. Chemicals and General Methods

All complexation reactions were performed under a nitrogen or argon atmosphere using a dual vacuum/nitrogen line and standard Schlenk-line techniques unless otherwise stated. All reaction solvents were dried by refluxing under an inert atmosphere over the appropriate drying agent and all samples were dried under vacuum. Reagents and solvents were purchased from commercial suppliers and used without further purification. $PdCl_2$ was kindly donated by Johnson-Mathey Inc. The thiosemicarbazone ligand **2.1** [33] and $K_2[PdCl_4]$ [34] were synthesized according to previously published methods.

7.4.2. Spectroscopic and Analytical Methods

Nuclear Magnetic Resonance (NMR) Spectra were recorded on a Varian Unity XR400 MHz (^{1}H at 399.95 MHz, ^{13}C at 100.58 MHz), Varian Mercury XR300 (^{1}H at 300.08 MHz, ^{13}C at 75.46 MHz) or Bruker Biospin GmbH (^{1}H at 400.22 MHz, ^{13}C at 100.65 MHz) spectrometer at ambient temperature. Chemical shifts for ^{1}H and ^{13}C{1H} NMR shifts are reported using tetramethylsilane (TMS) as the internal standard and ^{31}P{1H} NMR spectra were measured relative to H_3PO_4 as the external standard. NMR spectra were recorded in deuterated chloroform ($CDCl_3$-D_1) unless otherwise stated. Infrared (IR) absorptions were measured on Perkin-Elmer Spectrum 100 FT-IR Spectrometer using a Universal Diamond Attenuated Total Reflection (ATR) accessory. Microanalyses for C, H, and N were carried out using a Thermo Flash 1112 Series CHNS-O Analyser and melting points were determined using a Büchi Melting Point Apparatus B-540. Mass Spectrometry determinations were carried out on all new compounds using electrospray ionisation (ESI) on a Waters API Quattro Micro instrument in either the positive or negative mode.

*7.4.3. Synthesis of [Pd(3,4-Dichloroacetophenone thiosemicarbazone)]$_4$ (**7.1**)*

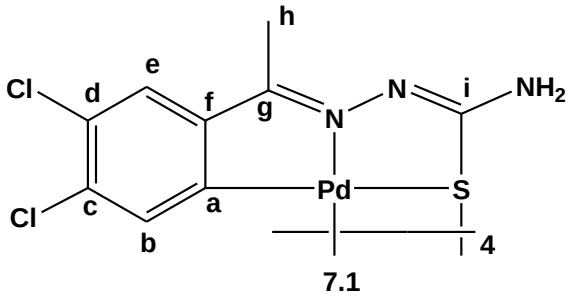

7.1

Potassium tetrachloropalladate (0.402 g, 1.230 mmol) was dissolved in deionised water (5 cm^3). Ethanol (40 cm^3) was added and 3,4-dichloro-acetophenone thiosemicarbazone (**2.1**) (0.355 g, 1.356 mmol) was added to the resulting yellow suspension. The reaction mixture was stirred at room temperature for 48 hours. The product (**7.1**) was collected as a yellow solid via filtration, washed with ethanol (3 x 10 cm^3) and dried under vacuum. Yield: 0.326 g, 73 %. M.p.: decomposition without melting 307-309 ºC. ^{1}H NMR (399.95 MHz, DMSO): δ (ppm) = 7.36 (s, 1H, H_b), 7.17 (s, 2H, NH_2), 6.71 (s, 1H, H_e), 1.99 (s, 3H, H_h). ^{13}C NMR (75.46 MHz, DMSO): δ (ppm) = 167.7 (C_i), 166.1 (C_g), 165.1 (C_a), 150.7 (C_f), 133.9 (C_c), 129.9 (C_d), 126.8 (C_e), 126.6 (Cb), 14.3 (C_h). IR (KBr, cm^{-1}) υ = 3442 (m, N-H), 3369 (m, N-H), 1597 (s, C=N), 1560 (m, C=N), 1524 (s, C=C aromatics). Elemental Analysis for $C_{36}H_{28}Cl_8N_{12}Pd_4S_4$: found C 29.14, H 2.43, N 10.87, S 8.56 %; calculated C 29.44, H 1.93, N 11.46, S 8.76 %. ESI-MS: *m/z* 1468 ($[M + 2H]^+$, 20%), 368 ($[M/4 + H]^+$, 100%).

*7.4.4. Synthesis of [Pd(3,4-Dichloroacetophenone thiosemicarbazone)(PPh_3)] (**7.2**)*

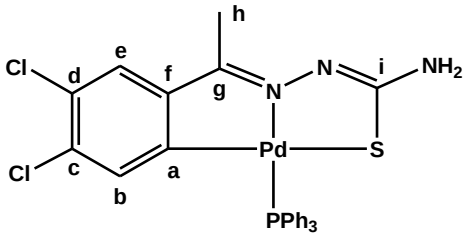

7.2

Compound **7.1** (0.100g, 0.069 mmol) was suspended in dry acetone (15 cm^3). Triphenylphosphine (0.073 g, 0.275 mmol) was added and the reaction was stirred under argon gas for 4 hours. The product (**7.2**) was collected as a bright yellow solid by filtration, washed with acetone (2 x 5 cm^3) and dried under vacuum. Yield: 0.129 g, 75 %. M.p.: decomposition without melting 290-291 ºC. ^{1}H NMR (300.08 MHz, DMSO): δ (ppm) = 7.42-7.64 (m, 15H, PPh_3), 7.20 (s, 1H, H_b), 6.79 (s, 2H, NH_2), 6.10 (s,1H, H_e), 2.76 (s, 3H, H_h). ^{13}C NMR (75.46 MHz, DMSO): δ (ppm) = 176.6 (C_i), 163.6 (C_g), 152.7 (C_a), 136.1 (C_g), 133.8 (C_d), 133.7 (C_c), 128.5-131.1 (PPh_3), 126.2 (C_e), 126.1 (C_h), 13.0 (C_h). ^{31}P NMR (121.47 MHz, DMSO): δ (ppm) = 38.75 (PPh_3). IR (KBr, cm^{-1}) υ = 3474 (m, N-H), 3332 (s, N-H), 1601 (s, C=N), 1579 (m, C=N), 1496 (s, C=C aromatics). Elemental Analysis for $C_{27}H_{22}Cl_2N_3PPdS$: found C 51.36, H 3.49, N 6.29, S 4.84 %; calculated C 51.57, H 3.53, N 6.68, S 5.10 %. ESI-MS: *m/z* 630 ($[M + H]^+$, 100%).

Compounds **7.3** and **7.4** were synthesised using the same procedure as for compound **7.2**.

7.4.5. Synthesis of [Pd_2(3,4-Dichloroacetophenone thiosemicarbazone)$_2$(trans-dppe)] ***(7.3)***

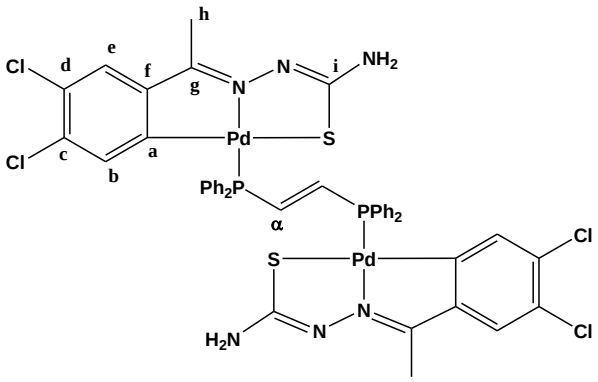

7.3

Bis(diphenylphosphinoethylene) (0.0592g, 0.149 mmol) was reacted with compound **7.1** (0.105 g, 0.0719 mmol). The product (**7.3**) was isolated as a yellow solid. Yield: 0.134 g, 79 %. M.p.: 211-213 ºC (decomp.). ^{1}H NMR (399.95 MHz, DMSO): δ (ppm) = 7.52-7.57 (m, 20H, PPh_2), 7.28-7.33 (m, 2H, H_α), 7.21 (s, 2H, H_b), 6.95 (s, 4H, NH_2), 6.23 (s, 2H, H_e), 2.28 (s, 6H, H_h). ^{13}C NMR (100.57 MHz, DMSO): δ (ppm) = 176.6 (C_i), 164.0 (C_g), 163.3 (C_a), 152.6 (C_f), 135.7 (C_d), 133.1-133.2 (PPh_2), 131.4 (C_α), 131.1 (C_c), 128.9-129.0 (PPh_2), 126.6 (C_e), 125.3 (C_b), 13.1 (C_h). ^{31}P NMR (161.90 MHz, DMSO): δ (ppm) = 34.18 (PPh_2). IR (KBr, cm^{-1}) υ = 3455 (m, N-H), 3317 (s, N-H), 1623 (m, C=N), 1605 (s, C=N), 1483 (s, C=C aromatics). Elemental Analysis for $C_{44}H_{36}Cl_4N_6P_2Pd_2S_2$: found C 46.84, H 3.25, N 7.29, S 5.74 %; calculated C 46.79, H 3.21, N 7.44, S 5.68 %. ESI-MS: *m/z* 1130.88 ($[M + H]^+$, 50 %), 565.95 ($[M/2 + 2H]^{2+}$, 100 %).

*7.4.6. Synthesis of [Pd_2(3,4-Dichloroacetophenone thiosemicarbazone)$_2$(dppf)] (**7.4**)*

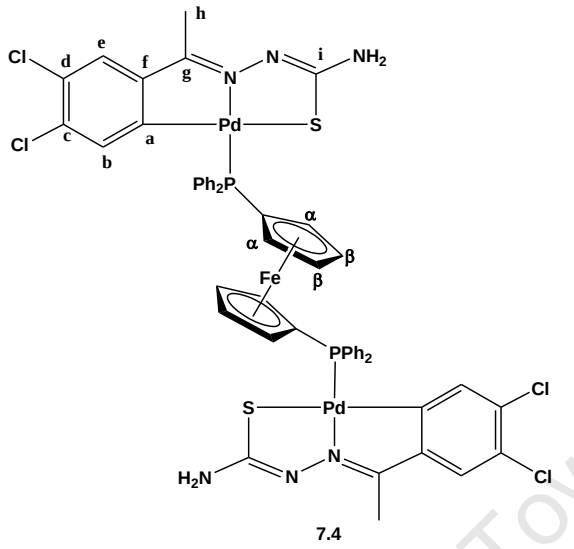

7.4

Bis(diphenylphosphinoferrocene) (0.0786 g, 0.142 mmol) was reacted with compound **7.1** (0.105 g, 0.0717 mmol). The product (**7.4**) was isolated as a yellow solid. Yield: 0.127 g, 90 %. M.p.: decomposition without melting 204-206 ºC. ^{1}H NMR (399.95 MHz, DMSO): δ (ppm) = 7.40-7.58 (m, 20H, PPh_2), 7.25 (s, 2H, H_b), 6.96 (s, 4H, NH_2), 6.08 (s, 2H, H_e), 5.07 (br s, 4H, Cp-H_α), 4.27 (br s, 4H, Cp-H_β), 2.31 (s, 6H, H_h). ^{13}C NMR (100.57 MHz, DMSO): δ (ppm) = 178.6 (C_i), 163.8 (C_g), 152.7 (C_a), 136.14 (C_f), 133.0-133.2 (PPh_2), 131.1 (C_d), 129.4 (C_c), 128.4-128.5 (PPh_2), 126.4 (C_e), 126.3 (C_b), 75.4-74.2 (C_α and C_β), 13.3 (C_h). ^{31}P NMR (161.90 MHz, DMSO): δ (ppm) = 29.19 (PPh_3). IR (KBr, cm^{-1}) υ = 3479 (m, N-H), 3383 (m, N-H), 1595 (s, C=N), 1574 (s, C=N), 1491 (s, C=C aromatics). Elemental Analysis for $C_{52}H_{42}Cl_4FeN_6P_2Pd_2S_2$: found C 48.96, H 3.52, N 6.22, S 4.10 %; calculated C 48.53, H 3.28, N 6.53, S 4.98 %. ESI-MS: *m/z* 1288.87 ($[M + H]^+$, 50 %), 644.94 ($[M/2 + 2H]^{2+}$, 100 %).

7.4.7. General Procedure for Suzuki-Miyaura Reactions

A Schlenk tube was charged with aryl boronic acid (0.4 mmol), K_3PO_4 (0.6 mmol) and the complex IV (0.5 mol%). The tube was connected to a vacuum line under argon and purged three times. N,N-dimethylformamide (2 mL) and aryl halide (0.3 mmol) were added. The reaction mixture was stirred at 130 °C between 24–48 h. At the end of the reaction, the reaction mixture was cooled to room temperature, diluted with diethyl ether and washed with water. The combined organic phase was dried over anhydrous Na_2SO_4. After removal of the solvent, the residue was subjected to column chromatography on silica gel using ethyl acetate and petroleum ether mixtures to afford the Suzuki-Miyaura product in high purity.

7.5. References

1. F. Diederic and P. J. Stang; *Metal-Catalyzed Cross-Coupling Reaction*; Wiley-VCH: Weinheim, 1998.
2. J. Tsuji; *Palladium Reagents and Catalysts*; John Wiley and Sons: Chichester, 1995.
3. Y. Li and M. Yang, *J. Mol. Cat. A: Chem.*, **2002**, *184*, 161.
4. C .-J. Li, W. T. Slaven, V. T. John and S. Banerjeeb, *J. Chem. Soc, Chem. Commun.*, **1997**, 1569.
5. R. W. Bates, C. J. Gabel, J. Ji and T. Rama-Devi, *Tetrahedron*, **1995**, *51*, 8199.
6. S. L. Hargreaves, B. L. Pilkington, S. E. Russell and P. A. Worthington, *Tetrahedron Lett.*, **2000**, *41* (10), 1653.
7. A. Zapf and M. Beller, *Top. Catal.*, **2002**, *19* (1), 101.
8. C. Mauger and G. Mignani, *Adv. Synth. Catal.*, **2005**, *347* (6), 773
9. H. Doucet and J. C. Hierso, *Curr. Opin. Drug Discov. Devel.*, **2007**, *10* (6), 672.
10. L. Yin and J. Liebscher, *Chem. Rev.*, **2007**, *107*, 133.
11. T. S. Lobana, R. Sharma, G. Bawa and S. Khanna, *Coord. Chem. Rev.*, **2009**, *253*, 977.
12. W. -H. Zhang, S. W. Chien and T. S. A. Hor, *Coord. Chem. Rev.*, **2011**, *255*, 1991.
13. P. Pelagatti, A. Venturini, A. Leporat, M. Carcelli, M. Costa, A. Bacchi, G. Pelizzi and C. Pelizzi, *J. Chem. Soc., Dalton Trans.*, **1998**, 2715.
14. D. Pandiarajan and R. Ramesh, *Inorg. Chem. Commun.*, **2011**, *14*, 686.
15. S. Datta, D. K. Seth, R. J. Butcher and S. Bhattacharya, *Inorg. Chim. Acta*, **2011**, *377*, 120.
16. S. Bonnet, M. Lutz, A. L. Spek, G. van Koten and R. J. M. K. Gebbink, *Organometallics*, **2010**, *29*, 1157.
17. N. J. M. Pijnenburg, M. Lutz, M. A. Siegler, A. Spek, G. van Koten and R. J. M. K. Gebbink, *New J. Chem.*, **2011**, *35* (10), 2356.
18. R. Gerber, O. Blacque and C. M. Frech, *Dalton Trans.*, **2011**, *40* (35), 8996.
19. V. A. Kozlov, D. V. Aleksanyan, Y. V. Nelyubina, K. A. Lyssenko, P. V. Petrovskii, A. A. Vasilév and I. L. Odinets, *Organometallics*, **2011**, *30* (11), 2920.
20. T. Stringer, P. Chellan, B. Therrien, N. Shunmoogam-Gounden, D. T. Hendricks and G. S. Smith, *Polyhedron*, **2009**, *28*, 2839.
21. P. Chellan, N. Shunmoogam-Gounden, D. T. Hendricks, J. Gut, P. J. Rosenthal, C. Lategan, P. J. Smith, K. Chibale and G. S. Smith, *Eur. J. Inorg. Chem.*, **2010**, 3520.

22. P. Chellan, S. Nasser, L. Vivas, K. Chibale and G. S. Smith, *J. Organomet. Chem.*, **2010**, *695*, 2225.

23. G. Xie, P. Chellan, J. Mao, K. Chibale and G. S. Smith, *Adv. Synth. Catal.*, **2010**, *352* (10), 1641.

24. A. G. Quiroga, J. M. Perez, I. Lopez-Solera, E. I. Montero, J. R. Masaguer, C. Alonso and C. Navarro-Ranninger, *J. Inorg. Biochem.*, **1998**, *69*, 275.

25. A. Amoedo, M. Graña, J. Martínez, T. Pereira, M. López-Torres, A. Fernández, J.J. Fernández and J.M. Vila, *Eur. J. Inorg. Chem.*, **2002**, 613.

26. A. G. Quiroga, J. M. Perez, I. Lopez-Solera, J. R. Masaguer, A. Luque, P. Roman, A. Edwards, C. Alonso and C. Navarro-Ranninger, *J. Med. Chem.*, **1998**, *41*, 1399.

27. S. Castro-Juiz, M. Lopez-Torres, A. Fernandez, R. Mosteiro, A. Suarez, J. M. Vila and J. J. Fernandez, *Polyhedron*, **2001**, *20*, 2925.

28. J. Albert, M. Gomez, J. Granell and J. Sales, *Organometallics*, **1990**, *9*, 1405.

29. J. Albert, J. Granell, J. Sales, M. Fon-Bardia and X. Solans, *Organometallics*, **1995**, *14*, 1393.

30. T. S. Lobana, G. Bawa, G. Hundal, R. J. Butcher and A. Castineiras, *Z. Anorg. Allg. Chem.*, **2009**, *635*, 1447.

31. A. Amoedo, L. A. Adrio, J. M. Antelo, J. Martínez, M. T. Pereira, A. Fernández and J. M. Vila, *Eur. J. Inorg. Chem.*, **2006**, 3016.

32. J. M. Vila, M. T. Pereira, J. M. Ortigueria, M. Graña, D. Lata, A. Suãrez, J. Fernández, A. Fernández, M. Lopez-Torres and H. Adams, *J. Chem. Soc., Dalton Trans.*, **1999**, 4193.

33. X. Du, C. Guo, E. Hansel, P. S. Doyle, C. R. Caffrey, T. P. Holler, J. H. McKerrow and F. E. Cohen, *J. Med. Chem.*, **2002**, *45*, 2695.

34. M.G. Abdullaev, *Pharm. Chem. J*, **2001**, *35* (1), 45.

CHAPTER 8

Conclusions and Future Outlook

8.1. Conclusions

8.1.1. Synthesis

New mono- and polynuclear complexes containing platinum, ruthenium, rhodium or iridium have been synthesized and fully characterized using several analytical and spectroscopic techniques. The complexes prepared consist of three different classes that are based on the type of ligand system used for their preparation.

Six new cycloplatinated thiosemicarbazone complexes (**2.2**-**2.7**) were prepared via C-H activation of the aromatic ring using the ligand 3,4-dichloroacetophenonethiosemicarbazone (**2.1**). Characterisation of complexes **2.2**-**2.7** using standard spectroscopic techniques revealed that the thiosemicarbazone ligand (**2.1**) acts as a tridentate dinegative donor to platinum. This was confirmed from the molecular structures of **2.2**-**2.4** which were determined using single crystal X-ray diffraction and show that the ligand coordinates to platinum in the expected tridentate manner via the *ortho*-carbon, imine nitrogen and thiolato sulfur. Reactivity studies of the mononuclear complex **2.4** with mono-, bis- and tris-(iodomethyl)benzene revealed that this complex was able to undergo oxidative addition reactions. This is noteworthy, as Pt(IV) complexes are believed to have pharmacological properties[1,2] thus the preparation of Pt(IV) cycloplatinated thiosemicarbazone complexes could be relevant to the search for alternative platinum therapies for cancer.

Two new pyridyl ether ligands (**4.1** and **4.2**) were synthesised using the Williamson Ether reaction. Both ligands were peripherally metallated with ruthenium, rhodium and iridium precursors to give the corresponding di- (**4.3**-**4.5**) and trinuclear (**4.6**-**4.8**) complexes. All of the compounds were isolated as air and moisture stable solids and were characterised using a variety of analytical and spectroscopic techniques. The molecular structure of **4.5** confirmed the monodentate coordination of the pyridyl ether ligands to each metal put forth by the spectroscopic and spectrometric characterisations of complexes **4.3** - **4.8**.

Two di- and tri-pyridyl ester ligands (**5.1** and **5.2**) have been synthesised by alkylation of the carboxylic acid. These ligands were functionalized with either [(p-cymene)$RuCl_2$], [(pentamethylcyclopentadienyl)$RhCl_2$] or [(pentamethylcyclopenta-dienyl)$IrCl_2$] moieties to give a series of new di- (**5.3**-**5.5**) and trinuclear (**5.6**-**5.8**) complexes. Spectroscopic characterisation revealed that, similar to the pyridyl ether ligands (**4.1** and **4.2**), the pyridyl ester ligands (**5.1** and **5.2**) act as monodentate donors to the metal via the pyridyl nitrogen. Proton NMR analyses of compounds **5.1**-**5.8** revealed that the proximity of the ester functionalities to the pyridyl ring influences the deshielding effect on the protons *ortho* to nitrogen. Minimal change in the ester methylene proton resonances confirmed no metal coordination occurs to the oxygen atoms of the ester functionality.

The molecular structures of **5.4** and **5.5** confirm the monodentate coordination of the pyridyl ester ligands to each metal put forth by the spectroscopic and spectrometric characterisations of complexes **5.3** - **5.8**. The elucidated molecular structures of the complexes **5.4** and **5.5** revealed a typical 'piano-stool' geometry around the metal and analysis of the dihedral angles formed between the central phenyl ring and the ester functionalities indicate that the pyridyl metal moieties position themselves almost perpendicular to the phenyl spacer thus minimizing electrostatic interactions.

8.1.2. In vitro Pharmacological Studies

The thiosemicarbazone complex **2.1** and its mono-, di- and tetranuclear complexes **2.2**-**2.6** were screened for antiparasitic activity against *Plasmodium falciparum* and *Trichomonas vaginalis* strains and for antitumor activity against cisplatin-sensitive and cisplatin-resistant human ovarian carcinoma cell lines. They were found to exhibit moderate to low parasite growth inhibition and antiproliferative activities. The *in vitro* activities obtained for **2.1**-**2.8** against the A2780 and A2780*cis*R cell lines revealed that cyclometalation of ligand **2.1** led to a decrease in *in vitro* activity. This is in contrast to previous reports where cycloplatination had a beneficial effect on activity.

The lipophilic nature of the phosphane in each complex may influence the antiproliferative activities of **2.3**-**2.6**. Complex **2.4** demonstrated the best IC_{50} out of all compounds tested against both cell lines and this activity may be due to the high hydrophilic nature of PTA which provides the right counter balance to the high lipophilicity of the platinum-thiosemicarbazone moiety. Overall, the moderate activities observed could be improved

through structural modification of the phosphanes to increase the hydrophilicity of the cycloplatinated complexes or by replacement of the phosphane with another type of ancillary ligand such as a monodentate nitrogen ligand.

Against the D10 and Dd2 *P. falciparum strains*, complexes **2.2**-**2.4** were much more active than their free ligand **2.1** and the inactivity of complexes **2.5** and **2.6** may be attributed to the presence of the diphosphane ligand. The highly lipophilic nature of complex **2.2** may result in the complex being unable to enter the acidic food vacuole of the parasite efficiently thus accounting for moderate antiplasmodial activity. Complex **2.3** displayed the best inhibitory activity against both strains yet was much less active against the A2780 and A2780*cis*R cell lines suggesting that complex **2.3** may be selective for *P. falciparum* over tumor cell lines. All of the compounds (**2.1** – **2.6**) with the exception of **2.4** displayed moderate to low effects on parasite viability in the *T. vaginalis* strain T1.

Evaluation of ligand **2.1** and complex **2.3** for their ability to inhibit β-hematin formation, it was found that these compounds do not target this process at the concentrations used in the assay. Preliminary stability studies of compounds **2.1** – **2.6** experiments with different short peptides and the amino acid methionine using ^{1}H NMR imply that these compounds may be stable in the blood and cytoplasm and they may reach their antitumoral target intact.

In vitro pharmacological evaluation of the two new series of di- and trinuclear ruthenium, rhodium and iridium complexes disclosed that all of the complexes and their free ligands (**4.1**-**4.8** and **5.1**-**5.8**) exhibited moderate to high antiplasmodial activity against the NF54 CQS *P. falciparum* strain. The trinuclear pyridyl ether complexes (**4.6**-**4.8**) and their free ligand demonstrated significantly higher activities than the other complexes tested and this was attributed to the incorporation of a central triazine moiety into their structures. The trinuclear complexes (**4.6**-**4.8** and **5.6**-**5.8**) display better activities compared to the dinuclear derivatives when strictly compared within each compound series (pyridyl ether and pyridyl ester) thus proposing that an increase in metal moieties leads to an increase in activity *in vitro*. All of the complexes showed better activity than the corresponding free ligand.

The most active compounds were assayed for inhibition of β-hematin formation and most of the compounds inhibited formation of synthetic hemozoin to some degree. This activity may be consequence of their polyaromatic structure. Should these compounds be able to enter the

acidic food vacuole of the parasite intact, then they may very likely inhibit parasite growth through inhibition of hemozoin.

Against the *Trichomonas vaginalis* strain G3, both the pyridyl ether and pyridyl ester compound series decreased parasite viability in a dose dependent manner. The complex **5.8** displayed the best inhibitory effect out of all complexes tested but as a whole, the pyridyl ether series (**4.2**-**4.8**) were much better inhibitors of the *T. vaginalis* strain G3.

Antitumoral studies against the A2780 and A2780*cis*R cell lines revealed that the trinuclear pyridyl ester complexes were the only active complexes. The tri-iridium complex (**5.8**) was found to be twice as active against the cisplatin resistant cell line (A2780*cis*R) compared to the A2780 cell line and also demonstrated the lowest toxicity against human embryonic kidney (HEK) cells. The rhodium complex **5.7** displayed the best inhibitory effect compared to its ruthenium (**5.6**) and iridium (**5.8**) derivatives.

The activity of the pyridyl ether (**4.1**-**4.8**) and pyridyl ester (**5.1**-**5.8**) series could be improved through modification of the ligand structure and/or the metal moieties may increase the activity of these compounds. The design of pyridyl ether or pyridyl ester ligands that can to chelate to the metal in a polydentante manner may lead to the formation of complexes that are more stable and hence display better pharmacological activites. Modification of the arene or cyclopentadienyl ligands of the metal moieties to give added hydrophilicity could also enhance activity.

8.1.3. Catalytic Evaluation

An initial screening of the four cyclopalladated complexes (**7.1**-**7.4**) that were prepared revealed these compounds to have moderate catalytic activity for the Suzuki-Miyaura cross coupling reaction with the exception of 7.4. This dinuclear complex, which contains the bis(diphenylphoshinoferrocene) spacer was a robust catalyst. It was able to efficiently catalyze the coupling of various aryl halides and aryl boronic acids, irrespective of the type of electron-withdrawing or electron-donating substituent on the aromatic ring.

8.2. Future Outlook

The moderate activities observed for the thiosemicarbazones (**2.1**-**2.7**) could be improved through structural modification of the phosphanes to increase the hydrophilicity of the cycloplatinated complexes or by replacement of the phosphane with another type of ancillary ligand such as a monodentate nitrogen ligand.

Further oxidative addition reactivity studies of **2.4** with other bromo-methyl substrates could prove useful as it offers another way of introducing hydrophilic groups to platinum thiosemicarbazone complexes and the increase in coordination number may further stabilize platinum. Pt(IV) complexes have been studied for pharmacological activity and are thought to act as pro-drugs, from which the active Pt(II) species is generated within the cancer cell.[2] It would be interesting to find out if Pt(IV) thiosemicarbazone complexes have improved antiproliferative and antiparasitic activities compared to Pt(II) derivatives.

The tri-pyridyl ether ligand **4.2** and its corresponding trinuclear ruthenium, rhodium and iridium complexes (**4.6**-**4.8**) displayed antiplasmodial activities in the nanomolar range. This was attributed to the incorporation of a central triazine moiety into their structures and should be kept in mind when designing future polynuclear complexes of this type for antiparasitic study.

The overall pharmacological activity of the pyridyl ether (**4.1**-**4.8**) and pyridyl ester (**5.1**-**5.8**) series could be improved through modification of the ligand structure and/or the metal moieties may increase the activity of these compounds. The design of pyridyl ether or pyridyl ester ligands that can to chelate to the metal in a polydentante manner may lead to the formation of complexes that are more stable and hence display better pharmacological activities. Modification of the arene or cyclopentadienyl ligands of the metal moieties to give added hydrophilicity could also enhance activity.

With respect to the catalytic activity of complex **7.4**, further studies of its ability to catalyze other coupling reactions should be undertaken. For example, tridentate mononuclear Pd(II) thiosemicarbazone complexes have shown high activity for the Heck coupling reaction.[3] Other mononuclear Pd(II) thiosemicarbazone complexes have displayed moderate to good activities for the Buchwald-Hartwig amination reaction.[4,5] It would be interesting to

determine if complex **7.4** would be able to catalyze other coupling reactions with similar high activities as it achieved for the Suzuki-Miyaura cross-coupling reactions.

8.3. References

1. L. Ronconi and P. J. Sadler, *Coord. Chem. Rev.*, **2007**, *251*, 1633.
2. M. D. Hall and T. W. Hambley, *Coord. Chem. Rev.*, **2002**, *232*, 49.
3. G. Xie, P. Chellan, J. Mao, K. Chibale and G.S. Smith, *Adv. Synth. Catal.*, **2010**, *352* (10), 1641.
4. J. Dutta, S. Datta, D. K. Seth and S. Bhattacharya, *RSC Advances*, **2012**, *2*, 11751.
5. R. N. Prabhu and R. Ramesh, *Tet. Lett.*, **2013**, *54*, 1120.